DOCTORAL THESIS

Investigation into the effects of chronic social stress on the regulation of feeding and metabolism in mice

Carneiro Nascimento, Simone

Award date:
2019

Awarding institution:
University of Roehampton

University of Roehampton London

Investigation into the effects of chronic social stress on the regulation of feeding and metabolism in mice

by

Simone Carneiro Nascimento, BSc.

A thesis submitted in partial fulfilment of the requirements for the degree of PhD

Department of Life Sciences

University of Roehampton

2019

To my God Almighty,

for it is His all honour and glory.

ABSTRACT

Stress is known to affect energy metabolism in humans and animals. This thesis aimed to investigate the effects of chronic social stress (CSS) on energy expenditure (EE), respiratory exchange ratio (RER), neuroendocrine regulators of feeding and the serotonergic system.

Adult male C57BL/6 mice were exposed to 15 days of social stress or control handling. In an iterative series of experiments, food intake (FI) and body weight (BW) were measured daily, indirect calorimetry was evaluated before and after the CSS period, and glucose homeostasis was evaluated using a glucose tolerance test. At termination, plasma and adipose tissues were collected for determination of ghrelin, leptin and insulin concentrations, as well as gene expression of leptin and leptin receptor. In discrete brain areas, ghrelin receptor (Ghs-r1a) immunopositive cell count, gene expression of ghrelin and leptin receptors, as well as serotonin 5-HT1A, 5-HT2A and 5-HT2C receptor binding (by means of autoradiography) and gene expression, were analysed.

The present results are consistent with CSS leading to a reduced conversion of FI into an increased BW, as demonstrated by an increased FI with an absence of BW effect or by unaffected FI with an attenuated BW increase. Increased RER was observed in CSS mice, indicating a greater carbohydrate utilisation as fuel source. This study also identified markers of increased hunger signalling i.e. increased plasma ghrelin and ventromedial hypothalamic *Ghs-r1a* mRNA expression, and decreased satiety signalling i.e. decreased plasma leptin and WAT *Lep* mRNA expression. The lower leptin levels were consistent with an increase in energy demand, as also

suggested by decreased insulin levels. CSS affected the serotonergic system through modifications of the binding activity and gene expression of serotonin receptors, and by modification of serotonin transporter gene expression.

In conclusion, the present thesis demonstrated that CSS in mice leads to both central and peripheral changes consistent with increased energetic requirements, which has important implications for brain function.

TABLE OF CONTENTS

ACKNOWLEDGEMENTS

I would like to express my sincere gratitude to my Director of Study, Professor Jolanta Opacka-Juffry, for her great support and guidance throughout my PhD, and for sharing her knowledge and passion for neuroscience. To my Supervisor Dr. Michael Patterson, for his essential supervision of my PhD research, and also for sharing such a vast knowledge of endocrinology. To my External Supervisor, Professor Christopher Pryce, for the training in the animal model used in this study, and the fundamental support for the in vivo research I conducted in his lab at the University of Zurich, as well as for his much-appreciated advice about data analysis and scientific writing.

I want to thank the laboratory technicians at the Department of Life Sciences, the University of Roehampton and the University of Zurich for the incredible support, particularly Hannes Sigrist for the assistance with animal handling and care, and sample collection in Zurich.

Finally, I would like to thank my boyfriend Andrea, for his amazing words of encouragement, and my parents, Carmem and Sinhuee, as without their support I would have never been able to achieve such goals. Your love is everything for me.

To all, I am deeply grateful.

AUTHOR'S DECLARATIONS

I declare that the work presented in this thesis is original and result of my own work, except where otherwise specified.

This study was performed in accordance with federal guidelines, under the license 149/2015 from the Zürich Cantonal Veterinary Office and approval of University of Roehampton Ethics Committee application LSC 16/175.

The present work was carried out with the support of the National Council for Scientific and Technological Development (CNPq) – Brazil process 200997/2015-7; Swiss National Science Foundation grant 31003A-160147 and the University of Roehampton activity 37996.

LIST OF PUBLICATIONS

Nascimento, S.C., Bergamini, G., Brugger, C.M., Rokni, A.F., Martins, L.A., Pryce, C.R., Opacka-Juffry, J. and Patterson, M. (2016) *The Effects of Chronic Psychosocial Stress on Ghrelin Receptor Immunoreactivity in the Hypothalamus and Ventral Tegmental Area*. Presented at: 10th FENS Forum of Neuroscience, Copenhagen, Denmark.

Nascimento, S.C., Bergamini, G., Brugger, C.M., Rokni, A.F., Martins, L.A., Pryce, C.R., Opacka-Juffry, J. and Patterson, M. (2017) *The Effects of Chronic Psychosocial Stress on Feeding Behaviour and the Battle against Obesity.* Presented at: Research Student Conference 2017, University of Roehampton, London, UK.

Nascimento, S.C., Buerge, M., Beyan, S., Lewis, C., Varathanathan, V., Pryce, C.R., Patterson, M. and Opacka-Juffry, J. (2017) *Effects of chronic social stress on 5-HT1A, 2A, and 2C receptor binding in mouse brain regions associated with reward processing.* Presented at: BNA2017 Festival of Neuroscience, Birmingham, UK.

Nascimento, S.C., Pryce, C.R., Opacka-Juffry, J. and Patterson, M. (2018) *The Effects of Chronic Social Stress on Energy Balance and The Potential Role of Neuroendocrine Regulators of Feeding.* Presented at: 11th FENS Forum of Neuroscience, Berlin, Germany.

Nascimento, S.C., Wiese, M., Pryce, C.R., Opacka-Juffry, J., Patterson, M. and Costabile, A. (2018) *The Effects of Chronic Social Stress on The Gut Microbiome in Mice.* Presented at: 11th FENS Forum of Neuroscience, Berlin, Germany.

Nascimento, S.C., Pryce, C.R., Powell, W., Uebel, M., Opacka-Juffry, J. and Patterson, M. (2018) *Animal-Model Evidence for Involvement of Leptin in the Regulation of Stress-induced Changes in Energy Balance.* Presented at: Pharmacology 2018, London, UK.

LIST OF ABBREVIATIONS

α-MSH – alpha melanocyte stimulating hormone

α_1, α_2, β – noradrenaline receptors

5-HT – serotonine

8-OH-DPAT – 8-hydroxi-2-(di-n-propylamino)tetralin

ACTH – adrenocorticotropic hormone

AgRP – agouti-related protein

Amy – amygdala

ANCOVA – analysis of covariance

ANOVA – analysis of variance

ARC – arcuate nucleus of the hypothalamus

ATP – adenosine triphosphate

AVP – arginine vasopressin

BAT – brown adipose tissue

BBB – blood-brain barrier

BDNF – brain-derived neurotrophic factor

BMI – body mass index

cAMP – cyclic adenosine monophosphate

CART – cocaine and amphetamine-regulated transcript

cDNA – complementary DNA

CHO – carbohydrate

CCK – cholecystokinin

CNS – central nervous system

CO_2 – carbon dioxide

CON – control

CRH – corticotropin-releasing hormone

CSDS – chronic social defeat stress

CSS – chronic social stress

CUMS – chronic unpredictable mild stress

CUS – chronic unpredictable stress

DA – dopamine

DLW – doubly-labelled water

DMH – dorsomedial hypothalamus

DRN – dorsal raphe nucleus

DS – dorsal striatum

EE – energy expenditure

eWAT – epididymal white adipose tissue

FDG – fluorodeoxyglucose

FW – forward primer

GABA – gaba-aminobutyric acid

GC – glucocorticoid

gDNA – genomic DNA

GH – growth hormone

GHS-R – growth hormone secretagogue receptor

GHS-R KO – growth hormone secretagogue receptor knockout

GI – gastrointestinal

GLP-1 – glucagon-like peptide 1

GLUT1/GLUT2/GLUT3/GLUT4 – glucose transporters

GOAT – ghrelin-o-acyl transferase

GPCR – G protein-coupled receptor

GR – glucocorticoid receptor

GTT – glucose tolerance test

HAM-A – Hamilton Rating Scales for Anxiety

HAM-D – Hamilton Rating Scales for Depression

HCl – hydrochloric acid

HFD – high-fat diet

Hipp – hippocampus

HPA – hypothalamic-pituitary-adrenal (axis)

Hyp – hypothalamus

i.c.v. – intracerebroventricular

i.v. – intravenous

i.p. – intraperitoneal

iBAT – interscapular BAT

IL-6 – interleukin-6

K^+ – potassium

LC – locus coeruleus

LEPR – leptin receptor

LEPRb – long form of LEPR

LHA – lateral hypothalamic area

LMM – linear mixed model

LSD – least significant difference

MA – motor activity

MC3R/MC4R – melanocortin receptors

MDD – major depressive disorder

mPFC – medial prefrontal cortex

MR – mineralocorticoid receptor

NAcc – nucleus accumbens

NE – norepinephrine (noradrenaline)

NPY – neuropeptide Y

NTC – no template control

NTS – nucleus tractus solitarius

O_2 – oxygen

OCT – optimal cutting temperature

PBS – phosphate-buffered saline

PET – positron emission tomography

POD – peroxidase

POMC – pro-opiomelanocortin

PTSD – post-traumatic stress disorder

PVN – paraventricular nucleus of the hypothalamus

PYY – peptide YY

RER – respiratory exchange ratio

RMR – resting metabolic rate

RN – raphe nucleus

RPa – raphe pallidus

rRNA – ribosomal RNA

ROI – region of interest

RT – room temperature

RT-qPCR – reverse transcription quantitative polymerase chain reaction

RV – reverse primer

sBAT – supraclavicular BAT

SD – standard deviation

SEM – standard error of the mean

SERT – serotonin transporter

SNS – sympathetic nervous system

SSRI – selective serotonin reuptake inhibitor

TEE – total energy expenditure

TMB – 3,3',5,5'-tetramethylbenzidine

TNF-α – tumour necrosis factor alpha

TRβ – thyroid hormone receptor beta

TRH – thyrotropin releasing hormone

Ucp-1 – uncoupling protein 1

VMH – ventromedial hypothalamus

VTA – ventral tegmental area

WAT – white adipose tissue

WT – wild type

LIST OF FIGURES

LIST OF TABLES

CHAPTER 1

General Introduction

1.1. Energy metabolism

Energy metabolism, as the set of biochemical reactions performed within a living organism (Kornberg, 2017), comprises the synthesis (i.e. anabolism) and breakdown (i.e. catabolism) of bioactive substances for energy production (Lazar and Birnbaum, 2012). Regulation of energy metabolism involves many factors, in particular: genetic, through expression of genes implicated in the regulation of food intake (Herrera and Lindgren, 2010) and energy expenditure (EE) (Almind and Kahn, 2004; Alonso et al., 2015), and environmental, such as diet, lifestyle (e.g. physical activity) and stress (Qi and Cho, 2008; Yamaoka and Tango, 2012; Bassi et al., 2014). This combination of genes and environment determines an individual's susceptibility to obesity (Romieu et al., 2017) and other metabolism-related disorders (Heindel et al., 2017).

Control of nutrient consumption and utilisation, as well as regulation of EE, have long been contemplated for development of interventions that better target diseases associated with obesity (Galgani and Ravussin, 2008; Geisler, 2011; Lam and Ravussin, 2016). To treat obesity and related disorders it is necessary to comprehend the mechanisms through which the body regulates energy intake *versus* EE, and how these are affected by environmental factors such as chronic stress.

1.1.1. Energy balance – Food intake *versus* Energy expenditure

Energy balance is a term used to describe the equilibrium between "energy in", in the form of calories taken, and "energy out", as EE (Hall et al., 2012). Feeding exerts

an essential role in the regulation of energy balance. Nonetheless, in order to maintain homeostasis, food intake must be balanced out by EE, and *vice versa*.

1.1.1.1. Energy expenditure

Energy expenditure can be described as the amount of energy an individual uses to maintain body homeostasis. Total energy expenditure (TEE) comprises three elements: *resting metabolic rate* (RMR), the main component of TEE (60-70%) that corresponds to the energy required for the performance of vital biological processes over 24 hours; *thermic effect of food,* or the energy required for nutrient utilisation and *physical activity* (Speakman, 2013; Westerterp, 2017).

Various factors influence EE (Romieu et al., 2017). Fat-free mass, for instance, is the best direct predictor of RMR (Cunningham, 1991; Westerterp, 2017). Body size can also exert an effect on RMR, however, indirectly: the larger the body size, the greater the amount of fat-free mass, consequently the greater the energy requirement. In regards to the thermic effect of food, it can take up to 10% of TEE when limited to homeostatic needs. However, in the case of overfeeding, there can be an increase not only in this element of TEE but also in RMR as a function of fat-free mass, since high-calorie intake commonly leads to increased body mass (Harris et al., 2006). Physical activity, on the contrary, is a far more variable component of TEE. For overweight individuals, there is a high energy cost in performing physical activity (Nantel et al., 2011), and although physical activity is highly recommended for weight loss, its frequency can be decreased for such reason.

1.1.1.2.1. Adaptive thermogenesis

EE is also subject to brown adipose tissue (BAT) thermogenesis (Morrison et al., 2014; Razzoli and Bartolomucci, 2016), activated during periods of chronic cold exposure or hyperphagia. This is the case in many species including mice (Virtue and Vidal-Puig, 2013) and humans (Ouellet et al., 2012; Saito, 2013). Whereas white adipose tissue (WAT) is accountable for energy storage, BAT is associated with EE. A transitional form of WAT characterised by the presence of brown adipocytes, named beige adipose tissue, has also been observed in rats and mice following cold stress (Young et al., 1984; Lonçar et al., 1988). The comparable features of the adipocytes in beige and brown adipose tissues were described recently (Ikeda et al., 2018).

The BAT is a thermogenic tissue that contains small brown adipocyte droplets surrounded by mitochondria, which allow for the production of heat. The thermogenic process associated with BAT is controlled foremost by the noradrenaline receptors (β, α_1, α_2) expressed on the membrane of the brown adipocyte (Ueta et al., 2012; Madden et al., 2013). Nevertheless, the adrenergic pathway seems not to be the only factor for cold-induced BAT browning (Razzoli et al., 2016). There are known effects of glucocorticoids (GC) on BAT, of relevance to stress, as addressed below in Section 1.3 of this chapter. Once activated, adrenergic receptors trigger a cascade of enzymatic reactions for triglyceride hydrolysis and fatty acid release, with subsequent activation of the mitochondrial transmembrane uncoupling protein 1 (Ucp-1) (Cannon and Nedergaard, 2004; Contreras et al., 2016). The Ucp-1 protein is accountable for heat production through non-shivering thermogenesis. Whenever this proton carrier is activated, through an oxidative process not "coupled" to the synthesis of ATP, dissipation of heat is prompted (Figure 1.1).

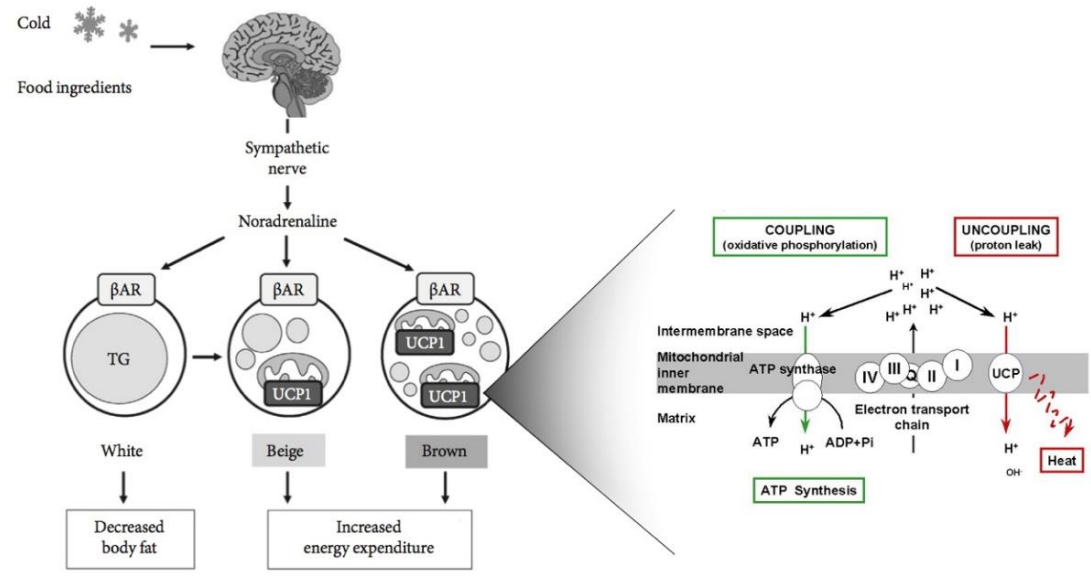

Figure 1.1. Effect of cold exposure and food intake on the sympathetic nervous system with subsequent activation of β-adrenergic receptors on white, beige and brown adipocytes. Electron transport chain forms an H^+ gradient between the mitochondrial intermembrane space and matrix, which can be used for the synthesis of ATP by ATP synthase or heat production by uncoupling proteins. Figure adapted from Saito et al. (2013), Diabetes and Metabolism Journal, p23, and Collins and Surwit (2001), The Endocrine Society, p310.

In mice, BAT is located subcutaneously, mainly in the dorsal back of the interscapular (iBAT) and subscapular (subscapular BAT) regions. Supraclavicular BAT (sBAT) was also recently characterised (Mo et al., 2017). In humans, BAT is reported to be primarily in the supraclavicular regions (Sacks and Symonds, 2013). Although human BAT is found prominently in newborns to control body temperature, studies using fluorodeoxyglucose (FDG)-positron emission tomography (PET) demonstrated the presence of metabolically active BAT in adult humans (Nedergaard et al., 2007). Despite localisation differences, sBAT and iBAT mitochondria from humans and mice, respectively, have comparable Ucp-1 function (Porter et al., 2016), validating the use of animal models in translational studies.

1.1.2. Neurocircuits of homeostatic feeding

The regulation of energy balance involves a complex interaction of peripheral organs and the central nervous system (CNS), the latter being responsible for detecting satiety and adiposity signals and responding according to the homeostatic body needs (Woods and Seeley, 2000; Chambers et al., 2013). Within CNS, the brain receives short-term satiety signals from peripheral organs via afferent fibres of the vagus nerve (Browning et al., 2017). Within the brainstem, nucleus tractus solitarius (NTS) neurons receive inputs from the gastrointestinal (GI) tract (e.g. volume of ingested food) and project to the paraventricular nucleus of the hypothalamus (PVN) (Katsurada et al., 2014) for the regulation of food intake. Ghrelin, for instance, stimulates appetite by inhibition of vagal afferent activity (Date et al., 2002). It also regulates feeding by acting directly on hypothalamic nuclei, more specifically the arcuate nucleus of the hypothalamus (ARC) (Riediger et al., 2003). Other gut peptide hormones such as glucagon-like peptide 1 (GLP-1), peptide YY (PYY) and cholecystokinin (CCK) are involved in the perception of satiety and meal termination (Little et al., 2005; Karra et al., 2009; Shah and Vella, 2014).

The brain also perceives variations in energy stores in the body. In a process referred to as 'adiposity negative feedback', long-term adiposity signals from hormones such as leptin and insulin, levels of which in the circulation are proportional to body fat stores, act directly at the ARC of the hypothalamus to reduce body fat and food intake (Cowley et al., 2001; Loh et al., 2017). The ARC of the hypothalamus acts therefore as an integrative centre of satiety and adiposity signals in order to determine food intake (Figure 1.2); its proximity to the third ventricle and median eminence means it is highly sensitive to circulating peripheral inputs (Rodríguez et al., 2010).

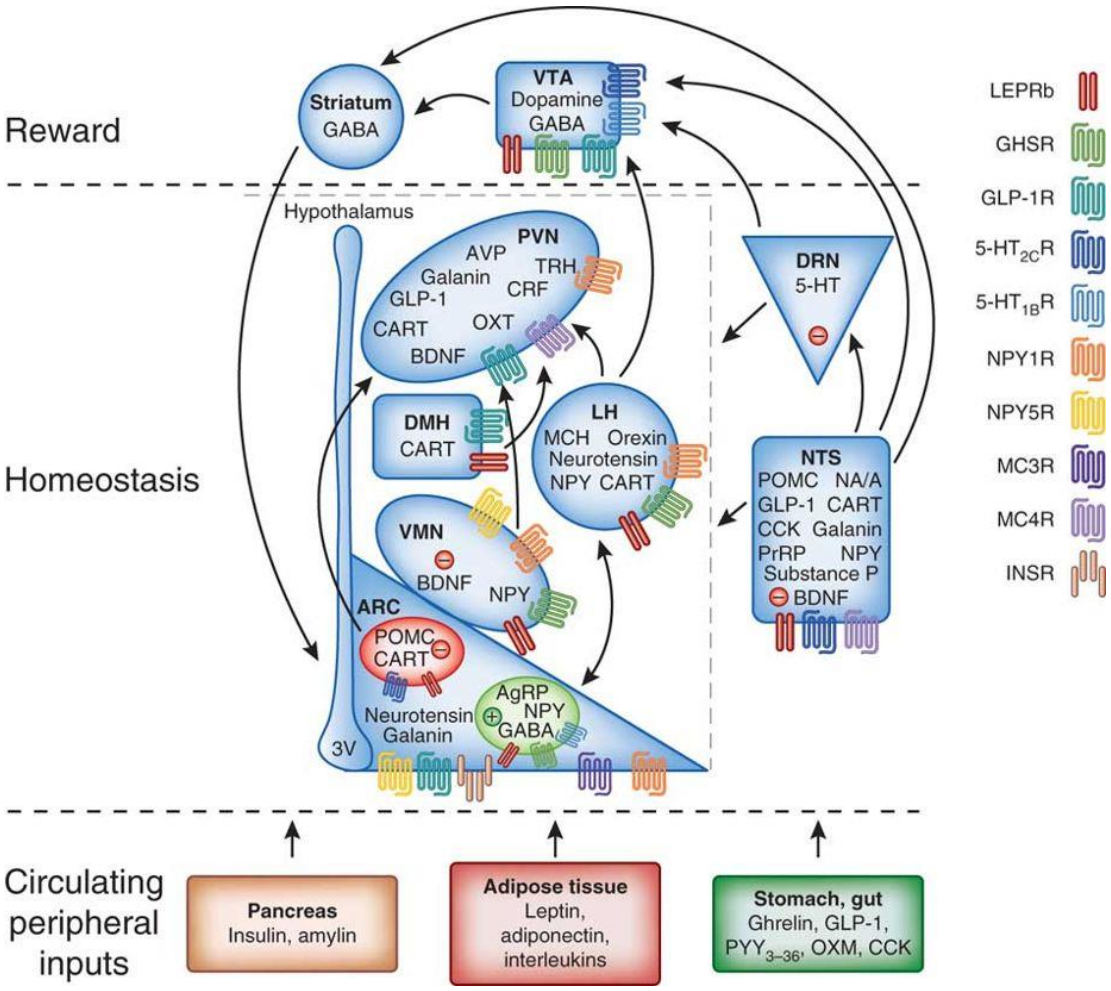

Figure 1.2. Schematic representation of the hypothalamic nuclei and main inputs from circulating peripheral peptides and reward-related brain regions. Abbreviations: ARC, arcuate nucleus of the hypothalamus; VMN, ventromedial hypothalamic nucleus; DMH, dorsomedial hypothalamic nucleus; LH, lateral hypothalamus; PVN, paraventricular nucleus; VTA, ventral tegmental area; DRN; dorsal raphe nucleus; NTS, nucleus tractus solitaries; CART, cocaine- and amphetamine-regulated transcript; CRF, corticotropin-releasing factor; GLP-1, glucagon-like peptide 1; MCH, melanin-concentrating hormone; OXT, oxytocin; AVP, vasopressin; TRH, thyrotropin-releasing hormone; NA, noradrenaline; A, adrenaline; PrRP, prolactin-releasing peptide; PYY, peptide YY residues; OXM, oxyntomodulin; CCK, cholecystokinin. MC3R and MC4R, melanocortin receptors; NPY1R and NPY5R, NPY receptors; LEPRb, long isoform of the leptin receptor; INSR, insulin receptor; GHS-R, ghrelin receptor; GLP-1R, GLP-1 receptor; 3V, third ventricle. Figure reprinted from Yeo and Heisler (2012), Nature Neuroscience, p1346, ©2012 Nature America, Inc.

1.1.2.1. Hypothalamic control of energy balance

1.1.2.1.1. Melanocortin system

The neurocircuitry regulating homeostatic feeding has two key neuronal subpopulations which are part of the melanocortin system, located in the ARC of the hypothalamus: neuropeptide Y (NPY) / agouti-related protein (AgRP) and pro-opiomelanocortin (POMC) / cocaine and amphetamine-regulated transcript (CART) (Figure 1.3). Activation of ARC NPY/AgRP neurons is known to increase motivation for feeding and enhance body weight gain (Krashes et al., 2011), whereas ARC POMC/CART neurons are known to inhibit food intake, by releasing α-melanocyte stimulating hormone (α-MSH) and activating neuronal melanocortin receptors (Cowley et al., 2001). While AgRP acts as an antagonist of melanocortin receptor type 3 (MC3R) and type 4 (MC4R) (Ollmann et al., 1997), NPY acts indirectly on melanocortin receptors, inhibiting POMC/CART neurons via NPY receptors (Nasrallah and Horvath, 2014).

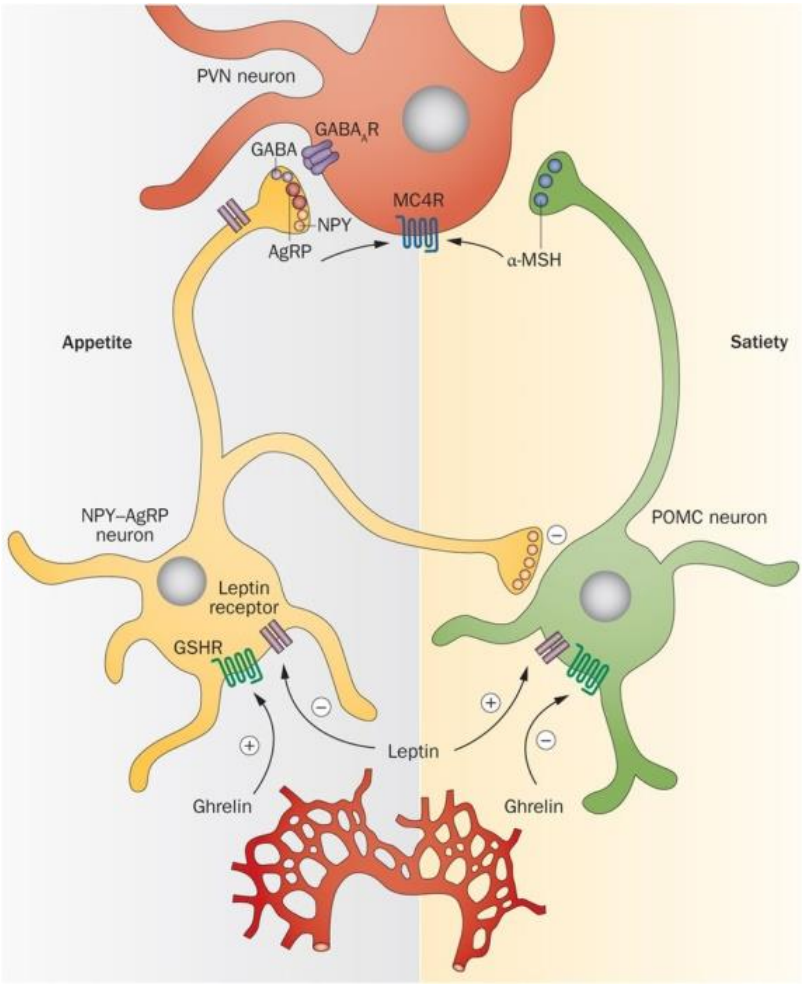

Figure 1.3. Hypothalamic melanocortin neuronal subpopulations. Abbreviations: PVN, paraventricular nucleus, GABA, gaba-aminobutyric acid; MSH, melanocortin stimulating hormone; MC4R, melanocortin receptor type 4; NPY, neuropeptide Y; AgRP, agouti-related protein; POMC, pro-opiomelanocortin; GHS-R, growth hormone secretagogue receptor. Figure reprinted from Nasrallah and Horvath (2014), Nature Reviews Endocrinology, p3, ©2014 Macmillan Publishers Ltd.

In addition to the NPY peptide, the gut hormone PYY also binds to NPY receptors located in ARC NPY/AgRP neurons, and it is thought to inhibit food intake (Batterham et al., 2002). Nonetheless, the mechanism by which PYY regulates food intake appears to be independent of the melanocortin system (Halatchev et al., 2004).

1.1.2.1.2. Intrahypothalamic connections

Much of the research on energy metabolism has focused on ARC. Nevertheless, homeostatic feeding and EE are also regulated through the interaction of ARC neuronal subpopulations with other hypothalamic nuclei (Waterson and Horvath, 2015) (Figure 1.2). For instance, ARC NPY/AgRP and POMC/CART neuronal subpopulations were shown to project to PVN, where MC4R is highly expressed and modulates feeding behaviour (Skibicka and Grill, 2009). For a full review on PVN pathways controlling energy homeostasis, see Hill (2012).

The connection between ARC and ventromedial hypothalamus (VMH) was also shown to be involved in the regulation of energy homeostasis (Sternson et al., 2005). Activation of VMH MC4R was shown to control energy balance, regulated by brain-derived neurotrophic factor (BDNF) (Xu et al., 2003). BDNF is a neurotrophic factor abundantly expressed in the brain, which regulates neuronal development and exerts neuroprotective effects (e.g. Greenberg et al., 2009). Interestingly, a selective BDNF knockdown in the VMH resulted in hyperphagia and obesity in mice (Unger et al., 2007). Furthermore, selective knockdown of the thyroid hormone receptor beta (TRβ) in the VMH stimulated an obese phenotype that was possibly due to a downstream modulation of hypothalamic regulators of feeding (Hameed et al., 2017).

In addition to PVN and VMH, ARC is also known to regulate energy balance by connecting to the lateral hypothalamic area (LHA) and dorsomedial hypothalamus (DMH). For instance, Betley et al. (2013) observed that optogenetic stimulation of AgRP projection from ARC to LHA increased feeding. Moreover, it was shown that the anorexigenic hormone leptin regulated ARC NPY and POMC neuronal subpopulations that project to LHA (Elias et al., 1999). Further, the ARC cells were

also shown to modulate DMH and exert an effect on feeding (Bellinger and Bernardis, 2002).

1.1.2.1.3. Extrahypothalamic connections

The hypothalamus is also connected with extrahypothalamic nuclei for the regulation of food intake and EE. An increase in feeding following optogenetic stimulation of GABAergic fibres originating in the LHA and projecting to the ventral tegmental area (VTA) was observed (Nieh et al., 2015). Stimulation of inhibitory GABAergic neurons projecting to the VTA may drive feeding by modulation of dopaminergic VTA neuronal activity and reward-related behaviour. It was also observed that activation of MC4R in the NTS, where they are highly expressed (Kishi et al., 2003), by ARC POMC descending projections suppressed food intake (Zheng et al., 2010). Additionally, PVN neurons were shown to control gastric distension and thus feeding behaviour by increasing the response of NTS neurons to vagal signals (Rogers and Hermann, 1985). In regard to the regulation of EE, neuronal projections from PVN to raphe pallidus (RPa) were shown to suppress BAT thermogenesis (Madden and Morrison, 2009), likely through the release of NPY peptides (Chao et al., 2011).

1.1.3. Satiety and adiposity signals

1.1.3.1. Ghrelin

Encoded by the *Ghrl* gene and first identified as growth hormone (GH) stimulating peptide, ghrelin is a 28 amino acid peptide hormone secreted from the stomach into the circulation and that functions to stimulate in meal initiation (for review, see Patterson et al., 2011 and Müller et al., 2015). Of note, ghrelin is the only

identified satiety-signal from the GI tract that increases meal size (Woods, 2003). It is found in two forms: acyl ghrelin, which activates cells expressing the growth hormone secretagogue receptor (GHS-R), and the non-modified des-*n*-octanoyl form of ghrelin (des-acyl ghrelin), which has no activity at the only known GHS-R. Circulating ghrelin consists of more than 90% of des-acyl ghrelin (Patterson et al., 2005), nevertheless, acylation of the serine 3 residue, by ghrelin-o-acyltransferase (GOAT), is imperative for its hormonal activity (Hosoda et al., 2000; Kojima et al., 2001).

Peptide hormones cannot generally freely access the brain, nevertheless, ghrelin crosses the blood-brain barrier (BBB) via passive diffusion (Schaeffer et al., 2013). This transport is limited to specific brain regions. Within the brain, *Ghrl* and *Ghs-r* gene expression were reported predominantly in the pituitary and in hypothalamic nuclei (Sun et al., 2004; Kineman et al., 2007). In humans and rodents, ghrelin is commonly associated with the hypothalamic regulation of energy homeostasis (Cummings et al., 2001; Nakazato et al., 2001; Klok et al., 2007). In rats, the highest levels of GHS-R expression were shown to be in ARC and VMH, with increased levels in ARC following fasting (Nogueiras et al., 2004). Following intracerebroventricular (i.c.v) administration of ghrelin, c-Fos protein, a marker of cellular activity, was found to be increased in NPY/AgRP neurons in rats (Nakazato et al., 2001).

In addition to the hypothalamus, GHS-R is found in other areas of the brain including VTA, nucleus accumbens (NAcc), hippocampus (Hipp) and amygdala (Amy); GHS-R expressed in the VTA could be of particular importance. VTA is part of the mesocorticolimbic dopamine system implicated in the motivational and learning aspects of feeding (Abizaid et al., 2006; Perelló and Zigman, 2012). Peripheral administration of ghrelin was reported to evoke a preference for energy-dense

palatable/rewarding foods (Egecioglu et al., 2010). Direct administration of ghrelin into VTA enhanced feeding in mice (Abizaid et al., 2006) and rats (Naleid et al., 2005). Furthermore, an attenuated feeding response was observed in GHS-R-deficient mice (Abizaid et al., 2006).

Ghrelin has not only been implicated in the regulation of food intake but also EE and thermogenesis. Various studies have shown that ghrelin favours adiposity by decreasing fat utilisation and promoting increase in carbohydrate (CHO) usage as a fuel source (Tschop et al., 2000; Tsubone et al., 2005; Patterson et al., 2013). When administrated peripherally in rats, ghrelin reduced BAT temperature thus decreasing EE (Yasuda et al., 2003). When administered centrally in mice, ghrelin reduced BAT *Ucp-1* expression, through inhibition of sympathetic innervation of BAT (Tsubone et al., 2005).

1.1.3.2. Leptin

Encoded by the *Ob* gene, leptin is a 146 amino acid peptide hormone secreted from adipocytes into the circulation and best understood as a long-term signal of adiposity, as a peripheral signal of nutritional status to the CNS, as well as in the regulation of EE (for review, see Friedman 2014). There is a consensus that leptin levels are correlated with adiposity (Caron et al., 2018). Leptin is mainly secreted from visceral WAT in rodents (Trayhurn et al., 1995) and subcutaneous WAT in humans (Hube et al., 1996). With the discovery of leptin, adipose tissue is no longer just a tissue correlated with body weight but an endocrine organ with feedback loops between the brain and peripheral organs (Coelho et al., 2013).

Via alternative mRNA splicing, a single leptin receptor (*Lepr*) gene produces six LEPR isoforms. However, it is only through the activation of the long form of the

leptin receptor (LEPRb) that leptin exerts its biological functions. *Leprb* (coding gene for LEPRb) was shown to be greatly expressed in many brain regions, and hypothalamus was identified as its principal site of action, particularly ARC (Elmquist et al., 1998; Scott et al., 2009).

Within ARC, NPY/AgRP and POMC/CART neuronal subpopulations were identified as fundamental for the leptin-associated homeostatic regulation of appetite. It was shown that leptin acts in part by activation of POMC and inhibition of AgRP neurons (Cowley et al., 2001; Van Den Top et al., 2004). Leptin i.c.v. injections were shown to decrease food intake in rodents while decreasing ARC *Npy* mRNA expression (Schwartz et al., 1996). Beyond the hypothalamus, studies also reported the effects of leptin on the regulation of energy balance via action on the midbrain and brainstem. Administration of leptin into VTA, for instance, decreased food intake (Hommel et al., 2006). Further, intravenous (i.v.) administration of leptin increased STAT3 phosphorylation in the brainstem of mice, a transcription factor essential for the metabolic actions of leptin (Hosoi et al., 2002).

Besides its function as an appetite regulator, leptin also contributes to the regulation of EE. Whenever leptin binds to its receptor in ARC and stimulates the production of POMC peptides, α-MSH peptides are produced. Binding of α-MSH to MC4R located in the pituitary was shown to stimulate secretion of thyrotropin releasing hormone (TRH) and increase EE (Flier et al., 2000). Moreover, direct leptin activation of NTS was shown to increase *Ucp-1* mRNA expression (Matheny et al., 2014). By acting on the sympathetic nervous system (SNS), studies showed that leptin promoted WAT triglycerides breakdown and browning (Dodd et al., 2015) and increased BAT glucose uptake (Haque et al., 1999). Interestingly, leptin levels were found to be decreased in situations of cold exposure and fasting (Hardie et al., 1996).

This suggests that leptin is more likely to reflect one's energy demand rather than body lipid content.

Leptin is known to play an important role in metabolic disorders, and there are significant links between leptin and obesity (Montague et al., 1997; Clément et al., 1998). Importantly, in obese humans and rodents, although leptin levels are recurrently high (Maffei et al., 1995), the leptin transport across BBB is impaired (Banks et al., 1999). Various studies support the strong association between obesity and leptin resistance (for review, see Zhou and Rui, 2014). Recently, Mazor et al. (2018) showed that obesity induced by high-fat diet (HFD) was associated with leptin receptor degradation and leptin resistance in mice. Further, dysfunctional LEPR-STAT3 signalling pathway was associated with an obese phenotype in mice (Saadat et al., 2012). Using adenoviral gene therapy to express ARC *Lepr*, Morton et al. (2003) reported that restoration of ARC *Lepr* mRNA expression was sufficient to attenuate obesity phenotype in leptin receptor-deficient rats. Nonetheless, it is still unclear whether leptin sensitivity is the cause or consequence of diet-induced obesity (de Git et al., 2018).

1.1.3.3. Insulin

Encoded by the *INS* gene, insulin biosynthesis begins with its precursor, preproinsulin, that undergoes posttranslational translocation and cleavage until the formation of the mature form of insulin (Liu et al., 2018). Insulin is a 51 amino acid peptide hormone secreted from pancreatic β-cells best known for its role in glucose homeostasis (for review, see Plum et al., 2006). The primary function of insulin is to control blood glucose levels by stimulating glucose uptake into cells. During a hyperglycemic state, insulin has potent physiological anabolic effects, promoting

synthesis of lipids, protein and carbohydrates and inhibiting their breakdown. It was shown to promote intestinal glucose absorption (Ussar et al., 2017), increase lipogenesis (Larger, 2005; Scherer et al., 2011) and liver glycogenesis (Han et al., 2016) and inhibit hepatic gluconeogenesis (i.e. glucose synthesis) (Lee et al., 2016).

For peripheral tissues, insulin is essential for the regulation of glucose homeostasis and energy balance. When insulin binds to its receptor in the membrane of target cells, it stimulates the translocation of glucose transporter type 4 (GLUT4) proteins to the plasma membrane, through exocytosis, at the same time that attenuates its endocytosis (Furtado et al., 2002). Whenever the concentration of GLUT4 proteins is enriched at the plasma membrane, transport of glucose into the cell is augmented. In the absence of insulin, GLUT4 recycles itself within the cell and glucose uptake is reduced (Huang and Czech, 2007).

Within the brain, glucose transport into most neurons is dependent on the glucose transporter type 3 (GLUT3) (Uemura and Greenlee, 2006), with the exception of a few selected nuclei that express GLUT4, and glia and brain endothelial cells that express glucose transporter type 1 (GLUT1) (McEwen and Reagan, 2004). Since insulin is not required for GLUT1- and GLUT3-mediated glucose transport, insulin is not necessary for glucose uptake into most brain cells (for review, see Gray et al., 2014).

Interestingly, the brain is an important target for insulin action. It reaches the brain by crossing the BBB, but the brain itself also produces endogenous insulin (Blázquez et al., 2014). Insulin receptors are widely expressed within the brain (Plum et al., 2005) and its activation, mostly within the hypothalamus, regulates feeding behaviour and energy stores (Obici et al., 2002). For instance, i.c.v. injection of insulin in fasted rats increased expression of POMC mRNA (Benoit et al., 2002).

There is considerable evidence for interactions between the leptin and insulin system. *In vitro* studies showed that insulin induced *Lep* mRNA expression in adipocytes, suggesting that insulin may stimulates leptin secretion (Leroy et al., 1996). Conversely, it was suggested that leptin interferes with glucose metabolism, mediating insulin secretion and sensitivity in peripheral tissues (for review, see Morton and Schwartz, 2011).

1.1.4. Neurocircuit of feeding motivation and behaviour

Based to a large extent on the inputs from the homeostatic system regarding metabolic needs, limbic and cortical regions such as Amy and NAcc modulate the motivational aspects of feeding, through control of food-directed behaviour (Volkow et al., 2011). The functional and anatomical overlap of the homeostatic and brain circuits suggests substantial interaction (Rossi and Stuber, 2017). Indeed, such interaction between the systems is required in order to remain healthy and prevent the development of metabolic abnormalities.

1.1.4.1. Monoaminergic systems

Monoamine neurotransmitters such as dopamine (DA) and serotonin (5-HT) are highly implicated in feeding motivation and behaviour. The mesolimbic dopaminergic pathway comprises neurons in the VTA that project to the ventral striatum (NAcc), Amy, Hipp and prefrontal cortex, whereas the serotonergic pathway comprises neurons from the raphe nuclei (RN) to the thalamus, hypothalamus, basal ganglia and cortex (Charnay and Léger, 2010) (Figure 1.4).

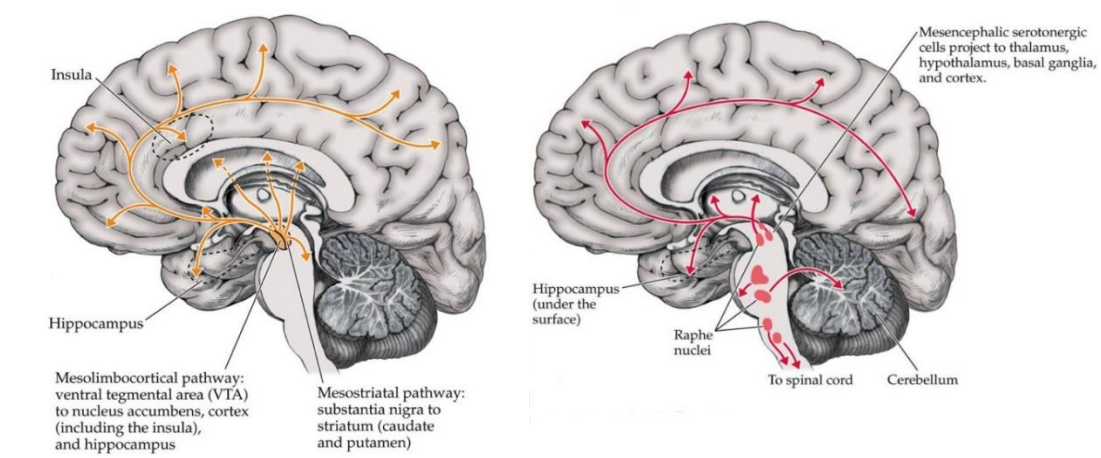

A. B.

Figure 1.4. Central dopaminergic (A) and serotonergic (B) pathways and their ascending projections, shown for human brain. Figure adapted from Kalat (1998).

1.1.4.1.1. Dopaminergic system

The role of the dopaminergic system in feeding motivation and behaviour has been well-characterised (Volkow et al., 2011; Salamone and Correa, 2012). DA modulates food intake and reward mechanisms mainly through neuronal projections from VTA to NAcc in the mesolimbic circuit. Studies showed that NAcc DA D2 receptor blocking following systemic injection of haloperidol in food-deprived rats significantly decreased lever pressing for food (Salamone et al., 1991). Moreover, mice showing chronic elevation of extracellular DA levels, by using DA transporter knockdown, had increased motivation for food reward (Cagniard et al., 2006).

In conditioned learning, potentially rewarding foods can promote eating and generate learning about a conditioned (initially neutral) stimulus associated with the reward (Dayan and Balleine, 2002). In studies using pairing sessions of conditioned cues (Pavlovian conditioned stimulus, CS) and food reinforcement (unconditioned stimulus, US), rats with lesioned NAcc were significantly impaired during the Pavlovian sessions (Parkinson et al., 1999). Interestingly, DA in the dorsal striatum

(DS) is also involved in food motivation in humans, independent of its role in NAcc. Exposure to conditioned non-palatable food cues as well as ingestion of palatable food promoted DA release in the DS that was associated with the desire to eat the food (Volkow et al., 2002; Small et al., 2003).

1.1.4.1.2. Serotonergic system

Serotonin, also known as 5-hydroxytryptamine or 5-HT, is a biogenic monoamine derivative of tryptophan, an essential amino acid obtained through diet nutrients; the pathway comprises two steps of hydroxylation and decarboxylation that occur almost instantaneously in the presence of tryptophan (Figure 1.5) (Mohammad-Zadeh et al., 2008).

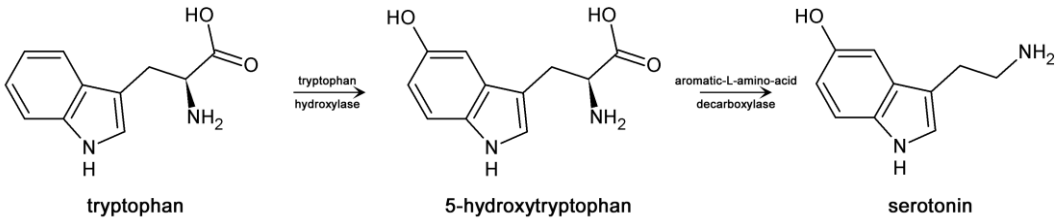

Figure 1.5. Chemical conversion of tryptophan into serotonin. Step 1. Loss of a hydroxyl group by tryptophan hydroxylase enzyme. Step 2. Loss of a carboxyl group by aromatic-L-amino-acid decarboxylase. Figure from Coelho (2014), Journal of the Brazilian Chemical Society.

5-HT is present in the brain, GI tract and blood platelets, although it is mostly linked with the enteric system (Gershon and Tack, 2007). Since 5-HT does not cross the BBB, its pool used in the nervous system must be produced within it. This neurotransmitter, with its various receptors, each of which is expressed in discrete brain regions, is the focus of much interest due to its implication in almost every physiological function (Charnay and Léger, 2010). Among its many functions, 5-HT

is accountable for the modulation of aversive stimuli and reward processing; it has been widely associated with the maintenance of mood and social behaviour, appetite and digestion, as well as with a wide range of neuropsychiatric and neurological conditions such as eating disorders and depression (Opacka-Juffry, 2008).

Serotonergic neurons are the main components of RN in the brainstem of humans and rodents. Based on its neuron clusters distribution and main projections, the serotonergic system is divided into two groups. The *rostral group*, which accounts for 85% of serotonergic neurons in the human brain, is restricted to the mesencephalon region and rostral pons (Hornung, 2003). Neurons from the rostral raphe complex within these areas project primarily to cortical areas, thalamus, hypothalamus, amygdala, basal ganglia and hippocampus. The *caudal group*, with the remaining 15% of the neurons, is confined to the caudal pons and medulla, and extends its projections to the caudal brainstem and spinal cord (for review on human serotonergic system, see Hornung, 2003).

1.1.4.1.2.1. Serotonin in the regulation of feeding

5-HT has been implicated in the regulation of satiety as well as reward behaviours. The properties of anti-serotonergic drugs used to modulate appetite have been observed since 1960 (Bergen, 1964, cited by Voigt and Fink, 2015). Increased serotonergic activity, as an effect of higher 5-HT synthesis that follows administration of tryptophan, was shown to decrease food intake (Gartner et al., 2018). Conversely, decreased serotonergic activity, due to activation of somatodendritic 5-HT1 autoreceptors for instance (Dourish et al., 1989), increases food intake. Surprisingly, low dose of the 5-HT receptor agonist 8-OH-DPAT was shown to increase food intake

in humans (Dourish et al., 1985); in pigs, tryptophan enhanced ghrelin expression and promoted feeding (Zhang et al., 2007).

The central serotonergic system has been implicated in the regulation of feeding behaviour, especially in hypothalamic regions (Lam et al., 2010). Within the hypothalamus, the effects of 5-HT are thought to be due to the modulation of the NPY peptide and melanocortin receptors (i.e. MC3R, MC4R) (Heisler et al., 2006). As previously mentioned, NPY is an essential stimulator of food intake, and projections from ARC NPY-expressing neurons to PVN are shown to mediate feeding effects of 5-HT (Kalra et al., 1991). For instance, acute and chronic systemic administration of fenfluramine, which causes 5-HT release by disrupting its vesicular storage, decreased hypothalamic *NPY* mRNA expression and NPY concentration, and resulted in anorexigenic effects in rats (Rogers et al., 1991; Choi et al., 2006). Additionally, the 5-HT antagonist methysergide increased NPY and induced feeding in rats (Dryden et al., 1995). Further, the 5-HT reuptake inhibitor sibutramine reduced appetite and induced weight loss (Luque and Rey, 2002). Although modulation of 5-HT affects feeding behaviour, anti-obesity drugs such as fenfluramine and sibutramine were removed from the market due to their adverse effects (Wharton, 2016).

1.1.4.1.2.2. Serotonin receptors

Allocated to seven different families, 5-HT receptors have structurally and pharmacologically distinct members that have been classified according to their location and function (Hoyer and Martin, 1997; Hoyer et al., 2002), as summarised in Table 1 below.

Table 1.1. 5-HT receptor subtypes and some of their functions, based on Hoyer and Martin (1997) and Hoyer et al. (2002)

Receptor type	Subtype	Function
5-HT1	5-HT1A*	mood, anxiety, appetite, thermoregulation
	5-HT1B*	mood, anxiety, aggression, addiction
	5-HT1D*	anxiety, vasoconstriction, locomotion
	5-HT1E	(unknown)
	5-HT1F	vasoconstriction, migraine
5-HT2	5-HT2A*	mood, anxiety, appetite, thermoregulation
	5-HT2B	anxiety, appetite
	5-HT2C	mood, anxiety, appetite, thermoregulation
5-HT3		anxiety, memory, gut motility
5-HT4		mood, anxiety, gut motility, appetite
5-HT5	5-HT5A	locomotion, sleep
	5-HT5B	(unknown)
5-HT6		mood, anxiety, memory
5-HT7*		mood, anxiety, thermoregulation

*Autoreceptor

Importantly, individual neurons can express more than one receptor (Berger et al., 2009). For instance, cultured rat dorsal root ganglion sensory neurons were shown to express 5-HT1B predominantly, but also 5-HT1D and 5-HT2A (Chen et al., 1998). The co-expression of 5-HT receptors may explain serotonin's pleiotropic behavioural effects and modulation of a wide variety of brain circuits (Berger et al., 2009). With the exception of the 5-HT3 receptor, a ligand-gated ion channel also known as ionotropic receptor, the other receptors are classified as metabotropic receptors; they belong to the G protein-coupled receptors (GPCRs) that couple to $G_{i/o}$ protein to inhibit the formation of cyclic adenosine monophosphate (cAMP) (Barnes and Sharp, 1999).

Some of these receptors are known as autoreceptors, such as 5-HT1A at somatodendritic locations of the RN or 5-HT1B at axon terminals (Riad et al., 2000;

Belmer and Maroteaux, 2018). They negatively regulate the excitability and firing rate of serotonergic neurons (Garcia-Garcia et al., 2014) (Figure 1.6). Other receptor subtypes such as 5-HT2C are expressed in post-synaptic regions of serotonergic, but also of non-serotonergic neurons (e.g. GABAergic neurons) (Serrats et al., 2005).

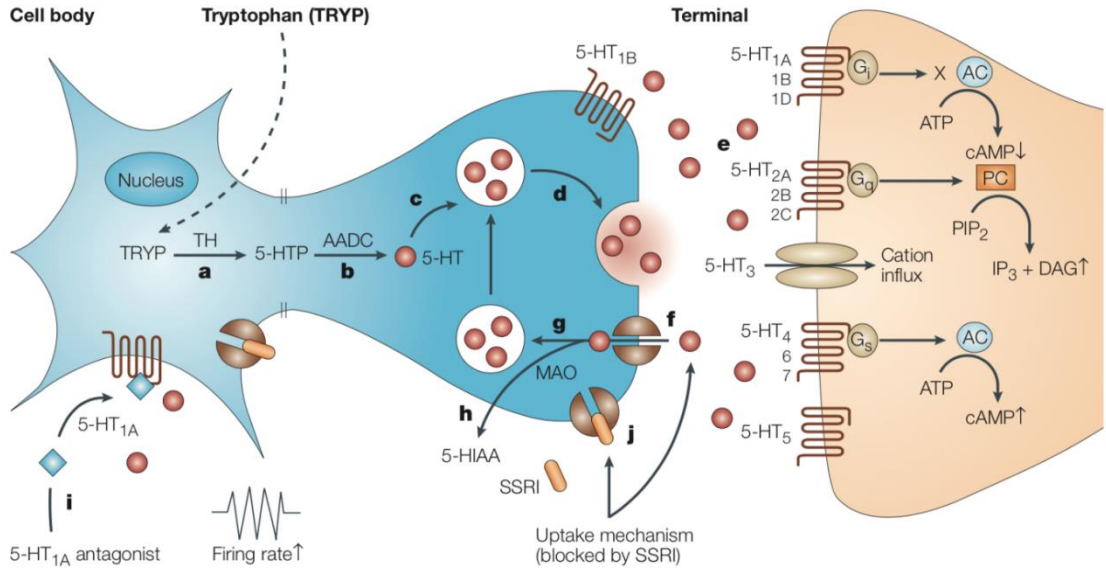

Figure 1.6. Schematic diagram depicting 5-HT synthesis, release, re-uptake and signalling. Abbreviations: TRYP, tryptophan; TH, tryptophan hydroxylase; AADC, aromatic amino acid decarboxylase; 5-HT, 5-hydroxytryptamine; 5-HIAA, 5-hydroxyindoleacetic acid; SSRIs, selective serotonin reuptake inhibitors, MAO, monoamine oxidase; ATP, adenosine triphosphate; cAMP, cyclic adenosine monophosphate; AC, adenylate cyclase; IP_3, inositol-1,4,5-trisphosphate; DAG, diacylglycerol; PIP_2, phosphatidylinositol-4,5-biphosphate. Figure reprinted from Wong et al., (2005), Nature Reviews Drug Discovery, p767, ©2005 Nature Publishing Group.

5-HT receptors, particularly 5-HT1A, 5-HT2A and 5-HT2C receptors, exert interesting effects on the regulation of food intake.

1.1.4.1.2.2.1. Serotonin 5-HT1A receptor

Encoded by the gene *HTR1A*, 5-HT1A receptors are GPCRs with seven transmembrane domains, expressed by all serotonergic neurons as autoreceptors, and by many non-serotonergic neurons as heteroreceptors (Charnay and Léger, 2010). They exert their effects through two different mechanisms: inhibition of adenylate cyclase activity and the opening of potassium (K^+) channels. In terminal areas of serotonergic innervation such as hippocampus and amygdala, 5-HT1A receptors are coupled to both effector systems. In the RN, however, they are located as presynaptic autoreceptors and coupled only to the opening of K^+ channels (Polter and Li, 2010). Whenever 5-HT concentration is enhanced, and inhibitory autoreceptors are stimulated, neurons are hyperpolarised, and firing is inhibited. Of note, 5-HT1A autoreceptors are also inhibited by dendritic 5-HT vesicular release, which occurs independently of action potentials by neuronal firing, and are induced by excitatory glutamatergic inputs to the dorsal raphe nucleus (DRN) (Belmer and Maroteaux, 2018).

Modulation of 5-HT1A has also been implicated in the regulation of food intake. In studies that used agonists of 5-HT1A receptors such as DPAT and NAN-190, these drugs stimulated feeding in rats (Williams and Dourish, 1992; Voigt et al., 2002), likely via a reduction in 5-HT release.

1.1.4.1.2.2.2. Serotonin 5-HT2A receptor

Encoded by the gene *HTR2A*, 5-HT2A receptors are also GPCRs (Guiard and Di Giovanni, 2015). Several factors are related to the signalling mechanisms that underpin the activity of this receptor and can be crucial in dictating the direction of response. Firstly, 5-HT2A receptor signalling can be regulated by its interactions with

other proteins such as β-arrestin, which plays an important role in the induction of behavioural effects such as head twitch in mice (Schmid et al., 2008); 5-HT2A can also be regulated by its homo- and hetero-dimerisation. Secondly, 5-HT2A effects can be direct or indirect and mediated via interactions with glutamatergic or GABAergic neurons (Di Giovanni, 2013). In the VTA, for instance, 5-HT2A receptors in GABAergic interneurons were shown to inhibit dopaminergic activity, presumably via the latters' inhibition of DA neurons (Doherty and Pickel, 2000), whereas 5-HT2A receptors in VTA dopaminergic neurons stimulated dopaminergic activity (Howell and Cunningham, 2015). In the DRN, GABAergic interneurons expressing 5-HT2A receptors project onto serotonergic neurons and regulate their firing activity (Guiard and Di Giovanni, 2015). It is a well-characterised receptor in the cerebral cortex; it mediates neuronal depolarisation and closing of potassium channels (Jiang et al., 2009).

5-HT2A receptors are linked not only to central physiological functions such as perception, mood, cognition and reward behaviour but also to neuropsychiatric disorders like depression and epilepsy. The central role of 5-HT2A in depressive disorders is not well-established. In the amygdala, 5-HT2A receptors are primarily located in GABAergic interneurons (Jiang et al., 2009); impaired modulation of 5-HT in the amygdala was shown to be implicated in the development of mood disorders (Cools et al., 2008).

5-HT2A receptors were also shown to modulate feeding behaviour, and appear critical for the anorectic action of GLP-1 agonists (Anderberg et al., 2017). Interestingly, reduction of hypothalamic *Htr2a* mRNA expression by liraglutide, a GLP-1 receptor agonist, reduced appetite in mice, independently of 5-HT synthesis (Nonogaki and Kaji, 2018). Earlier studies also described a relationship between 5-

HT2A polymorphism and eating disorders such as bulimia and anorexia nervosa (Ricca et al., 2002) and with food preference in humans on a stable diet (Prado-Lima et al., 2006).

1.1.4.1.2.2.3. Serotonin 5-HT2C receptor

Encoded by the gene *HTR2C*, 5-HT2C receptors (formerly 5-HT1C) are strategically localised in cortico-limbic regions implicated in the aetiology and modulation of emotional states. At post-synaptic level, its localisation is mainly in the choroid plexus, subthalamic nuclei, hypothalamus, hippocampus, periaqueductal grey matter and amygdala of rodents (Mengod et al., 1990). The receptor localisation in the mammalian brain is consistent with its potential involvement in states of anxiety and depression, since most of these brain regions belong to the main neural circuits that are implicated in emotional behaviours. However, the real understanding of the role of 5-HT2C receptors has been hampered by the lack of more selective ligands and by the very complex nature of these receptors. In the process of synthesis of 5-HT2C receptors, there may be changes in the mRNA transcription, with a consequent modification in protein synthesis and generation of up to 24 different isoforms (Gardiner and Du, 2006). As 5-HT is responsible for regulating a wide variety of behaviours, modulation of 5-HT signalling by RNA editing may be relevant to understanding mood-related psychopathologies. For instance, stress and depression states may alter mRNA editing, modifying the types of isoforms expressed in certain brain areas (Yamashita et al., 2011).

5-HT2C receptors are thought to be imperative in the relationship between food intake and energy balance. Pharmacological studies demonstrated some of the effects of 5-HT2C manipulation on the regulation of food intake, through its interactions with

ARC NPY/AgRP and POMC neurons (for review, see Voigt and Fink, 2015). For instance, 5-HT2C agonists were shown to decrease food intake (De Vry and Schreiber, 2000) and glucose consumption (Higgs et al., 2016), likely via downstream activation of MC4R (Lam et al., 2008); it also attenuated the motivation for palatable food (Ward et al., 2008). Of note, the 5-HT2C receptor agonist lorcaserin was approved as an anti-obesity drug (Brashier et al., 2014). Lorcaserin acts on POMC neurons causing α-MSH release and activation of PVN MC4R, thus decreasing appetite. Furthermore, selective activation of neurons expressing 5-HT2C receptors in NTS was shown to decrease food intake in mice; POMC-expressing neurons in both ARC and NTS were required for the reduction in food intake promoted by 5-HT2C agonists (D'Agostino et al., 2018). The 5-HT2C receptor antagonist RS-102221, on the other hand, increased feeding and promoted weight gain (Bonhaus et al., 1997). More recent studies showed that rats treated with the 5-HT2C antagonist risperidone had increased food intake and body weight, as well as decreased POMC mRNA expression in hypothalamic nuclei (Kursungoz et al., 2015).

1.1.4.1.2.3. Serotonin transporter

Encoded by the gene *SLC6A4*, serotonin transporter (SERT), situated on the presynaptic membrane of serotonergic neurons, is mainly involved in the regulation of serotonergic signalling. By taking up 5-HT from the synaptic cleft back into the pre-synaptic terminal for catabolism/re-utilisation, SERT plays an important role in the regulation of the availability of 5-HT to receptors (for review, see De Felice, 2016).

Regulation of SERT has also been shown to act on feeding behaviour. Sanders et al. (2007) demonstrated that inhibition of SERT reduced food intake and operant responding for food reward. Selective serotonin reuptake inhibitors (SSRIs) for

instance, such as sertraline, reduced food intake (Nielsen et al., 1992). The underlying mechanism is that by inhibiting 5-HT reuptake, 5-HT becomes increasingly available at the synaptic cleft thus increasing stimulation of serotonergic postsynaptic neurons.

As mentioned, the functional and anatomical overlap of homeostatic and motivation/behaviour systems suggests effective communication. For instance, LHA neurons combine VTA reward-related signals with ARC homeostatic inputs to orchestrate an adequate feeding response (Kampe et al., 2009).

In summary, regulation of energy metabolism involves the balance between feeding and EE, controlled by complex brain circuits, neurotransmitters, central and peripheral peptides. The influences of internal biological factors, as well as external environmental inputs such as stress, exert a great effect on this balance.

1.2. Stress

1.2.1. Definition

In most general terms, stress can be defined as the sum of physical and mental responses that allow living organisms to overcome difficulties caused by certain external or internal stressful stimuli (i.e. stressors). Hans Selye, who first introduced the concept of stress in his 'general adaptation syndrome' paper in 1936, described stress as "the non-specific response of the body for any demand for change". He also said that there are so many different situations involving stress that would not be possible to measure it, or even define it, thus indicating the complexity of this phenomenon (Selye, 1936).

Interestingly, stress-coping strategies might differ among those who have suffered from stressful situations in the past and those who have not. In that sense, stress develops from an interplay between external conditions (i.e. stressors) and individual variability. Stress is, therefore, a reaction which has physical, psychological, hormonal and mental components that can be developed in the face of situations that symbolise a challenge to the individual.

1.2.2. Categories

The current classification of stressors is based on two main categories: exteroceptive (e.g. electric shock) or interoceptive (e.g. stimuli through pharmacological agents) (Sawchenko et al., 2000). However, it is also critical to take into account aspects such as the nature of the stressor (e.g. metabolic, physical, psychosocial), the predictability and controllability of the stressor (Koolhaas et al.,

2011), as well as the extent of stressful challenge and the time point for evaluation of stress responses (Patchev and Patchev, 2006).

Stress can be categorised according to its duration. Thus acute stress, a physiological response to short-term stimuli (or stressors), often results in reversible physical and emotional effects. It is an adaptive response, which Selye referred to as "good stress" (Selye, 1976). Chronic stress, on the other hand, affects body and mind in a long-lasting and potentially harmful manner – a "bad stress" in Selye's words. It turns the physiological response of "good" stress into a maladaptive pathway that may verge towards the development of psychopathologies (Musazzi et al., 2017). Chronic stress was shown to be more strongly related to depression than acute stress in humans (McGonagle and Kessler, 1990) and rats (Katz et al., 1981).

1.2.3. Neurobiology of stress – HPA axis

The stress system works through a complex coordinated activation of endocrine responses from the hypothalamic-pituitary-adrenal (HPA) axis and the cardiorespiratory activity from the locus coeruleus/norepinephrine (LC/NE) autonomic sympathetic nervous system (SNS) (Chrousos, 2009).

Within seconds following stress stimulation, the catecholamines epinephrine and norepinephrine are released via activation of sympathetic preganglionic neurons in the spinal cord. The signal is then transferred to postganglionic neurons that project to peripheral organs in order to prepare the organism for the "fight-or-flight" response; it promotes, among other responses, an increase in heart rate and hepatic glucose release for enhanced active stress response (for review, see Wehrwein et al., 2016).

Different from the SNS, activation of the HPA axis occurs within minutes following stress initiation, lasting several hours (Herman et al., 2016). The first

component of the HPA axis is corticotropin-releasing hormone (CRH); dependent on neural afferents from the brainstem and limbic system, activation of CRH neurons in the parvocellular division of the PVN is followed by synthesis and release of CRH into the median eminence (Figure 1.7). Cawley et al. (2016) demonstrated that the release of CRH stimulated the transcription of the POMC gene via cAMP/protein kinase A and the secretion of POMC-related peptides such as adrenocorticotropic hormone (ACTH) from corticotropin cells of the anterior pituitary into the circulation. It is generally accepted that the CRH is an essential regulatory hormone of the HPA axis. Nevertheless, arginine vasopressin (AVP) is also considered an important regulator of ACTH secretion (Aguilera and Rabadan-Diehl, 2000); co-expressed with CRH neurons in the PVN, AVP potentiates the activity of CRH in releasing ACTH (Gillies et al., 1982). In the adrenal cortex, ACTH binds to melanocortin 2 receptors (MC2R) (Margioris and Tsatsanis, 2011), causing an increase in the synthesis of glucocorticoids.

Glucocorticoids are the end product of the HPA axis. Derived from cholesterol, GC influences the stress response through activation of the mineralocorticoid receptor (MR) and GC receptor (GR) located throughout the body (Oakley and Cidlowski, 2013). Although MR have a higher binding affinity to GC, a higher concentration of GC (e.g. following stressful stimuli) also occupy GR (Sapolsky et al., 2000, 2015); anti-inflammation and energy mobilisation are also mediated by this receptor.

Importantly, control of stress response is mediated via GC negative feedback at different levels of the HPA axis (Figure 1.7). Elevated GC acts at the PVN, where a high density of GR is found, reducing CRH synthesis and secretion from the hypothalamus, and eventually reducing the synthesis of POMC and secretion of ACTH in the anterior pituitary. The ceasing of ACTH release promotes a gradual return of

GC to baseline levels. This negative feedback loop controlled by GC is therefore vital to maintain the homeostasis of the stress system (Herman et al., 2016).

The activity of the HPA axis is also modulated by the time of the day. Under basal conditions, GC release follows a pulsatile one-hour ultradian rhythm and a predominant circadian pattern with a pronounced peak corresponding to the active phase, preparing the organism for daily activities (Fitzsimons et al., 2016). Excessive activation of the HPA axis and compromised negative feedback regulation by GC promotes a disruption in the circadian rhythm and is often associated with the development of endocrine and psychiatric disorders (Koch et al., 2017).

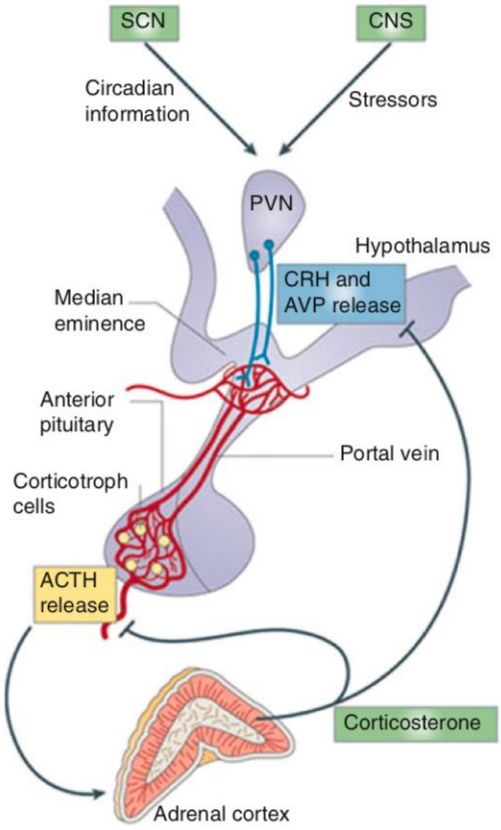

Figure 1.7. The hypothalamus-pituitary-adrenal (HPA) axis. Abbreviations: CNS, central nervous system; SCN, suprachiasmatic nucleus; PVN, paraventricular nucleus; CRH, corticotropin-releasing hormone; AVP, vasopressin, ACTH, adrenocorticotropic hormone. Figure from Lightman (2016), Research and Perspectives in Endocrine Interactions, p89, © Lightman 2016.

The efficiency of the stress response varies according to the type, intensity and duration of the stressor. Studies have suggested that physical and psychological categories of stress are recognised differently by the brain, supported by region-dependent c-*fos* expression (Dayas et al., 2001). In regards to the intensity, in general, the more severe the stressor, the more pronounced is the HPA responsiveness. For instance, daily repeated exposure to mild foot shock in rats resulted in higher HPA axis adaptation (i.e. reduction in ACTH and corticosterone) when compared to high-intensity foot shock (Rabasa et al., 2011).

Duration of stress exposure has also been shown to activate HPA axis differently. Acute stress induces a rapid release of CRH into the pituitary and an eventual inhibitory mechanism by GC. Conversely, prolonged stress exposure (i.e. chronic stress) may lead to impaired HPA axis negative feedback, characterised by GC receptor resistance (Cohen et al., 2012), adrenal hypertrophy (Ulrich-Lai et al., 2006) and insufficiency in terms of response to an ACTH challenge (Reber et al., 2007), and ultimately habituation of HPA axis response. For instance, 1h of immobilisation markedly increased ACTH and corticosterone in rats, however, this activation was reduced after the seventh immobilisation (Daviu et al., 2014). The initial elevation of corticosterone levels followed by its reduction may explain the absence of effect on corticosterone levels seen in models of chronic stress (Azzinnari et al., 2014).

Activation of the HPA axis and the SNS due to stress has also been shown to activate the immune system (Segerstrom and Miller, 2004; Chen et al., 2017), particularly in the pathophysiology of major depressive disorder (Otte et al., 2016). Markers of inflammation, e.g. interleukin-6 (IL-6) and tumour necrosis factor alpha (TNF-α), were shown to be increased in chronically stressed mice (Azzinnari et al., 2014). Once stress becomes chronic, enhanced inflammatory response concomitant

with the hyperactivity of the HPA axis and subsequent glucocorticoid resistance may lead to the development of depression (Raison et al., 2006), metabolic diseases (Pickup, 2004; Joseph and Golden, 2017) and other disorders.

In many cases, stressful stimuli can lead to considerable changes in the brain and body. Nonetheless, an organism`s adaptive (or maladaptive) response to acute or chronic stress is dependent on genetic factors, age, social support or previous stress experiences. The individual circumstances will ultimately dictate the possible susceptibility to stress-related diseases (Wood and Bhatnagar, 2014).

1.3. Stress-related mood disorders and energy metabolism

Among stress-related disorders, depression is most prevalent, estimated to affect 300 million people globally (World Health Organization, 2017). It affects people in different ways and with a varied severity. It can cause a wide variety of symptoms, such as the presence of continuously low mood or sadness, lack of motivation, feelings of anxiety and worthlessness, disturbed appetite, poor sleep, and suicidal tendencies (APA, 2013).

Stressful experiences throughout the life course are among the causes of affective disorders such as depression (Hammen, 2005). The etiological relationship between the exposure to stressful life events and the emergence of mental disorders has not been fully comprehended yet. Numerous studies have been conducted trying to elucidate the consequences of stress, within its different categories, on the brain and body, and to explain the cross-talk between these two in order to deal with these effects.

1.3.1. Stress and energy balance

1.3.1.1. Stress and feeding behaviour

In humans, chronic stress is a major risk factor for depression and related psychiatric disorders, in which changes in appetite and body weight are often a major symptom or co-occurring feature (Luppino et al., 2010). Many studies link stress with alterations in feeding behaviour (Maniam and Morris, 2012) and associations between stress and a preference for palatable, energy-rich food have been identified (Gibson, 2006; Dallman, 2010). There is growing consensus that particularly social stress

contributes to obesity (Scott, 2012), yet people respond differently to stress, and in some people stress leads to weight loss (Adam and Epel, 2007). Under conditions of perceived stress, 40% of humans eat more, and this group constitutes those who are at the upper range of normal in terms of body mass index (BMI), whilst 40% eat less (Oliver and Wardle, 1999). Nonetheless, independent of hyperphagia or hypophagia, there is an increase in the intake of highly palatable foods when individuals are subjected to stressful situations (Zellner et al., 2006).

The anatomical overlap of the HPA axis with the regulatory feeding system within the hypothalamus, considered the coordinating centre of the endocrine system, is a major indication that stress can influence feeding (Maniam and Morris, 2012). For instance, NPY/AgRP and POMC/CART neurons, centrally involved in the neuroendocrine regulation of feeding, project strongly to the PVN, containing among others CRH neurons that initiate the endocrine component of the stress response (Kalra et al., 1991; Jhanwar-Uniyal et al., 1993; Millington, 2007). Therefore, the long-lasting effects that stress has on feeding behaviour are partly due to the activation of HPA axis (Dallman et al., 2004). Secretion of GC has been shown to regulate hypothalamic *NPY* gene expression in rodents (Shimizu et al., 2008, 2010).

1.3.1.2. Stress and energy expenditure

With regards to EE, GC is also known to modulate BAT thermogenesis, nevertheless, there is a marked contrast between rodents and humans (Ramage et al., 2016). In rats, acute injection of the GR antagonist RU-486 promoted stimulation of BAT activity (Hardwick et al., 1989). When subcutaneous corticosterone was given to rats, levels of Ucp-1 content and BAT storage of lipid were suppressed in proportion to corticosterone increasing (Strack et al., 1995). A comparison between the effects of

ACTH and corticosterone on WAT browning and *Ucp-1* mRNA expression was performed; researchers observed that ACTH activated BAT and promoted WAT browning, but corticosterone counteracted these effects (Van Den Beukel et al., 2014). In humans, the effects of GC on BAT thermogenesis appear to oppose those in rodents (Figure 1.8). During hydrocortisone infusion, GC increased BAT temperature (Scotney et al., 2017). Further, the GC prednisolone increased the BAT glucose uptake, the supraclavicular temperature of the skin and the EE following cold exposure (Ramage et al., 2016). These opposing findings demonstrate one of the challenges in translating animal studies to humans, especially with regards to the effects of stress on EE and overall energy metabolism.

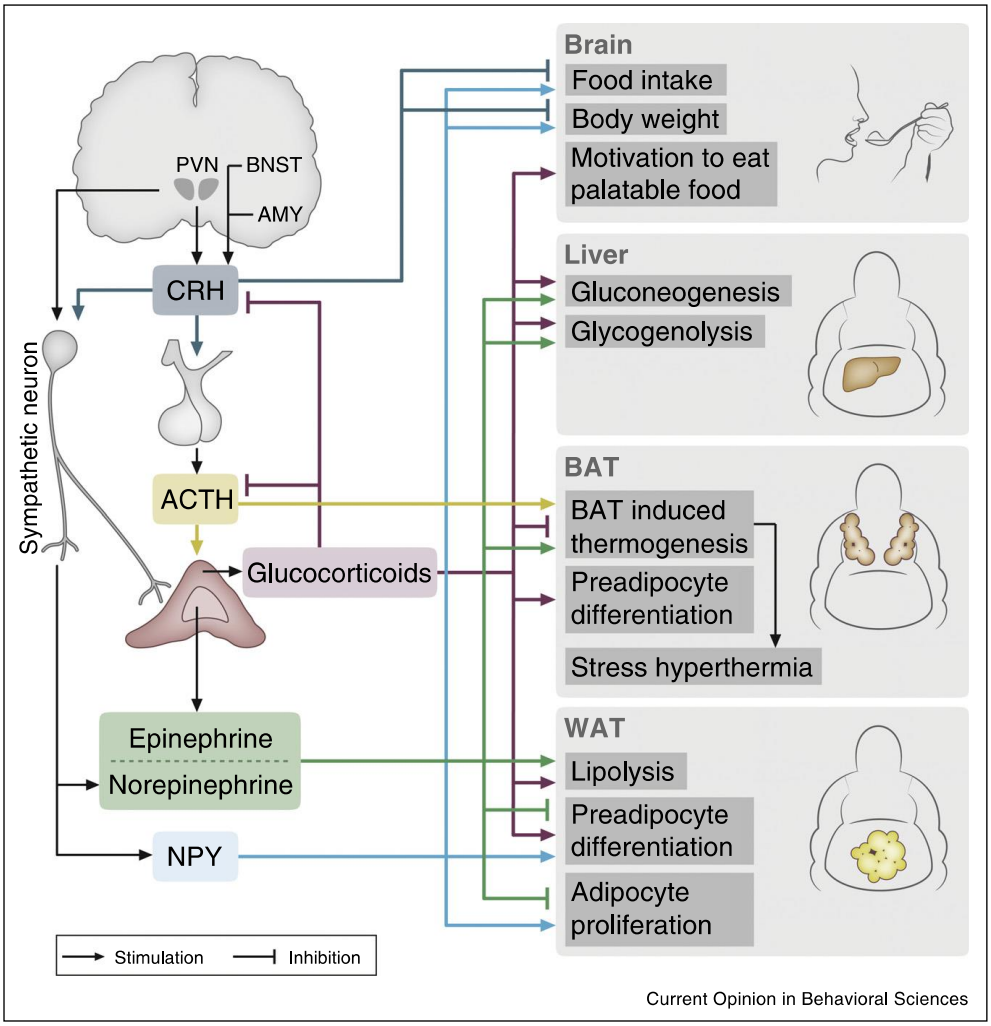

Figure 1.8. Schematic diagram depicting the different systems involved in the effects of stress on energy balance in different organs. Abbreviations: PVN, paraventricular nucleus; BSNT, bed nucleus of the stria terminalis; AMY, amygdala; CRH, corticotropin-releasing hormone; ACTH, adrenocorticotropic hormone; NPY, neuropeptide Y; BAT, brown adipose tissue; WAT, white adipose tissue. Figure from Rabasa and Dickson (2016), Current Opinion in Behavioural Sciences, p74.

Factors such as the severity and the duration of stress dictate the personal vulnerability on the regulation of feeding systems (Adam and Epel, 2007). For instance, acute and chronic stress manifest themselves differently. Perception of immediate threats (acute stress) and immediate activation of HPA axis to prepare the body for "fight-or-flight" action have often been shown to promote anorexigenic

effects (for review, see Maniscalco et al., 2012). Chronic stress, however, can have an orexigenic effect (Bartolomucci et al., 2009; Rabasa and Dickson, 2016) with consequences for body weight, and this can partially be explained by GC release (Rabasa and Dickson, 2016). GC receptors are particularly highly concentrated in visceral adipose tissue (Maniam and Morris, 2012). In the presence of insulin, cortisol promotes the accumulation of triglycerides resulting in an increase of visceral fat (Duclos et al., 2005). Chronic stress and, therefore, chronic secretion of GC might promote obesity through effects on fat accumulation. In patients with Cushing's syndrome (i.e. high levels of cortisol), obesity is a notable feature (Tiryakioglu et al., 2010).

The effects of chronic stress-induced corticosterone on food intake are not clear, and recent findings have suggested that stress-related changes in feeding behaviour might be glucocorticoid-independent (Patterson et al., 2013) (discussed in more details in Chapter 4). Interestingly, not all stress models that have reported an effect on food intake also observed elevated GC levels. For example, Pryce and colleagues reported an effect of chronic social stress on feeding behaviour (Bergamini et al., 2016) but no effect on basal plasma corticosterone (Azzinnari et al., 2014). Importantly nevertheless, Azzinnari et al. (2014) and others also reported adrenal hypertrophy, suggestive of hyperactivity of the HPA axis. Their findings suggested that the adrenal gland became insensitive to ACTH following chronic social stress, resulting in adrenal insufficiency.

It seems evident from an evolutionary point of view that chronic stressors promote the activation of mechanisms with obesogenic effects, for the reason that is considered advantageous to accumulate visceral fat and to store hepatic glycogen when life-threatening conflicts are existent in a long-lasting manner (Rabasa and Dickson,

2016). Nevertheless, this does not always happen, and it is still unknown what causes the absence of fat accumulation despite increased food intake being frequently observed. This gap in knowledge is aimed to be elucidated in the present thesis.

1.3.2. Stress and neuroendocrine regulators of feeding

Peptides such as ghrelin, a gastric hormone involved in meal initiation, and leptin, a long-term adiposity signal and also involved in meal termination, have been proposed to have a role in stress.

1.3.2.1. Stress and ghrelin

It has been proposed the peptide hormone ghrelin has a role in stress responses, nevertheless, it is still unknown whether ghrelin has a protective effect against stress-related symptoms, or, on the contrary, induces anxiogenic- and depressive-related symptoms. Ghrelin receptors are found within the PVN, although not co-localised with CRH producing neurons (Zigman et al., 2006; Cabral et al., 2012, 2016). When administered into the PVN, Wauson et al. (2015) reported that ghrelin exerted an anxiogenic effect in rats, attenuated if rats were allowed to eat immediately afterwards. A small number of studies reported the effects of different stress models on ghrelin levels in the course of the development of stress-related symptoms. Studies observed that ghrelin levels rose concurrently with ACTH levels following acute psychological stress in rats (Kristenssson et al., 2006). Furthermore, using a rodent model of post-traumatic stress disorder (PTSD), the stress-related increase in plasma ghrelin was necessary to increase Pavlovian fear learning in rats (Meyer et al., 2014). Interestingly, by systemically administrating ghrelin receptor agonist, Meyer et al. (2014) showed that the increase in fear conditioning was independent of an increase in CRH or

corticosterone (i.e. HPA activity); moreover, administration of ghrelin receptor antagonist prevented the fear learning increase caused by stress without affecting stress-related plasma corticosterone. Conversely, other studies suggested the role of HPA axis on ghrelin-induced stress-related symptoms. Peripheral administration of ghrelin increased *Crh* mRNA expression (Asakawa et al., 2001). Furthermore, intra-third-cerebroventricular and intraperitoneal (i.p.) administration of ghrelin increased anxiogenic behaviour in the elevated plus maze test in mice. Subsequent administration of CRH receptor antagonist was able to attenuate the ghrelin-induced anxiogenic effects (Asakawa et al., 2001).

In contrast to the studies above that describe the role of ghrelin in the development of stress-related symptoms, other studies reported an opposite role. Using a mouse model of acute restraint stress, Spencer et al. (2012) demonstrated that ghrelin receptor knockout (GHS-R KO) mice were more anxious compared to wild-type (WT) mice, and exhibited decreased corticosterone response. Contrary to the findings of Meyer et al. (2014), this study demonstrated that ghrelin reduced symptoms of anxiety (e.g. increased time spent in open arms in the elevated plus maze test) by stimulating HPA axis. Moreover, Lutter et al. (2008) showed that subcutaneous injection of ghrelin had antidepressant-like effects in mice exposed to social defeat stress (e.g. latency to immobility in the forced swim test). Lutter et al. (2008) further showed that antidepressant-like effects promoted by ghrelin were not present in mice lacking GHS-R.

1.3.2.2. Stress and leptin

Stress has been shown to have a regulatory effect on leptin, and studies have been conducted to elucidate the role of leptin in stress-related metabolic disorders

(Lutter and Elmquist, 2009; Chuang et al., 2010b). The adipokine leptin is thought to contribute to stress-related effects on energy metabolism through modulation of neuronal populations mostly within hypothalamic nuclei (for review, see Haleem, 2014). In rats, i.c.v. injection of leptin increased PVN *Crh* mRNA expression (Schwartz et al., 1996). Nonetheless, in mice, i.p. injection of leptin inhibited CRH release (Heiman et al., 1997). A more recent study reported that i.v. leptin infusion was able to normalise plasma levels of corticosterone in streptozotocin-diabetes mellitus rats (Morton et al., 2015). In line with this, following chronic unpredictable mild stress (CUMS), a rodent model of depression, rats displayed decreased serum leptin and *Lepr* mRNA expression in the hypothalamus; and *Lepr* mRNA expression was inversely correlated to serum corticosterone (Ge et al., 2013). Interestingly, women who had great adiposity and high plasma leptin levels when subjected to acute stress had high cardiovascular and inflammatory responsiveness to stress (Brydon, 2011).

As mentioned, stress is a major risk factor for depression and associated changes in appetite; leptin has also been associated with depressive states. Following chronic unpredictable stress (CUS), a rodent model of stress-induced anhedonia, Lu et al. (2006) also observed a reduction in leptin levels in rats; administration of leptin was able to reverse sucrose preference impairment promoted by CUS. Furthermore, following forced swim test, a rodent antidepressant screening test, administration of leptin into the hippocampus had antidepressant-like effects (Lu et al., 2006). Conversely, water-immersion restraint stress increased leptin levels in serum and adipose tissue (Konishi et al., 2006).

In humans, early-life stress, frequently accompanied by the development of depressive behaviour later in life, has been associated with increased plasma leptin

(Joung et al., 2014). Leptin has also been negatively associated with depression; patients with major depressive disorders were reported with low levels of leptin, potentially correlated with the pathogenesis of depression-linked obesity (Jow et al., 2006). Interestingly, leptin may be associated with depressive symptoms independently of body weight. Lawson et al. (2012) applied rating scales for mood disorders in order to establish the level of depression and anxiety of a patient, correlating that with leptin levels. Particularly in women, levels of leptin were inversely associated with Hamilton Rating Scales for Depression (HAM-D) and Anxiety (HAM-A), as well as with Perceived Stress scores, persisting significant after controlling for body weight or body fat (Lawson et al., 2012). A positive association between plasma leptin and DA release was also observed following stress pain challenge (Burghardt et al., 2012). Modulation of DA has an important role in the development of mood and eating disorders (Nestler and Carlezon, 2006; Johnson and Kenny, 2010).

Both ghrelin and leptin exert their effects on feeding through homeostatic and motivation/behaviour pathways. Ghrelin and its receptor GHS-R, similarly to leptin and its receptor Lepr, have been widely associated with the hypothalamic regulation of energy homeostasis, in both humans and rodents (Cummings et al., 2001; Nakazato et al., 2001; Klok et al., 2007). Nevertheless, the role of stress in the regulation of ghrelin and leptin and receptors is not fully understood. The present thesis aims to address this gap in knowledge.

1.3.2.3. Stress and insulin

Stress has been shown to alter insulin levels and glucose homeostasis; stress-induced increase in GC enhances hepatic gluconeogenesis and increases insulin

secretion (Dallman, 2010). Increased risk of type 2 diabetes is widely associated with stress-related human depression (for review, see Knol et al., 2006). For instance, use of antidepressant was associated with risk of diabetes (Rubin et al., 2010). Moreover, depression in diabetic patients was shown to worsen treatment outcomes and diabetes prognosis due to increased non-adherence to medical treatment (Goenzalz et al., 2008). Interestingly, the association between depression and impaired glucose homeostasis appears to be bidirectional (Mezuk et al., 2008; Bădescu et al., 2016). For instance, in limbic structures where insulin receptors are highly expressed (Hill et al., 1986), insulin resistance might cause neuronal damage and play a role in neuropsychiatric conditions such as depression (Cetinkalp et al., 2014; Kleinridders et al., 2015). Furthermore, it has been argued that rather than being the cause or consequence, both diabetes and depression are in fact symptoms of the same disease, namely metabolic syndrome (Anderson et al., 2001).

As previously mentioned, under conditions of perceived stress, 40% of people increase their caloric intake while 40% decrease their caloric intake (Oliver and Wardle, 1999). Those who are overweight appear to be more inclined to increase food intake and body weight under stressful periods, and the difference between anorexigenic or orexigenic effect during stressful periods may be due to peripheral insulin concentrations/functioning (Dallman, 2010). In humans, high BMI is associated with increased incidence of insulin resistance (Tatsumi et al., 2015) thus increased impaired insulin-induced glucose uptake (Ye, 2013) and, may as a consequence, also increase feeding behaviour. The role of stress in the modulation of glucose homeostasis by insulin and its implication in stress-related changes in feeding behaviour and body weight is not fully understood. The present thesis aims to address this gap in knowledge.

1.3.3. Stress and the serotonergic system

The monoamine theory of depression, which assumes a reduction in the biological activity of brain monoamines such as 5-HT and noradrenaline, facilitated the development of SSRI anti-depressant drugs. SSRI drugs are mediated via SERT and are meant to correct putatively low levels of 5-HT in depression (Rosenblatt et al., 1960; Schildkraut, 1965). Such a simplistic theory attracted criticism over the years; e.g. not all patients with depression treated with SSRI had their symptoms reversed (Bagby et al., 1997). Moreover, antidepressant effects were normally seen after 2 to 4 weeks of continuous treatment, which created a discrepancy between the immediate blockage of 5-HT reuptake and increase in synaptic 5-HT, and clinical improvement (Blier, 2001).

Currently, it is generally accepted that genetic, environmental and biological factors are implicated in depression. Although the monoamine theory of depression did not gain a long-lasting recognition, the serotonergic system remains at the core of recent neuroscience advances in the pathophysiology of depression (Fujita et al., 2017; James et al., 2017; Xu et al., 2018), and SSRIs are still widely used as antidepressants. For a review of the hypotheses that were proposed to explain the pathophysiology of depression, see Yohn et al. (2017).

Acute and chronic stress have different consequences for the serotonergic system. Studies about the effects of CRH on neuronal circuits showed that CRH afferent fibres to the DRN have contact with dendrites of both serotonergic neurons and GABAergic neurons (Homberg and Contet, 2009; Valentino et al., 2010). Acute stress was shown to activate preferably CRH1 receptors, increased the tonic inhibition of serotonergic neurons by GABAergic afferent and promoted the appearance of active coping strategy (swimming). Conversely, chronic stress (i.e. higher levels of CRH)

activated CRH2 receptors preferably and stimulated the internalisation of CRH1 receptors, increasing 5-HT release and promoting the appearance of passive coping strategies (floating, freezing) (Homberg and Contet, 2009).

The effects of stress on 5-HT and 5-HT receptors have been extensively studied for the potential involvement in the states of anxiety and depression. However, the particular effect of chronic social stress on the serotonergic system is poorly explained so far, and some questions remain to be answered. Via 5-HT receptor signalling, 5-HT is involved in the regulation of food intake (Voigt and Fink, 2015), and in the aetiology of depression (Risch et al., 2009) and anxiety (Lesch et al., 1996). Chronic psychosocial stress, an etiological risk factor for depression, causes several different alterations in the serotonergic system, with consequences for emotion, appetite, body temperature, higher cognitive functions such as memory consolidation, muscle contraction and many others (Pryce and Fuchs, 2017). Although 5-HT cell bodies are restricted to the discrete regions of the RN, their axonal projections innervate nearly every area of the mammalian brain, consequently being able to exert such wide variety of responses. The role of the stress in the modulation of the serotonergic system and its implication on feeding behaviour is not fully understood. The present thesis aims to address this gap in knowledge.

1.4. General hypotheses and aims

Animal experimental studies of stress have proved a valuable tool in elucidating how stress affects the brain and body (Patchev and Patchev, 2006), and have helped to understand how a physiological system can be driven to develop stress-related pathologies. Both behavioural and metabolic effects of stress have been observed in rodent models (Weiss et al., 2004; Pryce et al., 2005; Azzinnari et al., 2014), and comprehending the causal effects of environmental manipulations relevant to human endocrine and psycho-pathologies has the potential to further explain the relationship between stress, feeding and metabolism.

The overall aim of this thesis is to investigate the effects of chronic social stress on food intake and energy metabolism, as well as some of the main neural and hormonal regulatory systems underlying these fundamental physiological processes, in mice. In humans, chronic stress is a major risk factor for depression and related psychiatric disorders, in which changes in appetite and body weight are often a major symptom or co-occurring feature. Despite the importance of these associations, the causal pathways underlying them are complex and currently poorly understood, and animal studies are essential to increase the understanding.

In an established mouse model of chronic social stress, it was shown that stress led to increased feeding in the absence of change in body weight (Bergamini et al., 2016). The causal factors underlying the increase in food consumption and the dissociation between feeding and body weight are not well-defined. The present thesis aims to investigate some candidate mechanisms underlying these altered states. The

candidate mechanisms of interest are changes in EE, BAT activity, peripheral and central appetite hormone signalling, and peripheral glucose metabolism.

It is hypothesised that chronic social stress increases signalling of appetite-enhancing hormones as well as decreases signalling of appetite-suppressing hormones, leading to an increase in feeding behaviour. It is hypothesised that stressed animals have increased EE and adaptive thermogenesis and that this is associated with the previously observed lack of body weight gain. Given that increased food intake can be attributed to stress-induced changes in the processing of the reward valuation of food in addition to homeostatic appetite control, and given that 5-HT is a modulator of homeostatic appetite control, reward processing and stress-related pathologies such as depression, it is hypothesised that chronic social stress will affect the binding and expression of 5-HT receptors in the brain regions important for reward valuation.

CHAPTER 2

The chronic social stress mouse model

2.1. Theoretical background

2.1.1. Animal models for translational research into human pathophysiology

Animal modelling for the translational study of human disease has been proven to be a valuable tool in the process of characterisation of pathophysiology (Denayer et al., 2014; Vandamme, 2014). In providing a level of environmental and genetic manipulation that is not achievable in humans, animal experimental studies have become essential for the understanding of the biological basis of several different human disorders, including neuropsychiatric illnesses (Snyder et al., 2011; Chesselet and Carmichael, 2012). Although it is not possible to fully comprehend human physiology by means of laboratory animal research, homology/analogy between animal and human are sufficient for translational research; this combined with the availability of molecular research tools render the mouse as the foremost mammalian model for human health and disease studies (Nguyen and Xu, 2008).

In Great Britain, according to Home Office figures, in the year of 2016, 72.8% of total laboratory procedures involving animals were developed using mouse (*Mus musculus*), with the remaining 27.2% distributed among zebrafish (*Danio rerio, 11.1%*), rat (*Rattus novergicus, 6.3%*), domestic fowl (*Galilus domesticus, 3.6%*), guinea-pig (*Cavia porcellus, 0.7%)* and others (5.5%) (UK Home Office, 2017). Genetic manipulation techniques have developed immensely in the last few decades and have allowed geneticists to create a great variability of disease models to be used in the research field (Vandamme, 2014), of great importance to scientific progress.

2.1.2. Animal welfare

According to the Animal Welfare Act of 16 December 2005, Article 3, Section C (Appendix 1), an animal experiment is used with the aim of:

1) testing a scientific assumption

2) observing the effect of a particular measure in the animal;

3) testing a substance;

4) obtaining or testing cells, organs or bodily fluids, except when this is in the context of agricultural production, diagnostic or curative operations on the animal or for determining the health status of animal populations;

5) teaching or training.

(Swiss Confederation, 2011)

An experiment that does not meet the above criteria should not be continued.

2.1.3. The principle of 3Rs for animal experimentation ethics

For the purpose of protecting the dignity and welfare of animals, a Swiss Federation Act that prescribes rules of conduct in dealing with and handling animals (Appendix 1 – Animal Welfare Act) was established. As part of the national and international legislation which regulates animal laboratory experimentation, the principle of 3Rs (Replacement, Refinement and Reduction, described below), developed in 1959 by Willian Russel and Rex Burch (Russell and Burch, 1959, cited by Flecknell, 2002), is taken as synonym of high quality science research; a unifying concept and opportunity for achievement of scientific, economic and humanitarian benefits (NC3Rs, 2017).

Replacement – of the use of animals for other methods, such as computer models etc, states that animal models for research should be replaced with non-animal

alternatives whenever possible. Of the 3Rs, although it happens in infrequent circumstances, Replacement is the most frequently contemplated, not only replacement for *in vitro* models, but for which animal. In that sense, one of the great challenges of animal research still remains in the identification and selection of which animal model is the most appropriate for the respective study, hence database searches and consultation of literature is exceptionally required for consideration of alternatives (Wood and Hart, 2007).

Refinement – of methodological procedures, which aims at minimising unnecessary harm to the animal and improving its welfare, being applied to all aspects of experiments, from husbandry until the final sampling acquisition.

Reduction – of the number of animals used per experiment, either by obtaining the same results using less animals or by obtaining more information about the same number of animals. Research should employ the minimum suitable sample size, calculated using power analysis associated with statistical inferences based on the p-value and also effect sizes accompanied by confidence intervals (Sneddon et al., 2017).

The principle of 3Rs establishes the accepted standards for humane experimentation on animals, which shall be applied to every aspect of animal experimentation for achievement of excellence and distinction in any laboratorial research.

2.1.4. Validity criteria of animal models

Validity criteria have become highly relevant for assessment of animal models used in research (Bakshi and Kalin, 2002; Belzung and Lemoine, 2011). Elaborated by Willner in 1984, the multidimensional approach of evaluating a model in respect of its constructive, face and predictive validity were firstly proposed in relation to animal

models of depression. The criterion of *construct validity* sets the theoretical rationale behind the model. The criterion of *face validity* corresponds to observable behaviour and biological outcome of a model, looking for similarities between the animal model and the condition being modelled. Lastly, the criterion of *predictive validity* contemplates the ability of the animal model to identify therapeutic treatments for the disease and, in the case of depression, refers to selective responsiveness to antidepressants (Willner, 1984). These criteria have been recently revised and three further validity criteria have been added: *homological validity*, for choice of adequate species and strains; *pathogenic validity*, which takes into consideration the manipulation of the organism during developmental and adulthood periods for acquisition of pathological characteristics; and *mechanistic validity*, which identifies similarities of cognitive and biological mechanisms in both humans and animals (Belzung and Lemoine, 2011).

In addition to validity criteria, the endophenotype methodology, based on the modelling of discrete symptoms rather than the absolute illness, has contributed to the advancement in development of animal models for research. The endophenotype methodology is based on the study of a set of behavioural and physiological features of a basic process that are manifested in a disorder (Bakshi and Kalin, 2002). Such methodology has allowed the development of animal models with construct and predictive validity.

2.1.5. Animal models of stress

Experimental animal models of stress are used for the study of behavioural and biological reactions to the different forms of environmental threats, exploiting assorted circumstances within the laboratory boundaries. Various experimental models have

been formulated in order to study the associations between stress and its effects on the brain and body, by creating sophisticated methods for measuring the many components of stress (Lester et al., 1994; Torres and Nowson, 2007).

For experimental animals, depending on the stressor, a wide variety of responses can be generated. The monitoring of these stress responses is based on behavioural, physiological, metabolic, neurochemical, endocrine and immunological end points promoted by those models. Stress manipulations currently used include electric footshock, restraint, tail suspension, or forced swim test, that bear little resemblance to the challenges that animals commonly face in a natural environment. These stressors are solely physical and offer little validity compared to psychosocial stressors of relevance to humans (Tamashiro et al., 2005). Stress paradigms that evolve around the establishment of social hierarchy among individuals of a colony/society, on the other hand, will evoke behavioural and physiological responses of greater similarity to a more naturalistic ecosystem. Comprehending the causal effects of environmental manipulations relevant to human pathologies has the potential to help us gain a better understanding of the relationship between stress and stress-related pathological behaviours.

2.1.5.1. Social stress paradigms – mood and anxiety disorders

Social stress can be defined as social interactions that threatens an individual's well-being (Lazarus and Folkman, 1984, cited by Schneiderman et al., 2008). It can emerge in a number of different circumstances, and since many animal species, including humans, spend most of their time interacting with conspecifics (Koolhaas et al., 2017) and developing social hierarchies (Ely and Henry, 1978), such conditions are recurrent. Among the commonly used animal models of stress, the model of

psychosocial stress is considered to be one of the most severe stressors in terms of neuroendocrine stimulation (Koolhaas et al., 1997); numerous neuropeptide-secreting systems are activated by the brain, such as the HPA and the SNS systems (de Kloet et al., 2005).

In humans, stress is the most common risk factor for the development of associated numerous psychiatric disorders, such as mood and anxiety disorders (APA, 2013). With regards to depressive psychopathologies, some models of stress have been developed based on the variation of both physical and social environment, such as the chronic unpredictable mild stress (CUMS), whilst others are based on the variation of the social environment specifically (Razzoli et al., 2014). In the case of CUMS, the most widely-used stressor, several physical and social stressors are presented on an unpredictable schedule (Willner, 2017). Among the models based on psychosocial stressors only, the majority are dyadic-based (e.g. resident-intruder paradigms) and result in classification of subjects into dominant or submissive, according to social status, and winner or loser, according to the encounter outcome (Koolhaas et al., 2013; Razzoli et al., 2014).

In mice and other rodents, studies based on social stress are often gender-specific. Aggressive behaviour towards conspecifics and dominance hierarchy in dyadic encounters are more visually present in males due to their territorial characteristics (Palanza et al., 1993, 2001). Whenever grouped together, they can trigger a series of varied behaviours (Blanchard et al., 2001). In contrast, female rodents develop very low or no aggression when grouped together with other females, and only express detectable social hierarchy when reproductively active (Palanza et al., 1993) or during maternal care (i.e. lactation) (Vom Saal et al., 1995). Nevertheless, behavioural findings show differential effects of isolation and grouping in both female

and male rodents (Palanza et al., 2001), with female rats showing higher levels of corticosterone when individually-housed than when group-housed (Brown and Grunberg, 1995). Clear differentiation between social paradigms is therefore essential.

2.2. The model

2.2.1. Chronic social defeat stress

2.2.1.1. Rationale

Chronic social defeat stress, CSDS or simply CSS[1] (acronyms varying according to duration of stress protocol), is a well-established experimental mouse model of prolonged psychosocial stress that involves persistent exposure to social stress and results in behavioural and neurobiological changes analogous to those that are seen in human stress-related neuropsychiatric disorders, such as reduced social interaction and altered expression of genes in pathways of inflammation in the brain (Pryce and Seifritz, 2011; Azzinnari et al., 2014; Pryce et al., 2014; Bergamini et al., 2016). Protecting territory against invaders is a predictable behaviour of animal nature and this resident-intruder paradigm of male rodents has been broadly used on stress-related research as a tool for the better understanding of biological mechanisms and pathways of stress-related psychopathologies (Koolhaas et al., 2013; Wei et al., 2014).

Chronic social stress in combination with relevant readouts can constitute an animal model of anxiety/depression. It has been proposed to be distinguished from other environmental stressors by its ability to repeatedly activate the HPA axis over repeated social confrontations (Golden et al., 2011) and to promote changes in markers of anhedonic-like behaviours (e.g. deficit in evaluation of reward as seen by limited sucrose-seeking behaviour) (Riga et al., 2015). Moreover, it is also characterised by development of adaptive behaviours such as social avoidance that can only be reversed

[1] CSS applies specifically to the chronic social stress protocol that I applied in my Thesis.

by chronic antidepressant treatments (Kudryavtseva et al., 1991; Berton et al., 2006; Tsankova et al., 2006).

Chronic social defeat in mice was first described in 1991 by Kudryavtseva and colleagues, in which a series of behavioural outcomes, somatic symptoms and effects of chronic antidepressant (imipramine) treatment were examined following 20 consecutive days of social defeat and otherwise permanent sensory contact. Development of pathological forms of behaviour similar to depressive state was observed in this model, in parallel with development of somatic symptoms (e.g. weight loss) coincident with human depression (Kudryavtseva et al., 1991). Although one of the first papers published on social defeat stress model in mice was in 1991, social conflicts in mice have already been described since 1984.

A modified paradigm was established by Berton et al. (2006) with an abbreviated duration of stress exposure but still with continuous and unavoidable psychological stress from 24h of sensory interaction through a perforated divider in a shared home cage. In 2011, the standardized protocol was presented in details by Golden et al. (2011). The present study is based on a further development of the paradigm introduced by Kudryavtseva et al. (1991) (discussed subsequently).

2.2.1.2. Mouse strain

Regarding mouse strains, C57BL/6 (BL/6) is the most widely used inbred strain in social defeat models (Golden et al., 2011; Huang et al., 2013; Iñiguez et al., 2014, 2016), as well as several others research areas such as developmental biology, diabetes and obesity, genetics and immunology. BL/6 was the inbred strain of choice for this study, along with outbred CD-1 as the aggressive dominant mice.

2.2.1.3. Housing conditions

Prior to CSS manipulation, CSS and control (CON) mice were caged in brother pairs in standard in-house conditions (20-22°C temperature, 50-60% humidity). Mice were provided with tissue bedding and an igloo in the home cage as a retreat and for sleeping. Food and water were provided ad libitum, unless required otherwise (i.e. glucose tolerance test). Environmental conditions were controlled throughout.

During the CSS manipulation, CON mice remained in littermate pairs unless single caging was absolutely necessary for experimental purposes (i.e. Experiments B and C, as described elsewhere) and CSS mice were housed with CD-1 mice in a rota system.

2.2.1.4. Prior to CSS manipulation

A. 5 days prior to day 1 of CSS, BL/6 mice were handled daily for five minutes for familiarisation and acclimatisation of animals. Animal handling was carried out by taking the entire mouse in the hands and not by picking it up by the tail, aiming at reducing/avoiding any non-experimental stress.
B. Body weight was measured daily for baseline data and for allocation of mice to CSS or CON groups, by counterbalancing on this measure.
C. Motor activity (MA) test was also carried out prior to CSS manipulation for allocation of mice to CSS or CON groups.
D. CD-1 screening was conducted for identification of those that were aggressive, with latency to attack < 60s and total duration of attacks > 15s in 5 minutes.
E. Prior to day 1 of CSS manipulation, the CD-1 mice which were demonstrated to be aggressive (Golden et al., 2011) were placed in one compartment of a cage (1284L Eurostandard Type II L, Indulab, Gams, Switzerland), containing

a longitudinal divider made from transparent Plexiglas and perforated with multiple holes for sensory interactions. Care was taken to ensure the divider was firmly secure in order to prevent mice from escaping their overnight compartments.

2.2.1.5. CSS manipulation

The CSS manipulation used in the present study was adapted from that of Golden et al. (2011) (Azzinnari et al., 2014). This standard protocol for CSS was conducted by caging together a 10-12 weeks-old BL/6 mouse with a more aggressive mouse (CD-1) for a period of 15 consecutive days for a maximum 10 minutes per day or until a cumulative total of 60s of physical attack had occurred, subjecting therefore BL/6 mice to repeated bouts of social subordination (Figure 2.1). Social stress sessions were conducted under reversed light-dark cycle (07:00-19:00 h lights OFF), between 12:00-15:00 h.

On day 1, each CSS BL/6 mouse was taken out from its home cage, weighed and placed individually in the compartment of a CD-1 mouse. Physical attacks were observed and timed throughout. Mice remained together for the period of 10 minutes or until physical attacks summed up to 60s. Moreover, it was also scored for each stress session whether or not the CSS mouse fought back when attacked by the CD-1 mouse and whether or not the CD-1 mouse attacked CSS mouse. Frequency of behaviours per session was not scored, simply its presence or absence. Following the stress session, the CSS mouse was checked for bite wounds with a tissue paper and returned to the compartment where defeat occurred, whilst the CD-1 mouse was transferred to the other compartment, allowing continuous olfactory, visual and auditory contact

during the following 24 h. Resident-intruder pairs with behavioural observation and timing of attack durations were conducted with two cages at a time.

On day 2, a rotation of mice pairings was conducted, so that each CSS mouse was confronted with a novel CD-1 mouse and vice versa. This rotation was conducted throughout the 15 days of CSS manipulation. Control mice, as stated previously, remained in littermate pairs (separated by a divider or not), and were handled and weighed daily.

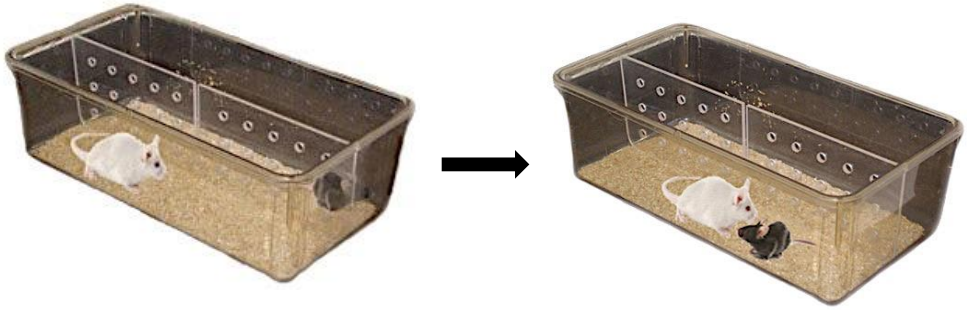

Figure 2.1. Mouse chronic social stress (CSS) mouse paradigm. BL/6 mouse is placed in the opposite compartment, where aggressor CD-1 is located, for 15 consecutive days (maximum 10 minutes per day or until a cumulative total of 60s of physical attack had occurred).

2.2.1.6. Protocol refinements

In the absence of any observation of the defeat period, there could be several minutes of biting, appearance of open bite wounds and eventually indispensable removal of animals from experiment, as reported to be common in the standard chronic social stress protocol (Golden et al., 2011). These factors somewhat impact on its aetiological validity as an emotional psychosocial stressor. Therefore, the protocol used in this study aimed to eliminate stress not of a psychosocial or emotional nature, including reducing physical injury to an absolute minimum (Azzinnari et al., 2014).

Refinements are described below:

A. Continuous observation of BL/6 and CD-1 throughout timing of defeat (10min/day). It allowed a more in-depth behaviour analysis when in face of the defeat;

B. Timing of attack periods. Mice were immediately separated when the cumulative time of attack reached 60s. In this case, attack was defined as chasing, boxing and biting;

C. Trimming of lower CD-1 mice incisors, which grew continuously, to markedly reduce surface wounds and completely eliminate deep bite wounds. Every 3 days, under brief 3% isoflurane anaesthesia, the lower incisors of CD-1 mice were trimmed using rodent tooth-cutting forceps (Precision Surgical International, USA) to remove the sharp edges. Food pellets were cut in pieces and provided to CD-1 mice so that the teeth blunting did not inhibit their feeding, thus avoiding significant weight loss.

Discontinuation of an experiment was established based on the following criteria:

A. Bite wound in chronic social defeat;

B. General loss of weight and physical condition.

2.3. Methodological framework

Experiment A (CON=12, CSS=12) investigated the effects of 15-day CSS on body weight, glucose tolerance, as well as motor activity test. Physiological valuations were also assessed. Experiment B (CON=8, CSS=10) investigated the effects of 15-day CSS on food intake, body weight and it also aimed at investigating the effects of CSS on indirect calorimetry. Physiological valuations were likewise assessed. However, due to methodological errors (i.e. inappropriate system calibration), metabolic studies in the calorimetry system had to be repeated. Therefore, Experiment C (CON=12, CSS=12) also investigated the effects of 15-day CSS on indirect calorimetry, in addition to body weight and food intake. Behavioural and physiological assessments were also conducted. Physiological samples collected were: plasma, interscapular brown adipose tissue (iBAT), epididimal white adipose tissue (eWAT), brain, stomach, and pancreas. Experimental designs are summarized in Figure 2.2 below and detailed subsequently.

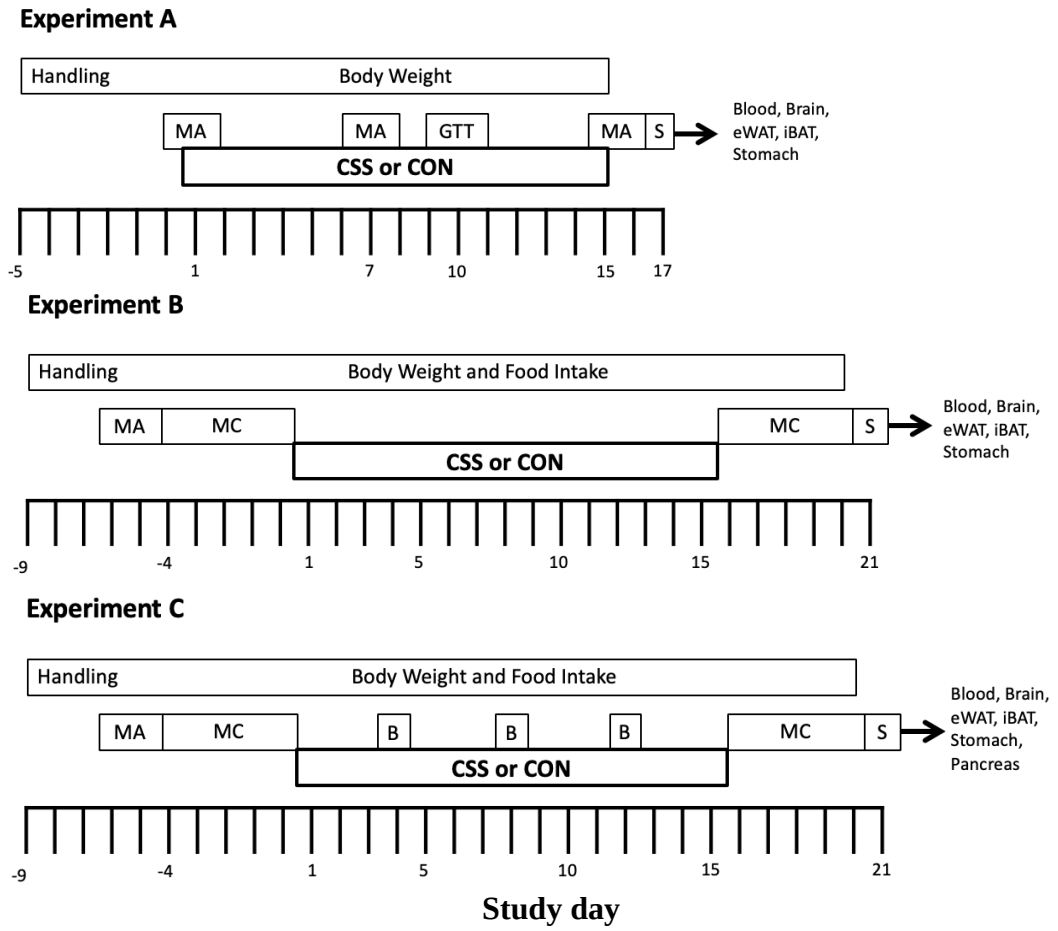

Figure 2.2. Experimental designs. Three cohorts of mice were exposed to chronic social stress (CSS) or control handling (CON) on days 1-15 and studied in three different experiments. Mice were handled and a motor activity test (MA) was conducted prior to experiments for balanced allocation of mice to CSS or CON groups. Body weight (Experiment A, B and C) and food intake (Experiment B and C) were monitored daily. Experiment A: Motor activity test was conducted on days 1, 7 and 15. A glucose tolerance test (GTT) was conducted on day 10 following 14h fasting. Mice were sacrificed and physiological samples (S) were collected on day 17. Experiment B: Mice were placed in metabolic cages (MC) for calorimetric data collection on day -4 for 5 days for baseline data and on days 16-20 for post-CSS data collection. Mice were sacrificed, and physiological samples were collected on day 21. Experiment C: Mice were placed in metabolic cages for calorimetric data collection on day -4 for 5 days for baseline data and on days 16-20 for post-CSS data collection. Behaviours (B) were scored on each of CSS/CON days 4, 8 and 12. Mice were sacrificed and physiological samples were collected on day 21. Abbreviations: eWAT, epididymal white adipose tissue; iBAT, interscapular brown adipose tissue.

2.4. Research considerations

2.4.1. Animal training

Animal training was completed (Introductory Course in Laboratory Animal Science – LTK Module 1 and Anatomy and Necropsy – Module 7E) according to the requirements of the Federation of Swiss Cantonal Veterinary Officers at Vetsuisse-Faculty, University of Zurich.

2.4.2. Health and safety

The majority of the risks to this project were related to laboratory procedures. For that purpose, detailed risk assessment forms for each experimental procedure were filled out to ensure fully understanding and management of the risks. The *in vivo* work carried out in Zurich presented some risks associated with animal handling. To ensure a safe working environment, personal protective equipment was used when appropriate, both at the University of Zurich and University of Roehampton.

2.4.3 Transport of samples

Import of non-infectious murine laboratory research samples from Switzerland to United Kingdom did not require any permit. Samples were sent via Dangerous Goods International (DGI) courier, authorised to transport and comply with packaging and health and safety regulations (Federal Express, FE) from Zurich to London, under FE's regulations and risk assessment.

CHAPTER 3

Effects of chronic social stress on energy metabolism

3.1. Introduction

3.1.1. Stress and feeding behaviour

Energy metabolism is essential for the maintenance of cell and organ functioning and individual survival. An organism's energy needs are subject to environmental factors, including social stress, which is known to affect body energy metabolism and more specifically feeding behaviour, body weight and EE. Previous studies on the effects of chronic social stress on feeding and EE have been conducted. Interestingly, the effects of stress on feeding behaviour appear to be different between mice and rats. Most of the studies performed in rats report decreases in food intake and body weight gain (Meerlo et al., 1996; Haller et al., 1999; Becker et al., 2008; Razzoli et al., 2009; Iio et al., 2012, 2014; Olivares et al., 2012; Ahnaou and Drinkenburg, 2016; Liu et al., 2017). In mice, the effects of stress on feeding behaviour are less consistent. Several studies report increased feeding without effects on body weight (Moles et al., 2006; Lutter et al., 2008; Sanghez et al., 2013; Bergamini et al., 2016), but increased feeding concomitant with increased body weight gain was also frequently observed (Chuang, et al., 2010a,b; Razzoli et al., 2010; Razzoli et al., 2011a,b; Patterson et al., 2013; Goto et al., 2014). The stress protocols associated with a HFD appears to play an essential role in determining body weight gain and fat content of mice under stressful circumstances. Chuang et al. (2010a) observed that control mice given HFD had higher body weight gain and more body fat than mice given a standard diet, as anticipated. Interestingly, stressed mice given HFD had significantly less body fat compared to control mice on HFD diet. Similarly, Balsevich

et al. (2014) reported significantly decreased body weight and body fat in stressed mice on HFD diet than control on HFD.

In mouse models of social stress similar to the one studied in this thesis, studies have observed increased calorie intake and increased body weight gain in stressed mice (Patterson et al., 2013). In the chronic social stress model (from Pryce laboratory) used in this thesis, increased calorie intake in the absence of an effect on body weight was observed (Bergamini et al., 2016). This is in agreement with several other studies previously mentioned.

3.1.2. Stress and energy expenditure

There is limited understanding of the neurobiological mechanisms that underpin the relationship between stress and energy balance. The reason for the absence of an effect on body weight despite an increase in calorie intake seen in this stress model is yet to be determined. A potential explanation could be due to changes in energy metabolism, more specifically, increased EE induced by chronic social stress.

Although present, studies on the effects of stress on EE using indirect calorimetry are scarce. Moles et al. (2006) reported increased food intake in stressed mice compared to the control mice, and higher body weight in subordinate mice compared with dominant mice. Increased EE was only observed in dominant mice, confirming the lack of body weight gain (Moles et al., 2006). Sanghez et al. (2013) observed increased feeding behaviour and similar body weight gain in subordinate mice compared to control mice, and a combination of increased feeding behaviour, decreased body weight gain and increased EE in dominant mice. More recently, Coccurello et al. (2017) reported decreased calorie intake and body weight at the end

of the stress period compared to the beginning of the stress period in stressed mice fed a standard diet; control mice maintained calorie intake and body weight over time. Compared to control mice, stressed mice had increased EE and respiratory quotient (i.e. increased usage of carbohydrate as energy fuel). Decreased body weight despite increased calorie intake over time was observed in stressed mice fed a high palatable diet compared to control mice, in combination with increased EE but decreased respiratory quotient (Coccurello et al., 2017). The increase in EE observed in the studies mentioned above indicates that stress leads to an increase in energy demand in comparison to control animals. Respiratory quotients appear to change according to dietary fat content, as observed by Coccurello et al. (2017). Further calorimetry studies are necessary to obtain a clear understanding of the energetic demands of a system under stressful conditions.

As previously mentioned, EE is also determined by BAT activity and its thermogenic uncoupling protein 1 (Ucp-1) located in the BAT. Since the discovery of *Ucp-1* in adult humans in 2009 (Cypess et al., 2009), it has received considerable attention as a potential target to treat obesity, given its ability to increase EE when activated. Under physiological conditions of low adaptive thermogenesis, it was reported that chronic social stress stimulated BAT activation and thermogenesis in mice, associated with increased resistance to diet-induced obesity despite the existence of hyperphagia (Razzoli et al., 2016). Stress responding in terms of activation of the SNS and acute increase in glucocorticoids levels were shown to suppress both *Ucp-1* and respiration in rodents but to enhance *Ucp-1* in humans (Ramage et al., 2016). In contrast, chronic increase in glucocorticoid levels were shown to suppress BAT activity and result in obesity (Ramage et al., 2016; Leitner et al., 2017).

Measuring body weight and food intake changes in this study was the first stage for a better understanding of the metabolic effects of CSS. Feeding efficiency was calculated as the ratio of body weight to energy intake. Assessment of EE through indirect calorimetry and evaluation of BAT thermogenesis was followed. Calorimetric techniques for assessment of EE and fuel selection are described below.

As previously mentioned, TEE could also be increased by physical activity; this could have been measured through beam breaks in the same indirect calorimetry system. Nevertheless, since the calorimetry system we used could not do such analysis, measurements of activity were performed in the home cage.

3.1.2.1. Calorimetry

Calorimetry is the discipline in which the energy of a system (i.e. organism) in terms of the heat exchange of this system with its surroundings is measured. Assessment of energy demands using calorimetry originates back to the research of Lavoisier and Laplace in the 1700s (Lavoisier 1783, cited by Schoffelen and Plasqui, 2018). There are currently two different calorimetric approaches commonly used for measuring EE in mammals: direct *versus* indirect calorimetry (Levine, 2005; Tschöp et al., 2011) (Figure 3.1).

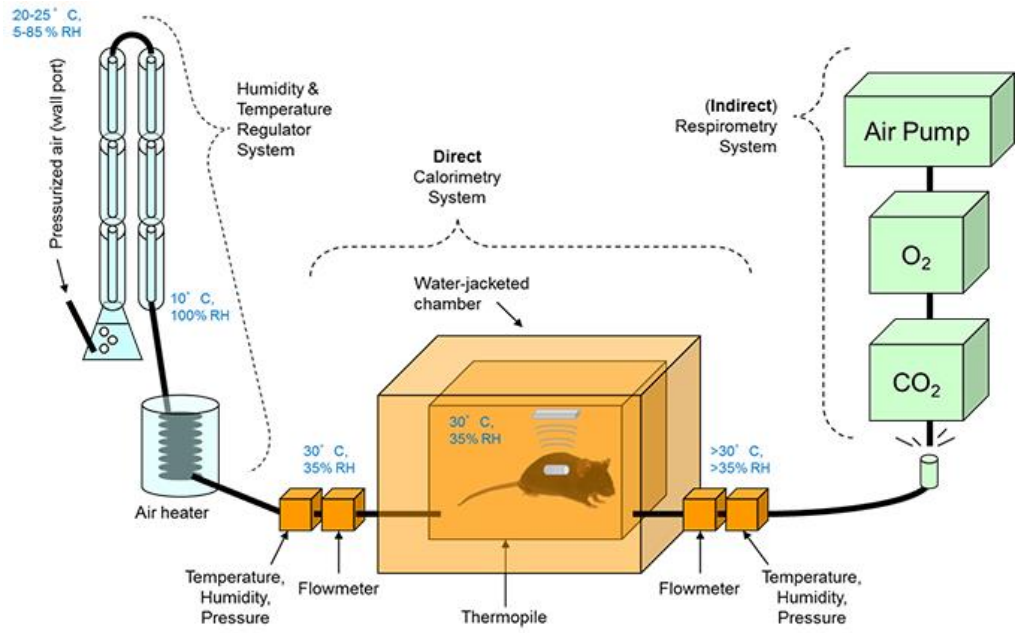

Figure 3.1. Diagram of direct calorimetry and closed-circuit indirect respirometry systems. Rodent is placed inside the calorimeter chamber for direct or indirect measurement of heat production. Humidity and temperature regulator systems calculate body metabolism directly through changes in the water temperature. Figure from Grobe Lab U Iowa, n.d.

Direct calorimetry is based on the direct measurement of body heat production in a water-enclosed calorimeter chamber. In addition to the technical difficulties of direct calorimetry in terms of measuring small amounts of heat and the requirement for numerous control steps to ensure appropriate system functioning, commercial equipment is not currently available for rodent experiments. Furthermore, it does not take into account the organism's heat storage throughout the test period; consequently, if body temperature would increase, the system would not compute for that increase and would, therefore, lead to a rather large error in the calculation of metabolic rate (Tschöp et al., 2011; Speakman, 2013; Lam and Ravussin, 2016).

Indirect calorimetry estimates the heat energy used by an organism based on gas exchange measurements – oxygen (O_2) consumption and carbon dioxide (CO_2) production. Relative to direct calorimetry, it requires a simple and inexpensive system,

and can be performed using different approaches. *Doubly-labelled water* (DLW), for instance, calculates EE by labelling the body with isotopes of oxygen (^{18}O) and hydrogen (^{2}H) and by evaluating elimination rate of these isotopes via water excretion (through the sampling of saliva, urine and blood) and respiration (Westerterp, 2017). The challenges from this method include the difficulty of injecting the isotopes into small animals, the washout speed from animals with high metabolic rate, and the limited body water for analysis with isotope ratio mass spectrometry (Speakman, 2013). Furthermore, a significant drawback is the inevitable stress caused by blood sampling. *Open-circuit system*, the most commonly used method for analysis of EE and the method of choice for this study, consists of placing the animal inside a metabolic cage that is connected to a flow of fresh air for measurements of the amount of O_2 consumed and CO_2 produced. Respiratory Exchange Ratio (RER) and Energy Expenditure (EE) are subsequently calculated by the values obtained (Tschöp et al., 2011; Gupta et al., 2017).

3.1.2.2. Assessment of energy expenditure and fuel selection

Oxidation of the three major energy substrates, namely carbohydrates, lipids and proteins, requires consumption of O_2 and production of CO_2 and water, with energy release in the form of ATP and/or heat (Jéquier et al., 1987), according to the functions below:

(1) 1g *carbohydrate* + 746ml O_2 → 746ml CO_2 + 0.6g H_2O + 15.7kJ

(2) 1g *lipid* + 2029ml O_2 → 1430ml CO_2 + 0.45g H_2O + 37.7kJ

(3) 1g *protein* + 966ml O_2 → 782ml CO_2+0.45g H_2O + 0.5g urea + 16.7kJ

The efficiency of oxidation in a living organism is reflected by the amount of ATP (representative of useful energy) retained for the performance of biological processes. For oxidation of glucose, for instance, 60% of the energy produced is wasted in the form of heat (Fine and Feinman, 2004). Any reduction in calorie efficiency, and consequent reduced ATP production, increases the likelihood that body stores of fat will be enlisted to yield the additionally required ATP, as represented in Figure 3.2. below.

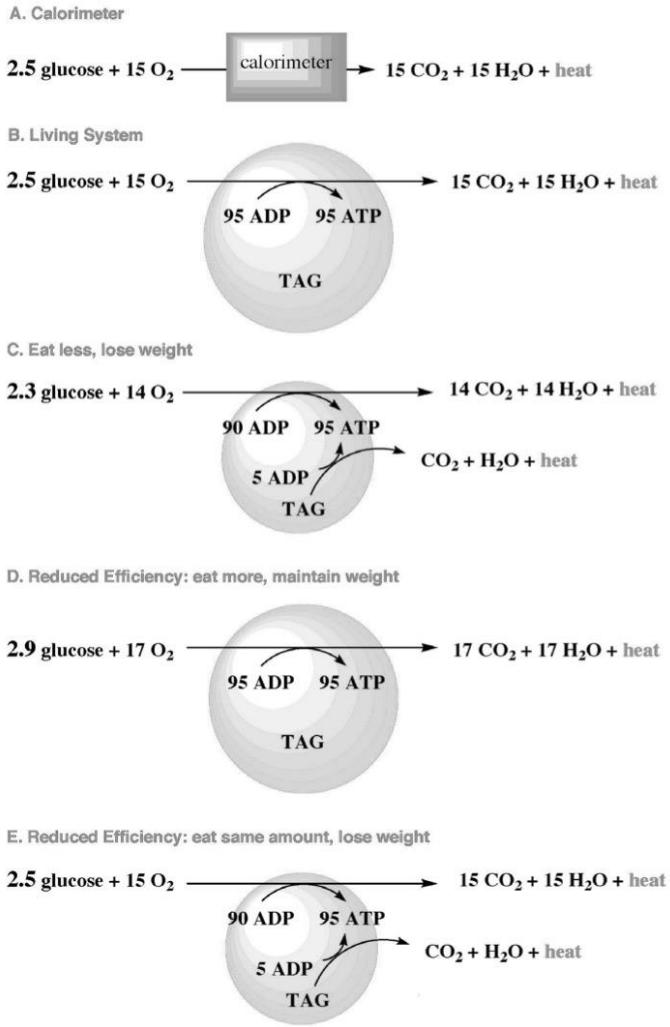

Figure 3.2. Representation of glucose oxidation efficiency in calorimetric and living systems with body weight outcomes. Figure from Fine and Feinman, 2004, Nutrition and Metabolism.

From O_2 and CO_2 measurements, it is possible to evaluate substrate utilisation preferences, by calculating the RER and EE according to the equations below:

$$^{1}\boldsymbol{RER} = \frac{CO_2}{O_2}$$

(1) 1g **carbohydrate** $= \frac{756ml}{746ml} = \mathbf{1.0}$

(2) 1g **lipid** $= \frac{1430ml}{2029ml} = \mathbf{0.7}$

(3) 1g **protein** $= \frac{782ml}{966ml} = \mathbf{0.8}$

$$^{2}\boldsymbol{EE}\ \left(\frac{kJ}{h}\right) = \frac{\left(16.3\ x\ O_2\left(\frac{ml}{h}\right)\right)+\left(4.57\ x\ CO_2\left(\frac{ml}{h}\right)\right)}{1000}\ *$$

**Weir equation for Energy Expenditure estimation*

Stress can also influence behaviour (Blanchard 2001, Beery 2015). Characterisation of behavioural phenotypes, to model certain aspects of psychiatric disorders, is an essential tool in the study of animal models relevant to stress-related disorders. In this study, various behaviours were measured in mice in their home cage.

3.2. Hypotheses

Chronic social stress in mice:

3.2.1. Increases calorie intake

3.2.2. Increases total energy expenditure

3.2.3. Increases *Ucp-1* mRNA expression

3.2.4. Promotes changes in spontaneous active behaviour

3.3. Aims

To investigate the effects of chronic social stress on:

3.3.1. Food intake, body weight and energy expenditure based on indirect calorimetry, in a comparison of CSS and control mice

3.3.2. mRNA expression of the heat generation protein, uncoupling protein 1 (*Ucp-1*), in brown adipose tissue, in a comparison of CSS and control mice

3.3.3. Active behaviour, based on period scan sampling, in a comparison of CSS and control mice

3.4. Methodology

Experiment B (CSS=10, CON=8) investigated the effects of 15-day CSS on food intake, body weight and it was used as a pilot study for calorimetry studies. Physiological samples of blood, brain, epididymal WAT (eWAT), interscapular BAT (iBAT) and stomach were also collected. Experiment C (CSS=12, CON=12) investigated the effects of 15-day CSS on indirect calorimetry, in addition to body weight and food intake. Behavioural and physiological assessments were also conducted. Experimental designs are summarised in the Figure 3.3 below.

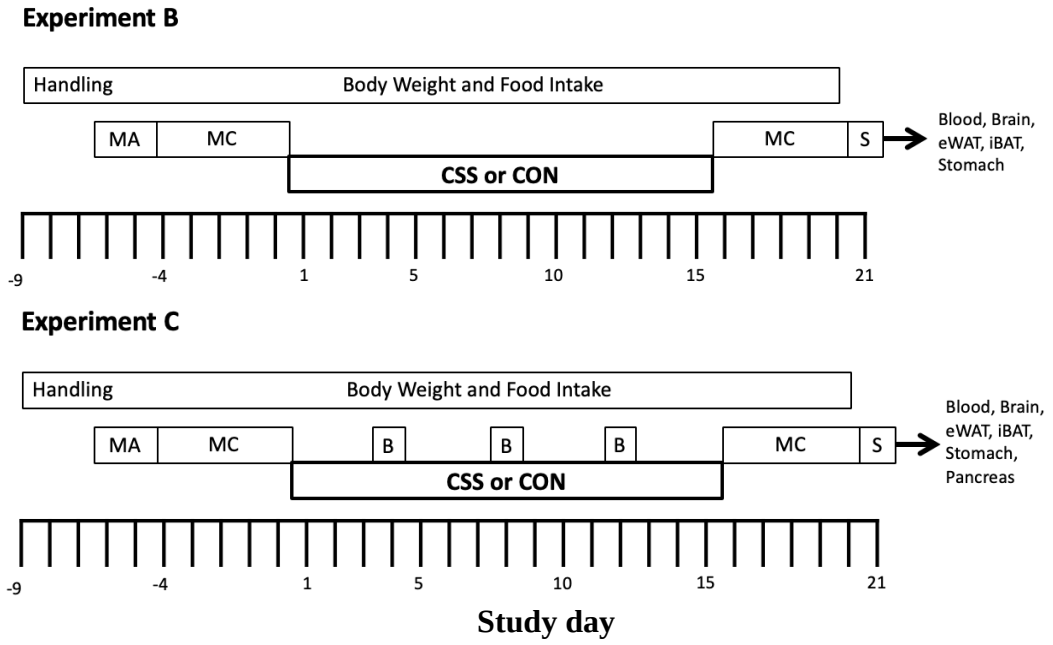

Figure 3.3. Study day of experimental designs. Mouse cohorts were exposed to chronic social stress (CSS) or control handling (CON) on days 1-15. Mice were handled, and a motor activity test (MA) was conducted before experiments for a balanced allocation of mice to CSS or CON groups. Body weight and food intake were monitored daily. Experiment B: Mice were placed in metabolic cages (MC) for calorimetric data collection on day -4 for 5 days for baseline data collection and on days 16-20 for post-CSS data collection. Mice were sacrificed and physiological samples were collected on day 21. Experiment C: Mice were placed in metabolic cages for calorimetric data collection on day -4 for 5 days for baseline data and on days 16-20 for post-CSS data collection. Behaviours (B) were scored on each of CSS/CON days 4, 8 and 12. Mice were sacrificed, and physiological samples were collected on day 21. Abbreviations: eWAT, epididymal white adipose tissue; iBAT, interscapular brown adipose tissue.

3.4.1. Food intake and body weight

Experiments B and C (please refer to Chapter 2 for 'Methodological framework').

Prior to, during and after CSS/CON, body weight and food intake were measured on a daily basis. Food intake was measured by weighing three food pellets in individual containers, placing inside the home cage and weighing the pellets again

24 hours later, using a 1 decimal place scale (Model XS6002SDR, Mettler Toledo). Mean value per 5-day block was calculated per mouse.

3.4.2. Indirect calorimetry

Experiment C (please refer to Chapter 2 for 'Methodological framework').

The indirect calorimetry study was carried out at the Institute of Veterinary Physiology, Vetsuisse, Zurich. Mice were transferred from the Department of Psychiatry 10 days before study onset. At both facilities, mice were maintained under a reversed light:dark cycle. During the 5-day pre-CSS/CON period (baseline) and the 5-day post-CSS/CON period, mice were single-housed in gas-tight metabolic cages of an automated open-circuit indirect calorimetry system (Type III, PhenoMaster Home Cage, TSE Systems, Inc.). Food and water were available ad libitum. The temperature and humidity of the room were kept at 23.4 ± 0.2°C and 54.7 ± 6%, respectively. Each cage was connected to a fresh air supply, which was also the sample switch unit for drawing air samples and measuring the flow rate from each cage. During the baseline period, the first 3 days (days -4 to -2) were used to acclimatise mice to the metabolic cages and baseline data were collected on days -1 and 0. In the post-manipulation period, day 16 was used to re-acclimatise mice to the cages and the data collected on days 17-20 were used for analysis. Each 20 min, measurements were obtained for each of the following parameters: O_2 consumption, CO_2 production, RER and EE, and the hourly average was then calculated. Following completion of calorimetry data collection on day 20, mice were fasted for 14 h and sacrificed at day 21.

3.4.3. Epididymal white adipose tissue dissection

Experiment C (please refer to Chapter 2 for 'Methodological framework').

Following completion of *in vivo* experiments on day 20 (Experiment C) mice were fasted overnight and sacrificed by decapitation for the collection of eWAT. The mouse was placed on its back and the pelage was rinsed with 70% ethanol to avoid tissue contamination with hair. The skin was lifted with tweezers and an incision was made along the abdomen, from the groin and towards the thorax. The eWAT was carefully detached from connective tissue, corresponding lymph nodes and blood vessels. Following dissection, eWAT was weighed for group comparison (in Experiment C) and stored at -80°C until subsequent steps.

3.4.4. Interscapular brown adipose tissue dissection

Following completion of *in vivo* experiments on day 20 (Experiments B and C) mice were fasted overnight and sacrificed for collection of iBAT. Dissection of iBAT was adapted from Mann et al. (2014) and performed as follows: the mouse was placed on its abdomen and the pelage was rinsed with 70% ethanol to avoid tissue contamination with hair. The skin was lifted with tweezers and an incision was made along the upper half of the spine and toward the shoulders, revealing the butterfly-shaped iBAT. The iBAT was carefully removed and separated from surrounding connective tissues, avoiding collection of muscular tissue closely associated with iBAT. Following dissection, iBAT was weighed for group comparison (in Experiment C) and stored at -80°C until subsequent steps.

3.4.5. Brown adipose tissue activity – *Ucp-1* mRNA expression

Experiments B and C (please refer to Chapter 2 for 'Methodological framework').

Expression of *Ucp-1* was measured as a marker of BAT activity, using the reverse transcription quantitative polymerase chain reaction (RT-qPCR) method.

3.4.5.1. RNA extraction

The RNA was extracted from iBAT using an RNeasy Lipid Tissue Mini Kit (Qiagen®), designed to purify RNA from small amounts of starting material. Tissue disruption was performed as follows: QIAzol Lysis Reagent (1mL/30mg) was added to each tube containing two stainless steel beads (ø 5mm, QIAgen®) and placed in a TissueLyser LT (QIAgen®) for 7 min at 50 Hz. The lysate was transferred to a new tube for an incubation period of 5 min at room temperature (RT). For phase separation, 200µL of chloroform was added, the tube was agitated vigorously for 15 sec, left for incubation for 3 min at RT, and centrifuged at 10000rpm for 15 min at 4°C. The upper aqueous phase (approx. 600µL) was transferred to a new tube, one volume of 70% ethanol was added to induce RNA precipitation and the tube vortexed. The solution was loaded onto a RNeasy Mini spin column placed in a collection tube and centrifuged at 12000rpm for 15 sec at RT. The flow-through was discarded. This procedure was performed twice until all tube content had been transferred. Washing Buffer RW1 (350µL) was added to the RNeasy MinElute spin column, centrifuged at 12000rpm for 15 sec at RT and flow-through was discarded. DNase I solution (80µL) diluted in RDD buffer (RNase-Free DNase Set, QIAgen®) was added directly to spin column membrane. The membrane was left for 15 min at RT to allow DNase digestion and genomic DNA (gDNA) removal. Washing buffer RW1 (350µL) was added to an Rneasy spin column, centrifuged at 12000rpm for 15 sec at RT. Flow-through was discarded, 500µL of washing buffer RPE were added to the RNeasy spin column for removal of salt traces, and it was centrifuged again at 12000rpm for 15 sec at RT. A

second centrifugation with buffer RPE was carried out for a more extended period (2 min) to ensure no ethanol was carried over during RNA elution. The RNeasy spin column was placed in a new collection tube and centrifuged at full speed (14800rpm) for 1 min. The RNeasy spin column was again placed in a new tube, 40µL of RNase-free water were added directly to the membrane, and centrifuged at 12000rpm for 1 min. A second centrifugation was performed using eluate for higher RNA yield concentration.

3.4.5.1.1. RNA purity and quantity

Assessment of RNA purity and quantity was performed using NanoVue™ Plus Spectrophotometer (GE Healthcare).

Two criteria were used for verification of RNA purity:

1. Ratio A260/280: 1.9 – 2.2. Ratios below 1.9 would be indicative of protein or phenol contamination;
2. Ratio A260/230: 2.0 – 2.2. Ratios below 2.0 would be indicative of contaminants which absorb at 230nm.

3.4.5.1.2. RNA integrity

Visual assessment of RNA integrity was conducted using 1% agarose gel electrophoresis (ThermoScientific™). RNA samples were stained with ethidium bromide (RNA Gel Loading Dye 2x, ThermoScientific™) and minimum 1µg of extracted RNA was loaded to the gel. The ratio of ribosomal RNA (rRNA) 28S and 18S bands (28S:18S) was checked. Smeared bands and a 28:18S rRNA ratio less than 2:1 are indicative of degradation and were therefore avoided. RNA was kept at -80°C with minimal freeze-thaw cycles, until further use.

3.4.5.2. Reverse transcription

For synthesis of complementary DNA (cDNA) from the RNA template, 1µg RNA was reverse transcribed using the High Capacity cDNA Reverse Transcription Kit (Applied Biosystems), as follows: thawed RNA and reagents were briefly vortexed and centrifuged. 2x Reverse Transcription Master Mix (RT Buffer, RT Random Primers, 100mM dNTP Mix and 50U/µL MultiScribe® Reverse Transcriptase) were prepared according to the manufacturer's instructions. Total RNA samples were added to the master mix, carefully homogenised and briefly centrifuged. Negative RT (absence of reverse transcriptase enzyme) was also prepared for identification of gDNA in downstream reactions. Samples were loaded into a thermal cycler (T100™, Bio-Rad Laboratories, Inc.) and optimum conditions were programmed (Table 3.1). cDNA was kept at -20°C until further use.

Table 3.1. Details of the 4-step cycling protocol for RNA reverse transcription

1. Primer annealing	10 min 25°C
2. DNA polymerisation	120 min 37°C
3. Enzyme deactivation	5 min 85°C
	Infinite hold 4°C

Please refer to Appendix 2 for reagents and solutions.

3.4.5.3. Quantitative polymerase chain reaction

By means of qPCR, specific quantification of cDNA targets was performed using the QuantiFast SYBR Green PCR Kit (QIAgen®) in the presence of ROX passive reference dye, according to the manufacturer's instructions. Briefly, 2x SYBR Green PCR Master Mix, 500nM forward and reverse primers and RNase-free water,

were mixed with 50ng/µL cDNA and prepared in duplicates. No template control (NTC) containing RNase-free water instead of cDNA was also prepared for analysis of quality primer pairs. Samples were loaded onto a MicroAmp™ Fast Optical 96-Well Reaction Plate (Applied Biosystems™). Care was taken to avoid the formation of air bubbles in the wells. The plate was placed in the StepOnePlus™ Real-Time PCR System (Applied Biosystems™) according to the cycling protocol shown in Table 3.2 below:

Table 3.2. Details of the 2-step cycling protocol for qPCR

1. Pre-incubation	5 min 95°C	denaturation
2. PCR (40 cycles)	10 sec 95°C	
	30 sec 60°C*	annealing/extension

* specific temperature of primer pairs described in *Section 'PCR efficiency'*.

Please refer to Appendix 2 for reagents and solutions.

3.4.5.3.1. Primer design

Primer pairs for *Ucp-1* were designed using NCBI Primer-BLAST, with the parameters set to create a product of 70-200bp and primer melting temperature ranging from 57°C to 63°C. BLAT (BLAST-Like Alignment Tool) from UCSC Genome Browser was used to check for primer sequence alignment. Primers were synthesised by Invitrogen (ThermoScientific™) and working stocks containing both forward (FW) and reverse (RV) primers at a concentration of 10µM were prepared. Two genes, *Gapdh* (Matoušková et al., 2014) and *Actb*, were used as housekeeping genes, for increased accuracy of the results (Kozera and Rapacz, 2013).

3.4.5.3.2. PCR efficiency

Presence of PCR inhibitors, inaccurate reagent pipetting and poor quality oligos/primers were some of the several parameters that could have affected the efficiency of the PCR reaction and were therefore avoided. Optimisation of PCR efficiency was achieved by performing a 5-fold cDNA dilution series for each target and each tissue. According to the length and composition of the primers, modifications of annealing temperature and extension time were necessary to achieve PCR efficiency of 90-110% (Table 3.3). A standard curve was generated for each primer pair setting and the slope of the curve was calculated.

Table 3.3. Gene description, primer sequences, qPCR parameters and primer efficiency

Gene	Primer sequence ('5 – 3')	PCR product (bp)	Annealing temp. (°C)	Extension (sec)	PCR *E* (%)
Ucp-1	FW: CTGCCAGGACAGTACCCAAG	110	63	40	100
	RV: GACCCGAGTCGCAGAAAAGA				
Actb	FW: GGCTGTATTCCCCTCCATCG	154	63	30	103
	RV: CCAGTTGGTAACAATGCCATGT				
Gapdh	FW: AGGTCGGTGTGAACGGATTTG	123	63	40	94
	RV: TGTAGACCATGTAGTTGAGGTCA				

3.4.6. Behavioural observation

Experiment C (please refer to Chapter 2 for 'Methodological framework').

To measure spontaneous behaviours in the home cage, the method of 'instantaneous scan sampling' was applied, in which each mouse was observed in turn for 10 sec every 2 min, and the most prominent behaviour during each 10 sec sample was scored (Dawkins et al., 1994). An ethogram comprising 10 behaviours was used, namely eating, drinking, self-grooming, foraging, sitting upright, resting, "at divider", locomoting, climbing and rearing. On each of CSS/CON days 4, 8 and 12, a 1-hour

observation was conducted at 8-9 h, 11-12 h, 16-17 h and 19-20 h (30 sample points per hour per mouse). The definition of each behaviour was as described below:

Eating – holding and biting food pellet

Drinking

Self-grooming – washing with front paws and licking of neck, trunk, abdomen or anogenital region; scratching coat

Foraging – burying nose into cage bedding, and also including moving of tissue paper in the mouth

Sitting upright – stationary with body weight supported by hind legs only, including some periods with head movement

Resting – stationary with body weight supported by front and hind legs and with abdomen resting on the ground. Includes periods of sleeping.

At divider – on front and hind legs or hind legs only and investigating with the nose either into the divider holes or at the divider base

Locomoting – walking or running on front and hind legs

Climbing – clinging with front and/or hind legs either vertically on the divider or upside down on the food grid

Rearing – standing on hind legs only with body and neck elongated and head oriented towards the top or corner of the cage

3.4.7. Statistical analysis

Statistical analysis of CSS effects on feeding, body weight, adipose tissue mass, calorimetry measures and home-cage behaviours was conducted using SPSS (version 24, SPSS Inc., Chicago IL, USA). In Experiment B, for food intake, repeated

measures analysis of covariance (ANCOVA) was conducted, with pre-CSS/CON body weight as a covariate. For body weight and food intake adjusted to body weight, repeated measures analysis of variance (ANOVA) was conducted. In Experiment C, for food intake and body weight, repeated measures ANCOVA was conducted, with pre-CSS/CON body weight as a covariate. For food intake adjusted to body weight, ANCOVA was conducted with pre-CSS/CON value as a covariate. Independent Student's *t*-test was conducted for feeding efficiency and adipose tissue mass. For calorimetric data, the linear mixed model (LMM) with baseline body weight as a covariate was used to study the effects of CSS on EE, O_2 production and CO_2 and the LMM was used to study the effects of CSS on RER. Significant main or interaction effects were analysed using *post hoc* testing with Bonferroni correction for multiple comparisons. For home-cage behaviours, ANOVA was conducted with group (CSS/CON) as between-subject factor and CSS/CON day and time as within-subject factors. Significant main or interaction effects were analysed using the least significant difference (LSD) post hoc test. For those behaviours that demonstrated a significant effect of group (CSS, CON) on a specific day and at a specific time point, additional non-parametric analysis of these specific effects was performed using the Mann-Whitney U test. Furthermore, to compensate for multiple testing, the level of significance was set at $p \leq 0.01$ for the Mann-Whitney U tests conducted. Data are given as means and the estimate of variance used is 1 standard deviation (SD). Analysis of iBAT *Ucp-1* expression was carried out using the $2^{-\Delta\Delta Ct}$ method and β-Actin was used as a control gene for normalisation; the independent Student's t-test was conducted. Data are given as fold change + standard error of the mean (SEM). Statistical significance was set at $p \leq 0.05$.

3.5. Results

3.5.1. Food intake and body weight

3.5.1.1. Experiment B

Please refer to Chapter 2 for 'Methodological framework'.

For the body weight and food intake parameters, measurements were averaged across 5-day blocks. There was no effect of Group on body weight (ANOVA: $F(1, 16)=0.193$, $p=0.67$, Figure 3.4A). Food intake was measured across the same time period: there was a Group x Day block interaction (ANCOVA with pre-CSS/CON body weight as covariate: $F(4, 56)=3.4$, $p=0.015$); *post hoc* tests demonstrated that CSS mice had increased food intake at days 16-20 post-CSS (Figure 3.4B). When food intake was adjusted for body weight, there was a Group x Day block interaction (ANOVA: $F(4, 52)=6.7$, $p<0.001$); at days 11-15 of CSS and 16-20 of post-CSS, food intake was increased in CSS mice compared to controls (Figure 3.4C). No difference in feeding efficiency was found between CSS and CON mice ($t(16)=-0.36$, $p=0.74$, Figure 3.4D). The increase in food intake and the absence of body weight gain observed in this experiment suggest an increase in EE, therefore EE was measured.

A.

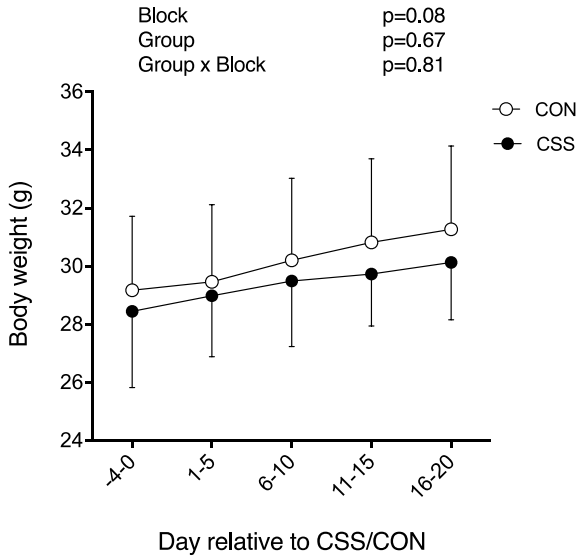
Block p=0.08
Group p=0.67
Group x Block p=0.81
CON
CSS
Body weight (g)
36
34
32
30
28
26
24
-4-0
1-5
6-10
11-15
16-20
Day relative to CSS/CON

B.

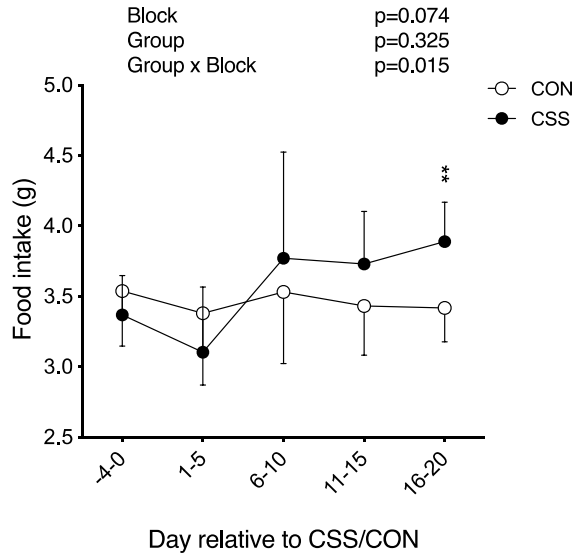
Block p=0.074
Group p=0.325
Group x Block p=0.015
CON
CSS
Food intake (g)
5.0
4.5
4.0
3.5
3.0
2.5
**
-4-0
1-5
6-10
11-15
16-20
Day relative to CSS/CON

C.

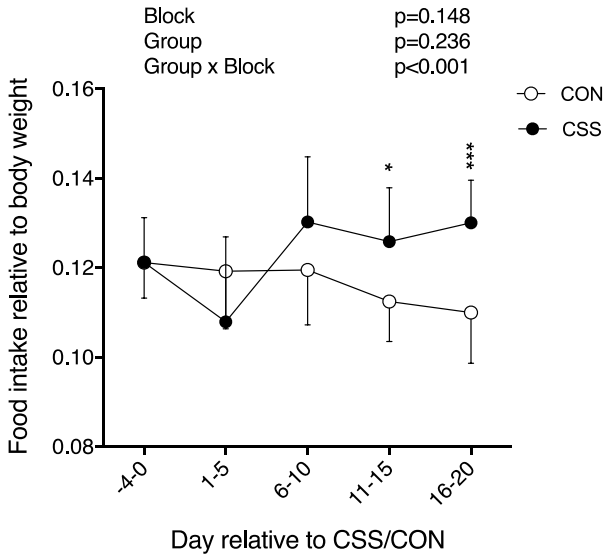

D.

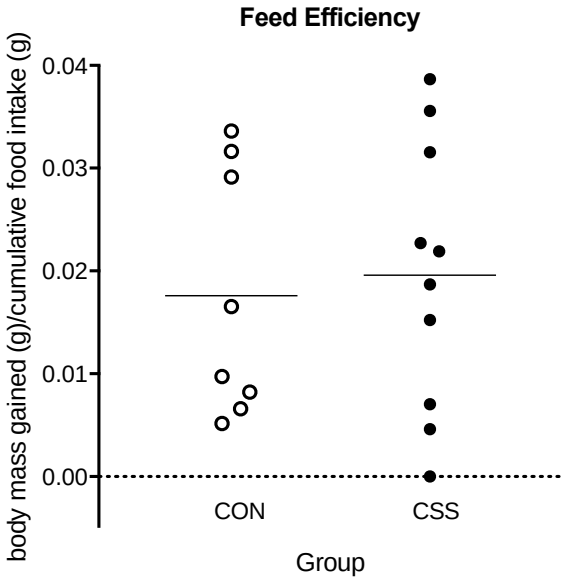

Figure 3.4. Effects of 15-day chronic social stress (CSS=10), versus control handling (CON=8) on body weight and food intake. (A) Absolute body weight. (B) Daily food intake. (C) Daily food intake adjusted for body weight. (D) Feeding efficiency. Values are overall means per 5-day block +/- standard deviation (SD). *p<0.05, **p<0.01, ***p<0.001 for CSS versus CON mice in day block indicated, using Group x Day block ANCOVA (Daily food intake) or Group x Day ANOVA (Absolute body weight and daily food intake adjusted for body weight), and in the case of significant interaction, day block-specific post hoc testing using LSD test.

3.5.1.2. Experiment C

Please refer to Chapter 2 for 'Methodological framework'.

There was a Group x Day block interaction effect on body weight (ANCOVA with pre-CSS/CON body weight as covariate: $F(2, 43)=11.9$, $p<0.0001$); *post hoc* tests demonstrated that CSS mice weighed less than CON mice at days 11-15 of CSS and 16-20 post-CSS (Figure 3.5A). Food intake was measured across the same time period: there was no effect of CSS on mean food intake per 5-day block (ANCOVA with pre-CSS/CON body weight as covariate: $F(1, 21)=1.92$, $p=0.18$, Figure 3.5B). When food intake was adjusted for body weight, there was no effect of Group (ANOVA: $F(1, 22)=2.8$, $p=0.11$) or Group x Day block interaction (ANOVA: $F(3, 73)=0.66$, Figure 3.5C). Therefore, although CSS mice failed to gain weight across the study whereas CON mice did gain weight, the two groups were consuming a similar amount of food. In regards to feeding efficiency, CSS mice showed lower feeding efficiency compared with CON mice ($t(22)=2.42$, $p<0.05$, Figure 3.5D).

A.

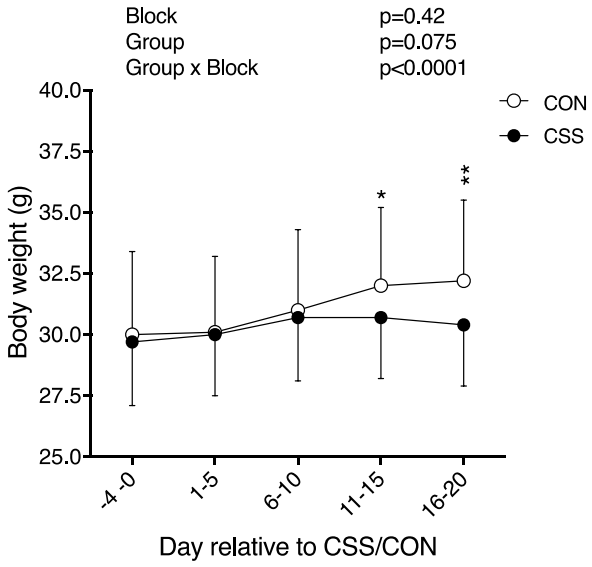

B.

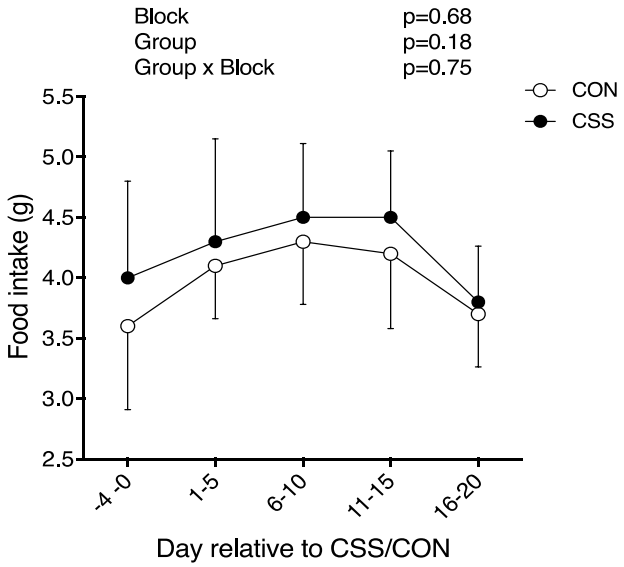
Block p=0.68
Group p=0.18
Group x Block p=0.75
CON
CSS
Food intake (g)
5.5
5.0
4.5
4.0
3.5
3.0
2.5
-4 -0
1-5
6-10
11-15
16-20
Day relative to CSS/CON

C.

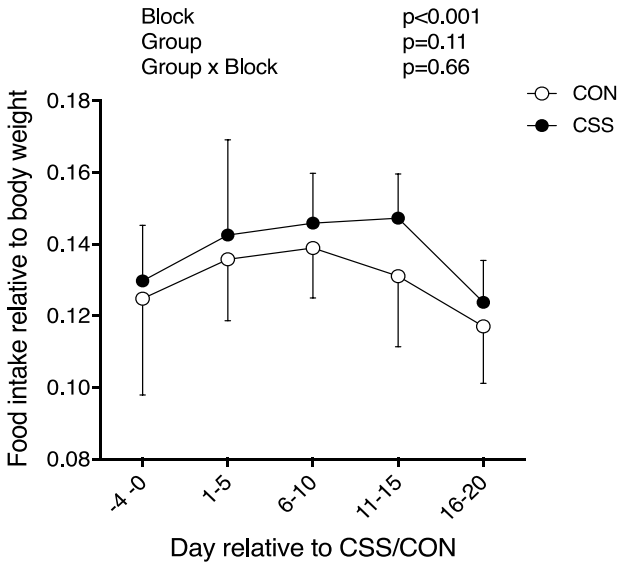
Block p<0.001
Group p=0.11
Group x Block p=0.66
CON
CSS
Food intake relative to body weight
0.18
0.16
0.14
0.12
0.10
0.08
-4 -0
1-5
6-10
11-15
16-20
Day relative to CSS/CON

D.

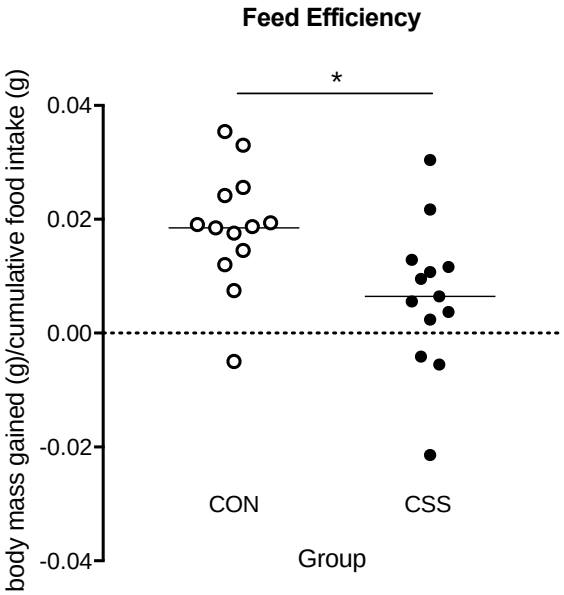

Figure 3.5. Effects of 15-day chronic social stress (CSS=12), versus control handling (CON=12) on body weight and food intake. (A) Absolute body weight. (B) Daily food intake. (C) Daily food intake adjusted for body weight. (D) Feeding efficiency. Values are overall means per 5-day block +/- standard deviation (SD). *p<0.05, **p<0.01 for CSS versus CON mice in day block indicated, using Group x Day block ANCOVA (Absolute body weight and daily food intake) or Group x Day block ANOVA (Daily food intake adjusted for body weight), and in the case of significant interaction, day block-specific post hoc testing using LSD test.

3.5.1.3. Adipose tissue weight

Experiment C (please refer to Chapter 2 for 'Methodological framework').

The BAT weight difference was found to be borderline significant: CSS mice had a lower BAT weight than CON mice ($t(22)=4.11$, $p=0.054$, Figure 3.6A). With regards to WAT weight, this was lower in CSS mice than CON mice ($t(22)=2.03$, $p<0.0001$, Figure 3.6B).

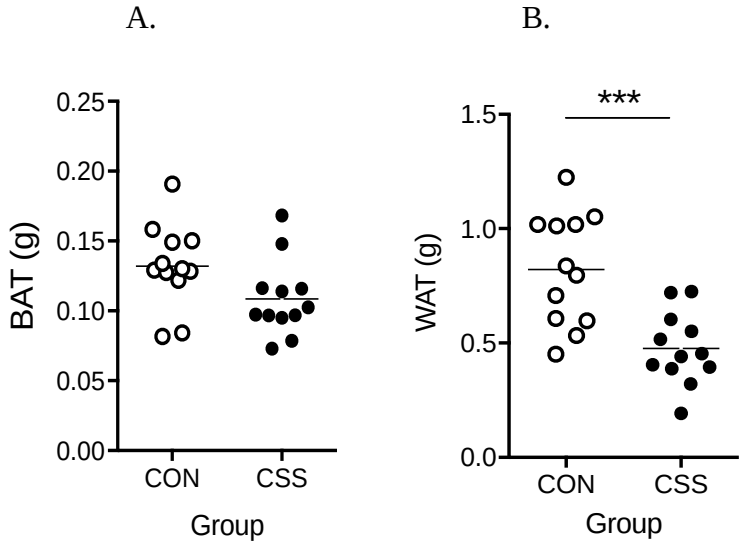

Figure 3.6. Effects of 15-day chronic social stress (CSS=12), versus control handling (CON=12) on BAT and WAT weight. (A) BAT. (B) WAT. ***p<0.001 for CSS versus CON mice following an Independent sample t-test.

3.5.2. Indirect calorimetry

Experiment C (please refer to Chapter 2 for 'Methodological framework').

As previously mentioned, the hourly average of parameters was calculated from the regular (every 20 min) measurements obtained on the indirect calorimetry system. As an illustration, the hourly data obtained for RER on day 19 of the experiment are presented in Figure 3.7. From these hourly data, the mean values were calculated for each 12-h dark phase (07-19:00 h) and each 12-h light phase (19-07:00 h). Statistical analysis was conducted for the dark and light phases separately.

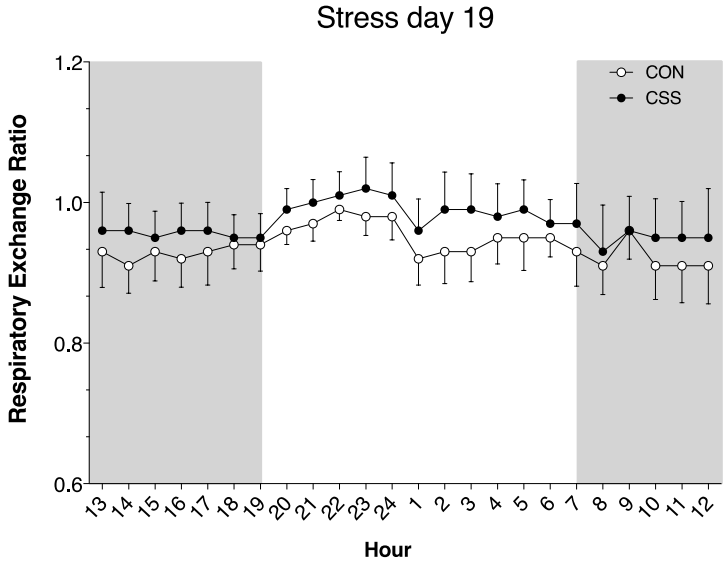

Figure 3.7. Data for respiratory exchange ratio obtained with CSS (N=12) and CON (N=12) mice for each hour on study day 19. One value was obtained each 20 min, and the mean hourly value per mouse was calculated. Values are overall group mean RER per hour +/- standard deviation for CSS and CON mice.

There is a general concern about the different approaches for measuring and calculating EE following an intervention. Since lean body mass was not measured and since variability in the metabolism of different adipose tissues might also generate inconsistency of analysis, for the present study pure values of O_2 consumption and CO_2 production were used followed by body weight correction when needed. Simple linear regression was performed to determine the association between parameters obtained from indirect calorimetry (O_2, CO_2, EE and RER) and body weight. For O_2 consumption, CO_2 production and EE, there was a clear positive association with body weight. There was no Group x BW interaction but a main effect of body weight. Body weight was used as a covariate in these cases and mixed model ANCOVA was conducted. Regarding RER, there was no relationship between RER and body weight; therefore, mixed model analysis was performed without body weight as a covariate (Figure 3.8).

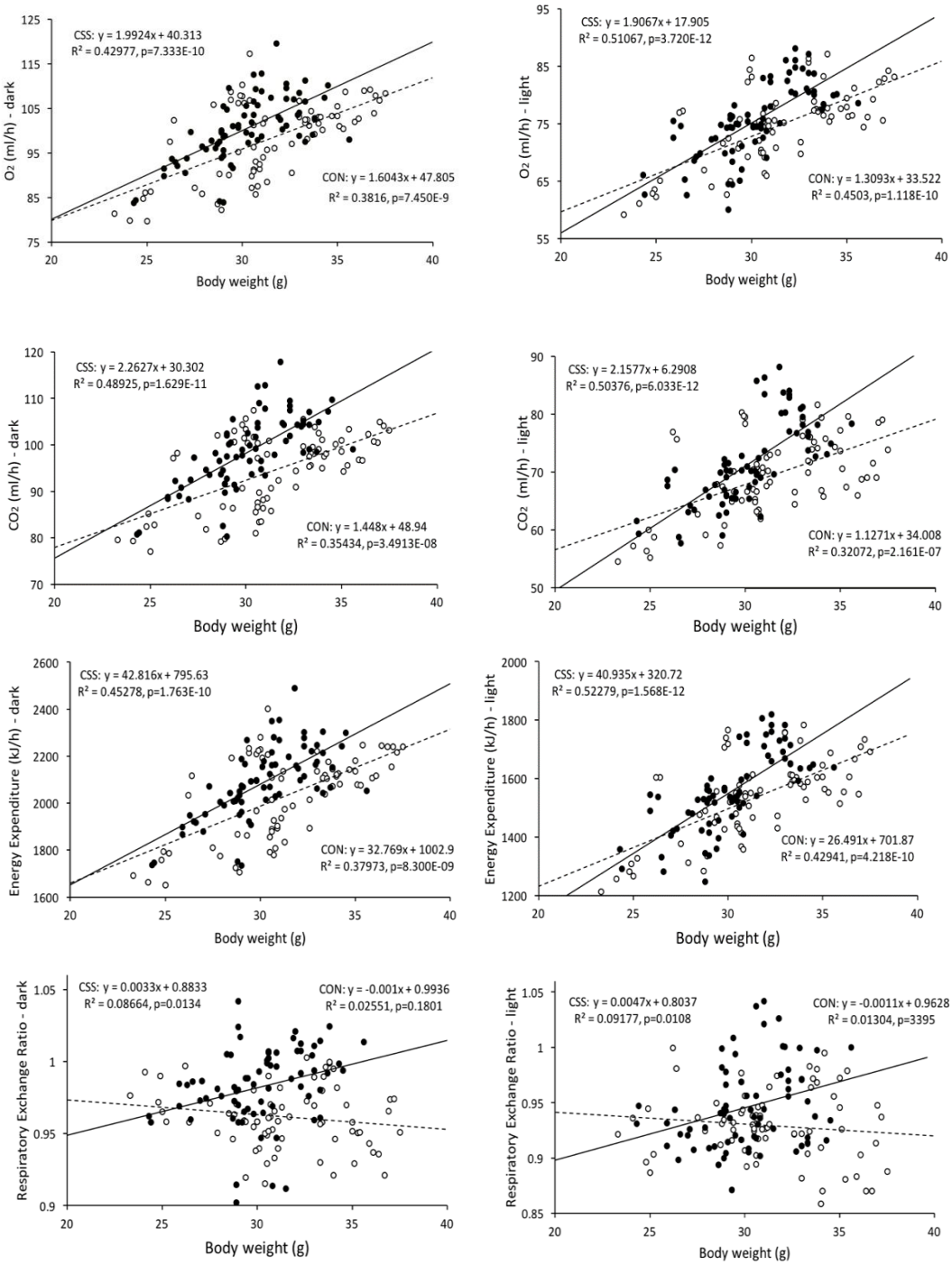

Figure 3.8. Simple linear regression analysis of O_2 consumption, CO_2 production, Energy Expenditure and Respiratory Exchange Ratio with body weight for both dark (left) and light (right) phases. CON (empty circle; dotted line), CSS (filled circle; continuous line).

For O_2 consumption, there was no effect of Group in either the dark or light phase. There was a main effect of Day during the light phase, indicating higher O_2 consumption at days 18-20 *versus* days -1/0 (Figure 3.9A).

For CO_2 production, there was a main effect of Group in the dark phase with CSS mice producing more CO_2 than CON mice; there was no effect of Group in the light phase. There was a main effect of Day during the light phase indicating higher CO_2 production at days 18-20 *versus* days -1/0. Furthermore, during the light phase, there was a Group x Day interaction effect; CSS mice produced more CO_2 than CON mice at days 19 and 20 (Figure 3.9B).

With regard to EE, there was no significant effect of Group (interaction or main effect) in either dark or light phases. There was a main effect of Day during the light phase, indicating higher EE at days 18-20 *versus* days -1/0 (Figure 3.9C). Despite the absence of a statistical effect, there was a clear positive association of EE with body weight, as shown previously in Figure 3.8; in mice of the same body weight, EE is typically higher in CSS than CON mice.

Lastly, regarding RER (Figure 3.9D), during the dark phase, there was a main effect of Group, with CSS mice showing higher RER values than CON mice. There was also a main effect of Day during the dark phase, indicating higher RER at day 17 *versus* day -1. There was a Group x Day interaction effect; CSS mice showed higher RER than CON mice at days 17-20. During the light phase, there was a main effect of Day indicating higher RER at day 17 *versus* day -1. There was a Group x Day interaction effect; CSS mice showed higher RER than CON mice at days 19 and 20.

A.

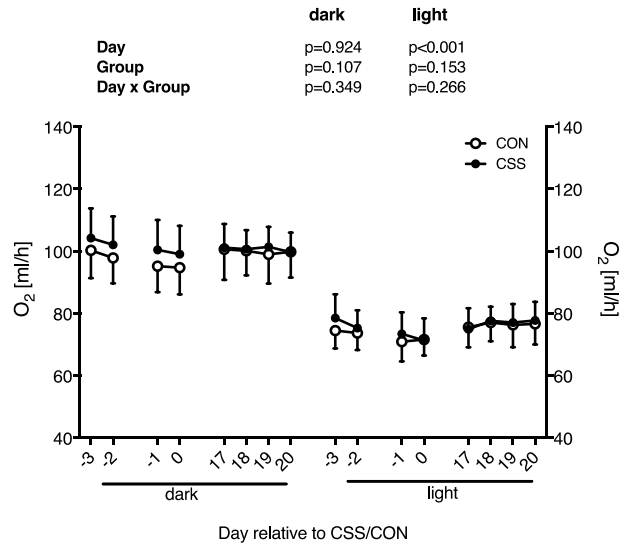
dark
light
Day p=0.924 p<0.001
Group p=0.107 p=0.153
Day x Group p=0.349 p=0.266
CON
CSS
O2 [ml/h]
dark
light
Day relative to CSS/CON

B.

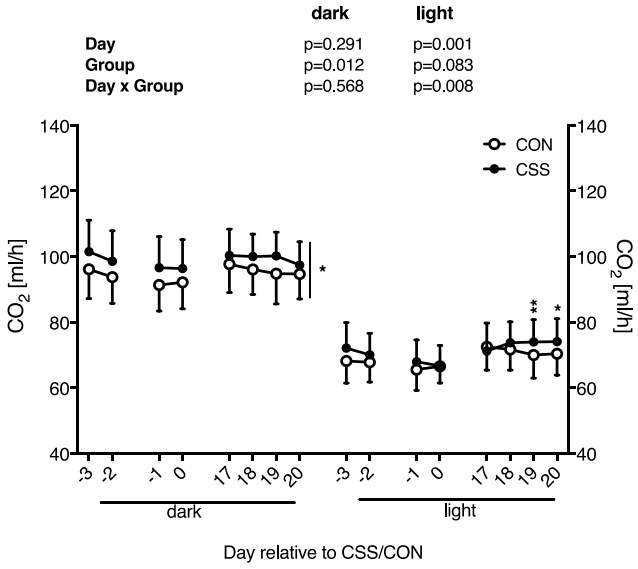
dark
light
Day p=0.291 p=0.001
Group p=0.012 p=0.083
Day x Group p=0.568 p=0.008
CON
CSS
CO2 [ml/h]
dark
light
Day relative to CSS/CON

C.

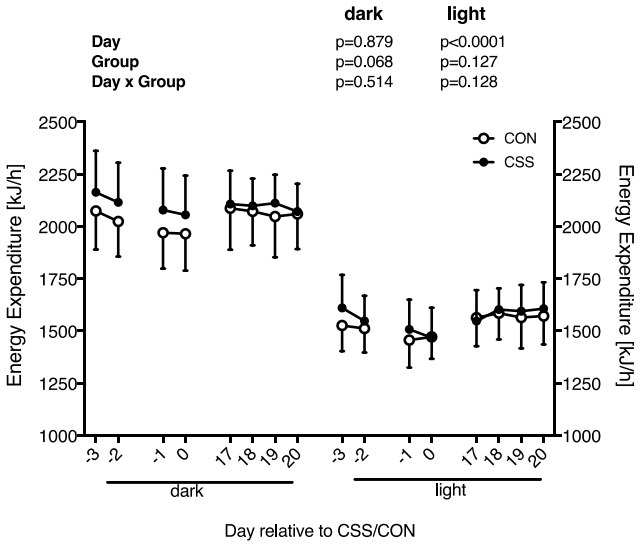

D.

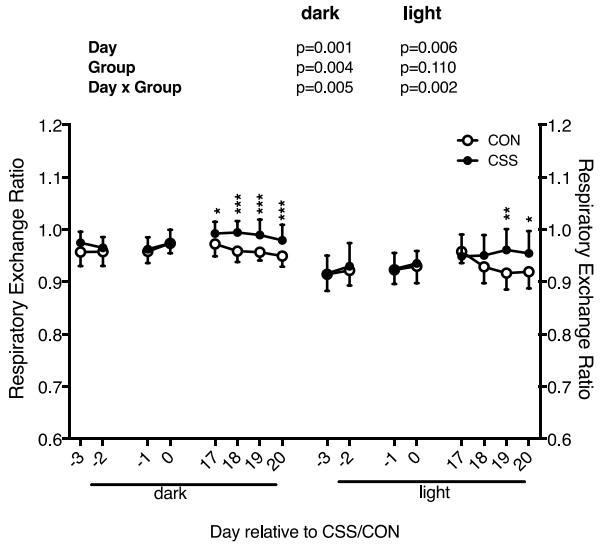

Figure 3.9. Effects of 15-day chronic social stress (CSS=12), versus control handling (CON=12) on indirect calorimetry. (A) O_2 consumption. (B) CO_2 production. (C) Energy Expenditure. (D) Respiratory Exchange Ratio. For each parameter, the left panel gives values during the dark phase and the right panel the values during the light phase. Values are overall mean +/- standard deviation. For statistical analysis, data were used for days -1, 0, 17, 18, 19, 20. *p<0.05, **p<0.01, ***p<0.001, for CSS versus CON mice following a main effect of Group in the mixed model ANCOVA (O_2, CO_2, EE) or ANOVA (RER), or in day-specific post hoc Bonferroni testing following a significant Group x Day interaction in ANCOVA or ANOVA.

3.5.3. Brown adipose tissue activity – *Ucp-1* mRNA expression

Experiments B and C (please refer to Chapter 2 for 'Methodological framework').

No difference in *Ucp-1* mRNA expression was found in iBAT of mice from Experiment B. For Experiment C, *Ucp-1* mRNA expression was increased in CSS mice when normalised to the housekeeping gene *Actb* (p=0.009, left Figure 3.10B), but no difference in expression was found when normalised to *Gapdh*.

Table 3.4. iBAT *Ucp-1* mRNA expression normalised to *Actb* and *Gapdh*, for Experiment B and Experiment C (specified in brackets). Values of ΔCt expressed as mean values ± SEM.

Gene	CON ΔCt	CSS ΔCt	Difference (%)	Fold change	*p* value	
Ucp-1_Actb(B)	**-2.17** ± 0.27	**-2.12** ± 0.35	5	1.39	0.924	
Ucp-1_Gapdh(B)	**0.01** ± 0.32	**-0.51** ± 0.37	52	1.20	0.330	
Ucp-1_Actb(C)	**-1.62** ± 0.13	**-2.11** ± 0.11	49	1.39	0.009	**
Ucp-1_Gapdh(C)	**0.19** ± 0.12	**-0.08** ± 0.13	27	1.20	0.136	

A.

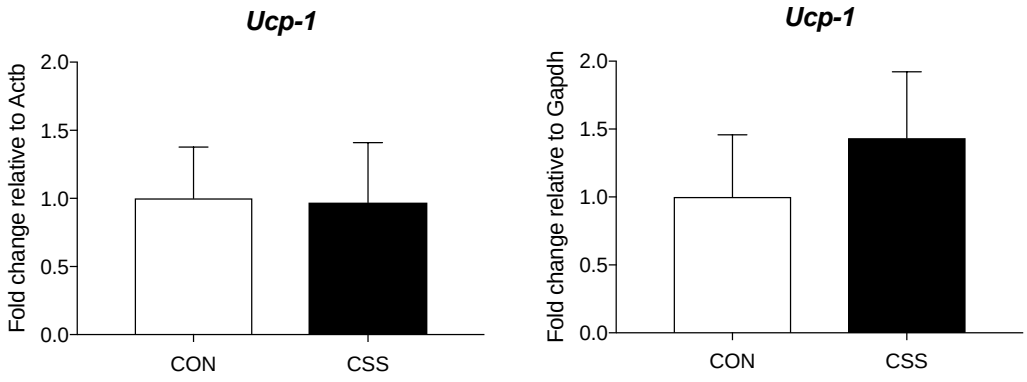

B.

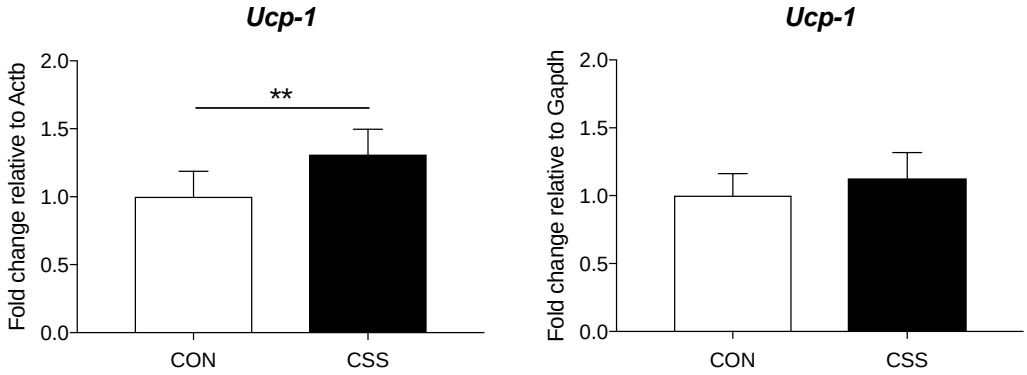

Figure 3.10. Effects of 15-day chronic social stress (CSS), versus control handling (CON) on iBAT Ucp-1 mRNA expression. (A) Experiment B (CSS=10, CON=8). (B) Experiment C (CSS=12, CON=12). Values are in terms of fold change relative to Actb (left) and Gapdh (right) housekeeping genes + SE. *p<0.05 for CSS versus CON mice following an independent Student's t-test.

3.5.4. Behaviour

Experiment C (please refer to Chapter 2 for 'Methodological framework').

For self-grooming, there was a main effect of Group ($F(1, 22)=30.16$, $p<0.0001$), with CSS mice self-grooming more than CON mice (Figure 3.12A). The Mann-Whitney test indicated that the self-grooming behaviour was greater for CSS mice (Mdn = 4.08) than for CON mice (Mdn=2.79), $U=8$, $p<0.01$. For sitting upright, there was a main effect of Group ($F(1, 22)=9.30$, $p<0.006$), with CSS mice sitting upright more than CON mice (Figure 3.12B). The Mann-Whitney test indicated that

sitting upright was greater for CSS mice (Mdn=1.04) than for CON mice (Mdn = 0.75), U=21.5, p<0.01. No main or interaction effect of Group was found for any of the other behaviours measured.

A.

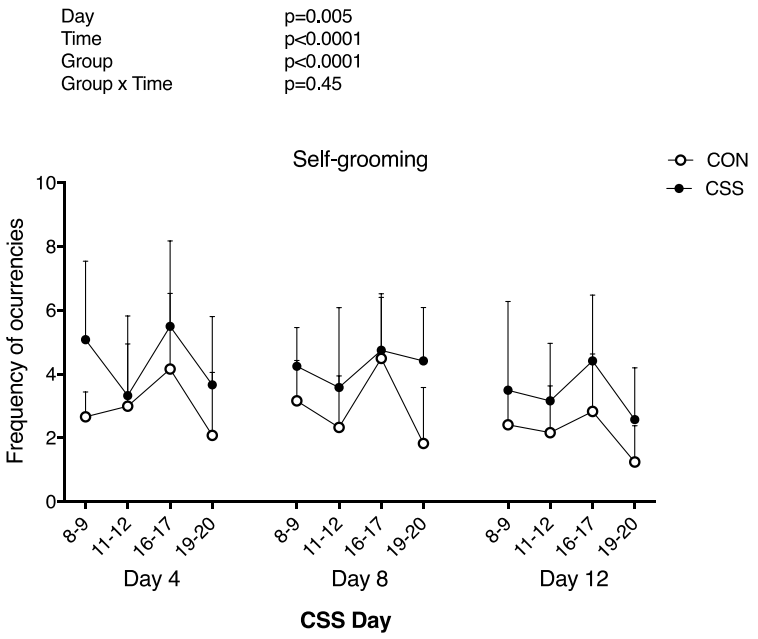

B.

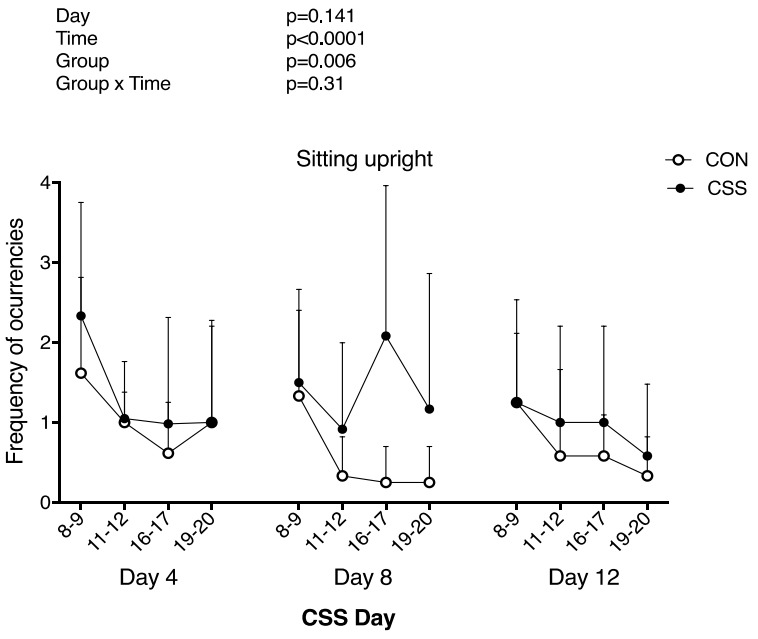

C.

Day	p=0.45
Time	p<0.0001
Group	p=0.91
Group x Time	p=0.10

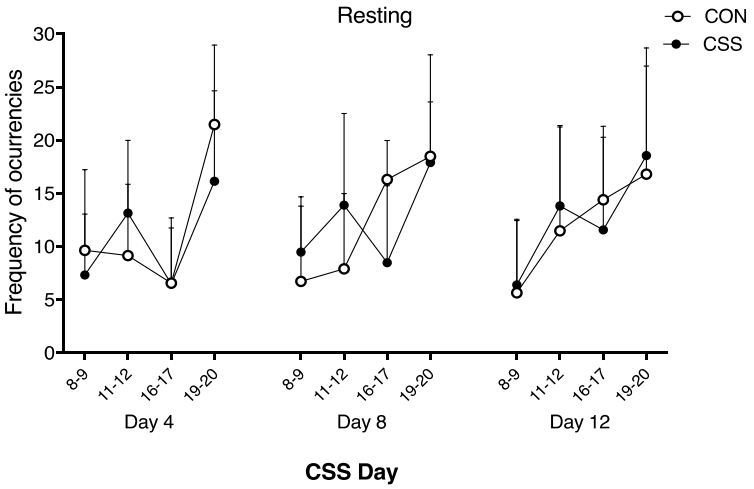

D.

Day	p=0.05
Time	p=0.01
Group	p=0.56
Group x Time	p=0.12

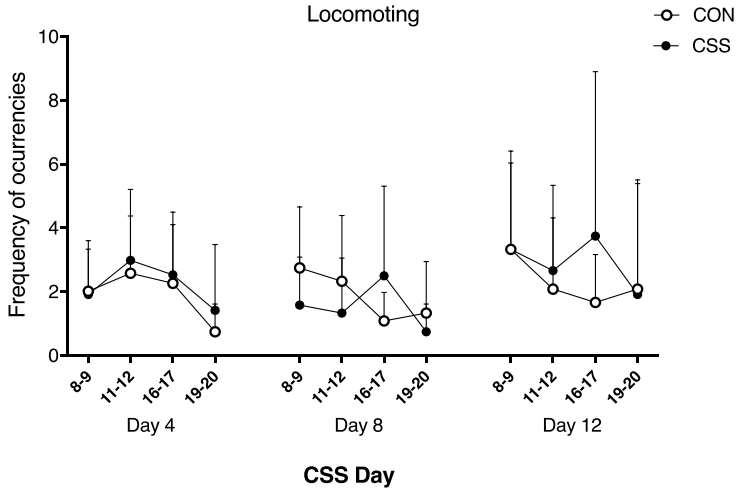

E.

Day	p=0.73
Time	p<0.0001
Group	p=0.45
Group x Time	p=0.72

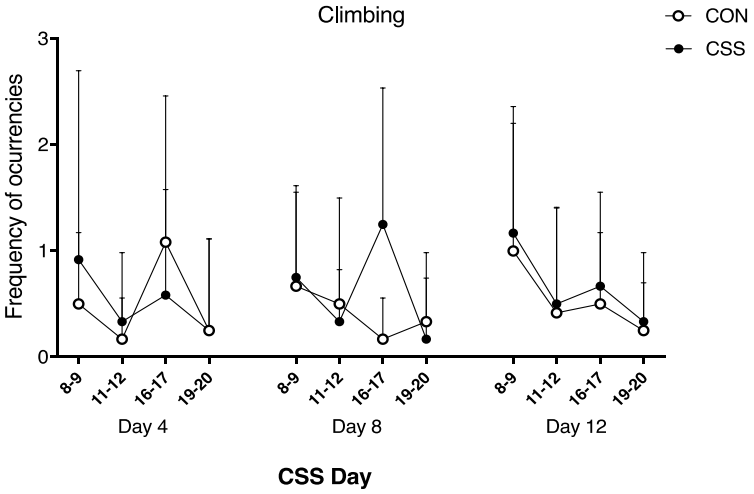

F.

Day	p=0.002
Time	p<0.0001
Group	p=0.89
Group x Time	p=0.36

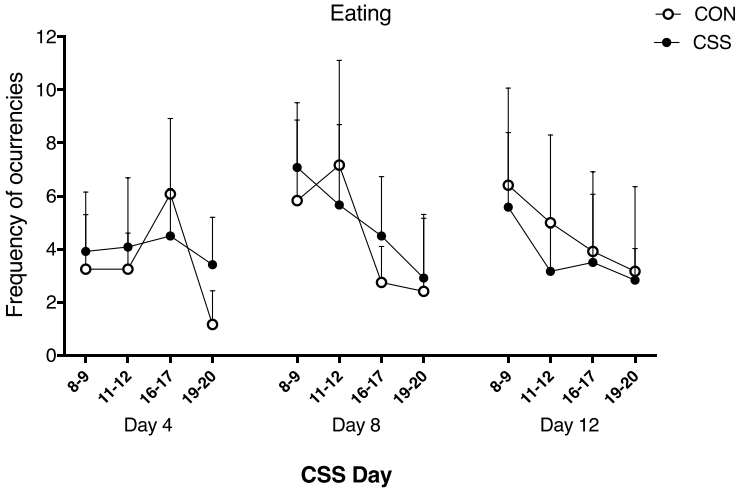

G.

Day	p=0.56
Time	p<0.0001
Group	p=0.62
Group x Time	p=0.18

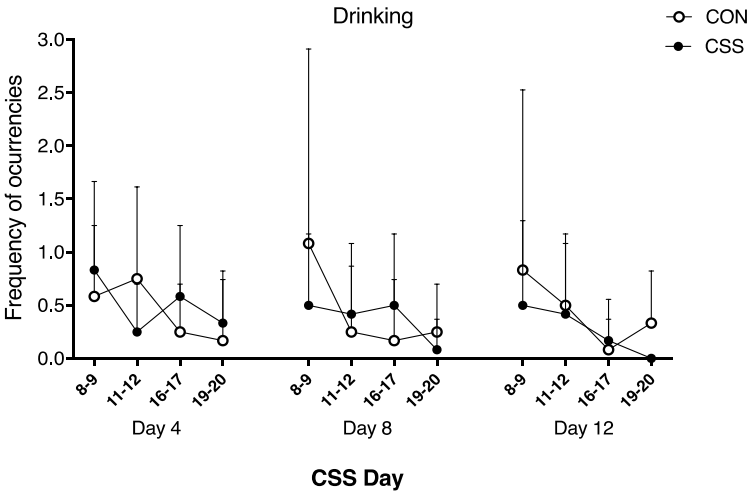

H.

Day	p=0.01
Time	p<0.0001
Group	p=0.15
Group x Time	p=0.09

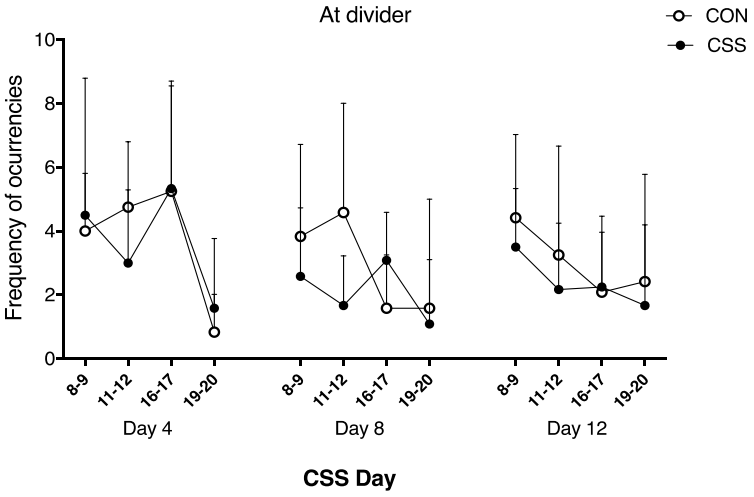

I.

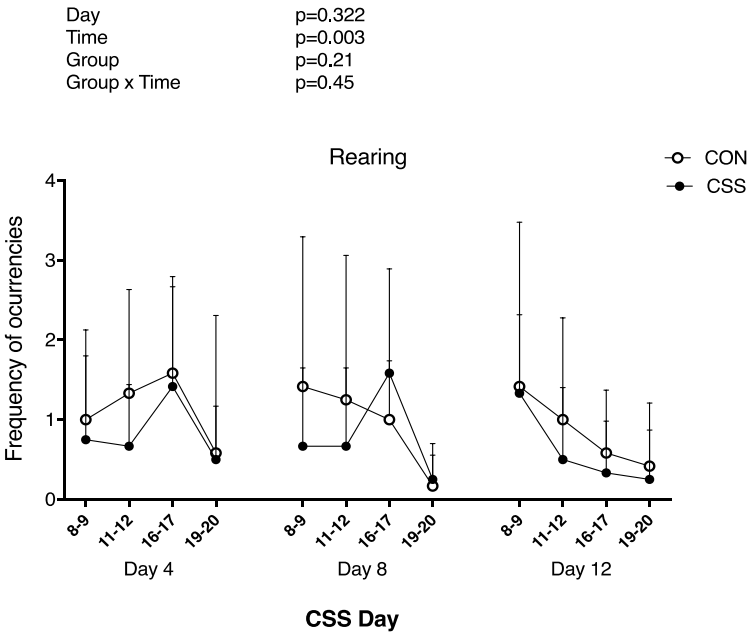

J.

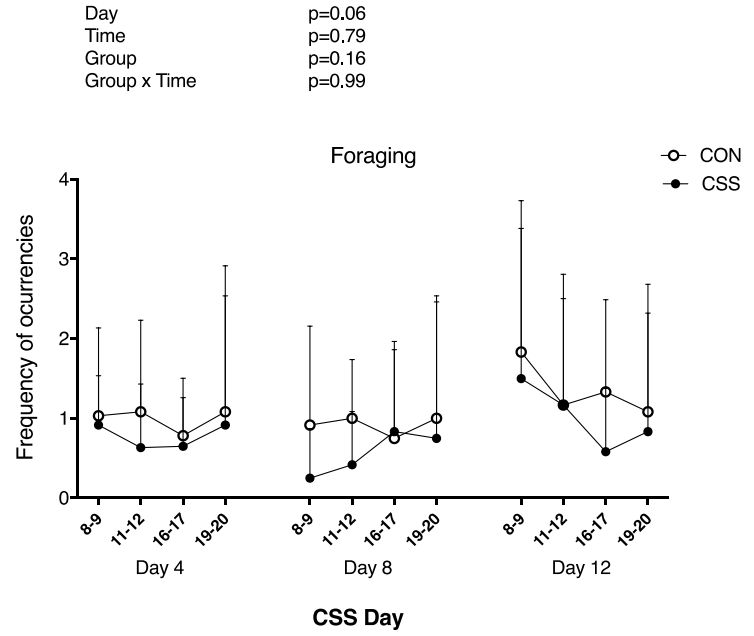

Figure 3.11. Comparison of CSS and CON mice in terms of behaviour on three days and at different time points, during the manipulation phase. (A) Self-grooming. (B) Sitting upright. (C) Resting. (D) Locomoting. (E) Climbing. (F) Eating. (G) Drinking. (H) At divider. (I) Rearing. (J) Foraging. Values are mean + standard deviation, N=12 per group. P values are for Group x Day x Time ANOVA.

3.6. Discussion

Changes in patterns of feeding behaviour and body weight are commonly observed as symptoms in depressive disorders (WHO, 2016) and are often seen in models of chronic social stress. Therefore, body weight and food intake were investigated in the current CSS model. An effect of CSS on energy metabolism was observed, in which stressed animals had either increased food intake with no change in body weight (Experiment B) or similar food intake with decreased body weight gain associated with lower eWAT (Experiment C) when compared to control animals. Calorimetric parameters were evaluated for a greater understanding regarding regulation of energy balance and fuel selection for homeostatic requirements, and *Ucp-1* mRNA expression analysed for evaluation of iBAT thermogenic activity. Indirect calorimetry revealed that EE was similar between stressed and control mice despite the reduced weight gain in the former. The RER was increased in stressed compared to control mice, indicating increased carbohydrate utilisation in the former, associated with lower eWAT. Gene expression of *Ucp-1* in iBAT was not significantly different between stressed and control mice. Additionally, the effect of CSS on individual home-cage behaviour was also studied. Stressed mice showed increased self-grooming behaviour as well as sitting upright behaviour when compared to control animals.

3.6.1. Food intake and body weight

For Experiment B, it was observed that CSS led to increased food intake, especially on the 5 last days of social stress and the post-CSS period. Previous studies also showed an increased feeding in chronically stressed mice (Moles et al., 2006;

Lutter et al., 2008; Chuang et al., 2010a,b; Razzoli et al., 2011a,b; Kumar et al., 2013; Goto et al., 2014; Bergamini et al., 2016). Moreover, there was no effect on body weight, in accord with some previous studies (Moles et al., 2006; Lutter et al., 2008; Savignac et al., 2011; Kumar et al., 2013; Sanghez et al., 2013; Azzinnari et al., 2014; Bergamini et al., 2016; Koch et al., 2016), suggesting a possible effect on EE. In contrast with the present findings, other studies observed increased body weight gain (Chuang et al., 2010a,b; Razzoli et al., 2010, 2011a,b; Patterson et al., 2013; Goto et al., 2014). Interestingly, the studies which demonstrated increased body weight performed slightly different stress protocol to the one presented here. For instance, Goto et al. (2014) performed a milder stress protocol of reduced social defeat duration (0.5 min *versus* 10 min in this study). Patterson et al. (2013) performed a stress protocol of 21 days, *versus* 15 days in this study. Chuang et al. (2010a) reported body weight gain at day 40, following 30 days of the 10-day stress protocol; it was not clear at which point the effects were seen.

For Experiment C, no change in feeding behaviour was found between CSS and CON mice, and CSS mice failed to gain weight across the study, in contrast to CON mice, which gained weight across the study period. This co-occurred with a decrease in eWAT. Absence of the effect of social stress on food intake was previously reported (Bartolomucci et al., 2004; Koch et al., 2016) as well as a decreased body weight gain (Bartolomucci et al., 2004; Balsevich et al., 2014). Of note, body weight loss was recently reported, but this was likely a consequence of the decreased food intake observed in the study (Coccurello et al., 2017). Interestingly, the effect of social stress on body weight may be dependent on various factors such as mouse strain (Razzoli et al., 2011b, c) and the time of the day in which the stress protocol is implemented (Koch et al., 2016). Razzoli et al. (2011c) observed that C57BL6/J

stressed mice did not exhibit altered body weight compared to control mice, whereas stressed Balb/c mice gained significantly less body weight than controls. Savignac et al. (2011) observed decreased body weight gain in stressed Balb/c mice compared to controls, but also increased body weight gain in C57BL6/J stressed mice. Most of the studies using social stress protocols were performed using the C57BL6/J strain, in which increased body weight gain, lack of body weight change (Lutter et al., 2008; Azzinnari et al., 2014; Bergamini et al., 2016) and decreased body weight gain were observed (Balsevich et al., 2014). Therefore, a clear comparison between Balb/c and C57BL6/J or other strains in terms of body weight change is not available. With respect to the time of the day, Koch and et al. (2016) observed that mice had greater body weight loss when the stress protocol was performed during the light phase, when animals are less active (Koch et al., 2016), which was not the case for the current study. Stress protocols performed during the light phase were linked with altered diurnal activity patterns and increased body temperature (Bartlang et al., 2015).

On the other hand, in contrast to mouse studies, various studies in socially stressed rats showed decreased body weight gain *versus* controls (Meerlo et al., 1996; Haller et al., 1999; Becker et al., 2008; Razzoli et al., 2009; Iio et al., 2012, 2014; Olivares et al., 2012; Ahnaou and Drinkenburg, 2016; Liu et al., 2017) and body weight loss (Albonetti and Farabollini, 1994), concomitant with anorexic behaviour (Meerlo et al., 1996; Becker et al., 2008; Iio et al., 2014). Repeated social stress seems to produce different effects between rats and mice as far as feeding behaviour and body weight gain are concerned.

Although Experiments B and C were performed under similar circumstances, results on food intake and body weight gain were different. We also measured body weight in a further study focused on glucose homeostasis, described in Chapter 4. In

this study, metabolic cages were not used, but otherwise the protocol was very similar. In this study, similar to Experiment B, no difference in body weight was observed. Furthermore, a previous study performed in the Pryce laboratory with the same CSS model again reported results similar to Experiment B (Bergamini et al., 2016). Our data suggest there can be some variance in the effects on feeding between experiments for yet unknown reasons. Nonetheless, despite differences in feeding results, in all these studies CSS mice displayed less weight gain per gram of food eaten, *versus* control mice, which suggests a less efficient use of food as energy or greater energy demand.

3.6.2. Indirect calorimetry

With regards to the effects of CSS on the regulation of EE, animals of Experiment C were placed in metabolic cages for measurements of O_2 consumption and CO_2 production, at baseline and post-CSS period. In the present study, we did not observe a significant effect of stress on EE. Nonetheless, these CSS mice displayed less weight gain than CON mice and had less WAT mass. The similar EE with a relatively low BW in stressed mice indicates reduced energy efficiency and/or higher energy requirement in CSS mice for metabolic processes. A recent study performed by Zhao et al. (2017) reported increased hippocampal levels of glycogen phosphorylase (glycogenolysis catalyser) in a mouse model of chronic unpredictable stress, an indication of rapid glycogen breakdown and brain energy demand (Zhao et al., 2017). A relatively novel angle of understanding of the effect of social stress on energy balance emerges.

Although inefficiency of body weight gain in socially stressed mice was previously shown (Moles et al., 2006; Lutter et al., 2008; Bergamini et al., 2016), the

usage of metabolic cages for the purpose of evaluating the effects of chronic social stress on regulation of energy metabolism is scarce. Moles et al. (2006) described the metabolic effects of social stress using indirect calorimetry; the period of 1 hour acclimatisation used was short for single-housing conditions (Stechman et al., 2010). Other studies performed similar experiments, with 6 hours of acclimatisation (Sanghez et al., 2013; Coccurello et al., 2017). Our experiment had a period of 3 days of acclimatisation and evaluated EE and RER in the course of 2 days instead of 17 hours (Moles et al., 2006), 20 hours (Coccurello et al., 2017) or 24 hours (Sanghez et al., 2013).

As previously stated, EE in humans is determined by four main factors: body size (i.e. the bigger the body the greater the RMR), body composition (i.e. RMR is greater when there is more free-fat mass), environment (i.e. ambient temperature) and behaviour (i.e. food intake and physical activity) (Westerterp, 2017). Body composition might wield influence on EE in both groups; however, since it was not determined in the current study, this limitation is present. Additionally, since calorimetric studies were performed at the same temperature, the environment had little to no influence on the regulation of EE in this case.

The previous study by Moles et al. (2006) that reported increased food intake with no change in body weight has also reported increased EE. Nevertheless, such increase was mostly observed when comparing dominant to submissive and control mice; dominant mice showed greater EE *versus* submissive mice, both at baseline and post-stress period and greater EE *versus* control mice at post-stress period. Furthermore, as previously stated, measurements in this study were performed for a total of about 17 hours only (Moles et al., 2006). A similar outcome was reported by Sanchez et al. (2013); however, dominant mice showed decreased body weight gain

in comparison to control mice in this case. The effect of social stress on metabolic rate appears to be dependent on social status (Moles et al., 2006; Sanghez et al., 2013). The recent study performed by Coccurello et al. (2017), using the same obesity-prone C57BL/6 mice strain used in our studies, found an increase of EE from socially stressed mice fed either a standard chow diet or high-fat/high-sugar diet, along with increased iBAT mass, but decreased overall body weight.

In comparison to our findings, these different outcomes could have been the result of fundamental methodological differences of maintaining control animals in brother pairs in the study performed by Coccurello et al. (2017), which was not applied in our case. The reasoning behind not housing together brother pairs of CON mice was that mice interaction following separation at the calorimetry stage might elicit undesired stress-related physiological and/or behavioural changes in the controlled group. Furthermore, physical contact between animals were showed to exert an effect on the physiology and behaviour of animals (Yamada et al., 2015), for the lack of social thermoregulation otherwise present. Group-housed animals can huddle, which reduces their thermoregulatory requirements. Comparison of EE between control animals housed in brother pairs (with lower thermoregulatory needs) and stressed animals single-housed throughout the stress period might exacerbates their difference in energy requirements. Nevertheless, a pilot study comparing CON mice pairs maintained together or separated from each other by a divider demonstrated no effects in tests of motor activity or fear acquisition (Azzinnari et al., 2014). Furthermore, the recent study by Coccurelo was performed following a 24-day stress protocol with 10-min social encounters twice a day, which could have had a prolonged impact on subjects' metabolism. Additionally, measurements of EE and RER were performed for 20 hours, at day 18 of social stress, following 6 hours of adaptation. The present study

instead performed indirect calorimetry prior and after stress protocol, for a period of 2 days and following 3 days of acclimatisation. This novel design allowed for a better longitudinal view on the effects of social stress on EE.

Studies using rats showed that EE increases during repeated restraint (Harris et al., 2006) or chronic mild stress (García-Díaz et al., 2007) and that it was combined to increased BAT temperature and psychosocial stress-induced body hyperthermia (Lkhagvasuren et al., 2011; Kataoka et al., 2014). This was likely mediated by the SNS and activation of β_3 adrenoceptors, which are abundantly expressed in BAT. This study found no consistent effect of stress in BAT activity, regarding *Ucp-1* mRNA expression (discussion addressed in the next section).

With regards to the effects of CSS on RER and fuel selection, the present study has shown that CSS mice have increased RER in comparison to CON mice during the dark phase. Increased RER is an indication of increased utilisation of carbohydrate as the energy source and as a consequence can lead to increase of fat tissue. While increased fat mass in social stress mice was previously reported (Patterson et al., 2013), our study instead observed reduced WAT weight. This may be explained by previous studies that showed enhanced lipid oxidation following social stress (Coccurello et al., 2017). In accord with our results, other studies reported decreased body fat in mice (Chuang et al., 2010b) and rats (Iio et al., 2014). An increase in carbohydrate oxidation observed through RER analysis could be a consequence of increased energy demand by the brain, which processes primarily glucose (Mergenthaler et al., 2013). Therefore, it is necessary to scrutinise the different fuel demands and metabolic profiles across different organs to better comprehend the effects of psychosocial stress on the maintenance of cerebral and peripheral energy homeostasis. The different forms of central and peripheral activation of energy balance

regulators were recently reviewed (Razzoli and Bartolomucci, 2016). Essentially, Razzoli and Bartolomucci (2016) described the three major neuroendocrine systems mediating the components of stress: HPA axis acting on adrenal cortex to stimulate release of glucocorticoids, sympatho-adrenomedullary axis innervating every organ in the body in a specific manner, and peptides, such as ghrelin, leptin and insulin, regulating feeding under different fat content conditions. Moreover, it described the molecular mechanisms of stress-induced positive and negative energy balance as well as the role of adaptive thermogenesis on energy homeostasis.

Research using modulatory neuroendocrine approaches for the investigation of stress-related diseases have increased continuously, despite the diverse metabolic effects of chronic social stress between rodents and humans. Nonetheless, studies using activation of BAT by a sympathetic purinergic system, independently of noradrenaline-dependent β-AR activation, have recently pointed out neuromodulation of adipose tissue in rodents for targeting metabolic disorders in humans. Studies on the effects of CSS on EE in the long-term are also required, for analysing the duration of psychosocial encounters on the regulation of energy balance.

3.6.3. Brown adipose tissue activity – *Ucp-1* mRNA expression

For this study, it was hypothesised that CSS increases *Ucp-1* mRNA expression and EE, which would enlighten the possible lack of calorie efficiency found in our results on food intake and body weight regulation. Activation of BAT were shown to increase energy utilisation for heat production rather than ATP formation (Morrison et al., 2014). Such an increase would subsequently result in less ATP production from fuel sources and would require greater triglycerides lipolysis and release of fatty acids from WAT for adaptive thermogenesis (Blondin et al., 2017), a

mechanism with consequent fat loss.

In order to evaluate the impact of BAT activation on energy metabolism, assessment of BAT depots and BAT *Ucp-1* mRNA expression were performed. In our studies, no difference in BAT mass was found between stress and control mice. Moreover, no significant change in *Ucp-1* mRNA expression was found in socially stressed mice compared to control when using *Gapdh* as the reference gene. When using *Actb* as the reference gene, however, *Ucp-1* was upregulated in stressed mice compared to controls; however that was only seen in Experiment C. Although no significant change was seen in the majority of cohorts, a tendency towards upregulation in stressed mice can be pictured. Overall, since our results have shown no substantial upregulation of mRNA *Ucp-1*, changes in BAT mass or regulation are unlikely to explain the calorie efficiency observed.

A potential explanation for the lack of calorie efficiency observed in this mouse model would be the altered nutrient absorption from the GI tract. The brain's response to stress has a direct effect on the gut; previous studies showed that stressed animals had altered levels of nutrient absorption (Toyoda et al., 2015), gut permeability (Yarandi et al., 2016) and gut microbiota (Bailey et al., 2011). Further studies on the role of CSS on GI nutrient absorption are required.

3.6.4. Behaviour

As previously mentioned, characterisation of behavioural phenotypes is an essential tool in the study of stress-related disorders. The aim of home-cage behaviour analysis performed in Experiment C was to investigate the behavioural frequency of mice subjected to CSS as well as evaluating advancement in the development of such behaviours by analysis of the 3 blocks of stress (CSS days 4, 8 and 12). CSS mice were

more often engaged in self-grooming and sitting upright behaviours, while no effect was found for the remaining behaviours (eating, drinking, foraging, resting, "at divider", locomoting, climbing and rearing).

Self-grooming (licking and scratching of body and head), beyond the primary purpose of hygiene and body care, were shown to act on the stimulation of skin, thermoregulation (Almeida et al., 2015) and also on stress reduction in rodents, with potential translational validity (Roth et al., 2013). Previous studies showed that i.c.v. injection of CRH in rats induced an increase in self-grooming behaviour (Sutton et al., 1982; Gargiufo and Donoso, 1996). Furthermore, a single episode of stress (i.e. acute stress) were also shown to significantly increase grooming behaviour (Füzesi et al., 2016). Nonetheless, chronic social stress seems to exert an opposite effect; a previous study had suggested a pronounced effect of chronic social stress on self-grooming frequency, time and patterning in mice (Denmark et al., 2010), in which a decrease in the percentage of grooming body transitions was observed. Moreover, decreased self-grooming behaviour were also observed in chronically stressed rats (Razzoli et al., 2007; Denmark et al., 2010; Ahnaou and Drinkenburg, 2016). Our study, in contrast, showed that CSS increases self-grooming frequency. Interestingly, an absence of effect on corticosterone were observed in the same animal model of stress (Azzinnari et al., 2014). Since stress paradigms such as the one used in the present study can include biting, one explanation for the increase in self-grooming behaviour would be intensification in wound licking. Nonetheless, since the frequency of bite wounds was low to none in this study due to CD-1 teeth-trimming, it is unlikely to have caused this increase. These conflicting results are possibly due to methodological differences in analysing self-grooming behaviour. The cumulative scores showed here provide little-

detailed analysis of this rather complex behaviour and therefore further observations should be made in the future.

3.7. Conclusion

In summary, the present experiments suggest that CSS in mice leads to reduced energy efficiency and/or increased energy requirements for metabolic processes. This is evident in both experiments despite the variation in the feeding and bodyweight results observed between the experiments. A change in metabolism following CSS is further supported by our observation of an increased respiratory exchange ratio as an indication of increased carbohydrate utilisation. It is plausible to speculate that the body adapts to chronic stress by making glucose preferentially available as a fuel. This is explored further in Chapter 4. However, this effect on fuel utilisation does not fully explain the metabolic inefficiency observed in the present model, and additional factors such as the potential effects of stress on GI absorption may play a role and should be investigated in further studies.

The variation in the feeding and body weight results observed between the two studies in this chapter highlights how groups of mice, like humans, can vary in their responses to social stress. It is possible that subtle undetected differences in the experimental environment may lead to substantial changes in the response to social stress or indeed, to the status of the mice in the control group. Indeed, these differences to the evidence that similar models of stress in different laboratories report varying effects on feeding and body weight.

CHAPTER 4

Effects of chronic social stress on neuroendocrine regulators of feeding and glucose metabolism

4.1. Introduction

The brain receives short-term and long-term satiety signals from peripheral organs important for the regulation of feeding behaviour and EE (Morton et al., 2014). The effects of CSS on the hormone ghrelin, a proposed appetite signal derived from the stomach, and leptin, a satiety signal derived from fat stores, are investigated in the current chapter. In addition, the effect of CSS on glucose homeostasis is examined.

4.1.1. Stress and neuroendocrine regulators of feeding

4.1.1.1. Ghrelin

Elevated ghrelin levels were previously reported in mouse models of chronic social stress (Lutter et al., 2008; Chuang et al., 2011; Patterson et al., 2013). There is evidence that this increase in ghrelin levels has anti-depressive effects including increased latency to immobility in the forced swim test, and that it acts as a defence mechanism in chronic social stress (Lutter et al., 2008) as well as in other models, e.g. chronic unpredictable mild stress (Huang et al., 2017).

Stress-related symptoms appear to be directly linked to the ghrelin receptor; for instance, following acute stress, GHS-R KO mice developed more anxiolytic behaviours compared to WT mice (Spencer et al., 2012). In chronic social stress, GHS-R KO mice displayed increased social avoidance (i.e. depression-like behaviour) (Lutter et al., 2008; Chuang et al., 2011). In regards to the effects of chronic social stress on ghrelin-associated feeding, a study reported an attenuated effect of chronic social stress on food intake and body weight gain in GHS-R KO mice (Patterson et al., 2013). Similar findings were reported in mice subjected to chronic unpredictable stress

(Patterson et al., 2010). Interestingly, corticosterone levels increased similarly in WT and GHS-R KO mice, suggesting that effects on feeding and body weight were due to the increase in ghrelin rather than the increase in corticosterone (Patterson et al., 2013).

The effect of chronic social stress on ghrelin appears to be consistent (Lutter et al., 2008; Kumar et al., 2013; Patterson et al., 2013), and interestingly it was observed in both models/studies that reported body weight increase (Patterson et al., 2013) and those which did not (Lutter et al., 2008).

Whilst it is clear that ghrelin levels are initially elevated after chronic social stress, the duration of this effect is unclear. Lutter et al. (2008) reported that plasma ghrelin concentrations remained elevated 4 weeks after the stress period. Nonetheless, Patterson et al. (2013) showed that effects were lost after a period of 3-weeks recovery. Recently, using a model of PTSD in rats with a history of stress exposure, a study reported elevation in acyl ghrelin for a period of 130 days following tail immobilisation stress (Yousufzai et al., 2018).

Also in humans, stress has been shown to increase plasma ghrelin levels; acute psychological stressors in the form of speech delivery and other mental challenges increased ghrelin in humans of normal weight (Rouach et al., 2007). Following exposure to a severe stressor, i.e. traumatised children affected by terrorist activities, adolescent humans also displayed increased ghrelin, for a minimum of 4 years (Yousufzai et al., 2018). Furthermore, in response to stressor anticipation, women displayed increased ghrelin in comparison to women in control conditions (Raspopow et al., 2014).

4.1.1.2. Leptin

Altered levels of leptin have also been frequently described in animal models of chronic social stress. Some studies reported that chronically stressed mice on both chow and HFD had decreased adipose tissue and decreased serum leptin (Chuang et al., 2010b; Balsevich et al., 2014), whereas another study reported decreased plasma leptin despite increased body weight (Finger et al., 2012). Decreased leptin levels were also reported in the absence of an effect on body weight (Kumar et al., 2013; Bergamini et al., 2016). As discussed in the Chapter 1, body fat exerts influence on leptin levels; nonetheless, the effect of chronic stress on leptin observed for various body weight outcomes suggests the altered leptin is independent of changes in adipose tissue mass.

No effect on plasma leptin was also reported in stressed mice (Razzoli et al., 2011a, b, c; Patterson et al., 2013). Equally in rats, in a protocol consisting of 3 daily social defeat experiences, Razzoli et al. (2009) reported similar levels of plasma leptin following one day of social stress; nevertheless, an increase in leptin was reported 21 days after the last defeat, despite body weight loss.

Dietary fat-content was reported to exert influence on the duration of stress-related changes in leptin levels (Finger et al., 2011, 2012); leptin levels were found to be decreased up to three weeks after chronic psychosocial stress (mix of social defeat and overcrowding) in mice on a low-fat diet, however this effect was prolonged to six weeks when on an HFD (Finger et al., 2012). Moreover, effects of time of the day on plasma leptin were also observed: mice under chronic social stress showed decreased leptin compared with control mice during the late light phase and early dark phase but not during the early light phase and late dark phase (Kumar et al., 2013).

While various studies described alterations in plasma concentrations of ghrelin and leptin in response to stress, the effects of chronic social stress on the brain-region expression of Ghs-r1a and the Lepr and their respective genes were not yet investigated. Such data are essential for the understanding of the effects of chronic social stress on ghrelin and leptin systems.

4.1.1.3. Insulin

Stress has been reported to exert both positive and negative effects on glucose homeostasis. For instance, chronic social stress were shown to promote the impairment of glucose tolerance (Tsuneki et al., 2013); it was associated with increased fasting glucose levels in both standard and HFD, accompanied by elevated insulin levels, which suggested a degree of insulin resistance, in the presence of body weight difference (Chuang et al., 2010a). Nonetheless, hypophagia and weight loss associated with chronic stress were shown to improve the obesity features of impaired glucose tolerance as well as insulin and leptin resistance (Balsevich et al., 2014); mice under HFD presented increased glucose and insulin levels, and hypophagia and weight loss induced by chronic social stress were able to counteract these effects (Balsevich et al., 2014). In line with that, Finger et al. (2011) observed that diet-induced obese mice were resistant to stress-induced depressive-like behaviour such as increased immobility in the forced swim test. Moreover, a recent study reported that subordinate mice which showed signs of metabolic syndrome and type 2 diabetes (e.g. hyperphagia, high leptin and dyslipidemia) were euglycemic when fed a standard diet; these results led to the hypothesis that stress might predispose mice to develop type 2 diabetes when combined with risk factors such as an HFD (Sanghez et al., 2013).

Preliminary studies from our laboratory reported increased food intake coupled with unchanged body weight (Bergamini et al., 2016), suggesting increased energy need and/or impaired calorie efficiency. Studies reviewed in Chapter 3 showed either no change in body weight or a decrease in body weight gain. The current CSS model therefore represents a good opportunity to study the effects of chronic social stress on glucose homeostasis in the absence of obesity. In order to assess the metabolic phenotype of this mouse model of chronic social stress, an intraperitoneal glucose tolerance test (GTT) was performed.

4.2. Hypotheses

Chronic social stress in mice:

4.2.1. Up-regulates the ghrelin system and down-regulates the leptin system

4.2.2. Leads to impaired glucose tolerance

4.3. Aims

To investigate the effects of chronic social stress on:

4.3.1. Plasma ghrelin and leptin levels

4.3.2. Ghrelin system

4.3.2.1. GHS-R1a-positive cells number in mouse arcuate nucleus (ARC), ventromedial hypothalamus (VMH) and ventral tegmental area (VTA)

4.3.2.2. *Ghs-r1a* gene expression in mouse paraventricular hypothalamic nucleus (PVN), arcuate nucleus (ARC), ventromedial nucleus (VMH) and ventral tegmental area (VTA)

4.3.3. Leptin system

4.3.1.1 *Lep* and *Lepr* gene expression in mouse eWAT

4.3.1.2. *Lepr* gene expression in mouse medial prefrontal cortex (mPFC), nucleus accumbens (NAcc), paraventricular hypothalamic nucleus (PVN), arcuate nucleus (ARC), ventromedial nucleus (VMH) and ventral tegmental area (VTA)

4.3.4. Glucose homeostasis, through evaluation of blood glucose and plasma insulin levels, following a glucose tolerance test

4.4. Methodology

4.4.1. Blood collection

Collection of blood followed the same procedure for all experiments. Following CSS on days 1-15, on day 16 (in Experiment A) or day 20 (Experiment C) mice were fasted overnight. On the following day mice were decapitated and the trunk blood (300-500μL) was collected into EDTA-coated tubes (Microvette 500 K3E, Sarstedt) and placed on ice. For plasma active ghrelin, 100μL blood was subsequently transferred into a second tube (Microvette 300 Z, Sarstedt) containing esterase inhibitor AEBSF (A8456, Sigma) to a final concentration of 1mg/mL. Blood was centrifuged at 3000 rpm and 4˚C for 10 min, plasma aliquots were transferred to cryotubes (Protein LoBind, Eppendorf) and, in the case of the sample for ghrelin determination, followed by HCl acidification (Merck Millipore) to a final concentration of 0.05N, to prevent catabolism of active ghrelin. For plasma leptin measurements, the trunk blood collected into EDTA-coated tubes was directly centrifuged for plasma separation. Plasma samples were stored at -80°C. Blood collection for the glucose tolerance test is explained later in this chapter.

4.4.2. Plasma active ghrelin – Enzyme immunoassay

Experiment A (please refer to Chapter 2, 'Methodological framework').

Analysis of plasma active ghrelin (acyl ghrelin) was performed using Rat/Mouse Sandwich ELISA (#EZRGRA-90K, Merck Millipore), according to the manufacturer's instructions. The sensitivity of the assay based on 20μL is 8pg/mL. All reagents were brought to room temperature prior to use. Assembled well strips were

washed three times using wash buffer (300µL/well), followed by the addition of Matrix solution (20µL) to blank, standards and quality control wells. Assay buffer was added to each of the blank and sample wells (20µL), as well as to each of the standard and quality control wells (10µL). Ghrelin standards, QC 1 and 2 and unknown samples were added in duplicate (20µL). Antibody solution mixture (1:1 capture and detection antibody) was added to each well (50µL) and left for incubation for 2 hours at RT on an orbital plate shaker, set at moderate speed. This first reaction consisted of the capture of ghrelin molecules in the sample by anti-ghrelin antibody and immobilisation of the resulting complex to plate wells, followed by binding of a second, biotinylated antibody to ghrelin. Well contents were aspirated and washed three times using wash buffer (300µL/well). The enzyme solution (100µL) was dispensed into wells and the plate was left for incubation for 30 mins at RT. This second reaction consisted of binding of horseradish peroxidase (POD) to the immobilised biotinylated antibodies. 3,3',5,5'-tetramethylbenzidine (TMB) substrate solution (100µL) was immediately dispensed into wells and left for 5 to 20 mins, depending on the colour development, for detection of the POD conjugate. The enzyme reaction was stopped by adding 100µl of the enzyme reaction stop solution. Absorbance (A_{490}/A_{620}) was measured within 5 min and ghrelin concentration was determined via interpolation using the standard curve generated by plotting absorbance *versus* the corresponding concentration of ghrelin standards.

Please refer to Appendix 3 for the standard curve of plasma ghrelin.

4.4.3. Plasma leptin – Enzyme immunoassay

Experiment C (please refer to Chapter 2 for 'Methodological framework').

Analysis of plasma leptin was performed using Mouse Sandwich ELISA (CrystalChem, #90030), according to the manufacturer's instructions. Sensitivity range of the assay based on 5µL is 0.2 – 12.8ng/mL. All reagents were brought to RT prior to use. Assembled well strips were washed two times using wash buffer (300µL/well), followed by addition of sample diluent (45µL) and guinea pig anti-mouse leptin serum (50µL). Standards and samples (5µL) were added to the wells, followed by overnight (16 – 20 hours) incubation at 4°C. This first reaction consisted of simultaneous binding of the mouse leptin in the sample to the rabbit anti-leptin antibody coated on the microplate well and the anti-leptin IgG of the guinea pig anti-mouse leptin serum added to each well. On the second day, well contents were aspirated and washed five times using wash buffer (300µL/well). The anti-guinea pig IgG enzyme conjugate (100µL) was dispensed into wells and the plate was left for incubation for 3 hours at 4°C. This second reaction consisted of binding of horseradish POD-conjugated anti-guinea pig IgG antibody to the guinea pig anti-leptin IgG of the complex immobilised to the microplate well. Well contents were aspirated, washed seven times using wash buffer (300µL/well), and the TMB substrate solution (100µL) was immediately dispensed into wells and left to react for 30 min at RT, for detection of the POD conjugate. The enzyme reaction was stopped by adding 100µl of the enzyme reaction stop solution. Absorbance (A_{490}/A_{620}) was measured within 30 min and leptin concentration was determined via interpolation using the standard curve generated by plotting absorbance *versus* the corresponding concentration of leptin standards.

Please refer to Appendix 3 for the standard curve of plasma leptin.

4.4.4. White adipose tissue – *Lep* and *Lepr* mRNA expression

Expression of *Lep* and *Lepr* was measured in eWAT by RT-qPCR.

4.4.4.1. Epididymal white adipose tissue dissection

Experiment C (please refer to Chapter 2 for 'Methodological framework').

As described in Chapter 3.

4.4.4.2. RNA extraction

Similar to the RNA extraction from iBAT tissue described in Chapter 3, the RNA from frozen eWAT was also extracted using RNeasy Lipid Tissue Mini Kit (Qiagen®). However, instead of disrupting tissue in TissueLyser LT (QIAgen®) for 7 min at 50 Hz, eWAT was disrupted for 5 min at 50 Hz, due to its softer consistency.

'RNA purity and quantity' and 'RNA integrity' steps were performed as shown in Chapter 3 for *Ucp-1* mRNA expression.

4.4.4.3. Reverse transcription

As performed for *Ucp-1* mRNA expression, described in Chapter 3.

4.4.4.4. Quantitative polymerase chain reaction

As performed for *Ucp-1* mRNA expression, described in Chapter 3.

4.4.4.4.1. Primer design

Primer pairs for *Lep* were designed using NCBI Primer-BLAST, with the parameters set similarly to *Ucp-1* and synthesised by Invitrogen (ThermoScientific™). Predesigned KiCqStart® primer pair for mouse *Lepr* was purchased from Sigma-

Aldrich. Two genes, *Gapdh* (Matoušková et al., 2014) and *Actb*, were used as housekeeping genes, for increased accuracy of the results (Kozera and Rapacz, 2013).

4.4.4.4.2. PCR efficiency

As performed for *Ucp-1* mRNA expression, described in Chapter 3.

Table 4.1. Gene description, primer sequences, qPCR parameters and primer efficiency

Gene	Primer sequence ('5 – 3')	PCR product (bp)	Annealing temp. (°C)	Extension (sec)	PCR *E* (%)
Lep	FW: TTTCACACACGCAGTCGGTA RV: GCACATTTTGGGAAGGCAGG	150	63	40	96
Lepr	FW: TTTCACACACGCAGTCGGTA RV: GCACATTTTGGGAAGGCAGG	138	60	30	109
Actb	FW: GGCTGTATTCCCCTCCATCG RV: CCAGTTGGTAACAATGCCATGT	154	63	30	103
Gapdh	FW: AGGTCGGTGTGAACGGATTTG RV: TGTAGACCATGTAGTTGAGGTCA	123	63	40	96

4.4.5. Brain region-specific – Ghs-r1a immunopositive cell number

Using stereological methodology, effects of CSS on the total GHS-R1a immunopositive cell number was also investigated. Areas of interest included arcuate nucleus (ARC) and ventromedial hypothalamus (VMH) within the hypothalamus and the ventral tegmental area (VTA) located in the midbrain. The brain samples used for this study were obtained from a previous experiment conducted in the same laboratory.

4.4.5.1. Brain tissue dissection and cryosectioning

On day 19, in a cohort of mice (CSS N=6, CON N=7) that had not been fasted overnight, brains were perfused with 4% paraformaldehyde, removed, post-fixed, cryopreserved in 30% sucrose solution and stored at -80°C prior to cryostat sectioning.

Frozen brains were placed in a cryostat set at -19˚C (Bright, model 11122/EX) and sectioned coronally at 25µm. Using a mouse brain atlas (Paxinos and Franklin, 2004), the following regions were harvested: arcuate nucleus, ventromedial hypothalamus and ventral tegmental area (Figure 4.1 and Table 4.2). Collected brain sections were stored in sucrose and anti-freezing solution at -20˚C for preservation prior to immunohistochemistry.

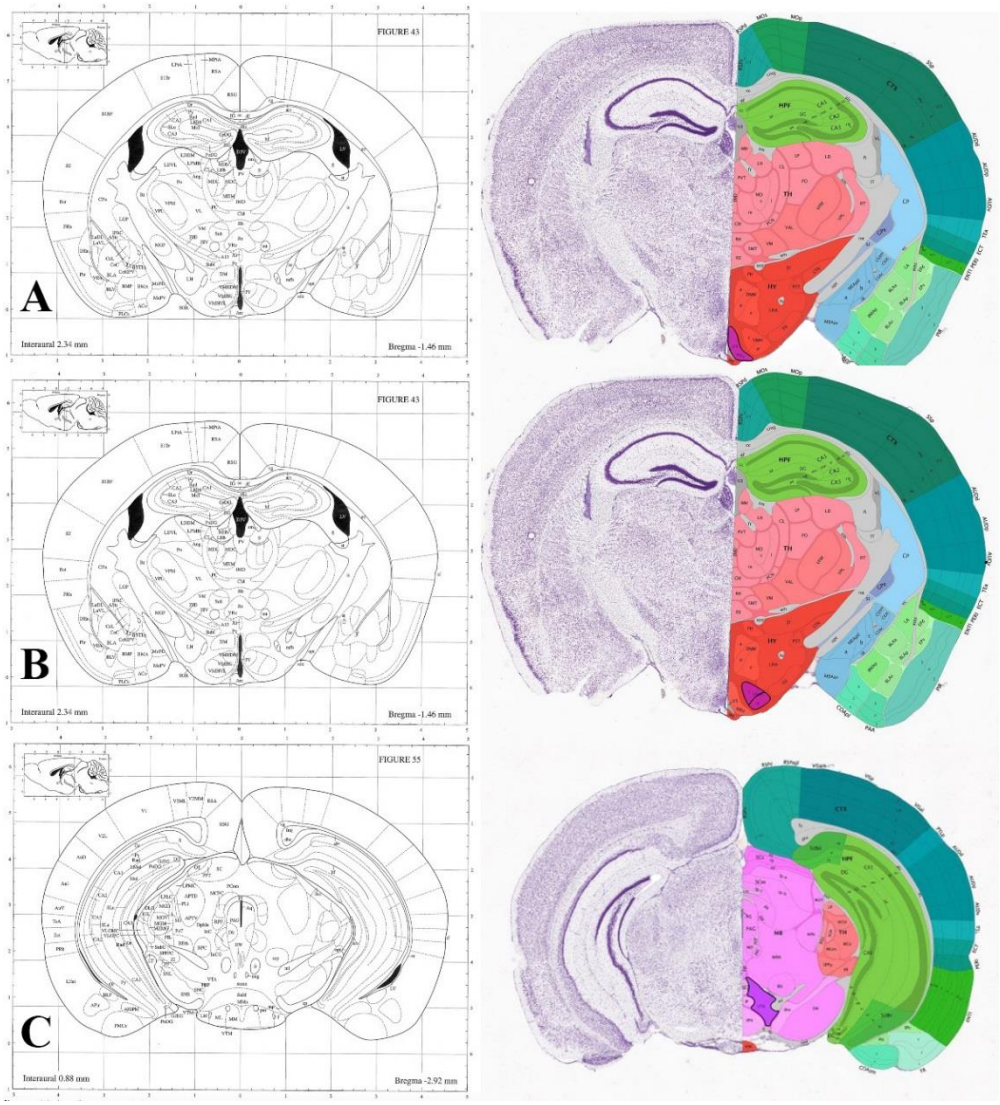

Figure 4.1. Representative coronal mouse brain sections depicting regions of interest for the investigation into effects of 15-day chronic social stress on GHS-R1a cell number, by immunohistochemistry. On the left, representative figures (from Paxinos and Franklin, 2004) depicting the target region for (A) ARC. (B) VMH. (C) VTA. On the right, representative images (from Allen Mouse Brain Atlas) illustrating regions of interest (dark purple).

Table 4.2. Fundamental details of brain region sectioning, according to The Mouse Brain in Stereotaxic Coordinates (Paxinos and Franklin, 2004)

Brain/region	**Bregma interval**
ARC, VMH	-1.34 – -1.70
VTA	-2.48 – -3.68

Abbreviations: ARC, arcuate nucleus; VMH, ventromedial hypothalamus; VTA, ventral tegmental area.

4.4.5.2. Immunohistochemistry incubation

The procedure was adapted from Abizaid et al. (2006). Optimisation of 1st Ab concentration was performed (1:2000, 1:1000, 1:500 and 1:250) for best staining result.

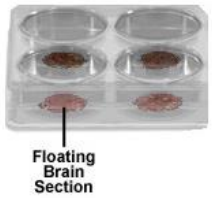

On day 1, brain sections from CSS and CON mice were taken out from the freezer and placed in a 4-well petri-dish (5-7 sections/well). Petri-dish wells were divided for CSS, CON and BLANK samples. In order to wash out storage sucrose solution, samples were washed 5x10min in 10mM phosphate buffered saline (PBS) on the vibrant shaker (200rpm/min, RT). Afterwards, sections were treated with 1% hydrogen peroxide (H_2O_2) (Sigma-Aldrich) in 10mM PBS for 15 min (200rpm/min, RT) in order to inhibit endogenous peroxidase, followed by additional rinsing steps in 10mM PBS (3x10min, 200rpm/min, RT). Blocking solution of 10% normal goat serum (VECTASTAIN® Elite® ABC System, Vector Laboratories) was added to each well and left for 1h incubation on the vibrant shaker (200rpm/min, RT). The blocking solution was then rinsed off with 10mM PBS on the vibrant shaker for 5x10min, followed by addition of the 1:250 1st Ab (Rabbit Anti-GHS-R1a, CYS0 330 336, Phoenix Pharmaceuticals) or vehicle solution (blank). The dish was left for 30 min on the vibrant shaker at RT, followed by overnight (20h) incubation in ice (200rpm/min).

On day 2, 1st Ab solution was rinsed off with 10mM PBS for 10 min and in 0.01% PBST for 5 min on the vibrant shaker, followed by additional rinsing steps in 10mM PBS (3x10min, 200rpm/min, RT) to remove any excess of unbound 1stAb. The second antibody (Goat anti-rabbit IgG, VECTASTAIN® Elite® ABC System, Vector Laboratories) was applied and left to incubate for 30 min on the vibrant shaker (150rpm/min). During the incubation period, ABC complex (Vectastain Elite streptavidin-avidin-peroxidase ABC Kit, PK 6100 Series, Vector Laboratories) was prepared and left standing for 30 min. The second Ab was rinsed off with 10mM PBS on the vibrant shaker (3x5min, 150/min, RT) followed by the addition of the ABC complex (30min, 150rpm/min, RT). This complex has a large protein avidin with a high affinity for biotin, a low molecular weight vitamin that can be conjugated with antibodies. Avidin can be labelled with peroxidase developed with 3'3 diaminobenzidine DAB (Sigma-Aldrich) to produce a coloured label. In this case, DAB was mixed with ammonium-nickel-sulphate (Sigma-Aldrich) solution to bring out details of immunoreactive structures in immunostained preparations, resulting in a black reaction production. For the removal of the ABC complex, sections were rinsed with 10mM PBS on the vibrant shaker (3x10min, 150/min, RT). The DAB solution was applied into wells, incubated for 2 min and the reaction was stopped by application of 1% H_2O_2 in PBS. The solution was aspirated quickly to avoid tissue damage and rinsed with 10mM PBS on the vibrant shaker (3x10min, 150/min, RT) to remove the excess of DAB. Sections were then gently mounted onto slides with a small brush and left to air-dry. Sections were dehydrated with a series of ethanol gradients (50%, 70%, 90% and 100%), for 5min each and left to air-dry for 10 min. Sections were protected with glass cover slips (22x22mm) using mounting media (Histomount®, National Diagnostics) and left to air-dry overnight.

Please refer to Appendix 2 for reagents and solutions.

4.4.5.3. Image analysis

GHS-R1a immunoreactive cells in the ARC, VMH and VTA were counted using the optical fractionator (Stereo Investigator®, Version 10, Microbrightfield Bioscience, Inc.). The neuroanatomical regions of interest were traced based on a mouse brain atlas (Paxinos and Franklin, 2004). Unbiased estimation of the total number of cells was achieved by choosing every 5th section yielding 5 to 7 sections per animal. Average mounted section thickness of 25µm was firstly manually entered in the analysis. Top and bottom guard regions of 4µm were used to compensate for cell post-processing section damage, and dissector height of 12µm was used for counting frame depth. Regions of interested were visualised and traced using a low magnification lens (2x); cell counting was performed under higher lens magnification (40x). Sampling frame and grid size (X: 100µm, Y: 100µm) were applied (Figure 4.2), comprising two inclusion lines (green) and two exclusion lines (red). An object (i.e. cell) was not included in the counting if it crossed or was outside the exclusion lines.

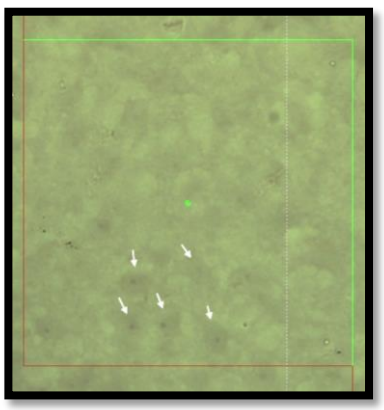

Figure 4.2. A representative example of a brain section depicting GHS-R1a positive immunoreactive cells and the visualisation of their clearly-defined nuclei (white arrows).

4.4.6. Brain region-specific – *Ghs-r1a* and *Lepr* mRNA expression

Experiment C (please refer to Chapter 2 for 'Methodological framework').

Expression of genes was measured in selected brain regions by RT-qPCR.

4.4.6.1. Brain tissue dissection, cryosectioning and micro-punching

Following completion of *in vivo* experiments on day 20 (Experiment C) mice were fasted overnight and sacrificed for brain collection by decapitation. Brains were quickly dissected from the skull, rinsed with ice-cold saline solution, snap-frozen at -40°C in 2-methylbutane (Sigma-Aldrich) and stored at -80˚C until analysis. Prior to brain sectioning and punching, all materials including cryostat chambers were decontaminated for removal of nucleic acid contaminants (DNA-ExitusPlus™, AppliChem). Frozen brains were embedded in optimal cutting temperature (OCT) compound, vertically mounted onto the cryostat chuck, placed in the cryostat which was previously set at -18˚C (Bright, model 5040 OTF/AS) and cut coronally into 300µm sections (Figure 4.3).

Figure 4.3. Brain mounting onto steel chuck followed by cryostat sectioning.

Using brain punches (Ø=0.5 and 1 mm, model 57397, Stoelting Europe) and a mouse brain atlas (Paxinos and Franklin, 2004), the following regions represented in Figure 4.4 and Table 4.3 were microdissected (model OTF5000, Bright) and transferred into 2 ml cryotubes (Protein LoBind, Eppendorf). The microdissection was conducted at -24˚C chamber temperature. Punches were stored at -80˚C until analysis.

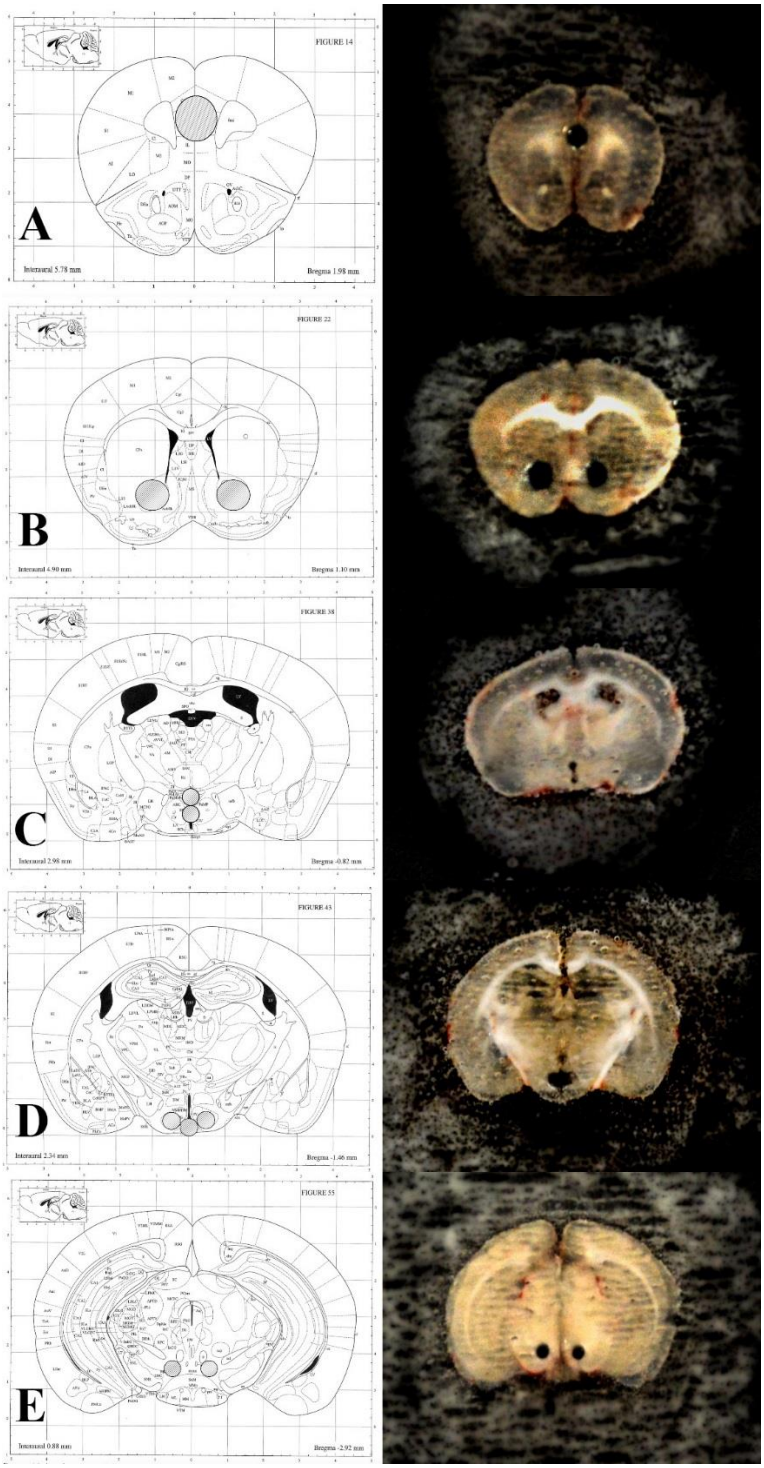

Figure 4.4. Neuroanatomical regions used for investigation into effects of 15-day chronic social stress on region-specific gene expression at day 21, using quantitative PCR with mRNA obtained from CSS mice (N=12) and CON mice (N=12). On the left, representative figures (from Paxinos and Franklin, 2004) depicting the target region for (A) mPFC. (B) NAcc. (C) PVN. (D) ARC and VMH. (E) VTA. On the right, representative computer-enhanced photographs of brain sections taken subsequently to the punch.

Table 4.3. Anatomical details of brain region microdissection, according to The Mouse Brain in Stereotaxic Coordinates (Paxinos and Franklin, 2004)

Brain/region	Bregma interval	Ø (mm)
mPFC	1.98 – 1.42	1
NAcc	1.42 – 0.74	1
PVN	0.02 – -1.94	0.5
ARC	-1.34 – -1.94	0.5
VMH	-1.34 – -1.94	0.5
VTA	-2.92 – -3.80	0.5

Abbreviations: mPFC, medial prefrontal cortex; NAcc, nucleus accumbens; PVN, paraventricular nucleus (including periventricular nucleus); ARC, arcuate nucleus; VMH, ventromedial hypothalamus; VTA, ventral tegmental area.

Initially, *Ghs-r1a* mRNA analysis was aimed to be completed for all the regions mentioned in the table above; nevertheless, due to limitations in the process of the RNA extraction, the amount of RNA extracted was not sufficient for investigation of the expression of *Ghs-r1a* mRNA in the mPFC and NAcc.

4.4.6.2. RNA extraction

The RNA was extracted from the brain using a RNeasy Micro Kit (Qiagen®), designed to purify RNA from small amounts of starting material (up to 5mg). Tissue disruption was performed as follows: QIAzol Lysis Buffer RLT (500µL mixed with 10 µL/ml of β-mercaptoethanol) was added to each tube containing two stainless steel beads (ø 5mm, QIAgen®) and placed in a TissueLyser LT (QIAgen®) for 3 min at 40 Hz. The lysate was transferred to a new tube and centrifuged for 3 min at full speed (14800rpm). The supernatant was then transferred to a new tube, one volume of 70% ethanol was added to induce RNA precipitation and the tube vortexed. The solution was loaded onto a RNeasy Mini spin column placed in a collection tube and centrifuged at 10000rpm for 15 sec at RT. The flow-through was discarded. This

procedure was performed twice until all tube content had been transferred. Washing buffer RW1 (350µL) was added to the RNeasy MinElute spin column, centrifuged at 10000rpm for 15 sec at RT and flow-through was discarded. DNase I solution (80µL) diluted in RDD buffer (RNase-Free DNase Set, QIAgen®) was added directly to the spin column membrane. The membrane was left for 15 min at RT to allow DNase digestion and gDNA removal. Washing buffer RW1 (350µL) was added to the RNeasy MinElute spin column, centrifuged at 10000rpm for 15 sec at RT. Flow-through and collection tube were discarded. With a new collection tube, 500µL of washing buffer RPE was added to the RNeasy MinElute spin column for removal of salt traces, and it was centrifuged again at 10000rpm for 15 sec at RT. 80% ethanol (500 µL) was added to the RNeasy MinElute spin column; flow-through and collection tube were discarded. The RNeasy spin column was placed in a new collection tube and centrifuged at full speed (14800rpm) for 5 min with the lid opened, in order to dry the spin membrane and ensure no ethanol was carried over during RNA elution. The RNeasy spin column was again placed in a new tube, 14µL of RNase-Free water were added directly to the membrane and centrifuged at full speed for 1 min.

4.4.6.2.1. RNA purity and quantity

As performed for *Ucp-1* mRNA expression, described in Chapter 3.

4.4.6.2.2. Quality control of RNA extraction

Assessment of quality control for RNA extraction was performed using a series of 6 punches (0.5-5) from the same brain region (e.g. cortex). Pearson's Correlation Coefficient (*r*) was calculated.

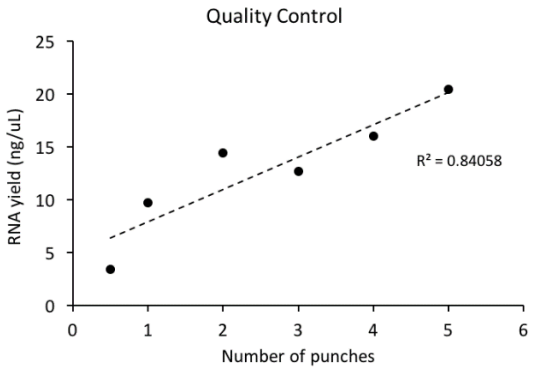

Figure 4.5. Linear correlation between the number of cortex punches and RNA yield achieved from RNA extraction. Coefficient of correlation *r*=0.92.

4.4.6.2.3. RNA integrity

Visual assessment of RNA integrity could not be performed as a minimum of 1µg of RNA is generally required in order to successfully run agarose gel electrophoresis.

4.4.6.3. Reverse transcription

Synthesis of cDNA from the RNA template was performed. Depending on the RNA yielded from each brain region punched, different amounts of RNA were used per region, but always the same amount was used for all the subjects within the same region (Table 4.4). The RNA was then reverse transcribed as performed for *Ucp-1* mRNA expression, described in Chapter 3.

Table 4.4. Amount of RNA (ng) used for reverse transcription according to brain region

Brain/region	RNA (ng)
mPFC	85
NAcc	110
PVN	100
ARC	30
VMH	50
VTA	65

Abbreviations: mPFC, medial prefrontal cortex; NAcc, nucleus accumbens; PVN, paraventricular nucleus; BLA, basolateral amygdala; ARC, arcuate nucleus; VMH, ventromedial hypothalamus; VTA, ventral tegmental area; RN, raphe nuclei.

4.4.6.4. Quantitative polymerase chain reaction

As performed for *Ucp-1* mRNA expression, described in Chapter 3.

Table 4.5. Details of the 2-step cycling protocol for qPCR

1. Pre-incubation	5 min 95°C	denaturation
2. PCR (40 cycles)	10 sec 95°C	
	30 sec 60°C*	annealing/extension

* specific temperature of primer pairs is described in *Section 'PCR efficiency'*.

4.4.6.4.1. Primer design

Predesigned primer pairs for *Ghs-r1a* and *Lepr* were purchased from KiCqStart® (Sigma-Aldrich). The *Actb* primer pair was designed using NCBI Primer-BLAST, with the parameters set to create a product of 70-200bp and primer melting temperature ranging from 57°C to 63°C. BLAT (BLAST-Like Alignment Tool) from UCSC Genome Browser was used to check for primer sequence alignment. Primers were synthesised by Invitrogen (ThermoScientific™) and working stocks containing both FW and RV primers at a concentration of 10μM were prepared.

4.4.6.4.2. PCR efficiency

As performed for *Ucp-1* mRNA expression, described in Chapter 3.

Table 4.6. Gene description, primer sequences, qPCR parameters and primer efficiency

Gene	Primer sequence ('5 – 3')	PCR product (bp)	Annealing temp. (°C)	Extension (sec)	PCR *E* (%)
Lepr	FW: TTTCACACACGCAGTCGGTA RV: GCACATTTTGGGAAGGCAGG	138	60	30	106
Ghs-r1a	FW: ACAAACAGACAGTGAAGATG RV: TGTAGAGAATGGGGTTGATG	197	60	30	102
Actb	FW: GGCTGTATTCCCCTCCATCG RV: CCAGTTGGTAACAATGCCATGT	154	63	30	103

4.4.7. Glucose tolerance test

Experiment A (please refer to Chapter 2 for 'Methodological framework').

Mice were fasted for 14 hours on CSS day 9. On CSS day 10, between 8-10am, a 20% β-D-glucose solution (Sigma-Aldrich) was administered intraperitoneally (10µL/g body weight), according to Bowe et al. (2014). Blood samples were drawn from the lateral tail vein (50µl/sample) immediately prior to (-1 min) and at 15, 30, 45, 60 and 120 min after glucose administration (total blood volume 6 x 50 = 300µl). For blood collection, the tail of the mouse was warmed with an infra-red lamp to cause vasodilatation and the mouse was then placed inside a restraint tube that allowed access to the tail (as shown in Figure 4.6).

Figure 4.6. Mouse restrainer, 2'' diameter tube with sliding nose restraint lock knob, ports and tail access for blood collection.

At the first blood sampling a 1-2mm incision was made on the lateral surface of the tail, approximately 15mm from the tip. The tail was then massaged gently, and 50µL of blood was collected into a capillary tube (Microvette® CB300µl, K2 EDTA, Sarstedt) and then placed on ice for analysis of plasma insulin levels. All subsequent samples were collected from the same incision site. Immediately after each blood draw, a small amount of blood was collected on a blood glucose test strip for immediate estimation of the blood glucose level using a hand-held blood glucose meter (ACCU-CHEK Aviva, Roche Diabetes Care Limited). Following blood sampling, capillary tubes were centrifuged at 3000 rpm and 4˚C for 10 min, plasma aliquots were transferred to cryotubes (Protein LoBind, Eppendorf) and stored at -80˚C.

Please refer to Appendix 2 for the detailed preparation of glucose solution.

4.4.8. Plasma insulin – Enzyme immunoassay

Analysis of plasma insulin was performed using Ultra-Sensitive Sandwich ELISA Assay for mouse samples (CrystalChem, #90080), according to the manufacturer's instructions. Sensitivity range of assay based on 5µL is 0.1 – 6.4ng/mL. The assay had 100% reactivity to mouse insulin but did not cross react with related peptides or degradation products. All reagents were brought to RT prior to use. In each well of the antibody-coated microplate, 95µL of sample diluent were dispensed, followed by 5µL of sample or mouse insulin working standards. This first reaction consisted of incubating the plasma with the guinea pig anti-insulin antibody that coated the wells of the plates, to allow the binding of insulin. The plate was left for incubation for 2 hours at 4˚C. Well contents were aspirated, and wells were washed five times using wash buffer (300µL/well). The anti-insulin enzyme conjugate (100µL) was dispensed into wells and the plate was left for incubation for 30 min at RT. This second

reaction consisted of incubating horseradish POD-conjugated anti-insulin antibody to the guinea pig anti-insulin antibody/mouse insulin complex immobilised to the microplate well. Well contents were aspirated and washed seven times using wash buffer (300µL/well). The TMB substrate solution (100µL) was immediately dispensed into wells and left to react for 40 min at RT, for detection of POD conjugate. During the enzyme reaction, exposing the microplate to light was avoided. The enzyme reaction was stopped by adding 100µl of the enzyme reaction stop solution. Absorbance (A_{490}/A_{620}) was measured within 30 min, and insulin concentration was determined via interpolation using the standard curve generated by plotting absorbance *versus* the corresponding concentration of mouse insulin standards.

Please refer to Appendix 3 for standard curves of plasma insulin.

4.4.9. Statistical analysis

Statistical analysis of the CSS effects on blood glucose, plasma ghrelin, leptin and insulin, central GHS-R1a cell number, central *Ghs-r1a* mRNA expression, eWAT *Lep* and *Lepr* mRNA expression and central *Lepr* mRNA expression, was conducted using SPSS (version 24, SPSS Inc., Chicago IL, USA). Independent Student's *t*-tests were conducted for plasma ghrelin and plasma leptin and central GHS-R1a cell number. Repeated measures analysis of variance (ANOVA) was conducted in cases of a between-subject factor of group (CSS, CON) and a within-subject factor of CSS day block (e.g. blood glucose). For the body weight of Experiment A and plasma insulin, repeated measures ANCOVA was conducted, with time -1 (i.e. baseline) insulin as the covariate. ANOVA and ANCOVA *post hoc* testing were conducted using Fisher's least significant difference (LSD). Gene expression analysis was carried out using $2^{-\Delta\Delta Ct}$ method and β-actin and GAPDH were used as the control genes for normalisation;

data are given as fold change + standard error of the mean (SEM). Independent Student's *t*-tests were conducted for each region within each gene study. Statistical significance was set at $p \leq 0.05$.

4.5. Results

4.5.1. Plasma active ghrelin (Experiment A)

There was an effect of Group with higher plasma acyl ghrelin levels in CSS compared with CON mice ($t(12.25)=-2.229$, $p\leq0.05$, Figure 4.7).

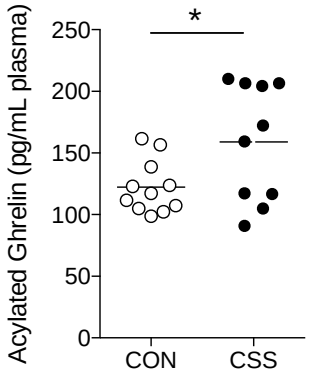

Figure 4.7. Effects of 15-day chronic social stress (CSS, N=10), *versus* control handling (CON, N=11) on levels of plasma ghrelin at day 17. *$p\leq0.05$ for CSS *versus* CON mice following an independent Student`s *t*-test.

4.5.2. Plasma leptin (Experiment C)

There was an effect of Group with lower plasma leptin levels in CSS mice compared with CON mice ($t(11.3)=5.97$, $p\leq0.001$, Figure 4.8).

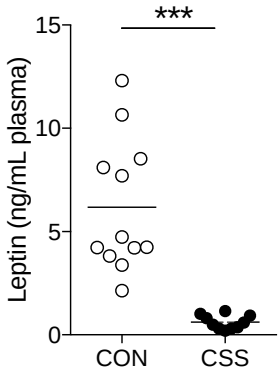

Figure 4.8. Effects of 15-day chronic social stress (CSS, N=10), *versus* control handling (CON, N=12) on levels of plasma leptin at day 21. ***p≤0.001 for CSS *versus* CON mice following an independent Student's t-test.

4.5.3. White adipose tissue – *Lep* and *Lepr* mRNA expression (Experiment C)

There was a significant decrease in eWAT *Lep* expression in CSS mice compared with CON mice, both when using either *Actb* ($t(20)=-3.06$, $p\leq0.01$) or *Gapdh* ($t(22)=-5.81$, $p\leq0.001$) as reference genes. There was no CSS effect on eWAT *Lepr* expression, neither when using *Actb* ($t(22)=0.0095$, $p=0.92$) nor *Gapdh* ($t(22)=-1.56$, $p=0.13$) (Figure 4.9, Table 4.7).

A.

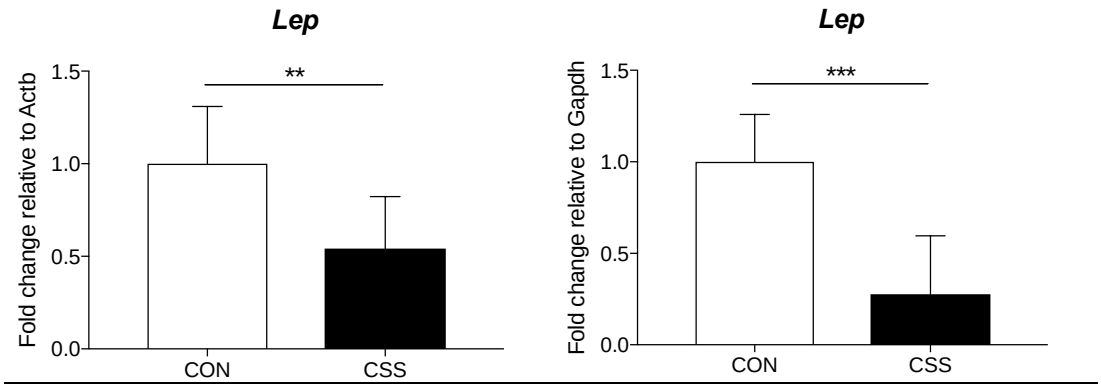

B.

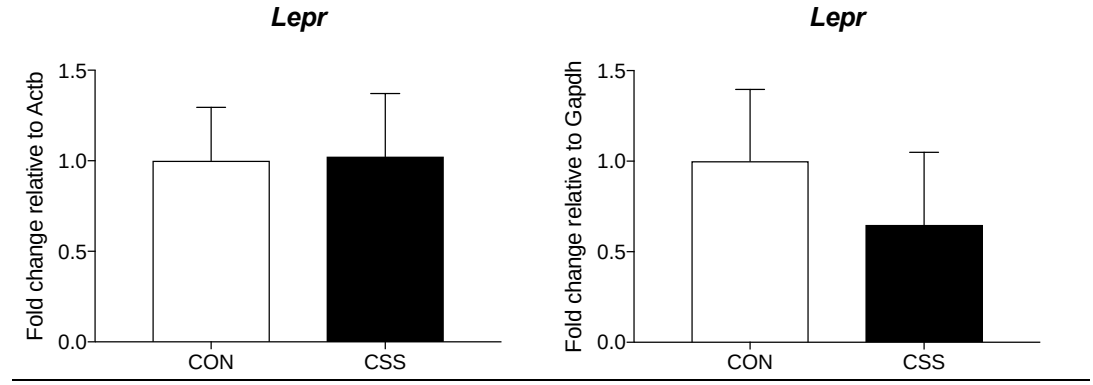

Figure 4.9. Effects of 15-day chronic social defeat stress (CSS, N=12), versus control handling (CON, N=12) on eWAT *Lep* and *Lepr* mRNA expression at day 21. Values are in terms of fold change + SEM. **p≤0.01, ***p≤0.001 for CSS versus CON mice following an independent Student's t-test.

Table 4.7. *Lep* and *Lepr* mRNA expression relative to *Actb* and *Gapdh* in eWAT.

Gene	CON ΔCt	CSS ΔCt	Difference (%)	Fold change	*p* value	
Lep_Actb	**1.16** ± 0.22	**2.04** ± 0.18	76.31	0.54	0.006	**
Lep_Gapdh	**0.60** ± 0.18	**2.45** ± 0.26	310.85	0.27	0.0001	***
Lepr_Actb	**8.27** ± 0.21	**8.24** ± 0.28	-0.39	1.02	0.927	
Lepr_Gapdh	**7.71** ± 0.28	**8.33** ± 0.29	8.13	0.64	0.133	

**p≤0.01, ***p≤0.001. Values of ΔCt expressed as mean ± SEM. n=12 per group.

4.5.4. Brain region-specific – GHS-R1a immunopositive cell number

There was no CSS effect on the number of GHS-R1a positive cells on ARC (t(12)=-0.9, p=0.38, Figure 4.10A), VMH (t(12)=-0.18, p=0.86) or VTA (t(10)=0.54, p=0.59), following an independent Student's *t*-test.

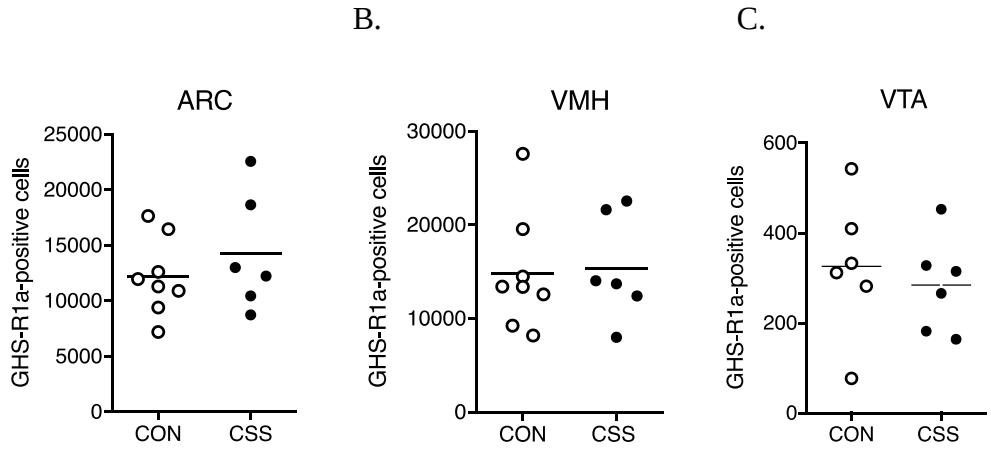

Figure 4.10. Effects of 15-day chronic social stress (CSS) *versus* control handling (CON) on number of GHS-R1a-positive cells in specific brain regions measured using immunohistochemistry and stereology at day 19. Individual and mean values are given for (A) ARC (CSS=6; CON=8). (B) VMH (CSS=6; CON=8). (C) VTA (CSS=6; CON=6).

4.5.5. Brain region-specific – *Lepr* and *Ghs-r1a* mRNA expression

4.5.5.1. *Ghs-r1a* mRNA expression (Experiment C)

There was a significant increase in *Ghs-r1a* expression in the VMH of CSS mice compared with CON mice (t(19)=2.92, p≤0.05) (Figure 4.11, Table 4.8). There was no significant difference in *Ghs-r1a* expression between the CSS and CON groups in any other region of the brain investigated.

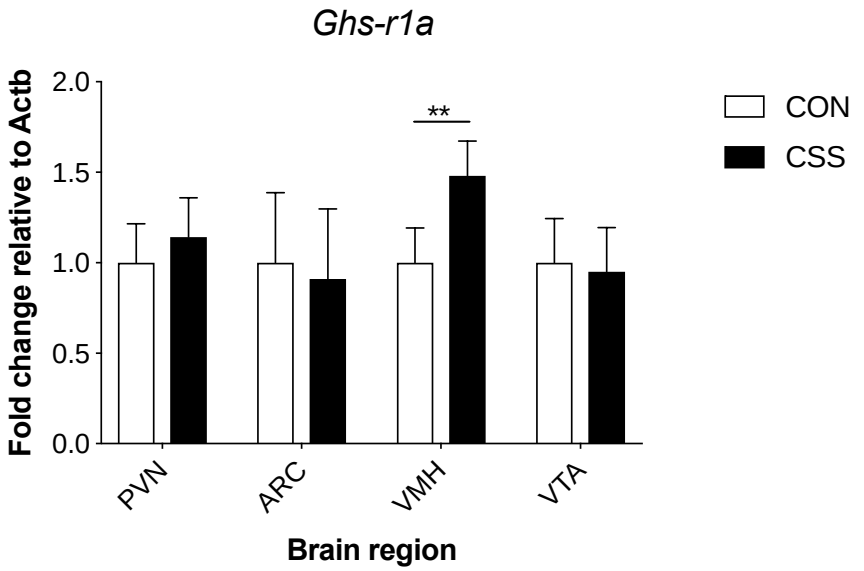

Figure 4.11. Effects of 15-day chronic social stress (CSS, N=12), versus control handling (CON, N=12) on region-specific *Ghr-r1a* mRNA expression at day 21. Values presented as mean fold change + SEM. **p≤0.01 for CSS versus CON mice following an independent Student's t-test. Abbreviations: PVN, paraventricular nucleus; ARC, arcuate nucleus; VMH, ventromedial nucleus; VTA, ventral tegmental area.

Table 4.8. *Ghs-r1a* mRNA expression in selected brain regions.

Brain/region	CON ΔCt	CSS ΔCt	Difference (%)	Fold change	*p* value	
PVN	**4.15** ± 0.16	**4.11** ± 0.14	-0.81	1.02	0.559	
ARC	**4.17** ± 0.32	**4.54** ± 0.22	2.97	0.91	0.717	
VMH	**9.92** ± 0.14	**9.35** ± 0.13	-5.70	1.48	0.009	**
VTA	**6.39** ± 0.15	**6.57** ± 0.19	2.83	0.88	0.779	

Abbreviations: PVN, paraventricular nucleus; ARC, arcuate nucleus; VMH, ventromedial nucleus; VTA, ventral tegmental area. **p≤0.01. Values of ΔCt expressed as mean ± SEM. n=12 per group.

4.5.5.2. *Lepr* mRNA expression (Experiment C)

There was no significant difference in *Lepr* expression between the CSS and CON groups in any region of the brain investigated.

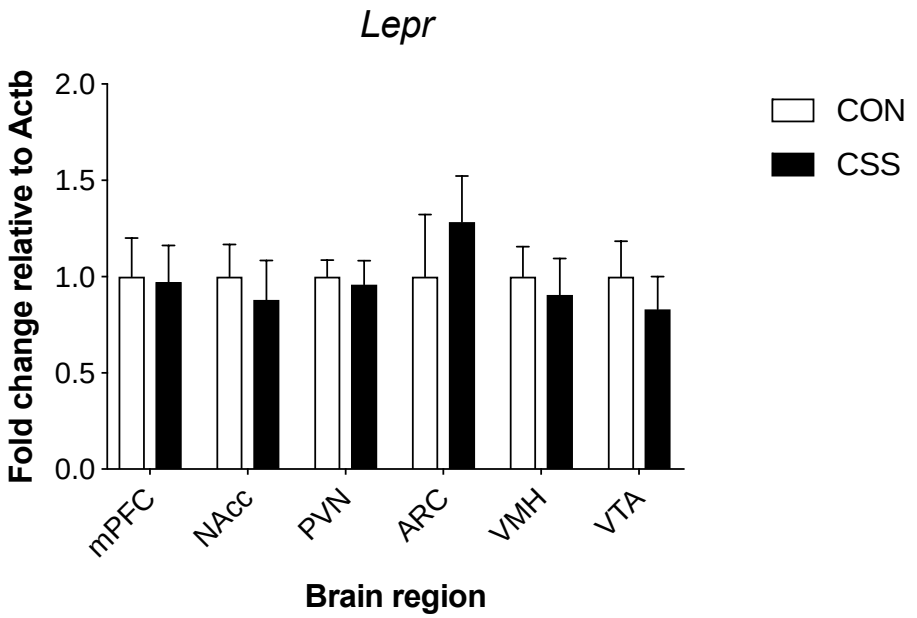

Figure 4.12. Effects of 15-day chronic social stress (CSS, N=12), versus control handling (CON, N=12) on region-specific *Lepr* mRNA expression at day 21. Values presented as fold change + SEM. Abbreviations: mPFC, medial prefrontal cortex; NAcc, nucleus accumbens; PVN, paraventricular nucleus; ARC, arcuate nucleus; VMH, ventromedial nucleus; VTA, ventral tegmental area.

Table 4.9. *Lepr* mRNA expression in selected brain regions.

Brain/region	CON ΔCt	CSS ΔCt	Difference (%)	Fold change	*p* value
mPFC	**9.18** ± 0.14	**9.22** ± 0.13	0.45	0.97	0.830
NAcc	**8.28** ± 0.12	**8.47** ± 0.17	2.38	0.87	0.379
PVN	**6.15** ± 0.06	**6.20** ± 0.11	0.77	0.97	0.744
ARC	**4.59** ± 0.23	**3.94** ± 0.07	-8.48	1.28	0.202
VMH	**8.61** ± 0.11	**8.76** ± 0.15	1.65	0.91	0.458
VTA	**6.20** ± 0.13	**6.47** ± 0.11	4.27	0.83	0.115

Abbreviations: mPFC, medial prefrontal cortex; NAcc, nucleus accumbens; PVN, paraventricular nucleus; ARC, arcuate nucleus; VMH, ventromedial nucleus; VTA, ventral tegmental area. Values of ΔCt expressed as mean ± SEM. n=12 per group.

4.5.6. Glucose tolerance test (Experiment A)

The GTT was performed on day 10 at which point there was no significant difference in body weight between CSS and CON mice (ANCOVA with pre-CSS/CON body weight as covariate: $F(1, 21)=0.005$, $p=0.94$). There was a Group x Day block interaction effect on body weight ($F(2, 42)=0.468$, $p\leq0.05$; however *post hoc* analysis demonstrated that CSS mice did not differ to CON mice in body weight at any time point) (Figure 4.13).

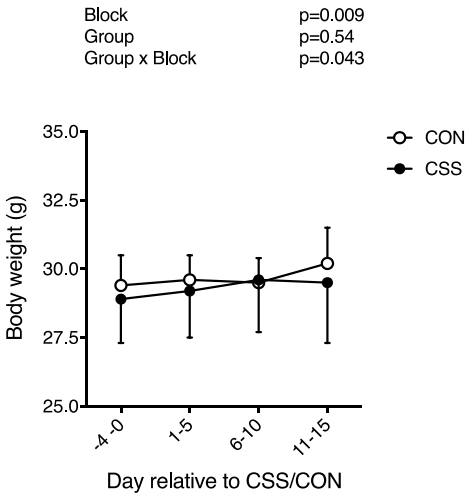

Figure 4.13. Effects of 15-day chronic social stress (CSS, N=12), versus control handling (CON, N=12) on absolute body weight. Values are overall means per 5-day block +/- standard deviation (SD). P values are for repeated measures ANCOVA. No significant interaction was found at any specific day block following LSD post hoc testing.

For blood glucose, there was a Group x Sampling time interaction effect: $F(3.23, 67.91)=3.05$, $p\leq0.05$; *post hoc* analysis demonstrated that at time 30 min, blood glucose was higher in CSS than CON mice ($p\leq0.05$) (Figure 4.14A). In terms of blood glucose area under the curve (AUC), there was no difference between groups for either periods Min -1 to 60 ($t(22)=-1.32$, $p=0.20$) or Min -1 to 120 ($t(22)=-0.63$, $p=0.53$) (Figure 4.14B).

A.

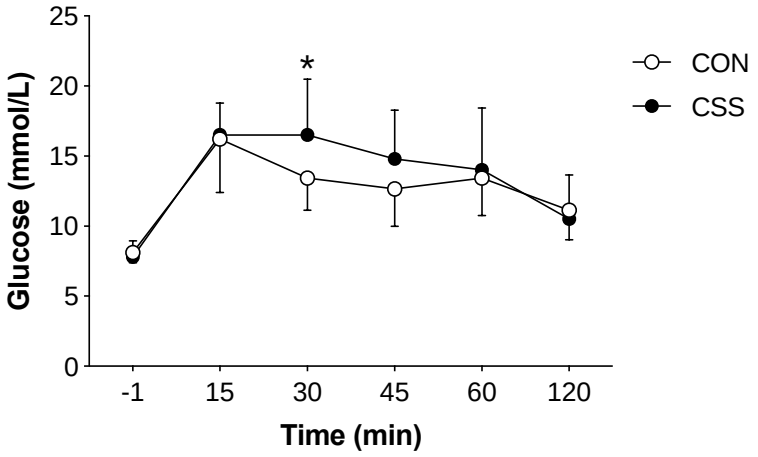

B.

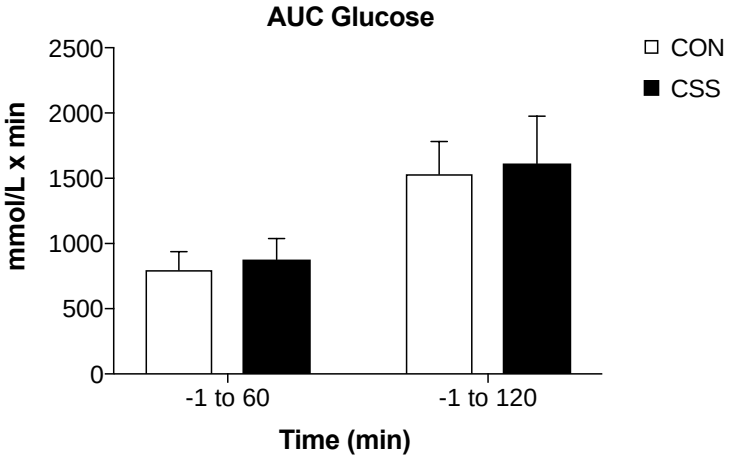

Figure 4.14. Effects of chronic social stress (CSS, N=12) *versus* control handling (CON, N=12) on levels of blood glucose at CSS day 10 following 14 h fasting. (A) Blood glucose of CON and CSS mice across the sampling period. (B) Total area under the curve for glucose at Min -1 to 60 and Min -1 to 120. (A) *p≤0.05 following Group x sampling time ANOVA and specific *post hoc* testing using LSD test.

4.5.7. Plasma insulin (Experiment A)

For plasma insulin, there was a Group x Sampling time interaction effect in ANCOVA with baseline insulin as covariate: $F(3.27, 62.16)=3.15$, $p\leq0.05$. *Post hoc* analysis demonstrated that plasma insulin was lower in CSS than CON mice at times

15 min ($p<0.01$) and 30 min ($p<0.05$) after glucose administration (Figure 4.15A). In terms of plasma insulin AUC, CSS mice had lower plasma insulin levels than CON mice at Min -1 to 60 ($t(22)=4.32$, $p\leq0.001$) and Min -1 to 120 ($t(22)=2.69$, $p\leq0.05$) (Figure 4.15B). When baseline insulin values were compared between groups, CSS mice had lower plasma insulin levels than CON mice ($t(21)=2.86)=0.009$, data not shown). Insulin AUC was also calculated after removing baseline values for each group, to determine whether there is a group effect for the insulin response to glucose injection; here also, CSS mice had lower plasma insulin levels than CON mice at Min -1 to 60 ($t(18)=2.67$, $p\leq0.05$) and Min -1 to 120 ($t(17)=2.49$, 0.023) (Figure 4.15C). Therefore, CSS led to a decrease in baseline insulin as well as a reduced plasma insulin response to glucose challenge compared with CON mice.

A.

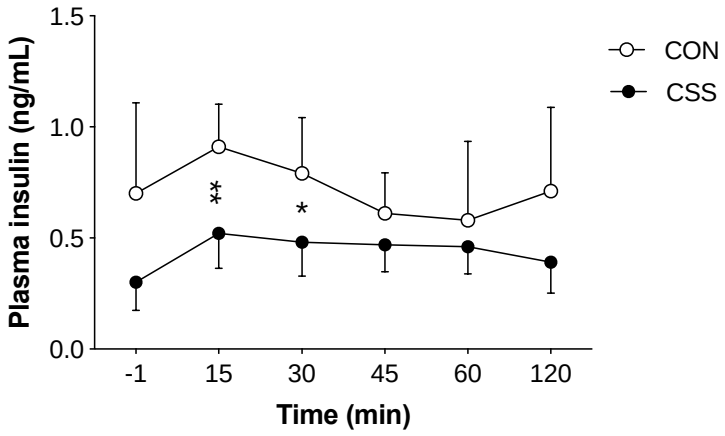

B.

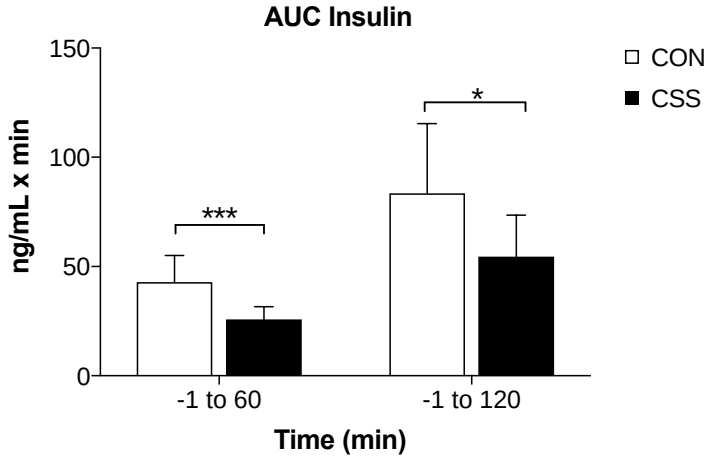

C.

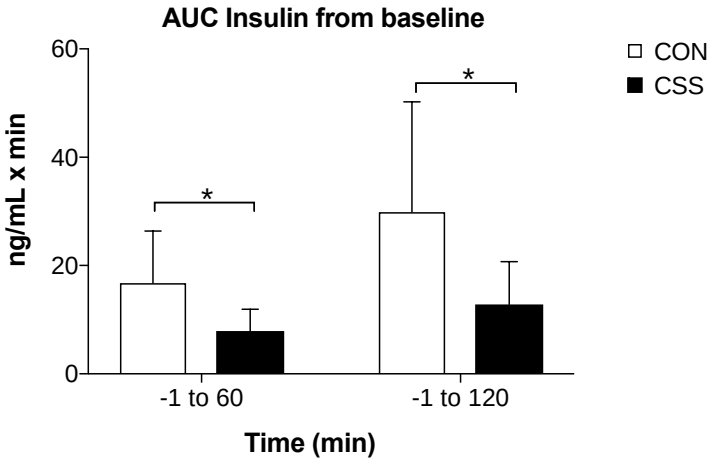

Figure 4.15. Effects of chronic social stress (CSS, N=12) *versus* control handling (CON, N=12) on levels of plasma insulin at CSS day 10 following 14 h fasting. (A) Plasma insulin of CON and CSS mice across the sampling period. (B) Total area under the curve for insulin at Min -1 to 60 and Min -1 to 120. (C) Total area under the curve for insulin at Min -1 to 60 and Min -1 to 120 after removing baseline values. (A) *p≤0.05, **p≤0.01 for CSS *versus* CON mice following Group x sampling time ANCOVA and specific *post hoc* testing using LSD test. (B) and (C) *p≤0.05, ***p≤0.001 for CSS *versus* CON mice following an independent Student's t-test.

4.6. Discussion

Neuroendocrine regulators of feeding, such as ghrelin and leptin, as well as glucose homeostasis, were evaluated for a better understanding of CSS effects on peripheral and central systems in the regulation of energy metabolism. Plasma concentration of ghrelin was increased in CSS mice compared with CON mice. Furthermore, there was a pronounced decrease in plasma levels of leptin, concomitantly with a decrease in eWAT mass. With regards to leptin (*Lep*) and leptin receptor (*Lepr*) gene expression in eWAT, CSS mice showed decreased eWAT *Lep* mRNA expression and no change in eWAT *Lepr* mRNA expression, compared with CON mice. In terms of hypothalamic levels of receptor expression, there was no effect of CSS on *Lepr* mRNA expression in any sub-region investigated, whilst *Ghs-r1a* expression was increased in VMH specifically. With respect to the number of GHS-R1a immunopositive cells, there was no CSS effect in the ARC, VMH or VTA. In fasted mice, the GTT revealed an increased blood concentration of glucose at time 30 min in CSS mice specifically. Plasma levels of insulin were consistently lower in CSS mice than in CON mice.

4.6.1. Ghrelin system

Assessment of plasma acyl ghrelin was performed on CSS day 17 of Experiment A. CSS mice had higher plasma ghrelin levels than CON mice. Similar studies using chronic social stress also observed an increase in plasma levels of ghrelin (Chuang et al., 2011; Kumar et al., 2013; Patterson et al., 2013) and at least up to four weeks post-stress (Lutter et al., 2008). Chronic stress studies using different protocols,

for example a study where rats were placed in a cage filled with water to a height of 2 cm, also reported increased plasma active ghrelin levels (Ochi et al., 2008). Moreover, Ochi et al. (2008) also reported an increase in the number of ghrelin-immunoreactive cells in the gastric body, as well as an increase in preproghrelin mRNA expression (Ochi et al., 2008). Effects of water avoidance stress (i.e. acute psychosocial stress) on circulating ghrelin levels were investigated in anxiety-associated rat strains; ghrelin levels were found to be increased by 80% in a low-anxiety rat strain and by 40% in a high-anxiety rat strain (Kristenssson et al., 2006). These results show consistent effects of stress on plasma ghrelin across protocols of different chronicity and methodologies.

In parallel to the evaluation of peripheral levels of acyl ghrelin, effects of CSS on central ghrelin receptor expression was also performed. As previously mentioned, some amelioration of stress-related symptoms appears to be mediated by the ghrelin receptor. Thus, Lutter et al. (2008) demonstrated that mice lacking ghrelin receptor exhibited increased depressive-like symptoms. Furthermore, Patterson et al. (2013) demonstrated that stress-induced increase in body weight gain and a tendency to increase in food intake was ablated in GHS-R KO mice. Although previous studies showed that the effects of chronic social stress on body weight and food intake were linked to central GHS-R1a (Patterson et al., 2013), effects of CSS on central GHS-R1a were not investigated. The GHS-R1a is found prominently in hypothalamic nuclei such as ARC and VMH, and in the VTA, implicated in food reward and addition (Guan et al., 1997; Zigman et al., 2006; Chuang et al., 2011). Therefore, we examined the mRNA expression of *Ghs-r1a* by qPCR in discrete hypothalamic sub-regions associated with regulation of feeding, and the number of GHS-R1a positive cells in these sub-regions.

There was a significant increase in *Ghs-r1a* mRNA expression in the VMH of CSS mice compared with CON mice. There was no significant difference in *Ghs-r1a* mRNA expression between the CSS and CON groups in any other region of the brain investigated. There was no effect of CSS on GHS-R1a positive cell number in the ARC, VMH or VTA.

Increased levels of ghrelin and enhanced ghrelin signalling through activation of central GHS-R1a have been shown to play an important role in protecting chronically stressed rodents from the development of depressive-like symptoms (Kanehisa et al., 2006; Lutter et al., 2008; Chuang et al., 2011). Furthermore, another recent study reported that chronic peripheral treatment with ghrelin was able to alleviate anxiety- and depression-like symptoms promoted by CUMS (Huang et al., 2017). Nevertheless, the mechanisms by which ghrelin modulates depressive-related behaviour is yet unclear; the well-defined influence of ghrelin on food intake indicates that ghrelin may exert a role as anxiolytic and antidepressant at the cost of increased food intake, as suggested by Lutter et al. (2008). The majority of neuroendocrine systems are regulated by a process of negative feedback, in which increased levels of hormones induce downregulation of central receptors, counterbalancing hormonal signalling. Therefore, it is particularly striking that an increase in *Ghs-r1a* mRNA expression in a hypothalamic nucleus is co-occurred with an increase in plasma acyl ghrelin levels. Of note, mRNA levels of both stomach ghrelin and hypothalamic *Ghs-r1a* were upregulated together after fasting (Kim et al., 2003).

4.6.2. Leptin system

Stress is known to affect regulation of energy balance through changes in body fat storage and metabolism. With regards to the effects of CSS on fat tissue mass,

eWAT mass was evaluated. A decrease in eWAT in CSS mice in comparison to CON mice was observed. This is in accord with previous studies (Bartolomucci et al., 2004; Chuang et al., 2010b; Balsevich et al., 2014). Nevertheless, an increase in the visceral fat pad in stressed mice following chronic social stress protocol was also observed in other studies (Patterson et al., 2013; Coccurello et al., 2017).

With regards to the effects of CSS on leptin levels, a previous study from the same laboratory reported a decrease in plasma leptin (-60%) in non-fasted CSS mice relative to CON mice (Bergamini et al., 2016). Consistent with this finding, CSS mice again had lower (-90%) leptin levels compared with CON mice. The larger decrease in plasma leptin observed in the present study is likely due to decreased body weight gain and fat pads in CSS mice, compared to no change in body weight observed by Bergamini et al. (2016). Findings with the current CSS model are in accord with other studies that observed a decrease in plasma leptin in various rodents models of stress (Lu et al., 2006; Chuang et al., 2010b; Finger et al., 2011, 2012; Ge et al., 2013; Balsevich et al., 2014; Iio et al., 2014). In mice, decreases in plasma leptin have been observed up to several weeks after chronic social stress. A decrease in plasma leptin was observed 30 days after the 10-day stress period in mice under chow or HFD by Chuang et al. (2010b), as well as following 21 days of chronic social stress by Balsevich et al. (2014). Moreover, reduced plasma leptin following chronic social stress in mice on both low and HFD was observed, but interestingly the effect was more pronounced in mice on an HFD (Finger et al., 2011, 2012). As previously mentioned, a decrease in plasma leptin following 10-day stress period was also observed by Kumar et al. (2013) specifically during the late night/early dark phase. Interestingly, an absence of the stress effect on plasma leptin was also observed: despite a decrease in abdominal fat mass (Razzoli et al., 2011a, b, c), with an increase

in body weight gain (Razzoli et al., 2011a, b), and without a change in body weight (Razzoli et al., 2011c). The protocol developed by Razzoli and colleagues comprised four weeks of single housing in addition to the 10-day chronic social stress. A previous study in isolated rats reported increased plasma leptin levels (Perelló et al., 2006), thus the included single housing period in Razzoli studies might have exerted counterbalancing effect on the leptin lowering often observed in stressed animals. A recent meta-analysis conducted on the effects of single housing on visceral fat mass in rodents reported a significant increase in fat mass in individually housed compared with socially housed animals (Schipper et al., 2018); this would be expected to co-occur with an increase in plasma leptin levels. Chronic social stress and social isolation may influence fat metabolism and leptin signalling in different manners, possibly explaining the leptin findings observed by Razzoli et al. (2011a, b, c).

Furthermore, in order to consider the genetic expression of leptin in WAT and therefore evaluate the self-regulatory function of adipocytes in protein synthesis, assessment of *Lep* mRNA expression was performed. In the same cohort used for plasma leptin analysis, a significant decrease in expression of eWAT *Lep* mRNA in CSS mice compared with CON mice was observed. This demonstrates that the reduction in plasma leptin observed is related not only to the decrease in eWAT mass but also to the reduced eWAT *Lep* mRNA expression, the latter possibly being associated with adipocyte size (Guo et al., 2004) and not necessarily with WAT mass. To my knowledge, this is the first study to assess the effects of CSS on *Lep* mRNA expression in eWAT in mice. In rats, Iio et al. (2014) observed a decrease in *Lep* mRNA expression in eWAT, concomitant with a decrease in plasma leptin and fat tissue, following five weeks of daily social defeat.

Therefore, in this experiment, CSS led to no change in food intake despite a decrease in plasma leptin, a decrease in eWAT mass and a decrease in eWAT *Lep* mRNA expression, and, as would be predicted, there was a decrease in body weight gain. Assessment of *Lepr* mRNA expression by qPCR, in brain regions associated with homeostatic regulation of feeding, was performed, however the present study did not show any significant difference in *Lepr* in any of the brain regions investigated. To my knowledge, assessment of *Lepr* mRNA expression within the brain, in animal models of depression has not been conducted until the present moment.

4.6.3. Glucose homeostasis

In rodents, stress is known to affect glucose metabolism (Black, 2006; Chuang et al., 2010a; Kanarik et al., 2011). For evaluation of the effects of CSS on glucose homeostasis, a fasted GTT was performed at day 10. CSS mice had a higher blood concentration of glucose at 30 min following i.p. administration of glucose compared with CON mice. This increase in blood glucose at time point 30 min indicates a mild impairment in glucose processing/homeostasis in CSS mice. This might be attributable to reduced insulin release/secretion from the pancreas into the bloodstream. Indeed, lower plasma insulin levels were observed in these CSS mice compared with CON mice. A decrease in plasma insulin was observed in a previous chronic stress study in mice, by Balsevich et al. (2014), and under conditions of both normal chow diet and HFD. It will be important to investigate whether plasma insulin is also reduced in non-fasting mice. A possible cause of the decrease in insulin may be the enhanced plasma ghrelin found in CSS mice compared with CON mice. Previous studies showed that mice overexpressing the active form of ghrelin had attenuated glucose-stimulated insulin release (Bewick et al., 2009). In line with this, blockade of endogenous ghrelin

were shown to increase levels of insulin, likely by preventing Ca^{2+} signalling in β-cells (Dezaki et al., 2004). The majority of studies of chronic social stress observed the development of insulin resistance. For instance, Chuang et al. (2010a) observed increased fasting glucose levels accompanied by elevated insulin levels. Increased insulin levels and insulin resistance have been mostly observed in chronically stressed mice on a HFD (Finger et al., 2012; Sanghez et al., 2013). Indeed, when observed under a chow diet, no change in insulin levels was observed in chronically stressed mice (Sanghez et al., 2013; Tsuneki et al., 2013).

Interestingly, glucose homeostasis is regulated not only by insulin but also by the fasting hormone leptin, both acting in the central nervous system to regulate food intake and adiposity (Benoit et al., 2004). Previous studies showed that insulin enhanced leptin synthesis and secretion, in order to promote a decrease in food intake and therefore to regulate body weight gain (Inui et al., 2012). A decrease in levels of insulin in CSS mice might lead to reduced leptin secretion from adipose tissue, resulting in the observed lower leptin levels. Conversely, an increase in leptin levels was reported to promote a reduction in glucose-stimulated pancreatic insulin secretion, insulin delivery and lipogenesis (Paz-Filho et al., 2012); thus low levels of leptin observed here could be expected to enhance insulin secretion; nevertheless, this is not the situation.

In addition, ghrelin has also been shown to regulate glucose homeostasis and insulin secretion in both rodents and humans. In mice, ghrelin inhibited glucose-stimulated insulin secretion in a dose-dependent manner (Reimer et al., 2003). In rats, ghrelin did not significantly alter basal insulin, but it inhibited insulin secretion in response to increased blood glucose (Egido et al., 2002). In humans, administration of ghrelin promoted hyperglycemia and suppressed insulin secretion (Broglio et al.,

2001; Arosio et al., 2003). Moreover, low levels of ghrelin were associated with increased insulin and insulin resistance in mice (Pöykkö et al., 2003). Conversely, insulin infusion decreased plasma ghrelin (Saad et al., 2002). Therefore, an increase in ghrelin levels observed in the present study might explain the low levels of insulin in CSS mice.

The decreased levels of insulin found in this study suggest that CSS in mice might be leading to reduced efficiency in the use of glucose or increasing glucose demand for metabolic processes such as for brain function and execution of stress-coping tasks. The brain does not require insulin in a direct manner; therefore it can be speculated that decreased insulin levels correspond to lower (or slower) peripheral glucose storage thus increased likelihood of brain glucose uptake. The speculation that CSS mice might be using up available glucose for metabolic processes is reinforced by the increased RER and the decreased accumulation of eWAT observed here, suggesting that great energy requirements by stressed animals limit fat storage. Increased fat mass is not observed in CSS mice in the present study, and CSS mice might be using the available glucose at an increased rate, not allowing sufficient time for fat storage and usage. The great energy demand for brain function, believed to be occurring in this case, has limited glucose availability to peripheral organs, making insulin secretion and fat storage unnecessary.

4.7. Conclusion

In summary, the results presented in this chapter demonstrated that CSS in mice led to peripheral metabolic changes consistent with increased energetic requirements; CSS induced changes in the neuroendocrine regulators of energy metabolism and feeding, leptin and ghrelin in a pattern associated with increased appetite. CSS also led to a decrease in plasma insulin co-occurring with impaired glucose metabolism. We can speculate that stress induces changes in areas including the brain, which leads to increased demand for glucose for energy metabolism. This may lead to neuroendocrine changes consistent with increasing the drive to eat, impaired insulin response and reduced anabolic processes.

CHAPTER 5

Effects of chronic social stress on the serotonergic system

5.1. Introduction

The emergence of psychopathology in humans is widely associated with stressful events experienced throughout life. Recent neuroscience research advances in the pathophysiology of mood-related disorders, e.g. depression, have been focused on the regulatory mechanisms of the serotonergic system (Fujita et al., 2017; James et al., 2017; Xu et al., 2018). Anatomical and molecular similarities of the human and rodent serotonergic systems facilitate translational research; it makes experimental studies of 5-HT and its receptors in mice relevant to answering research questions which also refer to human physiology and neurobiology (Figure 5.1).

A. B.

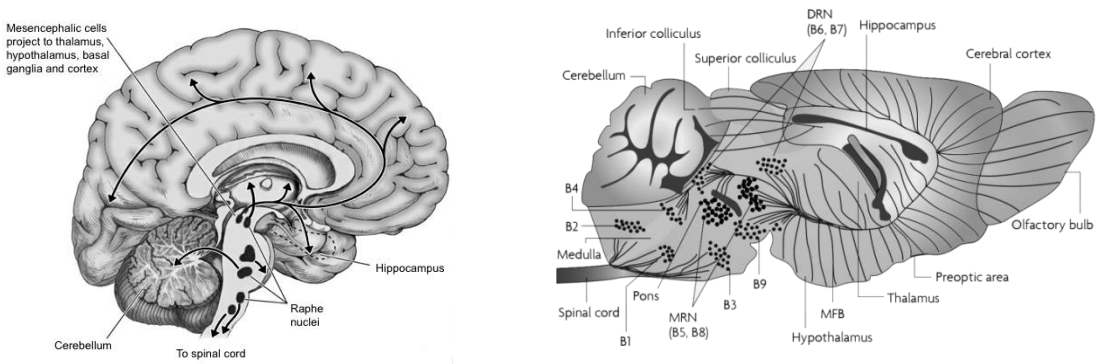

Figure 5.1. Schematic sagittal view of serotonergic projections in human and mouse brains, depicting 5-HT neuron clusters allocated within the raphe nuclei. (A) Serotonergic pathway of the human brain. Figure adapted from Kalat (1998), Biological Psychology 6th edition. (B) Serotonergic pathway of the mouse brain. Figure adapted from Murphy and Lesch (2008), Nature Reviews Neuroscience, p91, ©2008 Springer Nature. Abbreviations: B1, raphe pallidus nucleus; B2, raphe obscurus nucleus; B3, raphe magnus nucleus; B4, dorsolateral raphe obscurus; (B5, B8) MRN, medial raphe nucleus; (B6, B7) DRN, dorsal raphe nucleus; B9, pontis oralis nucleus; MFB, medial frontal bundle.

The serotonergic system not only plays a role in the development of stress-related depressive symptoms, as addressed below, but it also modulates reward processing and feeding regulation (Kranz et al., 2010). Anticipatory reward of and gratification through food consumption can activate a range of brain regions, e.g. nucleus accumbens, ventral tegmental area, prefrontal and cingulate cortices, some of the hypothalamic nuclei, and amygdala (Yager et al., 2015), which triggers a repetitive behaviour in order to keep experiencing this positive sensation. Brain reward signals can override signals of satiety, leading to overeating and, as a result, obesity (Yu et al., 2015)**.** Mice subjected to chronic social stress in adulthood showed an increased food intake, for at least one month after the defeat period, in the absence of weight gain, but with reduced effortful motivation to obtain the gustatory reward (Chuang et al., 2011; Pryce and Fuchs, 2017). An increased intake of highly palatable foods was reported in socially stressed mice, independent of signs of hyperphagia or hypophagia (Chuang et al., 2011). There is growing evidence that brain reward activation can buffer stress effects and there are plausible links between reward and resilience to stress, as recently reviewed (Dutcher and Creswell, 2018).

The role of stress in the modulation of the serotonergic system, including 5-HT receptors and transporter, and its implication in feeding behaviour is not fully understood. This chapter is therefore focused on the effects of stress on the three selected 5-HT receptors known to modulate mood-related and eating behaviours: 5-HT1A, 5-HT2A and 5-HT2C, and the serotonin transporter, SERT.

5.1.1. Stress and serotonin receptors

5.1.1.1. Stress and serotonin 5-HT1A receptor

5-HT1A receptor is involved in the stress-related regulation of the HPA axis with the limbic system and modulation of depressive-like symptoms in humans and rodents, as explained below. Thus in depressed and chronically psychosocially stressed subjects, PET studies showed reduced 5-HT1A binding potential (BP) in the limbic brain regions such as the hippocampus, insular cortex, anterior cingulate and RN (Sargent et al., 2000; Jovanovic et al., 2011). In regards to the role of 5-HT1A in the HPA axis regulation, the 5-HT1A agonist 8-OH-DPAT administered into the PVN was shown to activate PVN CRH neurons (Bovetto et al., 1996), increase plasma ACTH (Pan and Gilbert, 1993; Petrunich-Rutherford et al., 2018) and corticosterone release (Bovetto et al., 1996). It was also able to relieve depressive symptoms in rats (Jiang et al., 2014). In the hippocampus, however, activation of 5-HT1A appears to have an opposing role. In hippocampal cell cultures, stimulation of 5-HT1A by application of 5-HT increased GR density (McAllister-Williams et al., 1998). The role of hippocampal GR in the HPA axis regulation is to inhibit CRH release via the inhibitory feedback to PVN CRH neurons (Herman et al., 2016). The involvement of glucocorticoid resistance in depression, due to impaired GR function, has been considered (Anacker et al., 2011).

In mice, chronic mild stress (CMS) led to a reduced sensitivity of DRN 5-HT1A autoreceptors, likely in response to their overactivation (property displayed by many GPCRs), but not in GR-impaired mice (i.e. mice bearing GR antisense RNA) with a deficit in the HPA negative feedback (Froger, 2004). A slow increase in the inhibition of DRN following 5-HT1A agonist (i.e. reduced sensitivity) and a reduced serotonergic firing activity was also reported in rats following chronic unpredictable

stress, co-occurring with anhedonic-like symptoms (Bambico et al., 2009). Acute suppression of RN 5-HT1A autoreceptors by administration of small interference RNA (siRNA) enhanced 5-HT release and promoted antidepressant-like effects in mice under stressful conditions (Ferrés-Coy et al., 2013).

In the context of feeding regulation, as mentioned in Chapter 1, 5-HT1A agonists were shown to stimulate feeding in rats (Williams and Dourish, 1992; Voigt et al., 2002). It is plausible that stress causes an increase in food intake through the modulation of the 5-HT1A receptor and decreasing availability of extracellular 5-HT in animal models of stress such as the chronic mild stress and chronic unpredictable stress (Froger, 2004; Bambico et al., 2009).

5.1.1.2. Stress and serotonin 5-HT2A receptor

In regards to the 5-HT2A receptor, its modulation seems to play an essential role in depressive-like symptoms, however, studies are divergent. A downregulation of *Htr2a* was reported in BLA of rats under learned helplessness stress (Jiang et al., 2009) and mice following chronic social stress and co-occurring with increased acquisition of fear and helplessness (Azzinnari et al., 2014). As previously mentioned, 5-HT2A receptors are highly expressed in GABAergic interneurons in various regions of the brain, e.g. amygdala and VTA (Guiard and Di Giovanni, 2015); administration of 5-HT2A agonist in the BLA increased the frequency and amplitude of inhibitory postsynaptic currents (Jiang et al., 2009). In rats, acute injection of 5-HT2A agonist into the mPFC, a region with extensive neural connectivity with the limbic structures e.g. amygdala (Arco and Mora, 2009; Park et al., 2018), was able to block depression-like behaviours, such as a deficit in perseveration and shorter latency of immobility, following chronic mild stress (Natarajan et al., 2017).

The 5-HT2A receptor agonist DOI can cause an up-regulation of the BDNF in selected brain regions, including the hippocampus, prefrontal cortex, amygdala and nucleus accumbens in a rat model of acute psychosocial stress (Jiang et al., 2016). BDNF is widely associated with neuronal differentiation and development, and is essential for the molecular mechanisms of synaptic plasticity; the survival of 5-HT neurons depends on trophic factors such as BDNF (Martinowich and Lu, 2008). Interestingly, rats exposed to acute swim stress produced rapid transcriptional changes in BNDF isoforms and chronic treatment with the serotonin-noradrenaline reuptake inhibitor antidepressant duloxetine was able to modulate these effects (Molteni et al., 2009).

In contrast, inactivation of this receptor was also shown to be beneficial in animal models of depression. For instance, the 5-HT2A antagonist BIP-1 decreased duration of immobility in mice during a forced swim test (Pandey et al., 2010). Furthermore, i.p. administration of the 5-HT2A antagonist SR-46349B in mice partially reverted the delayed nesting (i.e. motivation behaviour) promoted by acute social stress (Otabi et al., 2017).

5-HT2A receptors are also thought to be implicated in the modulation of feeding, however, studies are limited. For instance, 5-HT2A gene polymorphism of the promoter region was associated with eating disorders such as anorexia nervosa (Collier et al., 1997; Ricca et al., 2002). Further studies on the role of 5-HT2A in feeding behaviour are required.

5.1.1.3. Stress and serotonin 5-HT2C receptor

5-HT2C receptors appear to be involved in the response to stress, as 5-HT2C-KO mice are more responsive to repeated stress than WT mice, displaying increased

levels of ACTH and corticosterone (Chou-Green et al., 2003). However, the role of stress in the modulation of 5-HT2C receptors and the relevance of this to stress-related depressive symptoms are not well established.

5-HT2C receptors are also implicated in the regulation of mood and anxiety disorders. Thus 5-HT2C agonists increased anxiety in a social interaction test in mice (Mongeau et al., 2010), whereas 5-HT2C antagonists were anxiolytic in both mice (Rainer et al., 2012) and humans (Demyttenaere, 2014). It was recently shown that the 5-HT2C antagonist SB242,084 works in parallel to SSRIs, potentiating antidepressant effects in patients (Demireva et al., 2018).

In the context of feeding regulation, as previously mentioned, 5-HT2C receptors are thought to be necessary for the control of eating behaviour. 5-HT2C agonists were shown to decrease food intake (De Vry and Schreiber, 2000) whereas the 5-HT2C antagonist risperidone increased food intake and body weight (Kursungoz et al., 2015). Effects of CSS on the modulation of 5-HT2C receptors with implications in feeding behaviour are not yet established.

5.1.2. Stress and serotonin transporter

Stress is known to exert effects not only on the 5-HT receptors but also on SERT. In response to social stress in rodents, *Sert* mRNA and SERT protein expression were found to be upregulated in DRN (Filipenko et al., 2002; Zhang et al., 2012) and amygdala (Azzinnari et al., 2014). However, a decrease in SERT binding in RN was also found in chronically stressed rats (McKittrick et al., 2000). In primates, the gene encoding SERT contains a regulatory variation that contributes to individual differences in anxiety-related traits and susceptibility for depression (Canli and Lesch, 2007). In line with that, SERT became a recognised target for treating stress-related

disorders such as depression; by functionally blocking SERT activity in the presynaptic neurons, SSRIs increase the availability of 5-HT at the synaptic cleft (for review, see Otte et al., 2016). SSRI drugs such as fluoxetine and citalopram were shown to revert stress-induced decrease in the locomotor activity and rearing behaviour in rats submitted to a chronic social stress regimen (Rygula et al., 2006a, b). The inhibitory effect of SSRIs on 5-HT signalling is linked to the overactivation of 5-HT1A autoreceptors in the DRN. The SSRI-promoted increase in 5-HT activates presynaptic inhibitory 5-HT1A autoreceptors and leads to a subsequent decrease in serotonergic firing rate (Celada et al., 2013). It was shown that 5-HT1A antagonists did not reverse these inhibitory effects in the DRN, but 5-HT2A antagonist (MDL100,907) reversed the signal response, an indication that inhibition of both receptors was required for the prevention of these inhibitory effects (Quesseveur et al., 2013) and effective treatment of depression.

In humans, PET imaging and postmortem studies also demonstrated reduced SERT binding and expression in the brains of individuals with depression (Arango et al., 1995; Malison et al., 1998; Willeit et al., 2000; Parsey et al., 2006). Although effects of stress on SERT have been widely investigated in RN, amygdala and other brain areas, the results are somewhat controversial and stressor-dependent. Further investigation into the effects of stress on the regulation of SERT and expression of its gene *Slc6a4* is required.

In the present study, complementary to the experiments on the effects of CSS on homeostatic regulators of feeding presented in Chapter 4, the ligand-binding activity of the 5-HT1A, 5-HT2A, 5-HT2C receptors in mouse brain regions implicated in the central regulation of food intake or reward evaluation was investigated using

quantitative autoradiography. Moreover, the effects of CSS on the gene expression of the aforementioned 5-HT receptors as well as *Sert* were investigated using quantitative polymerase chain reaction. Quantification of 5-HT receptors and *Sert* in such regions provides a better understanding of the effects of CSS on the central regulatory mechanisms of feeding and reward.

5.2. Hypotheses

Chronic social stress in mice:

5.2.1. Alters ligand-binding activity of the 5-HT receptors in mouse brain regions that are implicated in the central regulation of food intake or reward evaluation.

5.2.2. Alters mRNA expression of the 5-HT receptors and serotonin transporter in mouse brain regions that are implicated in the central regulation of food intake or reward evaluation.

5.3. Aims

To investigate the effects of chronic social stress on:

5.3.1. 5-HT1A, 5-HT2A and 5-HT2C receptor binding in mouse medial prefrontal cortex (mPFC), nucleus accumbens (NAcc), ventral tegmental area (VTA), amygdala (Amy), hypothalamus (Hyp), dorsal raphe nucleus (DRN), hippocampus (Hipp) and locus coeruleus (LC), by means of quantitative autoradiography.

5.3.2. *Htr1a*, *Htr2a*, *Htr2c* and *Slc6a4* (*Sert*) mRNA expression in mouse medial prefrontal cortex (mPFC), nucleus accumbens (NAcc), paraventricular nucleus of hypothalamus (PVN), basolateral amygdala (BLA), arcuate nucleus (ARC), ventromedial hypothalamus (VMH), ventral tegmental area (VTA) and raphe nuclei (RN), by means of quantitative PCR.

5.4. Methodology

5.4.1. 5-HT1A, 2A and 2C receptor binding – quantitative autoradiography

Quantitative autoradiography is a highly specific method that uses radioactive biochemical substances for detection of pharmacologically characterised receptors in biological tissue. This technique requires radioligands of high affinity, high receptor specificity and low non-specific binding. Elimination of non-specific binding and appropriate system calibration provides an anatomically discrete, reproducible quantification of specific binding of the binding sites of interest.

5.4.1.1. Study design

In a cohort of mice exposed to CSS or control handling (CSS N=8, CON N=8), quantitative autoradiography of 5-HT1A, 5-HT2A and 5-HT2C receptors was performed in brain sections of medial prefrontal cortex (mPFC), nucleus accumbens (NAcc), ventral tegmental area (VTA), amygdala (Amy), hypothalamus (Hyp), dorsal raphe nucleus (DRN), hippocampus (Hipp) and locus coeruleus (LC).

5.4.1.2. Brain tissue dissection and cryosectioning

On day 17 after CSS, animals were sacrificed by means of decapitation. Brains were quickly dissected from the skull, rinsed with ice-cold saline solution, snap-frozen at -40°C in 2-methylbutane (Sigma-Aldrich) and stored at -80˚C. Coronal 25µm brain sections were cut and stored at -80°C prior to autoradiography. Sections from a total of 16 mouse brains were used per radioligand assay. *Performed by Michaela Buerge (2016).*

5.4.1.3. Material for autoradiography

The following radioligands were used: [O-methyl-^{3}H]WAY 100635 as selective 5-HT1A receptor antagonist, [^{3}H]ketanserin as 5-HT2A receptor antagonist and [^{125}I]DOI as 5-HT2C receptor agonist. Due to the absence of high specificity of the last two radioligands, masking drugs were used to exclude interfering activities.

The radioligands for 5-HT1A and 5-HT2C receptors, [O-methyl-^{3}H]WAY 100635 (specific activity 80 Ci/mmol) and [^{125}I]DOI (specific activity 2200 Ci/mmol) were purchased from American Radiolabelled Chemical Ltd. The radioligand for 5-HT2A, ketanserin hydrochloride [ethylene-^{3}H] (specific activity 43 Ci/mmol), methysergide, MDL 100907 and RS-102221, were purchased from Tocris/Biotechne Biosciences UK; tritium microscales were purchased from Amersham UK. Tritium sensitive Hyperfilm was purchased from GE Healthcare Life Sciences. All other chemicals were purchased from Sigma-Aldrich (Poole, UK).

For each radioligand, a range of 32 to 48 slides was used, according to the number of regions examined, with 2-3 sections per region per subject. Two slides per cassette were selected as the block for non-specific binding. 0.5M Tris buffer was prepared for stock in advance; pH was adjusted to 7.5 by adding HCl to the stock solution. On the day of the experiment, (0.5M) Tris-HCl stock was diluted 10x and its pH was re-adjusted to 7.5.

Please refer to Appendix 2 for reagents and solutions.

5.4.1.4. Serotonin 5-HT1A receptor binding

The procedure was based on Leventopoulos et al. (2009). Frozen brain sections were left to thaw for 3 hours before the incubation procedure. Brain sections were pre-incubated in 0.05M Tris-HCl buffer pH 7.5 for 30 min at room temperature. This step

ensured that endogenous 5-HT was removed from the brain sections. After the period of pre-incubation, Tris-HCl buffer was poured from slides into a glass beaker, and the surplus buffer was blotted off the slides with absorbent paper. Brain sections were then incubated with 2nM [O-methyl-^{3}H]WAY 100635 (specific activity 80 Ci/mmol) with 10μM pargyline, a monoamine oxidase inhibitor, for 2h at RT. Non-specific binding was determined using 10μM unlabelled 5-HT. A paraffin pen was used to ensure block solution did not slip to the other half of sections. Slides were then washed in ice-cold Tris-HCl buffer for 2 min and rinsed 3x in cold deionised water, very briefly each time. Slides were removed from the racks and placed on plastic trays covered with paper tissue. They were left to air dry for 24 hours.

5.4.1.5. Serotonin 5-HT2A receptor binding

The procedure was based on Dawson et al., (2014). Brain sections were preincubated in 0.05M Tris-HCl buffer with pH 7.5 for 5 min at room temperature and incubated with 1nM [^{3}H]ketanserin (specific activity 43 Ci/mmol) in 0.05M Tris-HCl buffer pH 7.5 with 1μM prazosin (to block binding to adrenergic receptors) and 100nM tetrabenazine (to block binding to the vesicular transporter) for 60 min at RT. Non-specific binding was assessed in the presence of 200μM methysergide (block solution). Slides were then washed twice for 30 min in ice-cold Tris-HCl buffer, replacing buffer after the first wash and rinsed in cold deionised water for 10 sec.

5.4.1.6. Serotonin 5-HT2C receptor binding

The procedure was based on Li et al., 2003. Brain sections were preincubated in assay buffer (0.05M Tris-HCl buffer pH 7.5, 0.5mM EDTA, 10mM $MgSO_4$, 0.1% ascorbic acid, 0.1% bovine serum albumin, 10uM pargyline) for 30 min at room

temperature and incubated in 0.2nM [^{125}I]DOI (specific activity 2200 Ci/mmol) with 100nM MDL 100907 for 1h at room temperature. Non-specific binding was assessed using 10μM RS-102221. Sections were washed in ice-cold assay buffer for 2x10min and rinsed 3x with cold deionised water.

5.4.1.7. Film exposure

Once dried, radiolabelled slides were placed inside cassettes (RPN13642 18x24cm, Amersham Biosciences). Tritium standard strips were put in the centre. 2-3 layers of heavy paper (160g/m^2) were cut at the same size as the Amersham™ Biosciences [^{3}H]Hyperfilm, with a small notch cut on the upper right-hand side, and placed at the bottom of the cassette. Autoradiography films were placed on the top of the emulsion facing the slides and then 3-4 layers of heavy paper on top to provide more pressure and light protection. Cassettes were closed, sealed with silver foil and placed at 4°C for the required period of exposure. The same procedure was carried out for [^{3}H]ketanserin, [O-methyl-^{3}H]WAY 100635 and [^{125}I]DOI, with 8 weeks, 6 weeks and 2 days of exposure, respectively.

5.4.1.8. Film development

After the appropriate time, the cassettes were opened in a dark room, completely isolated from any light source. Films were placed glossy-side down into a tray filled with the developing solution: this fluid contains reducing agents in alkaline solution that enable the conversion of the remaining silver ions within a crystal to metallic silver and the formation of a "negative visual image". Ensuring that the films remained immersed in Kodak™ D19 developer solution, they were gently agitated for 1 min. Using tweezers, films were removed from the developing tray and placed into

another tray filled with stop solution, for another minute. Next, they were submerged into a fixer solution for 3 min, in order to remove any remaining silver bromide/halide. The contact with the fixing solution lasted for a long enough period to remove all silver ions. Once fixed, films were transferred into an empty tray and washed with running filtered water for a minimum of 30 min. Lastly, developed films were hung up in a fume cupboard to air dry overnight. The same procedure was carried out for all the films.

Please refer to Appendix 2 for reagents and solutions.

5.4.1.9. Calibration and image grabbing

For quantification of radiolabelled tissue sections, MCID™ Image Analysis Software (MCID Basic 7.0, Imaging Research In., Interfocus Ltd, UK) was used. A Northern Light desktop illuminator B95 with a Nikon 50mm, f2.8 lens was used to capture images. Prior software calibrations were required for reliable image acquisition and analysis: Magnification and Focus, Flat Field Correction, Distance and Density Calibration.

Magnification and Focus calibration was performed by adjusting the distance between the objective lens of the microscope and the light box until a focused image was achieved. In order to do so, the autoradiography film sheet was placed on the light box and image was digitalised. Camera height was adjusted until the coronal brain section occupied most of the field of view (FOV). As camera images can display some intensity variation due to uneven illumination, a *Flat Field Correction* was made for compensation of shading error. The film sheet was removed, and light box intensity illumination was adjusted until a blank FOV appeared bluish-pink. A new image was acquired, and the flat field correction was completed pixel by pixel. From then on,

MCID Basic scanned the blank field and was able to determine how much each pixel deviated from the mean grey level value. Once established, this correction became part of the camera's default configuration and images acquired were then automatically corrected for uneven illumination, providing standardised regulated images. Flat field correction was established whenever there was a change in the illumination pattern and when a new autoradiography film was used. *Distance Calibration* was then conducted. It established the pixel definition according to FOV distance in centimetres, by placing a glass scale in FOV and calibrating horizontal and vertical distances. *Density Calibration* was the last step before the image grabbing. In order to express autoradiography data in units of isotope or ligand concentration, a standard curve was constructed from the set of standards (RPA510 – RPA506 + RPA507, Amersham^{TM} Microscales^{TM}) co-exposed with the tissue sections and their related value. Pre-existing standard values were used for that purpose (Amersham Biosciences, Inc., [^{3}H] Microscales RPA506 and RPA507). As each standard was digitalised and sampled, MCID Basic plotted the standard curve (density vs. standard values). The system's internal density measurement unit for the standard values was ROD (Relative Optical Density). From the constructed curve, a ROD value corresponded to the concentration of ligand bound to the tissue area, in nCi/mg. Tritium standards were used for [O-methyl-^{3}H]WAY 100635 (5-HT1A), [^{3}H]ketanserin (5-HT2A). For [^{125}I]DOI, the results were kept expressed as ROD and receptor binding was averaged among the three films; density calibration was not applied in that case. After following the calibration steps, an image of each section was acquired and saved. The above steps were completed whenever a new film was placed on the light box.

5.4.1.10. Image analysis and quantification

Prior to image analysis, blank sections were sampled for the establishment of non-specific binding. On each image, ROI around the specific areas of interest (mPFC, NAcc, VTA, Hipp, Hyp, Amy, LC and DRN) were traced freehand for quantification, based on a mouse brain atlas (Paxinos and Franklin, 2004) (as shown in Figure 5.2, left column). Neuroanatomical images on the left side of Figure 5.2 were taken from the Allen Mouse Brain Atlas (Brain Explorer 2.3.2, Allen Institute from Brain Science), a digital high-resolution anatomic reference atlas accompanied by a systematic, hierarchically organised taxonomy of mouse brain structures. Specific binding of each neuroanatomical region was calculated automatically by subtraction of non-specific binding from total binding.

Measurements of standards of each cassette were used for the establishment of standard curves, which correlated ROD values with its specific binding in nCi/mg. As no reliable iodine standards were available, specific binding of films developed for 5-HT2C remained shown as ROD.

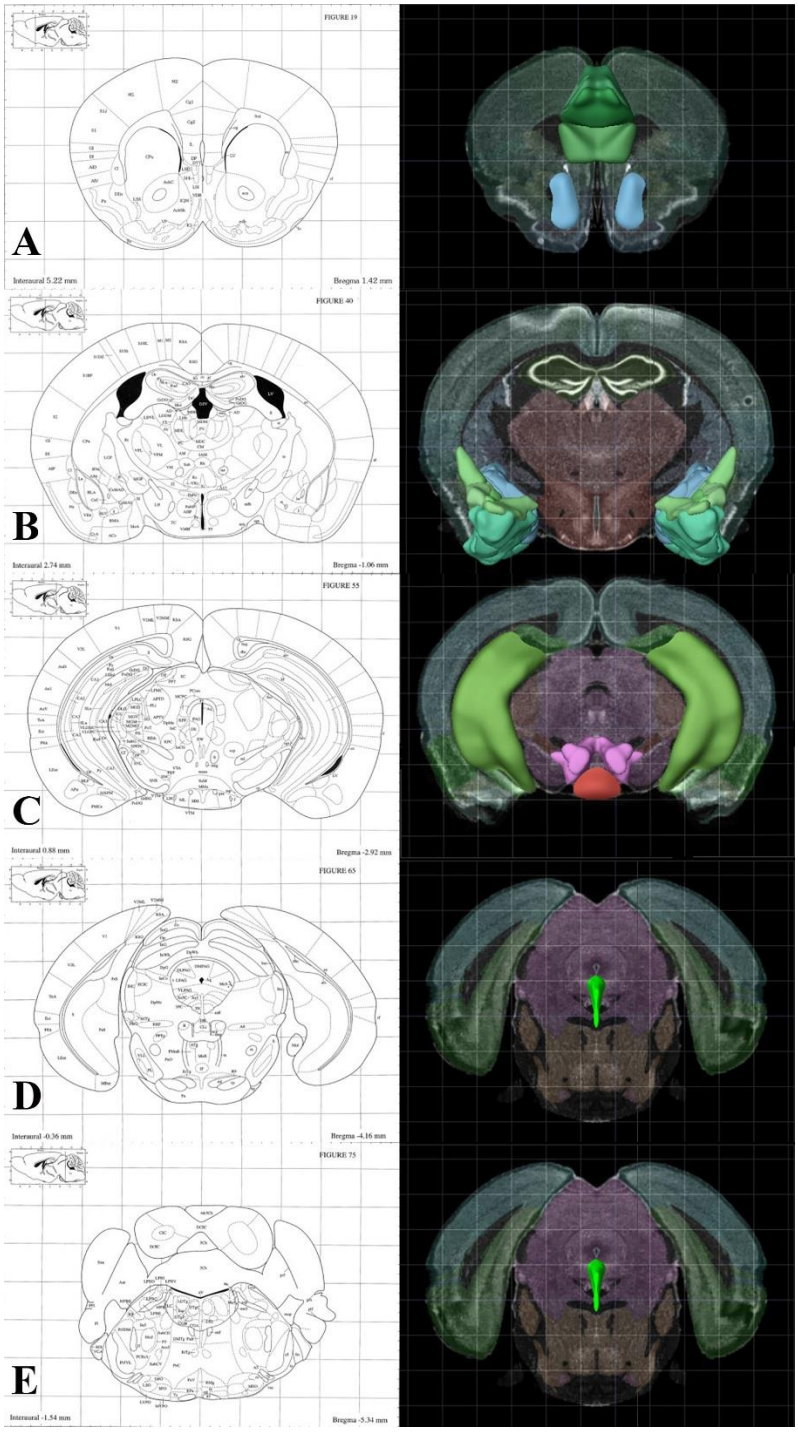

Figure 5.2. Neuroanatomical regions used for specific-binding quantification of 5-HT receptors. (A) mPFC (green) and NAcc (blue): bregma 1.98. (B) Amy (green and blue): bregma -1.06. (C) Hipp (green), VTA (pink), Hyp (red): bregma -2.50. (D) DRN (green): bregma -4.16. (E) LC (green): bregma -5.34. Figures on the left were taken from The Mouse Brain in Stereotaxic Coordinates (Paxinos and Franklin, 2004). Figures on the right were taken from Allen Mouse Brain Atlas software (Brain Explorer 2.3.2, Allen Institute from Brain Science).

5.4.2. Brain-region specific – *Htr1a, 2a, 2c, Slc6a4* mRNA expression

Experiment A (please refer to Chapter 2 for 'Methodological framework').

Expression of genes was measured in selected brain regions by RT-qPCR.

5.4.2.1. Brain tissue dissection, cryosectioning and micro-punching

Performed as shown in Chapter 4 for *Ghs-r1a* and *Lepr* mRNA expression. The following regions represented in Figure 5.3 and Table 5.1 were microdissected.

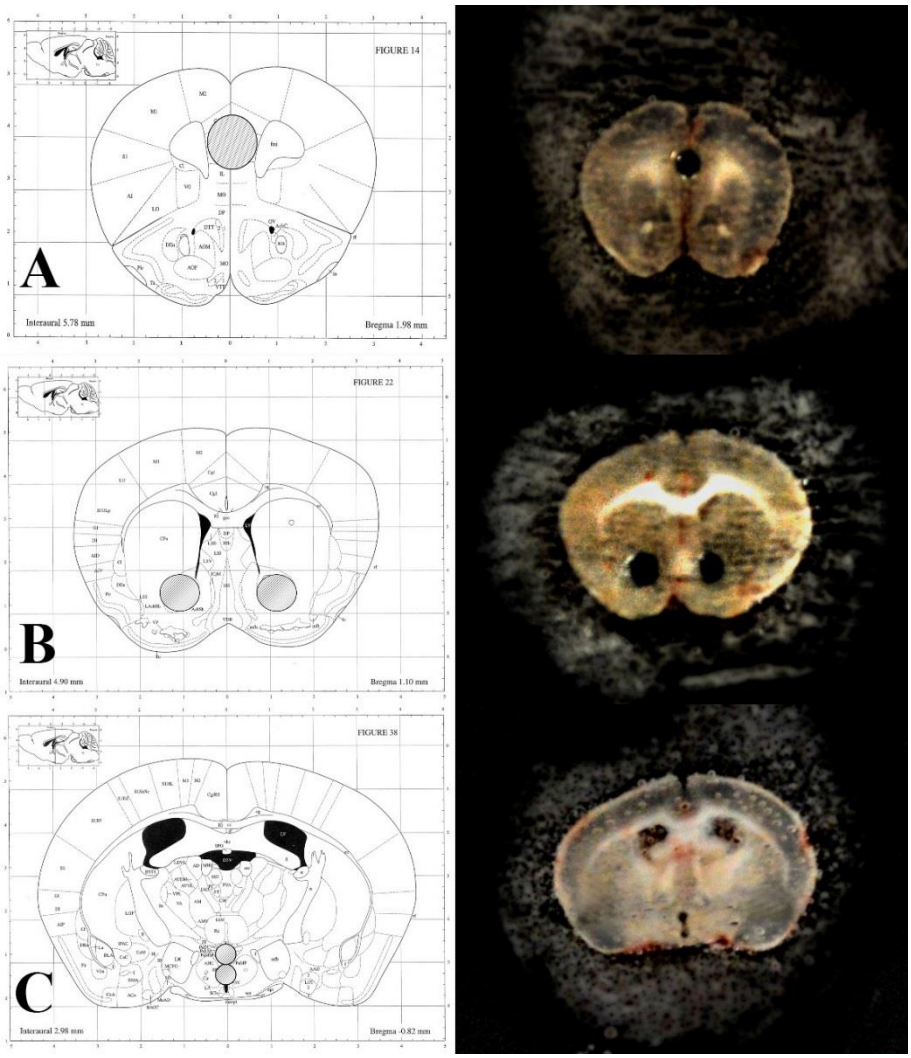

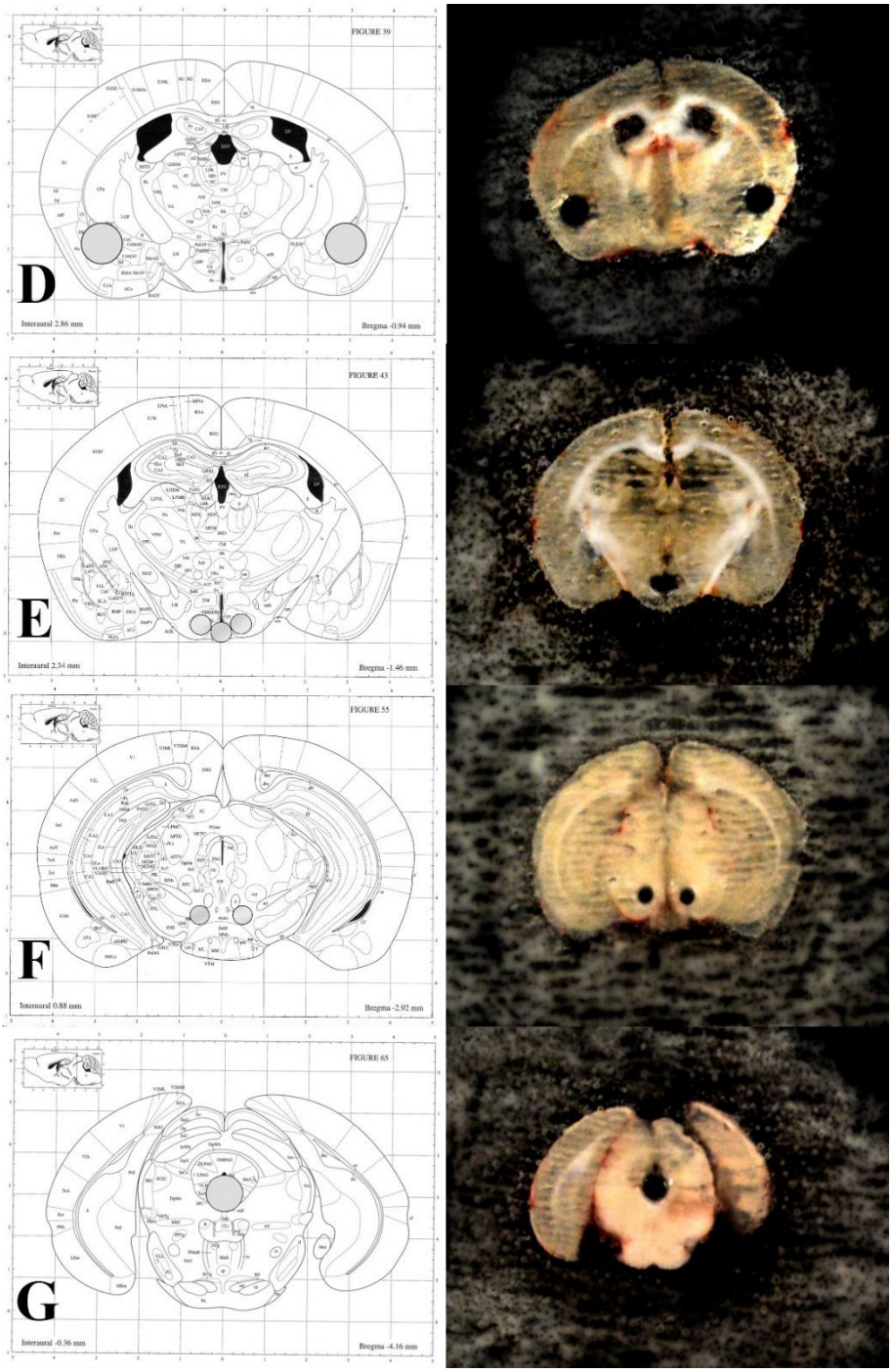

Figure 5.3. Neuroanatomical regions used for investigation into effects of 15-day chronic social stress on region-specific gene expression at day 16, using quantitative PCR with mRNA obtained from CSS mice (N=12) and CON mice (N=12). On the left, representative figures from Paxinos and Franklin (2004) depicting the target region for (A) mPFC. (B) NAcc. (C) PVN. (D) Amy. (E) ARC and VMH. (F) VTA. (G) RN. On the right, representative computer-enhanced photographs of brain sections taken after micro-punching.

Table 5.1. Anatomical details of brain region microdissection, according to The Mouse Brain in Stereotaxic Coordinates (Paxinos and Franklin, 2004)

Brain/region	**Bregma interval**	**Ø (mm)**
mPFC	1.98 – 1.42	1
NAcc	1.42 – 0.74	1
PVN	0.02 – -1.94	0.5
BLA	-0.82 – -1.94	1
ARC	-1.34 – -1.94	0.5
VMH	-1.34 – -1.94	0.5
VTA	-2.92 – -3.80	0.5
RN	-4.36 – -4.84	1

Abbreviations: mPFC, medial prefrontal cortex; NAcc, nucleus accumbens; PVN, paraventricular nucleus; BLA, basolateral amygdala; ARC, arcuate nucleus; VMH, ventromedial hypothalamus; VTA, ventral tegmental area; RN, raphe nuclei.

5.4.2.2. RNA extraction

Performed as shown in Chapter 4 for *Ghs-r1a* and *Lepr* mRNA expression.

Visual assessment of RNA integrity (ratio 2:1 for 28S/18S RNA bands) could not be performed since a minimum of 1µg of RNA is generally required to run agarose gel electrophoresis.

5.4.2.3. Reverse transcription

Synthesis of cDNA from RNA template was performed. Depending on the RNA yield for each brain region, different amounts of RNA were used (Table 5.2). RNA was then reverse transcribed, as performed for *Ucp-1* mRNA expression, described in Chapter 3.

Table 5.2. Amount of RNA (ng) used for reverse transcription according to the brain region.

Brain/region	RNA (ng)
mPFC	85
NAcc	110
PVN	100
BLA	100
ARC	30
VMH	50
VTA	65
RN	100

Abbreviations: mPFC, medial prefrontal cortex; NAcc, nucleus accumbens; PVN, paraventricular nucleus; BLA, basolateral amygdala; ARC, arcuate nucleus; VMH, ventromedial hypothalamus; VTA, ventral tegmental area; RN, raphe nuclei.

5.4.2.4. Quantitative polymerase chain reaction

As performed for *Ucp-1* mRNA expression, described in Chapter 3.

5.4.2.4.1. Primer design

Predesigned KiCqStart® primer pairs for mouse *Htr1a*, *Htr2a* and *Htr2c* were purchased from Sigma-Aldrich. *Slc6a4* primer pair sequence was obtained from Filipenko (2002) and synthesised by Invitrogen (ThermoScientific™). *Actb* primer pair was designed using NCBI Primer-BLAST, with the parameters set to create a product of 70-210bp and primer melting temperature ranging from 57°C to 63°C. BLAT (BLAST-Like Alignment Tool) from UCSC Genome Browser was used to check for primer sequence alignment and synthesised by Invitrogen (ThermoScientific™). Working stocks containing both forward (FW) and reverse (RV) primers at a concentration of 10μM were prepared.

5.4.2.4.2. PCR efficiency

As performed for *Ucp-1* mRNA expression, described in Chapter 3.

Table 5.3. Gene description, primer sequences, qPCR parameters and primer efficiency

Gene	Primer sequence ('5 – 3')	PCR product (bp)	Annealing temp. (°C)	Extension (sec)	PCR *E* (%)
Htr1a	FW: CTCACCCTCAGTTTCTTTTC	165	60	30	106
	RV: TCTAAGTCTCCAACCTCTTG				
Htr2a	FW: ATGAAAAGGTTAGCTGTGTG	208	60	30	95
	RV: GGCAATGTTAAAAGCATCAC				
Htr2c	FW: GTCTGGATTTCACTAGATGTG	172	60	30	99
	RV: GAAACTCCTATTGATATTGCCC				
Slc6a4	FW: TTTGCCATCATCTTCTTCCTCATG	363	60	30	100
	RV: GGCCACCCAGCAGATCCTC				
Actb	FW: GGCTGTATTCCCCTCCATCG	154	63	30	103
	RV: CCAGTTGGTAACAATGCCATGT				

5.4.3. Statistical analysis

Statistical analysis of the CSS effects on 5-HT receptor binding and mRNA expression was conducted using Statistical Package for the Social Sciences (version 22, SPSS Inc., Chicago IL, USA). Gene expression analysis was carried out using the $2^{-\Delta\Delta Ct}$ method, with β-Actin as the control gene for normalisation. Independent Students's t-test was conducted for each region within each receptor study. Statistical significance was set at $p \leq 0.05$.

5.5. Results

5.5.1. Serotonin 5-HT1A, 2A and 2C receptor binding

5.5.1.1. Serotonin 5-HT1A

The radioligand distribution of tritium-dependent signal was consistent with a high density of 5-HT1A receptors in DRN of the rodent brain. There was a significant increase in [O-methyl-^{3}H]WAY 100635 binding in the DRN of CSS mice compared with CON mice ($t(8.15)=-4.52$, $p\leq0.01$, Figure 5.4). There was no significant difference in [O-methyl-^{3}H]WAY 100635 binding between the CSS and CON groups in any other region of the brain.

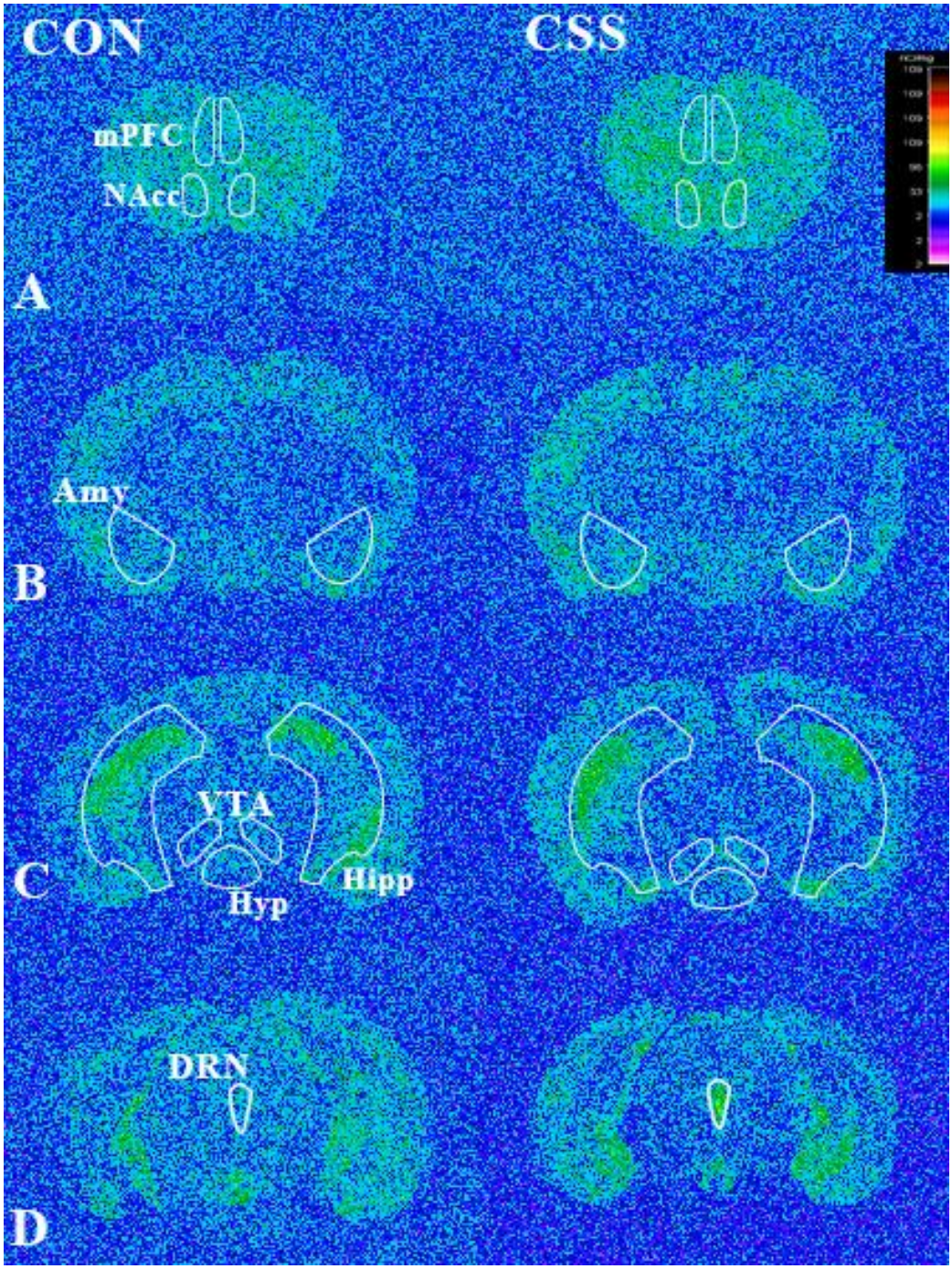

Figure 5.4. Representative computer-enhanced autoradiograms of [O-methyl-^{3}H]WAY 100635 total binding in mouse brain, CON and CSS groups. Coronal brain sections were incubated with 2nM [O-methyl-^{3}H]WAY 100635 in Tris–HCl with 10μM pargyline for 2 hours at room temperature. Non–specific binding was defined in the presence of 10mM 5–HT. ROIs outlined in white: (A) mPFC and NAcc. (B) Amy. (C) Hipp, VTA, Hyp. (D) DRN, based on Paxinos and Franklin (2004). Abbreviations: mPFC, medial prefrontal cortex; NAcc, nucleus accumbens; Amy, amygdala; Hyp, hypothalamus; VTA, ventral tegmental area; Hipp, hippocampus; DRN, dorsal raphe nucleus.

Table 5.4. Quantitative autoradiography of 5-HT1A receptors visualised by means of [O-methyl-^{3}H]WAY 100635 in selected brain regions.

Brain/region	CON	CSS	Difference (%)	*p* value	
mPFC	**13.52** ± 1.10	**13.80** ± 1.49	2.01	0.886	
NAcc	**15.08** ± 1.25	**18.83** ± 1.85	24.90	0.115	
Amy	**12.42** ± 1.52	**13.43** ± 1.76	8.13	0.671	
Hyp	**6.10** ± 0.77	**6.30** ± 0.46	3.26	0.834	
VTA	**7.42** ± 1.15	**7.55** ± 0.98	1.84	0.930	
Hipp	**17.71** ± 2.53	**21.44** ± 2.81	21.08	0.340	
DRN	**10.63** ± 0.89	**25.15** ± 3.09	136.58	0.002	**

Abbreviations: mPFC, medial prefrontal cortex; NAcc, nucleus accumbens; Amy, amygdala; Hyp, hypothalamus; VTA, ventral tegmental area; Hipp, hippocampus; DRN, dorsal raphe nucleus. **p≤0.01. Data expressed as mean values ± SEM in nCi/mg, n=8 per group.

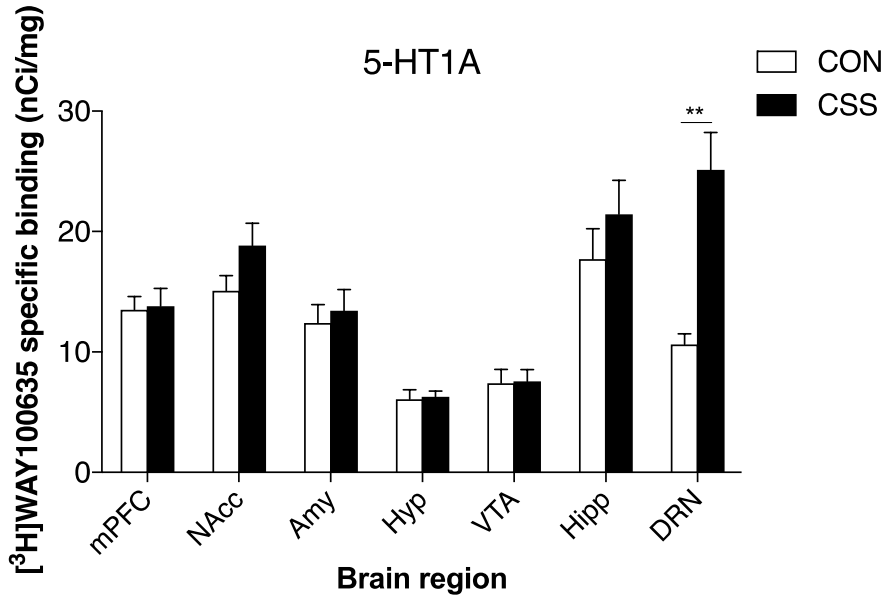

Figure 5.5. Effects of 15-day chronic social stress (CSS, N=8), versus control handling (CON, N=8) on [O-methyl-^{3}H]WAY 100635 specific binding at 5-HT1A receptor sites. Values presented as mean + SEM in nCi/mg. Abbreviations like in Table 5.4. **p≤0.01 for CSS versus CON mice following an independent Student's t-test. Abbreviations: mPFC, medial prefrontal cortex; NAcc, nucleus accumbens; Amy, amygdala; Hyp, hypothalamus; VTA, ventral tegmental area; Hipp, hippocampus; DRN, dorsal raphe nucleus.

5.5.1.2. Serotonin 5-HT2A

The radioligand distribution of tritium-dependent signal was consistent with the lower density of 5-HT2A receptors in CSS mice compared with CON mice in both amygdala and VTA. There was a significant decrease in [^{3}H]ketanserin binding in the VTA ($t(14)=-4.83$, $p\leq0.001$) and amygdala ($t(14)=2.32$, $p\leq0.05$) of CSS mice compared with CON mice (Figure 5.6B). There was no significant difference in [^{3}H]ketanserin binding between the CSS and CON groups in the other regions of the brain studied.

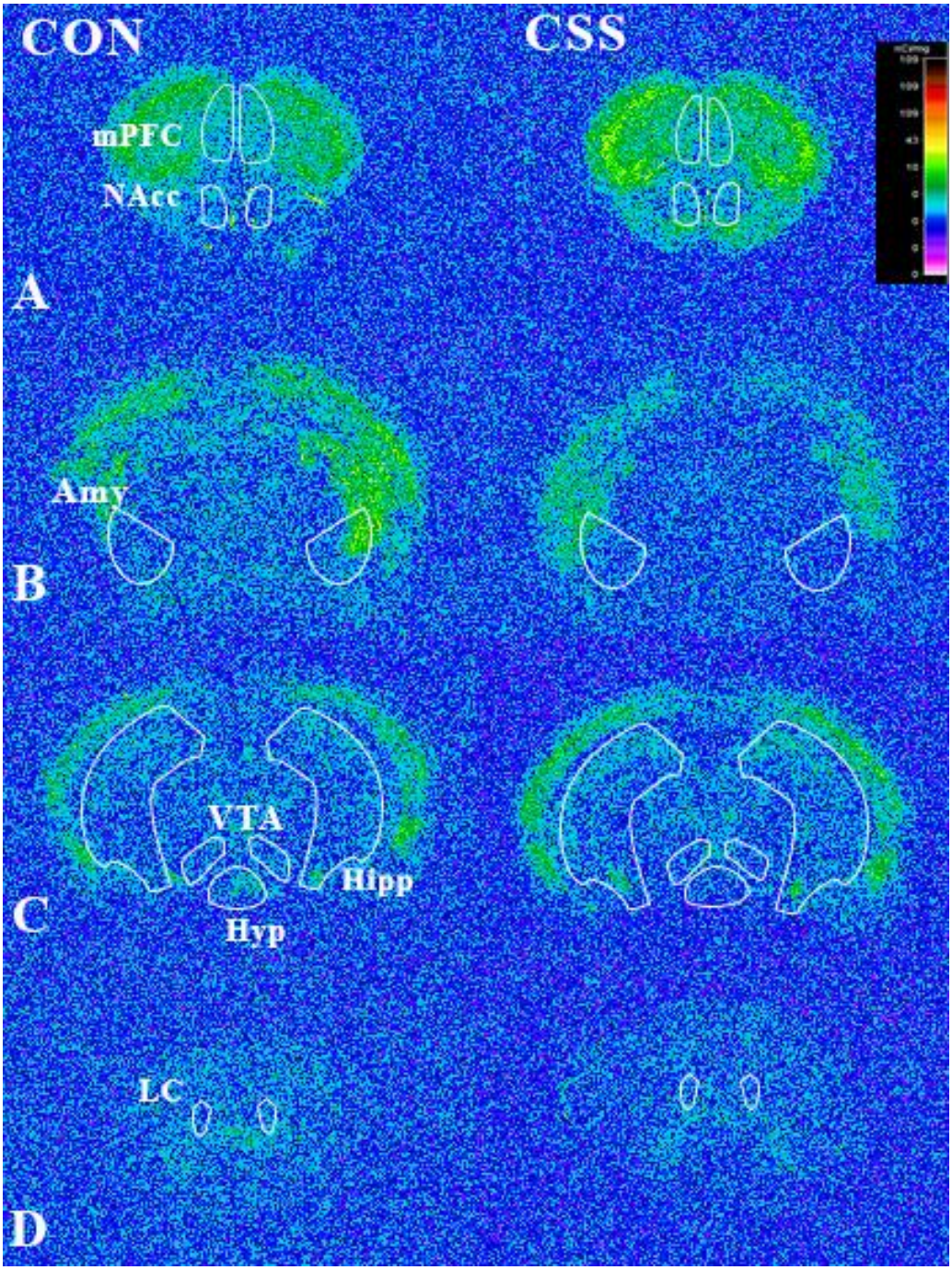

Figure 5.6. Representative computer-enhanced autoradiograms of [^{3}H]ketanserin total binding in mouse brain, CON and CSS groups. Coronal brain sections were incubated with 1nM [^{3}H]ketanserin in Tris-HCl buffer with 1μM prazosin and 100nM tetrabenazine for 1h at room temperature. Non-specific binding was defined in the presence of 200μM methysergide. ROIs outlined in white: (A) mPFC and NAcc. (B) Amy. (C) Hipp, VTA, Hyp. (D) LC (Paxinos and Franklin, 2004). Abbreviations: mPFC, medial prefrontal cortex; NAcc, nucleus accumbens; Amy, amygdala; Hyp, hypothalamus; VTA, ventral tegmental area; Hipp, hippocampus; LC, locus coeruleus.

Table 5.5. Quantitative autoradiography of 5-HT2A receptors visualised by means of [^{3}H]ketanserin in selected brain regions.

Brain/region	CON	CSS	Difference (%)	*p* value	
mPFC	**4.77** ± 0.68	**3.11** ± 0.63	-34.70	0.098	
NAcc	**2.02** ± 0.43	**1.74** ± 0.48	-14.10	0.667	
Amy	**1.30** ± 0.24	**0.67** ± 0.14	-48.22	0.036	*
Hyp	**1.53** ± 0.35	**1.25** ± 0.31	-18.16	0.607	
VTA	**0.81** ± 0.08	**0.32** ± 0.07	-60.62	0.0002	***
Hipp	**0.95** ± 0.13	**0.62** ± 0.13	-35.17	0.088	
LC	**1.20** ± 0.20	**0.74** ± 0.14	-38.21	0.082	

Abbreviations: mPFC, medial prefrontal cortex; NAcc, nucleus accumbens; Amy, amygdala; Hyp, hypothalamus; VTA, ventral tegmental area; Hipp, hippocampus; LC, locus coeruleus. *p≤0.05; ***p≤0.001. Data expressed as mean ± SEM in nCi/mg, n=8 per group.

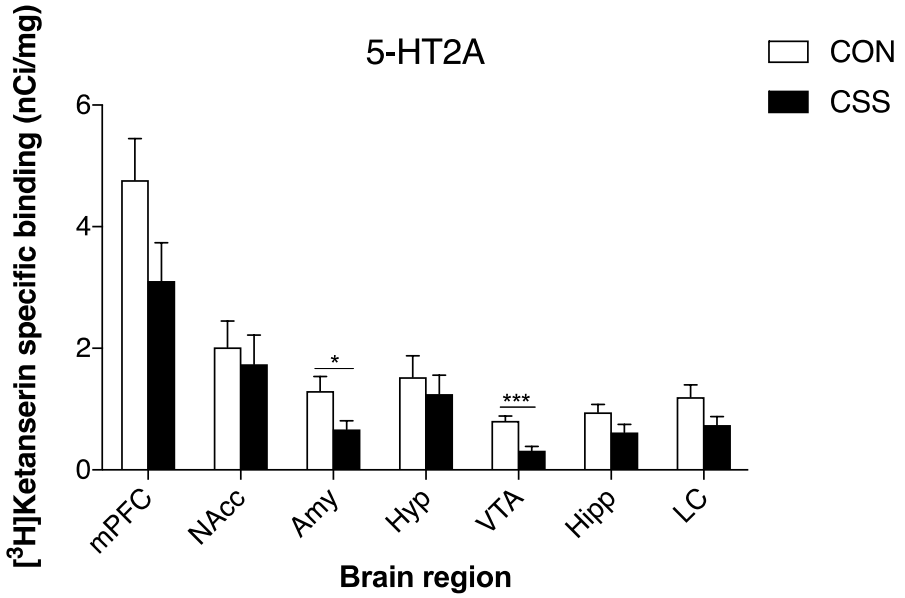

Figure 5.7. Effects of 15-day chronic social stress (CSS, N=8), versus control handling (CON, N=8) on [^{3}H]ketanserin specific binding of [^{3}H]ketanserin at 5-HT2A receptor sites. Values presented as mean + SEM. Abbreviations like in Table 5.5.*p≤0.05, ***p≤0.001 for CSS versus CON mice following an independent Student's t-test. Abbreviations: mPFC, medial prefrontal cortex; NAcc, nucleus accumbens; Amy, amygdala; Hyp, hypothalamus; VTA, ventral tegmental area; Hipp, hippocampus; LC, locus coeruleus.

5.5.1.3. Serotonin 5-HT2C

There was a significant decrease in [^{125}I]DOI binding in the DRN ($t(13)=2.36$, $p \leq 0.05$) of CSS mice compared with CON mice (Figure 5.8, Table 5.6). There was no significant difference in [^{125}I]DOI binding between the CSS and CON groups in any other region of the brain studied.

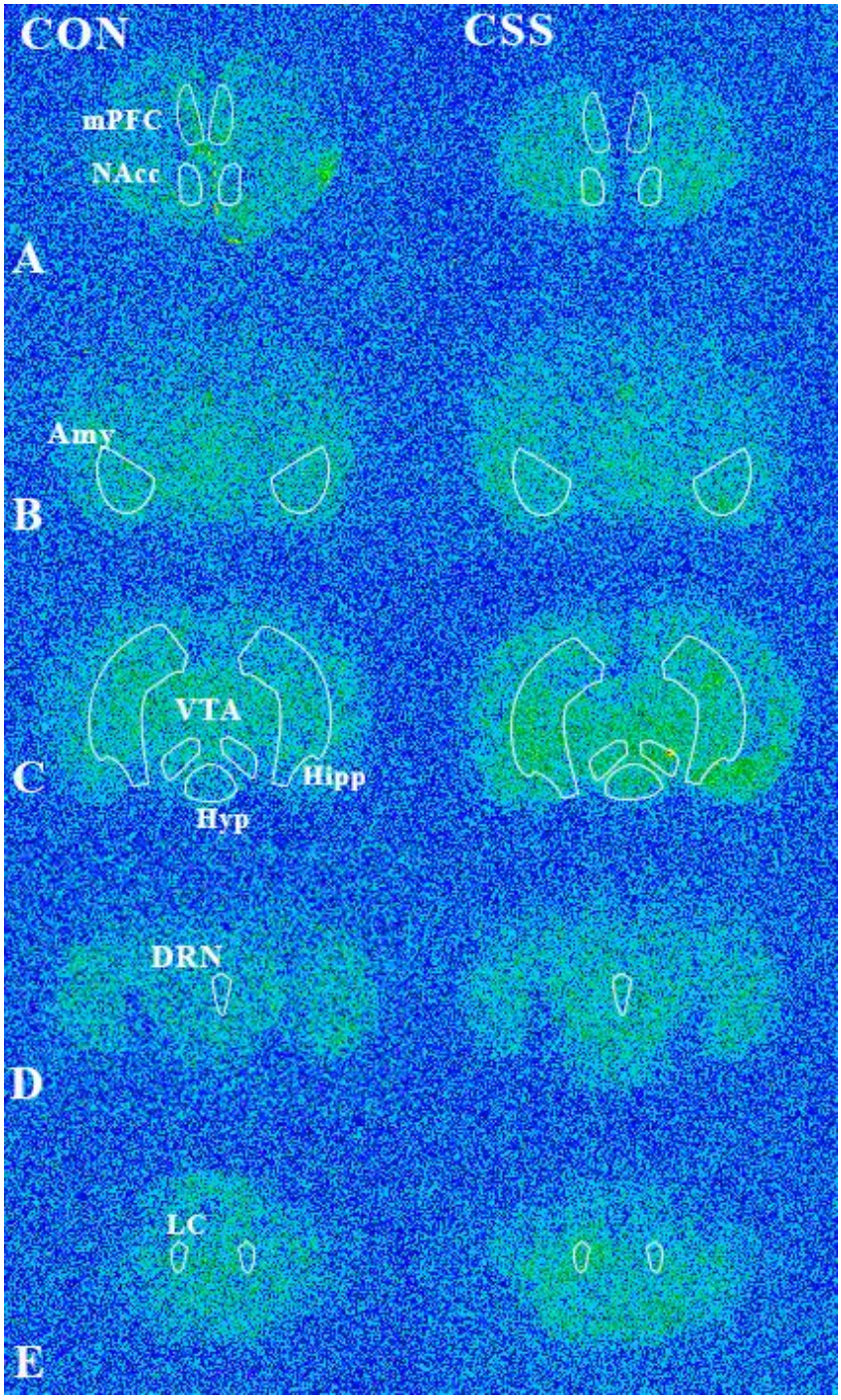

Figure 5.8. Representative computer-enhanced autoradiograms of [^{125}I]DOI total binding in mouse brain, CON and CSS groups. Coronal brain sections were incubated with 0.2nM [^{125}I]DOI with 100nM MDL 100907 for 1h at room temperature. Non-specific binding was assessed using 10μM RS-102221. ROIs outlined in white: (A) mPFC and NAcc. (B) Amy. (C) Hipp, VTA, Hyp. (D) DRN. (E) LC (Paxinos and Franklin, 2004). Abbreviations: mPFC, medial prefrontal cortex; NAcc, nucleus accumbens; Amy, amygdala; Hyp, hypothalamus; VTA, ventral tegmental area; Hipp, hippocampus; DRN, dorsal raphe nucleus; LC, locus coeruleus.

Table 5.6. Quantitative autoradiography of 5-HT2C receptors visualised by means of [^{125}I]DOI in selected brain regions.

Brain/region	CON	CSS	Difference (%)	*p* value	
mPFC	**0.0203** ± 0.0041	**0.0196** ± 0.0047	-3.88	0.901	
NAcc	**0.0232** ± 0.0038	**0.0204** ± 0.0047	-12.05	0.650	
Amy	**0.0264** ± 0.0031	**0.0237** ± 0.0044	-10.29	0.622	
Hyp	**0.0228** ± 0.0026	**0.0139** ± 0.0046	-38.93	0.099	
VTA	**0.0264** ± 0.0039	**0.0179** ± 0.0016	-32.01	0.080	
Hipp	**0.0188** ± 0.0032	**0.0137** ± 0.0022	-27.08	0.223	
DRN	**0.0398** ± 0.0058	**0.0232** ± 0.0041	-41.62	0.034	*
LC	**0.0297** ± 0.0070	**0.0257** ± 0.0048	-13.25	0.645	

Abbreviations: mPFC, medial prefrontal cortex; NAcc, nucleus accumbens; Amy, amygdala; Hyp, hypothalamus; VTA, ventral tegmental area; Hipp, hippocampus; DRN, dorsal raphe nucleus; LC, locus coeruleus. *p≤0.05. Data expressed as mean ± SEM in ROD, n=8 per group.

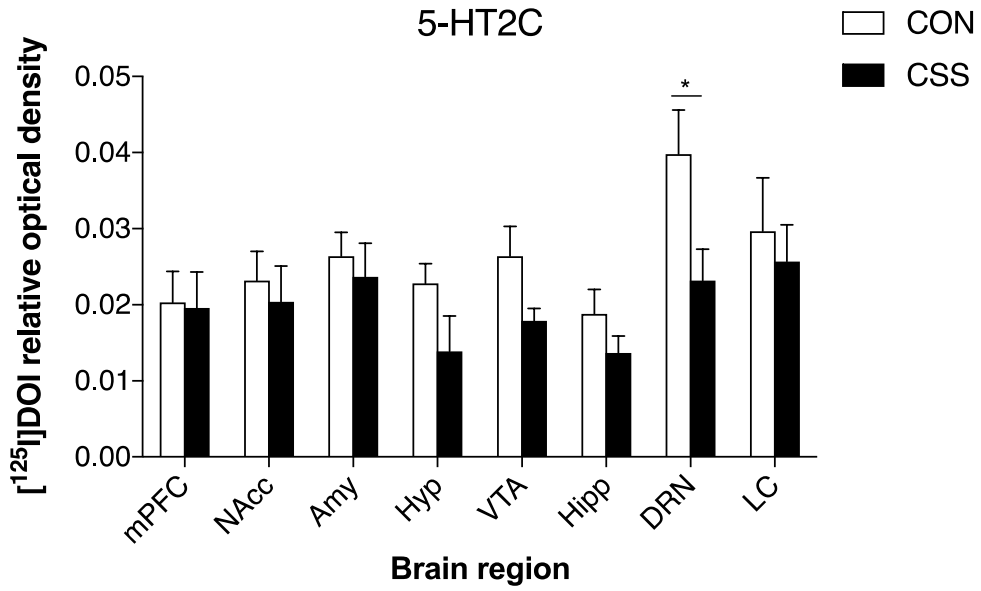

Figure 5.9. Effects of 15-day chronic social stress (CSS, N=8), versus control handling (CON, N=8) on [^{125}I]DOI specific binding at 5-HT2C receptor sites. Values presented as mean + SEM. Abbreviations like in Table 5.6. *p≤0.05 for CSS versus CON mice following an independent Student's t-test. Abbreviations: mPFC, medial prefrontal cortex; NAcc, nucleus accumbens; Amy, amygdala; Hyp, hypothalamus; VTA, ventral tegmental area; Hipp, hippocampus; DRN, dorsal raphe nucleus; LC, locus coeruleus.

5.5.2. Brain-region specific – *Htr1a, 2a, 2c* and *Slc6a4* mRNA expression (Experiment A)

In Experiment A, gene expression of *Htr1a*, *Htr2a*, and *Htr2c* were investigated in medial prefrontal cortex (mPFC), nucleus accumbens (NAcc), paraventricular nucleus of hypothalamus (PVN), basolateral amygdala (BLA), arcuate nucleus (ARC), ventromedial hypothalamus (VMH), ventral tegmental area (VTA) and raphe nuclei (RN) including DRN, by means of quantitative PCR.

5.5.2.1. *Htr1a*

There were significant increases in *Htr1a* expression in CSS mice compared with CON mice in the mPFC ($t(19)=2.92$, $p\leq0.01$), PVN ($t(20)=2.08$, $p\leq0.05$), VMH ($t(20)=3.15$, $p\leq0.01$) and RN ($t(16)=2.18$, $p\leq0.05$) (Table 5.7, Figure 5.10). There was no CSS effect in the other regions studied.

Table 5.7. *Htr1a* mRNA expression in selected brain regions.

Brain/region	CON ΔCt	CSS ΔCt	Difference (%)	Fold change	*p* value	
mPFC	**6.92** ± 0.09	**6.49** ± 0.11	-6.22	1.35	0.009	**
NAcc	**9.94** ± 0.14	**9.89** ± 0.21	-0.44	1.03	0.872	
PVN	**7.12** ± 0.10	**6.85** ± 0.08	-3.85	1.21	0.050	*
BLA	**7.60** ± 0.16	**7.61** ± 0.19	0.08	1.00	0.981	
ARC	**7.43** ± 0.12	**7.01** ± 0.21	-5.74	1.34	0.100	
VMH	**6.41** ± 0.13	**5.95** ± 0.09	-7.23	1.38	0.005	**
VTA	**7.02** ± 0.09	**6.86** ± 0.15	-2.27	1.12	0.412	
RN	**5.38** ± 0.10	**5.12** ± 0.06	-4.67	1.19	0.044	*

Abbreviations: mPFC, medial prefrontal cortex; NAcc, nucleus accumbens; PVN, paraventricular nucleus; BLA, basolateral amygdala; ARC, arcuate nucleus; VMH, ventromedial nucleus; VTA, ventral tegmental area; RN, raphe nuclei. *p≤0.05, **p≤0.01. Values of ΔCt expressed as mean ± SEM. n=12 per group.

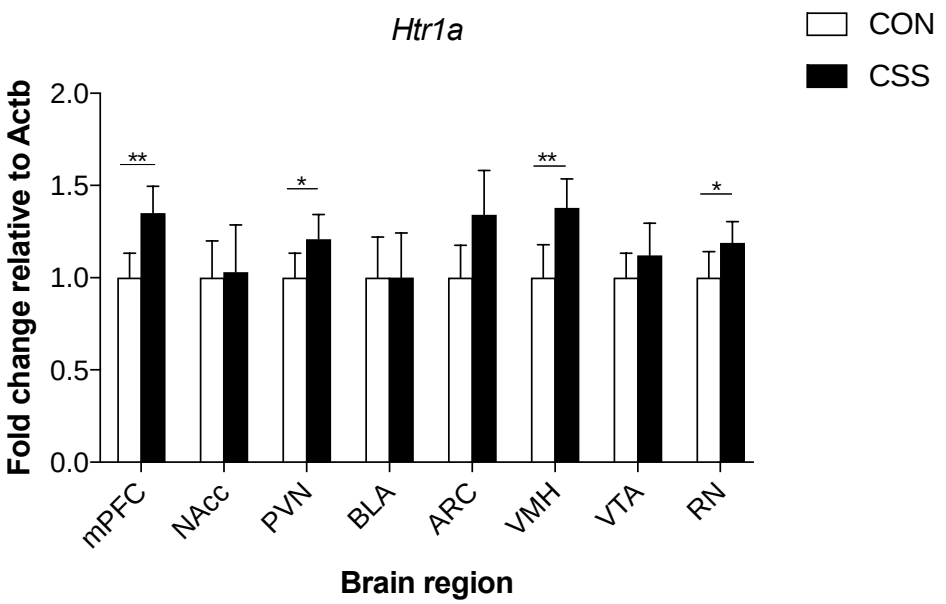

Figure 5.10. Effects of 15-day chronic social stress (CSS, N=12), versus control handling (CON, N=12) on region-specific *Htr1a* mRNA expression. Values presented as fold change + SEM. *p≤0.05, **p≤0.01 for CSS versus CON mice following an independent Student's t-test. Abbreviations: mPFC, medial prefrontal cortex; NAcc, nucleus accumbens; PVN, paraventricular nucleus; BLA, basolateral amygdala; ARC, arcuate nucleus; VMH, ventromedial nucleus; VTA, ventral tegmental area; RN, raphe nuclei.

5.5.2.2. *Htr2a*

There was a significant increase in Htr2a expression in CSS mice compared with CON mice in the BLA ($t(14.14)=4.284$, $p\leq0.001$) (Table 5.8, Figure 5.11). There was no significant difference in Htr2a expression between the CSS and CON groups in any other region investigated.

Table 5.8. *Htr2a* mRNA expression in selected brain regions.

Brain/region	CON ΔCt	CSS ΔCt	Difference (%)	Fold change	*p* value	
mPFC	**6.55** ± 0.21	**6.61** ± 0.09	0.92	0.96	0.797	
NAcc	**10.07** ± 0.27	**9.47** ± 0.19	-5.97	1.52	0.080	
PVN	**6.32** ± 0.10	**6.23** ± 0.10	-1.39	1.06	0.545	
BLA	**5.80** ± 0.24	**4.69** ± 0.11	-19.15	2.16	0.0004	***
ARC	**7.95** ± 0.16	**7.68** ± 0.11	-3.32	1.20	0.201	
VMH	**6.56** ± 0.08	**6.36** ± 0.09	-2.94	1.14	0.136	
VTA	**8.32** ± 0.11	**8.55** ± 0.16	2.76	0.85	0.268	
RN	**8.73** ± 0.26	**9.04** ± 0.11	3.53	0.81	0.288	

Abbreviations: mPFC, medial prefrontal cortex; NAcc, nucleus accumbens; PVN, paraventricular nucleus; BLA, basolateral amygdala; ARC, arcuate nucleus; VMH, ventromedial nucleus; VTA, ventral tegmental area; RN, raphe nuclei. ***p≤0.001. Values of ΔCt expressed as mean ± SEM, n=12 per group.

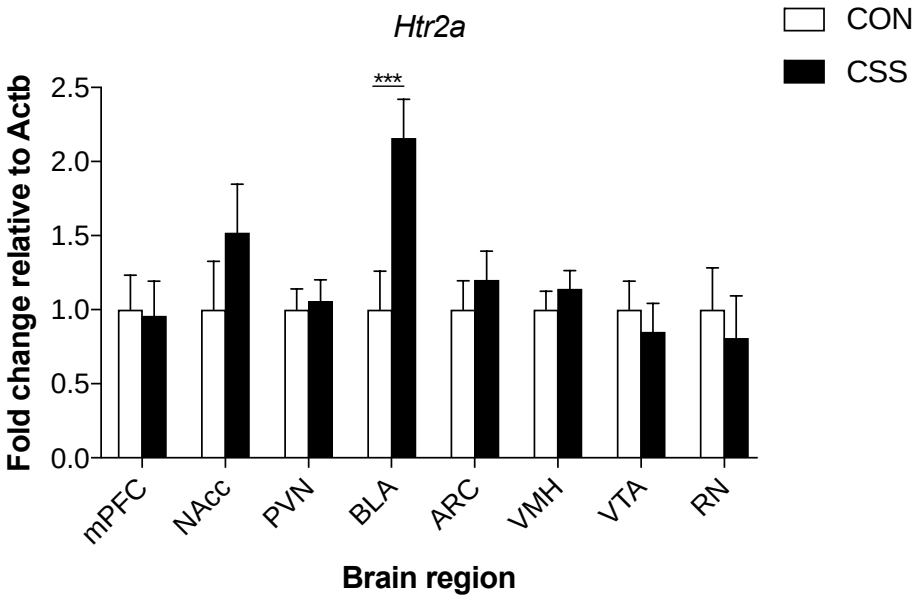

Figure 5.11. Effects of 15-day chronic social stress (CSS, N=12), versus control handling (CON, N=12) on region-specific *Htr2a* mRNA expression. Values presented as fold change + SEM. ***p≤0.001 for CSS versus CON mice following an independent Student's t-test. Abbreviations: mPFC, medial prefrontal cortex; NAcc, nucleus accumbens; PVN, paraventricular nucleus; BLA, basolateral amygdala; ARC, arcuate nucleus; VMH, ventromedial nucleus; VTA, ventral tegmental area; RN, raphe nuclei.

5.5.2.3. *Htr2c*

No effect of CSS on *Htr2c* mRNA expression in any brain region of interest was observed (Table 5.9, Figure 5.12).

Table 5.9. *Htr2c* mRNA expression in selected brain regions.

Brain/region	CON ΔCt	CSS ΔCt	Difference (%)	Fold change	*p* value
mPFC	**7.51** ± 0.07	**7.38** ± 0.18	-1.68	1.09	0.535
NAcc	**5.50** ± 0.10	**5.60** ± 0.19	1.93	0.93	0.648
PVN	**4.51** ± 0.04	**4.40** ± 0.08	-2.52	1.08	0.254
BLA	**5.32** ± 0.12	**5.60** ± 0.15	5.23	0.82	0.202
ARC	**7.41** ± 0.17	**7.31** ± 0.11	-1.34	1.07	0.615
VMH	**4.43** ± 0.10	**4.52** ± 0.14	2.13	0.94	0.590
VTA	**6.19** ± 0.06	**6.22** ± 0.12	0.55	0.98	0.809
RN	**4.66** ± 0.08	**4.46** ± 0.08	-4.24	1.15	0.087

Abbreviations: mPFC, medial prefrontal cortex; NAcc, nucleus accumbens; PVN, paraventricular nucleus; BLA, basolateral amygdala; ARC, arcuate nucleus; VMH, ventromedial nucleus; VTA, ventral tegmental area; RN, raphe nuclei. Values of ΔCt expressed as mean ± SEM. n=12 per group.

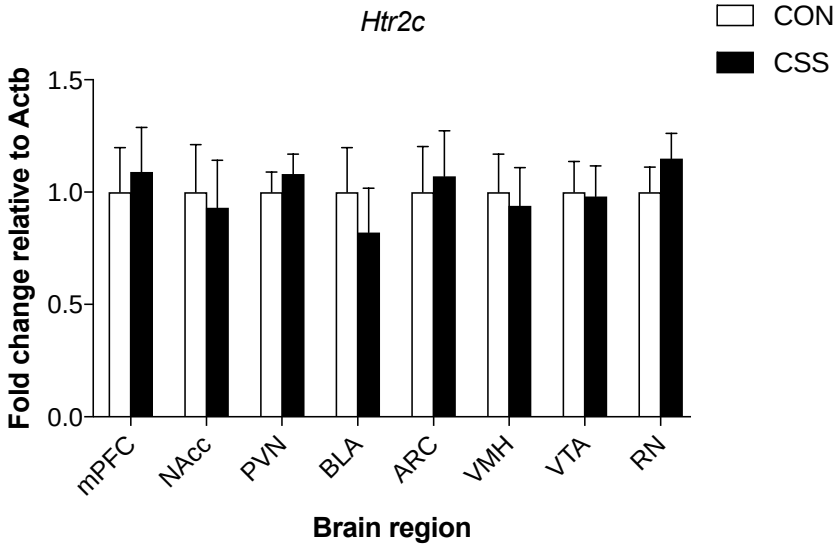

Figure 5.12. Effects of 15-day chronic social stress (CSS, N=12), versus control handling (CON, N=12) on region-specific *Htr2c* mRNA expression. Values presented as fold change + SEM. Abbreviations: mPFC, medial prefrontal cortex; NAcc, nucleus accumbens; PVN, paraventricular nucleus; BLA, basolateral amygdala; ARC, arcuate nucleus; VMH, ventromedial nucleus; VTA, ventral tegmental area; RN, raphe nuclei.

5.5.2.4. *Slc6a4*

There was a significant increase in *Slc6a4* expression in the RN of CSS mice compared with CON mice ($t(18)=3.11$, $p \leq 0.05$) (Table 5.10). Expression of *Slc6a4* was also investigated in some other brain regions (mPFC, NAcc, PVN, BLA, VTA, ARC and VMH). In NAcc and BLA, expression was increased in CSS compared with CON mice (data not shown). However, in all regions except RN, there were methodological issues with the expression signals in terms of delayed amplification; these were probably related to the low expression levels of *Slc6a4* in these regions and the low cDNA template used.

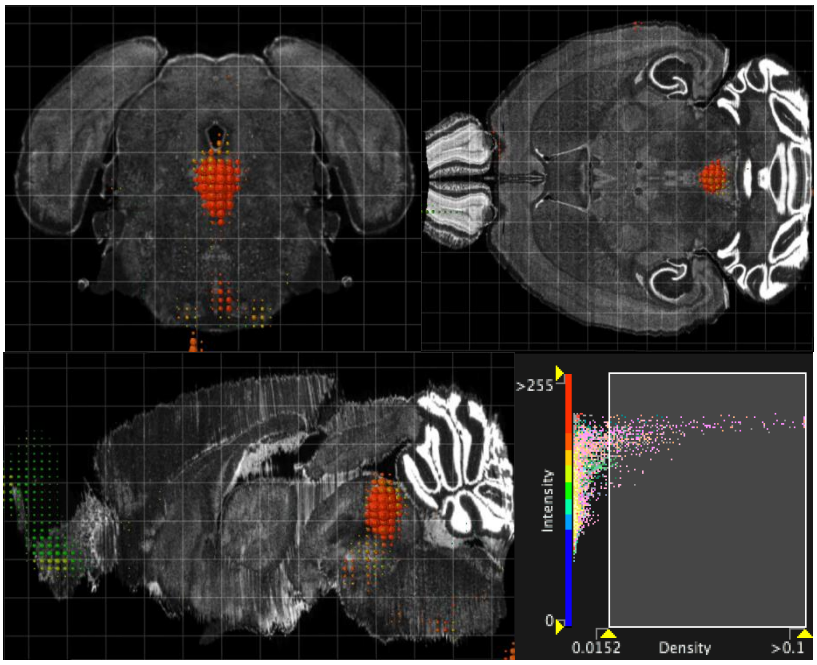

Figure 5.13. Coronal, axial and sagittal view of mouse brain displaying regions where Slc6a4 are found expressed, using in situ hybridisation data. Figures were taken from Allen Mouse Brain Atlas software (Brain Explorer 2.3.2, Allen Institute from Brain Science).

Table 5.10. *Slc6a4* mRNA expression in selected brain regions.

Brain/region	CON ΔCt	CSS ΔCt	Difference (%)	Fold change	*p* value	
RN	**1.24** ± 0.15	**0.58** ± 0.15	-53.56	1.59	0.006	**

Abbreviation: RN, raphe nuclei. **p≤0.01. Values of ΔCt expressed as mean ± SEM. n=12 per group.

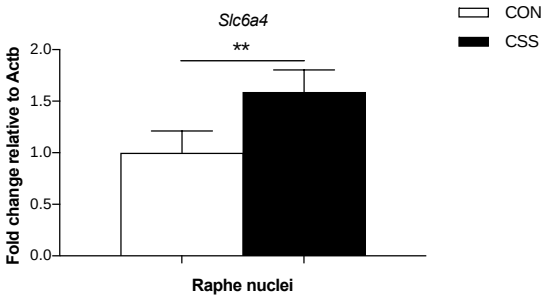

Figure 5.14. Effects of 15-day chronic social stress (CSS, N=12), versus control handling (CON, N=12) on region-specific *Slc6a4* mRNA expression. Values presented as fold change + SEM. **p≤0.01 for CSS versus CON mice following an independent Student's t-test.

5.6. Discussion

Numerous lines of evidence favour the hypothesis that serotonergic neurotransmission is sensitive to diverse stressors and it is involved in the processes of adaptation to aversive events through stress-related eating behaviours. In this sense, the present study also hypothesised that CSS promotes changes in 5-HT receptor binding, which therefore can disturb the food-related reward mechanisms. Through the analysis of 5-HT receptor localisation, also referred to as "receptor mapping", it was possible to quantify the specific binding of each receptor within the brain regions of interest in mice that underwent social stress and compare with controls. The present study aimed at investigating the effects of CSS particularly on 5-HT1A, 5-HT2A, and 5-HT2C receptor binding by means of *in vitro* quantitative autoradiography, as well as *Htr1a, 2a, 2c* and *Slc6a4* mRNA expression by means of quantitative PCR in mouse brain regions associated with reward processing.

5.6.1. Serotonin 5-HT1A receptor and *Htr1a*

The present study found a markedly increased 5-HT1A specific binding in the DRN of CSS mice, as well as *Htr1a* mRNA expression in the RN, in comparison with CON mice. In addition, *Htr1a* was also significantly increased in the mPFC, PVN and VMH of CSS mice compared with CON mice.

In the RN, 5-HT1A is a somatodendritic inhibitory autoreceptor located on 5-HT neurons; it acts by reducing neuronal serotonergic firing rate and 5-HT release in all projection targets, including those of interest in this study. In the context of mood disorders, it has been shown that subjects with major depressive disorder (MDD) exhibit increased 5-HT1A receptor binding in several brain regions, including the RN

(Hesselgrave and Parsey, 2013; Kaufman et al., 2016). Nevertheless, reduced 5-HT1A specific binding in the RN of patients with depression was also observed (Drevets et al., 1999; Sargent et al., 2000). In preclinical studies, higher levels of 5-HT1A autoreceptors augmented a depressive phenotype in mice (Richardson-Jones et al., 2010). It is plausible that the present increase in *Htr1a* mRNA expression in RN, and the increase in the autoreceptor 5-HT1A binding activity in DRN in CSS mice can result in reduced serotonergic cell firing, diminished synaptic 5-HT levels and depressive-like behaviours.

In the context of feeding regulation, it was shown that activation of 5-HT1A receptors exerted hyperphagic effects (Williams and Dourish, 1992; De Vry and Schreiber, 2000; Voigt et al., 2002; Oury and Karsenty, 2011). Further, it has been proposed that this is mediated by 5-T1A autoreceptors and a decreased firing activity of serotonergic neurons that project from the RN to hypothalamic areas (Magalhães et al., 2010). In rats, injection of exogenous 5-HT in the DRN induced feeding, likely by promoting activation of 5-HT1A autoreceptors and thus decreasing firing rate of 5-HT neurons (Fletcher and Davies, 1990). In accordance with previous findings in the CSS model used here (Bergamini et al., 2016), Experiment B in the present study identified an increase in food intake in CSS mice compared with CON mice. Bringing these findings together, it is appropriate to suggest that the increased expression of 5-HT1A in the RN, potentially leading to a decreased 5-HT release, contributes to the increased feeding in CSS mice. There was no evidence for 5-HT1A specific binding changes in the hypothalamus in the present study.

As a result of enhanced 5-HT1A binding activity, a decrease in extracellular 5-HT concentrations could, through negative feedback, promote expression and externalisation of putative post-synaptic 5-HT receptors such as 5-HT1A, to maintain

synaptic signalling in the projection areas. Indeed, CSS mice displayed increased *Htr1a* expression in the mPFC, PVN and VMH. In the mPFC, 5-HT1A receptors seem to modulate anxiogenic-like behaviours in rats (Solati et al., 2011). Electrical stimulation of the mPFC, as well as application of the 5-HT1A agonist 8-OH-DPAT in the mPFC, can reduce the firing rate of DRN 5-HT neurons (Celada et al., 2001). Therefore, an increase in the mPFC *Htr1a* expression shown in this study would likely reduce the serotonerginc activity in the DRN thus decreasing 5-HT output in the terminal areas such as mPFC. Challis and Berton (2015) discussed that the socioemotional processing impaired in MDD is controlled by the serotonergic system in the mPFC-DRN pathway.

In the PVN, 5-HT activity is shown to modulate the HPA axis, thus being involved in stressful stimulation processing (Goel et al., 2011). Rats treated with the 5-HT1A agonist flesinoxan exhibited high levels of corticosterone, likely via CRH neurons in the PVN (Compaan, 1996). An increased *Htr1a* mRNA expression observed in the PVN in this study would be expected to increase the number of 5-HT1A receptors and enhance the HPA-stress response in the socially stressed mice.

Htr1a expression was also increased in the VMH of CSS mice in the present study. 5-HT1A immunoreactive neurons were previously described in the VMH from DRN ascending projections (Biagioni et al., 2016). Of note, one should not exclude sampling overlap of VMH with the surrounding regions such as ARC, considering the small size of these subregions. 5-HT binding to the 5-HT1A receptor in ARC was described to favour feeding behaviour (Oury and Karsenty, 2011). Thus, the increased expression of ARC/VMH *Htr1a* would enhance the appetite and food intake, consistent with the present observations.

5.6.2. Serotonin 5-HT2A receptor and *Htr2a*

The present study showed a decrease in the specific binding of 5-HT2A receptors in the amygdala and VTA of CSS mice in comparison with CON mice. In addition, an increase in *Htr2a* mRNA expression in the BLA of CSS mice versus CON mice was observed.

The present increase in the binding of 5-HT1A in the DRN of CSS mice would be expected to decrease 5-HT release and, in turn stimulate an up-regulation of other 5-HT receptors at different post-synaptic sites. Indeed, CSS mice showed a noticeable increase of *Htr2a* expression in BLA. Intriguingly, results of 5-HT2A receptor binding are at odds with *Htr2a* expression findings. It is commonly presumed that levels of protein are linked with levels of the mRNA for that gene. Although the production rate of a protein, in general, is proportional to the concentration and translational efficiency of its mRNA, there are at least three reasons assumed to be linked with the deficiency mRNA-protein correlation observed in the literature. Firstly, there are several complex post-transcriptional factors involved in converting mRNA into protein (Gout et al., 2017). Secondly, half-lives of proteins might be significantly distinct *in vivo*. Thirdly, the generation of membrane asymmetry by vertical and lateral diffusion of phospholipids (i.e. flip-flop translocation), which are involved in protein internalisation and externalisation, may be linked with the different 5-HT2A specific binding and mRNA expression of its encoding gene found in this study (Contreras et al., 2010). Lastly, there is a considerable possibility of error coming from mRNA and protein experiments performed (for more information, see Greenbaum et al. (2003) and Hershey et al. (2012)). It is therefore important to consider all those aforementioned factors in the establishment of the gene expression and protein concentration and/or binding in any study.

The present study also demonstrated a reduced 5-HT2A binding in the amygdala and VTA. The amygdala is an integrative centre of emotional processing, and 5-HT activity in this region has been linked with fear processing and development of stress-related disorders (Holmes, 2008; Bocchio et al., 2016). Administration of the 5-HT2A antagonist MDL100,907 was shown to reverse increased CRH, ACTH and corticosterone release promoted by the 5-HT2A agonist DOI (Van de Kar et al., 2001; Hemrick-Luecke and Evans, 2002). It is theoretically possible that the present reduced 5-HT2A binding activity in the amygdala may lead to a decreased HPA axis response in CSS mice. 5-HT2A receptors in the VTA are thought to play a role in anxiety and mood disorders by regulating monoaminergic systems (Doherty and Pickel, 2000; Blier and El-Mansari, 2013). Nonetheless, studies on this receptor in the VTA and its implication in mood disorders are limited.

5.6.3. Serotonin 5-HT2C receptor and *Htr2c*

The present study showed a decrease in the specific binding of 5-HT2C receptors in DRN in CSS mice. No change in *Htr2c* mRNA expression was found in any of the regions targeted. Similar to this study, Leventopoulos et al. (2009) described a reduced 5-HT2C binding in the DRN of adult rats exposed to early life stress.

The 5-HT2C receptor has been shown to regulate 5-HT firing activity in the DRN. For instance, Boothman et al. (2003) demonstrated that the 5-HT2C agonist DOI decreased 5-HT cell firing. Inhibition of the 5-HT2C receptor using the receptor antagonist SB242,084 was shown to reverse cell firing inhibition promoted by the antidepressant SSRI citalopram (Sotty et al., 2009). Furthermore, Spoida et al. (2014) demonstrated that impaired 5-HT cell firing induced by DRN 5-HT2C activation

relieved anxiety behaviour in mice. Thus, the decreased DRN 5-HT2C binding observed in this study might enhance 5-HT cell firing in stressed mice. This contradicts the present idea that increased 5-HT1A binding in stressed mice reduces 5-HT cell firing. It also differs from previous findings suggesting that stressed mice and depressed humans display reduced serotonergic activity (Smith et al., 1997; Stockmeier et al., 1998; Miyagawa et al., 2015) which may be ascribed to the different methodology of stress induction.

In the context of the regulation of feeding, evidence suggests the role of this receptor in controlling eating behaviour. Animals with a knockout of this receptor showed signs of mild hyperphagia, and stimulation of hypothalamic 5-HT2C promoted specific hypophagic effect, by accelerating the satiety process (Tecott et al., 1995). Furthermore, the 5-HT2C agonist was shown to decrease food intake (De Vry and Schreiber, 2000). As mentioned, 5-HT2C receptor agonist lorcaserin was recently approved for the treatment of obesity (Brashier et al., 2014). The decreased 5-HT2C receptor binding in the DRN observed in the present study is consistent with the present and previous studies that demonstrated that CSS mice led to increased food intake, as discussed in the Chapter 3.

5.6.4. *Slc6a4*

The present study showed an increase in the expression of *Slc6a4* mRNA in the RN of CSS mice compared with CON mice, and as observed in previous studies (Filipenko et al., 2002; Zhang et al., 2012). Interestingly, various studies have suggested that depression-like behaviour in rodents and depression in humans might be associated with decreased SERT binding and *Slc6a* expression (Arango et al., 1995; Malison et al., 1998; McKittrick et al., 2000; Willeit et al., 2000; Newberg et al., 2012,

2015). It is not obvious why there are such conflicting results concerning the regulation of *Slc6a4* and SERT protein in the various chronic stress-related studies. It is worth mentioning that acute stress has caused a decrease in *Slc6a4* mRNA expression in the RN of rats (Vollmayr et al., 2000). Thus increased *Slc6a4* mRNA expression could be a compensatory phenomenon observed in the long-term exposure to social stress used in this study, as also noted by others (Filipenko et al., 2002; Zhang et al., 2012). Further investigation into the possible causal factors is required.

5.7. Conclusion

This study supports the hypotheses and demonstrates that CSS changes the expression and binding activity of 5-HT receptors and its transporter. In particular, CSS resulted in an upregulation of DRN 5-HT1A autoreceptor binding, as well as of *Htr1a* and *Sert* mRNA expression in RN, the brain area from which serotonergic neuronal cell bodies project to the limbic and cortical brain regions. CSS also led to changes in the gene expression and binding of the 5-HT2A and 5-HT2C in the important RN projection areas associated with emotional processing and reward-seeking behaviour. Taken together, the present findings add new evidence to the relationship between social stress and the serotonergic system, of relevance to the regulation of feeding motivation and behaviour.

CHAPTER 6

General Discussion

The present study aimed at investigating the effects of chronic social stress on the regulation of feeding and metabolism in mice. The mouse model of CSS used in this thesis is representative of prolonged exposure to psychosocial stress in humans, as it results in behavioural, physiological and neurobiological states of relevance to human major depressive disorder (Pryce and Seifritz, 2011). This experimental mouse model was used here to investigate the relationship between CSS and energy allostasis, as it has been shown that CSS often increases feeding that is not reflected in corresponding body weight gain (Moles et al., 2006; Lutter et al., 2008; Razzoli et al., 2011c; Bergamini et al., 2016). The underlying mechanisms by which stress-affected mice do not gain weight despite increased feeding are not understood. The present study hypothesised that CSS induces endocrine, metabolic and neurobiological changes that result in increased calorie intake in conjunction with elevated energy metabolism, that are ultimately associated with a lack of body weight gain. Chronic psychosocial stress has also been shown to lead to changes in the serotonergic system (McKittrick et al., 1995; Blanchard et al., 2001), and therefore the present study hypothesised that CSS affects the serotonergic system in brain regions essential for the regulation of feeding and emotional processing.

6.1. Evaluation of the present findings against the background of existing research

In order to evaluate the effects of CSS on energy balance, a number of variables such as food intake, body weight, adipose tissue mass, EE and iBAT activity were assessed. Experiments presented in this thesis consistently suggested that CSS mice required more calories to maintain their body weight. Increased energy demand and/or

paucity of energy resources following CSS may be the underlying mechanisms by which stress promotes development of various diseases, including depression (Østergaard et al., 2018). Whilst experiments consistently indicated that CSS mice required more calories to maintain their body weight, there were some variations in the results of feeding and body weight between the Experiments B and C. Consistent with a previous study using the same mouse model (Bergamini et al., 2016), in Experiment B mice undergoing CSS increased their food intake with no change in body weight gain, in accord with Bergamini et al. (2016). In contrast, in Experiment C there was no CSS effect on food intake, but a decrease in body weight gain in CSS relative to control mice. Experiments B and C had identical protocols, consisting of the indirect calorimetry in addition to the CSS paradigm. Therefore, the current study highlights how individual or group responses to stress can vary in mice and/or how uncontrolled factors can influence specific outcomes. Conceivably, individual mouse variability in the response to stress may explain these differences. In addition, and rather more likely, differences in unidentified environmental variables may play a role (Chesler et al., 2002). Taken together with the individual stress-response variability, these differences demonstrate the complexity of experimental research on the effects of stress on energy metabolism in mice, and it is probably similar in humans.

The studies presented in this thesis were the first to assess EE in the current CSS mouse model. The previous studies that used indirect calorimetry included longer stress periods than the 15-day CSS model used for this thesis, and included a much shorter period of acclimatisation to the metabolic cages (Moles et al., 2006; Sanghez et al., 2013; Coccurello et al., 2017). Given that a change of environment can be considered a stressor in itself, the short acclimatisation period used in the previous studies may have led to inaccuracies in the assessment of EE. Moreover, to my

knowledge, this is the first study to record EE in mice fed a standard diet for a period longer than 20 hours (compared to 17 hours (Moles et al., 2006) and 20 hours (Coccurello et al., 2017), or 24 hours recording in mice fed an HFD (Sanghez et al., 2013)), thus allowing an extended evaluation of the CSS effects on EE. This is of importance since the endocrinological and metabolic responses to stress do not remain constant over time, and adaptation can occur.

The present study observed a significant increase in RER, suggesting that CSS mice have a higher carbohydrate oxidation in comparison with CON, possibly shifting towards glucose as the most rapid energy source. Increased carbohydrate oxidation allows the body to respond rapidly to the energy demands that stressful stimuli may generate. The previous studies that described an increased EE in socially stressed mice reported that this co-occurred with various combinations of changes in food intake and body weight; nonetheless, there was a consistent indication that increased EE in stressed mice was sufficient to reduce their body weight gain relative to CON mice (Moles et al., 2006; Sanghez et al., 2013; Coccurello et al., 2017). In my study with indirect calorimetry study, whilst a trend towards increased EE was observed in CSS relative to CON mice, this was not significant. Nevertheless, overall results presented in this thesis are consistent with an increased requirement for energy intake in CSS mice, which is in accord with the existing literature (Moles et al., 2006; Lutter et al., 2008; Razzoli et al., 2011c; Sanghez et al., 2013; Bergamini et al., 2016). Taken together, these findings indicate that CSS may cause a shift to the utilisation of carbohydrates relative to lipids as fuel, and increased energy demand for the maintenance of body weight. However, it is still unclear whether the current CSS procedure leads to increased EE, or whether effects on other mechanisms such as gut nutrient absorption explain the requirement for additional energy intake.

To evaluate the effects of CSS on the neuroendocrine regulators of feeding, ghrelin and leptin peripheral and central systems were assessed, as were circulating insulin levels and glucose homeostasis. Earlier studies have also looked at social stress effects on plasma ghrelin and leptin in mice (Chuang et al., 2011; Kumar et al., 2013; Patterson et al., 2013). However, to my knowledge, the studies presented in this thesis were the first to evaluate effects of CSS on the mRNA expression of ghrelin and leptin receptors in a number of brain regions. The current CSS model also represented a good opportunity to evaluate glucose homeostasis in the absence of body weight gain. The present results suggested that CSS led to an upregulation of the ghrelin system and a downregulation of the leptin system. In regard to ghrelin, this study observed that CSS increased plasma ghrelin and led to an upregulation of VMH *Ghs-r1a* mRNA expression. In regard to leptin, it was shown that CSS decreased plasma leptin concentrations and eWAT *Lep* mRNA expression but had no effect on eWAT or central *Lepr* mRNA expression. These findings are consistent with an increased motivation to eat, possibly due to a higher energy demand for maintenance of body weight. The glucose tolerance test in the present study revealed that CSS mice had significantly decreased plasma insulin concentrations compared with CON, which led to a slower initial clearance of glucose. Previous studies have also observed effects of chronic social stress on glucose homeostasis, however in the presence of increased weight gain (Chuang et al., 2010a; Tsuneki et al., 2013) or reduced weight gain (Balsevich et al., 2014). To my knowledge, the current study is the first to report alteration in glucose homeostasis independent of body weight changes in mice fed a standard diet. In the present study, reduced insulin availability in the plasma would limit the glucose influx into peripheral issues and thus reduce energy storage in CSS mice. These findings suggest that CSS increased the availability of peripheral glucose,

further supporting the idea of increased energy demand. These findings are of importance to the evaluation of the underlying mechanisms of stress-related changes in energy allostasis and body weight.

In order to investigate the effects of CSS on the serotonergic system and its involvement in feeding behaviour, the specific binding of 5-HT1A, 5-HT2A and 5-HT2C receptors and mRNA expression of their respective encoding genes were investigated, as well as the expression of the serotonin transporter gene (*Sert*), in brain regions implicated in the regulation of food intake and emotional processing. Previous studies have looked into the effects of stress on the regulation of 5-HT synthesis (review by Miura et al., 2008) and the role of 5-HT and 5-HT receptors in the regulation of feeding (Lam et al., 2010). Nonetheless, the role of CSS in the modulation of 5-HT receptors and the 5-HT transporter in such a wide range of brain regions had not been studied previously. The increased specific binding of the 5-HT1A autoreceptor and increased *Htr1a* mRNA expression in the RN presented in this study suggest that CSS acts on the serotonergic system by decreasing neuronal activity in the RN, where serotonergic neuronal cell bodies are located, and is thus likely to cause a reduction in 5-HT availability in the projection areas. This result is of importance for several reasons. Firstly, because brain 5-HT deficiency can lead to increased susceptibility to psychosocial stress, as shown in genetically modified mice (Sachs et al., 2015). Secondly, reduced 5-HT activity has been proposed as an aetio-pathological factor in clinical depression (Stockmeier et al., 1998). Thirdly, with regard to energy balance, as 5-HT is known to promote hypophagic effects (Gartner et al., 2018), reduced extracellular 5-HT would further increase feeding in CSS mice. Decreased 5-HT2A specific binding but enhanced *Htr2a* mRNA expression in the amygdala described in the present study suggests the presence of a molecular error in translating

mRNA into protein, possibly associated with post-transcriptional factors (Gout et al., 2017). The present reduction in the 5-HT2A binding in the amygdala and VTA of CSS mice may play a role in the pathophysiology of fear processing and other stress-related behaviours (Doherty and Pickel, 2000; Blier and El-Mansari, 2013; Bocchio et al., 2016). This study also observed a decreased 5-HT2C specific binding in the DRN. Impaired 5-HT2C activation has been shown to promote hyperphagia (Kursungoz et al., 2015), which may be an underlying mechanism for the increased calorie intake observed in this study. Lastly here, the present increased *Sert* mRNA expression in the DRN suggests that CSS increases re-uptake of 5-HT in pre-synaptic neurons, further limiting serotonergic activity in projecting areas. Although a link between 5-HT and feeding behaviour in the CSS model has been proposed in this thesis, it is done with caution, as there has been variation in terms of feeding results through our experiments with this mouse model. In the cohort of mice used for the 5-HT experiments, there was no difference in body weight, which would lead us to speculate food intake had increased in accord with our other experiments with no body weight change, but food intake was not measured. Nevertheless, the present data support the hypothesis that social stress alters the serotonergic system through changes in gene expression and binding activity of the 5-HT receptors and the 5-HT transporter.

6.2. Additional limitations of the present study not discussed elsewhere

- Quantitative mouse body composition was not performed in the present study, although it would help differentiate between fat or fat-free mass when evaluating EE.

- Food intake was not evaluated in the animals used for the serotoninergic study (Experiment A) as discussed above. Measurements of food intake were then performed for the subsequent experiments.

6.3. Future studies

The results from the present study suggest that stressed mice have a greater energy demand that results in:

1. an increased food intake but no change in body weight or

2. no change in food intake but a lack of body weight gain.

Such effects could be explained by an increased glucose uptake by peripheral organs such as the skeletal muscle and/or the liver. It is known that skeletal muscles increase membrane permeability to glucose upon contraction (Richter and Hargreaves, 2013), important function to be exercised on "fight-or-flight" stressful situations. In the liver, it was observed that stressed mice increased expression of the glucose transporter 2 (GLUT2) (Chuang et al., 2010a). By looking at the expression of glucose transporters for instance, in skeletal muscles and liver, it would be possible to comprehend better the reasons behind CSS increased energy demand.

These effects could also be tentatively explained by increased central glucose uptake. It has been suggested that the brain, under the conditions of psychosocial stress, acts by diminishing the energy supply (i.e. glucose) to peripheral organs and allocating it to itself, in what is called 'allocative brain-pull mechanism' (Peters, 2011a, b). By this mechanism, the brain is thought to activate the stress system to favour glucose self-allocation. In the 'direct brain-pull mechanism', astrocytes can increase GLUT-1-dependent glucose transport via the blood-brain-barrier thus

increasing intracerebral glucose supply (Pellerin et al., 2007). To verify this, mouse cerebral hemodynamic post-CSS would have to be measured by means of fMRI to monitor changes in local cerebral blood flow as an indicator of brain activity, or to measure brain regional glucose utilisation by means of PET; it would give an insight into the metabolic brain demands.

Potential effects of stress on the GI nutrient absorption may also play an important role in the inefficient use of fuel observed in the present mouse model. Firstly, an assessment of the energy usage could be performed by looking at energy ingested *versus* energy excreted. Moreover, by examining the intestinal glucose absorption through gene quantification of duodenal sodium-dependent glucose transporter 1 (SGLT-1) and GLUT2 (Nguyen et al., 2015), it would be possible to further understand some of the physiological consequences of prolonged stress exposure and the underlying mechanism behind inefficient energy storage. In addition, there are new lines of evidence that social stress affects gut microbiota (Yarandi et al., 2016; Szyszkowicz et al., 2017; Yang et al., 2017) which can alter the absorption of nutrients from the gut (Cani et al., 2019).

6.4. Conclusion

The present study demonstrated that CSS led to a range of endocrine, metabolic and neurobiological changes that are associated with an increased requirement for food in order to maintain body weight, possibly due to enhanced metabolic demands in mice. The results of this study encourage speculating that there is an increased demand for energy in the periphery and/or brain under CSS. The present thesis contributes novel insights into the underlying mechanisms of stress-related changes in energy

metabolism in mice, of relevance to human pathophysiology and psychopathology in stress-related disorders.

BIBLIOGRAPHY

Abizaid, A., Liu, Z. W., Andrews, Z. B., Shanabrough, M., Borok, E., Elsworth, J. D., Roth, R. H., Sleeman, M.W., Picciotto, M. R., Tschöp, M. H., Gao, X. B., and Horvath, T. L. (2006). Ghrelin modulates the activity and synaptic input organization of midbrain dopamine neurons while promoting appetite. *Journal of Clinical Investigation*, 116(12), 3229–3239.

Adam, T. C., and Epel, E. S. (2007). Stress, eating and the reward system. *Physiology and Behavior*, 91(4), 449–458.

Aguilera, G., and Rabadan-Diehl, C. (2000). Vasopressinergic regulation of the hypothalamic-pituitary-adrenal axis: Implications for stress adaptation. *Regulatory Peptides*, 96(1–2), 23–29.

Ahnaou, A., and Drinkenburg, W. H. I. M. (2016). Simultaneous Changes in Sleep, qEEG, Physiology, Behaviour and Neurochemistry in Rats Exposed to Repeated Social Defeat Stress. *Neuropsychobiology*, 73(4), 209–223.

Albonetti, M. E., and Farabollini, F. (1994). Social stress by repeated defeat: effects on social behaviour and emotionality. *Behavioural Brain Research*, 62(2), 93.

Almeida, M. C., Vizin, R. C. L., and Carrettiero, D. C. (2015). Current understanding on the neurophysiology of behavioral thermoregulation. *Temperature*, 2(4), 483–490.

Almind, K., and Kahn, C. R. (2004). Genetic Determinants of Energy Expenditure and Insulin Resistance in Diet-Induced Obesity in Mice. *Diabetes*, 53(12), 3274–3285.

Alonso, R., Farías, M., Alvarez, V., and Cuevas, A. (2015). The Genetics of Obesity. *Translational Cardiometabolic Genomic Medicine*, (October), 161–177.

Anacker, C., Zunszain, P. A., Carvalho, L. A., and Pariante, C. M. (2011). The glucocorticoid receptor: Pivot of depression and of antidepressant treatment? *Psychoneuroendocrinology*, 36(3), 415–425.

Anderberg, R. H., Richard, J. E., Eerola, K., López-Ferreras, L., Banke, E., Hansson, C., Nissbrandt, H., Berqquist, F., Gribble, F. M., Reimann, F., Asterholm, I. W., Lamy, C. M., and Skibicka, K. P. (2017). Glucagon-like peptide 1 and its analogs act in the dorsal raphe and modulate central serotonin to reduce appetite and body weight. *Diabetes*, 66(4), 1062–1073.

Anderson, R. J., Freedland, K. E., Clouse, R. E., and Lustman, P. J. (2001). The prevalence of comorbid depression in adults with diabetes: A meta-analysis. *Diabetes Care*, 24(6), 1069–1078.

APA. (2013). *Manual Diagnóstico e Estatístico de Transtornos Mentais - DSM - 5*. (Fifth, Ed.), *Manual Diagnóstico E Estatístico De Transtornos Mentais - Dsm - V*.

Arango, V., Underwood, M. D., Gubbi, A. V., and Mann, J. J. (1995). Localized alterations in pre- and postsynaptic serotonin binding sites in the ventrolateral prefrontal cortex of suicide victims. *Brain Research*, 688(1–2), 121–133.

Arco, A. Del, and Mora, F. (2009). Neurotransmitters and prefrontal cortex-limbic system interactions: Implications for plasticity and psychiatric disorders. *Journal of Neural Transmission*, 116(8), 941–952.

Arosio, M., Ronchi, C. L., Gebbia, C., Cappiello, V., Beck-Peccoz, P., and Peracchi, M. (2003). Stimulatory effects of ghrelin on circulating somatostatin and pancreatic polypeptide levels. *Journal of Clinical Endocrinology and Metabolism*, 88(2), 701–704.

Asakawa, A., Inui, A., Kaga, T., Yuzuriha, H., Nagata, T., Fujimiya, M., Katsuura, G., Makino, S., Fujino, M. A., and Kasuga, M. (2001). A role of ghrelin in neuroendocrine and behavioral responses to stress in mice. *Neuroendocrinology*, 74(3), 143–147.

Azzinnari, D., Sigrist, H., Staehli, S., Palme, R., Hildebrandt, T., Leparc, G., Hengerer, B., Seifritz, E., and Pryce, C. R. (2014). Mouse social stress induces increased fear conditioning, helplessness and fatigue to physical challenge together with markers of altered immune and dopamine function. *Neuropharmacology*, 85, 328–341.

Bădescu, S. V, Tătaru, C., Kobylinska, L., Georgescu, E. L., Zahiu, D. M., Zăgrean, A. M., and Zăgrean, L. (2016). The association between Diabetes mellitus and Depression. *Journal of Medicine and Life*, 9(2), 120–125.

Bagby, R. M., Kennedy, S. H., Schuller, D. R., Dickens, S. E., E. Minifie, C., Levitt, A., and Joffe, R. (1997). Differential pharmacological treatment response in high angry hostile and low angry hostile depressed patients: A retrospective analysis. *Journal of Affective Disorders*, 45(3), 161–166.

Bailey, M. T., Dowd, S. E., Galley, J. D., Hufnagle, A. R., Allen, R. G., and Lyte, M. (2011). Exposure to a social stressor alters the structure of the intestinal microbiota: Implications for stressor-induced immunomodulation. *Brain, Behavior, and Immunity*, 25(3), 397–407.

Bakshi, V. P., and Kalin, N. H. (2002). Animal models and endophenotypes of anxiety and stress disorders. In K. L. Davis, D. Charney, J. T. Coyle, and C. Nemeroff (Eds.), *Neuropsychopharmacology* (pp. 883–900). Pennsylvania: American College of Neuropsychopharmacology.

Balsevich, G., Uribe, A., Wagner, K. V, Hartmann, J., Santarelli, S., Labermaier, C., and Schmidt, M. V. (2014). Interplay between diet-induced obesity and chronic stress in mice: potential role of FKBP51. *The Journal of Endocrinology*, 222(1),

15–26.

Bambico, F. R., Nguyen, N. T., and Gobbi, G. (2009). Decline in serotonergic firing activity and desensitization of 5-HT1A autoreceptors after chronic unpredictable stress. *European Neuropsychopharmacology*, 19(3), 215–28.

Banks, W. A., DiPalma, C. R., and Farrell, C. L. (1999). Impaired transport of leptin across the blood-brain barrier in obesity. *Peptides*, 20(11), 1341–1345.

Barnes, N. M., and Sharp, T. (1999). A review of central 5-HT receptors and their function. *Neuropharmacology*, 38(8), 1083–1152.

Bartlang, M. S., Oster, H., and Helfrich-Förster, C. (2015). Repeated psychosocial stress at night affects the circadian activity rhythm of male mice. *Journal of Biological Rhythms*, 30(3), 228–241.

Bartolomucci, A., Cabassi, A., Govoni, P., Ceresini, G., Cero, C., Berra, D., Dadomo, H., Franceschini, P., Dell'Omo, G., Parmigiani, S., and Palanza, P. (2009). Metabolic consequences and vulnerability to diet-induced obesity in male mice under chronic social stress. *PLoS ONE*, 4(1).

Bartolomucci, A., Pederzani, T., Sacerdote, P., Panerai, A. E., Parmigiani, S., and Palanza, P. (2004). Behavioral and physiological characterization of male mice under chronic psychosocial stress. *Psychoneuroendocrinology*, 29(7), 899–910.

Bassi, N., Karagodin, I., Wang, S., Vassallo, P., Priyanath, A., Massaro, E., and Stone, N. J. (2014). Lifestyle Modification for Metabolic Syndrome: A Systematic Review. *The American Journal of Medicine*, 127(12), 1242.e1-1242.e10.

Batterham, R. L., Cowley, M. A., Small, C. J., Herzog, H., Cohen, M. A., Dakin, C. L., Wren, A. M., Brynes, A. E., Low, M. J., Ghatei, M. A., Cone, R. D., and Bloom, S. R. (2002). Gut hormone PYY(3-36) physiologically inhibits food intake. *Nature*, 418, 650–654.

Becker, C., Zeau, B., Rivat, C., Blugeot, A., Hamon, M., and Benoliel, J. J. (2008). Repeated social defeat-induced depression-like behavioral and biological alterations in rats: Involvement of cholecystokinin. *Molecular Psychiatry*, 13(12), 1079–1092.

Bellinger, L. L., and Bernardis, L. L. (2002). The dorsomedial hypothalamic nucleus and its role in ingestive behavior and body weight regulation: Lessons learned from lesioning studies. *Physiology and Behavior*, 76(2), 431–442.

Belmer, A., and Maroteaux, L. (2018). Regulation of raphe serotonin neurons by serotonin 1A and 2B receptors. *Neuropsychopharmacology*, 44(1), 218–219.

Belzung, C., and Lemoine, M. (2011). Criteria of validity for animal models of psychiatric disorders: focus on anxiety disorders and depression. *Biology of Mood & Anxiety Disorders*, 1, 9.

Benoit, S. C., Air, E. L., Coolen, L. M., Strauss, R., Jackman, A., Clegg, D. J., Seeley, R. J., and Woods, S. C. (2002). The catabolic action of insulin in the brain is mediated by melanocortins. *Journal of Neuroscience*, 22(20), 9048–9052.

Benoit, S. C., Clegg, D. J., Seeley, R. J., and Woods, S. C. (2004). Insulin and leptin as adiposity signals. *Recent Progress in Hormone Research*, 59, 267–285.

Bergamini, G., Cathomas, F., Auer, S., Sigrist, H., Seifritz, E., Patterson, M., Gabriel, C., Pryce, C. R. (2016). Mouse psychosocial stress reduces motivation and cognitive function in operant reward tests: A model for reward pathology with effects of agomelatine. *European Neuropsychopharmacology*, 26(9), 1448–1464.

Bergen, S. S. (1964). Appetite Stimulating Properties of Cyproheptadine. *American Journal of Diseases of Children*, 108, 270–273.

Berger, M., Gray, J. A., and Roth, B. L. (2009). The Expanded Biology of Serotonin. *Annual Review of Medicine*, 60(1), 355–366.

Berton, O., McClung, C. A., Dileone, R. J., Krishnan, V., Renthal, W., Russo, S. J., Graham, D., Tsankova, N. M., Bolanos, C. A., Rios, M., Monteggia, L. M., Self, D. W., and Nestler, E. J. (2006). Essential role of BDNF in the mesolimbic dopamine pathway in social defeat stress. *Science*, 311(5762), 864–868.

Betley, J. N., Cao, Z. F. H., Ritola, K. D., and Sternson, S. M. (2013). Parallel, redundant circuit organization for homeostatic control of feeding behavior. *Cell*, 155(6), 1337–13350.

Bewick, G. A., Kent, A., Campbell, D., Patterson, M., Ghatei, M. A., Bloom, S. R., and Gardiner, J. V. (2009). Mice with hyperghrelinemia are hyperphagic and glucose intolerant and have reduced leptin sensitivity. *Diabetes*, 58(4), 840–846.

Biagioni, A. F., de Oliveira, R. C., de Oliveira, R., da Silva, J. A., Anjos-Garcia, T. dos, Roncon, C. M., Corrado, A. P., Zangrossi, H., and Coimbra, N. C. (2016). 5-Hydroxytryptamine 1A receptors in the dorsomedial hypothalamus connected to dorsal raphe nucleus inputs modulate defensive behaviours and mediate innate fear-induced antinociception. *European Neuropsychopharmacology*, 26(3), 532–545.

Black, P. H. (2006). The inflammatory consequences of psychologic stress: Relationship to insulin resistance, obesity, atherosclerosis and diabetes mellitus, type II. *Medical Hypotheses*, 67(4), 879–891.

Blanchard, R. J., McKittrick, C. R., and Blanchard, D. C. (2001). Animal models of social stress: Effects on behavior and brain neurochemical systems. *Physiology and Behavior*, 73(3), 261–271.

Blázquez, E., Velázquez, E., Hurtado-Carneiro, V., and Ruiz-Albusac, J. M. (2014). Insulin in the brain: Its pathophysiological implications for states related with central insulin resistance, type 2 diabetes and alzheimer's disease. *Frontiers in*

Endocrinology, 5, 1–21.

Blier, P. (2001). Pharmacology of rapid-onset antidepressant treatment strategies. *Journal of Clinical Psychiatry*, 62(Suppl 15), 12–17.

Blier, P., and El-Mansari, M. (2013). Serotonin and beyond: Therapeutics for major depression. *Philosophical Transactions of the Royal Society of London, Series B, Biological Sciences*, 368(1615), 20120536.

Blondin, D. P., Frisch, F., Phoenix, S., Guérin, B., Turcotte, É. E., Haman, F., Richard, D., and Carpentier, A. C. (2017). Inhibition of Intracellular Triglyceride Lipolysis Suppresses Cold-Induced Brown Adipose Tissue Metabolism and Increases Shivering in Humans. *Cell Metabolism*, 25(2), 438–447.

Bocchio, M., McHugh, S. B., Bannerman, D. M., Sharp, T., and Capogna, M. (2016). Serotonin, Amygdala and Fear: Assembling the Puzzle. *Frontiers in Neural Circuits*, 10, 24.

Bonhaus, D. W., Weinhardt, K. K., Taylor, M., DeSouza, A., McNeeley, P., Szczepanski, K., … Eglen, R. (1997). RS-102221: A Novel High Affinity and Selective, 5-HT2C Receptor Antagonist. *Neuropharmacology*, 36(4–5), 621–629.

Boothman, L. J., Allers, K. A., Rasmussen, K., and Sharp, T. (2003). Evidence that central 5-HT 2a and 5-HT 2B/C receptors regulate 5-HT cell firing in the dorsal raphe nucleus of the anaesthetised rat. *British Journal of Pharmacology*, 139(5), 998–1004.

Bovetto, S., Rouillard, C., and Richard, D. (1996). Role of CRH in the effects of 5-HT-receptor agonists on food intake and metabolic rate. *American Journal of Physiology*, 271(5 Pt 2), R1231-1238.

Bowe, J. E., Franklin, Z. J., Hauge-Evans, A. C., King, A. J., Persaud, S. J., and Jones, P. M. (2014). Assessing glucose homeostasis in rodent models. *Journal of Endocrinology*, 222(3), 13–25.

Brashier, D. S., Sharma, A., Dahiya, N., Singh, S., and Khadka, A. (2014). Lorcaserin: A novel antiobesity drug. *Journal of Pharmacology and Pharmacotherapeutics*, 5(2), 175–178.

Broglio, F., Arvat, E., Benso, A., Gottero, C., Muccioli, G., Papotti, M., Van Der Lely, A. J., Deghenghi, R., and Ghigo, E. (2001). Ghrelin, a natural GH secretagogue produced by the stomach, induces hyperglycemia and reduces insulin secretion in humans. *Journal of Clinical Endocrinology and Metabolism*, 86(10), 5083–5086.

Brown, K. J., and Grunberg, N. E. (1995). Effects of housing on male and female rats: crowding stresses male but calm females. *Physiology & Behavior*, 58(6), 1085–1089.

Browning, K. N., Verheijden, S., and Boeckxstaens, G. E. (2017). The Vagus Nerve in Appetite Regulation, Mood, and Intestinal Inflammation. *Gastroenterology*, 152(4), 730–744.

Brydon, L. (2011). Adiposity, leptin and stress reactivity in humans. *Biological Psychology*, 86(2), 114–120.

Burghardt, P. R., Love, T. M., Stohler, C. S., Hodgkinson, C., Shen, P.-H., Enoch, M.-A., and Goldman, D., and Zubieta, J.-K. (2012). Leptin Regulates Dopamine Responses to Sustained Stress in Humans. *Journal of Neuroscience*, 32(44), 15369–15376.

Cabral, A., Portiansky, E., Sánchez-Jaramillo, E., Zigman, J. M., and Perello, M. (2016). Ghrelin activates hypophysiotropic corticotropin-releasing factor neurons independently of the arcuate nucleus. *Psychoneuroendocrinology*, 67, 27–39.

Cabral, A., Suescun, O., Zigman, J. M., and Perello, M. (2012). Ghrelin indirectly activates hypophysiotropic CRF neurons in rodents. *PLoS ONE*, 7(2), 1–10.

Cagniard, B., Balsam, P. D., Brunner, D., and Zhuang, X. (2006). Mice with chronically elevated dopamine exhibit enhanced motivation, but not learning, for a food reward. *Neuropsychopharmacology*, 31(7), 1362–1370.

Cani, P. D., Van Hul, M., Lefort, C., Depommier, C., Rastelli, M., and Everard, A. (2019). Microbial regulation of organismal energy homeostasis. *Nature Metabolism*, 1(1), 34–46.

Canli, T., and Lesch, K. P. (2007). Long story short: The serotonin transporter in emotion regulation and social cognition. *Nature Neuroscience*, 10(9), 1103–1109.

Cannon, B., and Nedergaard, J. (2004). Brown adipose tissue: function and physiological significance. *Physiological Reviews*, 84(1), 277–359.

Caron, A., Lee, S., Elmquist, J. K., and Gautron, L. (2018). Leptin and brain-adipose crosstalks. *Nature Reviews Neuroscience*, 19(3), 153–165.

Cawley, N. X., Li, Z., and Loh, Y. P. (2016). Biosynthesis, trafficking, and secretion of pro-opiomelanocortin-derived peptides. *Journal of Molecular Endocrinology*, 56(4), T77–T97.

Celada, P., Bortolozzi, A., and Artigas, F. (2013). Serotonin 5-HT1Areceptors as targets for agents to treat psychiatric disorders: Rationale and current status of research. *CNS Drugs*, 27(9), 703–716.

Celada, P., Puig, M. V., Casanovas, J. M., Guillazo, G., and Artigas, F. (2001). Control of dorsal raphe serotonergic neurons by the medial prefrontal cortex: Involvement of serotonin-1A, GABA(A), and glutamate receptors. *The Journal of Neuroscience : The Official Journal of the Society for Neuroscience*, 21(24),

9917–9929.

Cetinkalp, S., Simsir, I. Y., and Ertek, S. (2014). Insulin resistance in brain and possible therapeutic approaches. *Current Vascular Pharmacology*, 12(4), 553–564.

Challis, C., and Berton, O. (2015). Top-Down Control of Serotonin Systems by the Prefrontal Cortex: A Path toward Restored Socioemotional Function in Depression. *ACS Chemical Neuroscience*, 6(7), 1040–1054.

Chambers, A. P., Sandoval, D. A., and Seeley, R. J. (2013). Integration of satiety signals by the central nervous system. *Current Biology*, 23(9), R379-388.

Chao, P. T., Yang, L., Aja, S., Moran, T. H., and Bi, S. (2011). Knockdown of NPY expression in the dorsomedial hypothalamus promotes development of brown adipocytes and prevents diet-induced obesity. *Cell Metabolism*, 13(5), 573–583.

Charnay, Y., and Léger, L. (2010). Brain serotonergic circuitries. *Dialogues in Clinical Neuroscience*, 12(4), 471–87.

Chen, J. J., Vasko, M. R., Wu, X., Staeva, T. P., Baez, M., Zgombick, J. M., and Nelson, D. L. (1998). Multiple subtypes of serotonin receptors are expressed in rat sensory neurons in culture. *Journal of Pharmacology and Experimental Therapeutics*, 287(3), 1119–1127.

Chen, X., Gianferante, D., Hanlin, L., Fiksdal, A., Breines, J. G., Thoma, M. V., and Rohleder, N. (2017). HPA-axis and inflammatory reactivity to acute stress is related with basal HPA-axis activity. *Psychoneuroendocrinology*, 78, 168–176.

Chesler, E. J., Wilson, S. G., Lariviere, W. R., Rodriguez-Zas, S. L., and Mogil, J. S. (2002). Influences of laboratory environment on behavior. *Nature Neuroscience*, 5(11), 1101–1102.

Chesselet, M.-F., and Carmichael, S. T. (2012). Animal Models of Neurological Disorders. *Neurotherapeutics*, 9(2), 241–244.

Choi, S. J., Blake, V., Cole, S., and Fernstrom, J. D. (2006). Effects of chronic fenfluramine administration on hypothalamic neuropeptide mRNA expression. *Brain Research*, 1087(1), 83–86.

Chou-Green, J. M., Holscher, T. D., Dallman, M. F., and Akana, S. F. (2003). Repeated stress in young and old 5-HT2C receptor knockout mice. *Physiology and Behavior*, 79(2), 217–226.

Chrousos, G. P. (2009). Stress and disorders of the stress system. *Nature Reviews Endocrinology*, 5(7), 374–381.

Chuang, J. C., Cui, H., Mason, B. L., Mahgoub, M., Bookout, A. L., Yu, H. G., Perello, M., Elmquist, J. K., Repa, J. J., Zigman, J. M., and Lutter, M. (2010a). Chronic

social defeat stress disrupts regulation of lipid synthesis. *Journal of Lipid Research*, 51(6), 1344–1353.

Chuang, J. C., Krishnan, V., Yu, H. G., Mason, B., Cui, H., Wilkinson, M. B., Zigman, J. M., Elmquist, J. K., Nestler, E. J., and Lutter, M. (2010b). A β3-Adrenergic-Leptin-Melanocortin Circuit Regulates Behavioral and Metabolic Changes Induced by Chronic Stress. *Biological Psychiatry*, 67(11), 1075–1082.

Chuang, J. C., Perello, M., Sakata, I., Osborne-Lawrence, S., Savitt, J. M., Lutter, M., and Zigman, J. M. (2011). Ghrelin mediates stress-induced food-reward behavior in mice. *Journal of Clinical Investigation*, 121(7), 2684–2692.

Chuang, J. C., and Zigman, J. M. (2010). Ghrelin's roles in stress, mood, and anxiety regulation. *International Journal of Peptides*, 2010, 1–5.

Clément, K., Vaisse, C., Lahlou, N., Cabrol, S., Pelloux, V., Cassuto, D., Gourmelen, M., Dina, C., Chambaz, J., Lacorte, J. M., Basdevant, A., Bougnères, P., Lebouc, Y., Froguel, P., and Guy-Grand, B. (1998). A mutation in the human leptin receptor gene causes obesity and pituitary dysfunction. *Nature*, 392(6674), 398–401.

Coccurello, R., Romano, A., Giacovazzo, G., Tempesta, B., Fiore, M., Giudetti, A. M., Marrocco, I., Altieri, F., Moles, A., and Gaetani, S. (2017). Increased intake of energy-dense diet and negative energy balance in a mouse model of chronic psychosocial defeat. *European Journal of Nutrition*, 57(4), 1485–1498.

Coelho, A. G., Aguiar, F. P. C., and Jesus, D. P. de. (2014). A Rapid and Simple Method for Determination of 5-Hydroxytryptophan in Dietary Supplements by Capillary Electrophoresis. *Journal of the Brazilian Chemical Society*, 24(4), 783–787.

Coelho, M., Oliveira, T., and Fernandes, R. (2013). Biochemistry of adipose tissue: An endocrine organ. *Archives of Medical Science*, 9(2), 191–200.

Cohen, S., Janicki-Deverts, D., Doyle, W. J., Miller, G. E., Frank, E., Rabin, B. S., and Turner, R. B. (2012). Chronic stress, glucocorticoid receptor resistance, inflammation, and disease risk. *Proceedings of the National Academy of Sciences*, 109(16), 5995–5999.

Collier, D. A., Arranz, M. J., Li, T., Mupita, D., Brown, N., and Treasure, J. (1997). Association between 5-HT(2A) gene promoter polymorphism and anorexia nervosa. *Lancet*, 350(9075), 412.

Collins, S., and Surwit, R. S. (2001). The {beta}-Adrenergic Receptors and the Control of Adipose Tissue Metabolism and Thermogenesis. *Recent Progress in Hormone Research*, 56, 309–328.

Compaan, J. C. (1996). 5-HT1A receptor agonist flesinoxan enhances fos immunoreactivity in rat central amygdala, bed nucleus of the stria terminalis and

hypothalamus. *European Journal of Neuroscience*, 8(11), 2340–2347.

Contreras, C., Nogueiras, R., Diéguez, C., Medina-Gómez, G., and López, M. (2016). Hypothalamus and thermogenesis: Heating the BAT, browning the WAT. *Molecular and Cellular Endocrinology*, 438, 107–115.

Contreras, F. X., Sánchez-Magraner, L., Alonso, A., and Goñi, F. M. (2010). Transbilayer (flip-flop) lipid motion and lipid scrambling in membranes. *FEBS Letters*, 584(9), 1779–1786.

Cools, R., Roberts, A. C., and Robbins, T. W. (2008). Serotoninergic regulation of emotional and behavioural control processes. *Trends in Cognitive Sciences*, 12(1), 31–40.

Cowley, M. A., Smart, J. L., Rubinstein, M., Cerdán, M. G., Diano, S., Horvath, T. L., Cone, R. D., and Low, M. J. (2001). Leptin activates anorexigenic POMC neurons through a neural network in the arcuate nucleus. *Nature*, 411(6836), 480–484.

Cummings, D. E., Purnell, J. Q., Frayo, R. S., Schmidova, K., Wisse, B. E., and Weigle, D. S. (2001). A Preprandial Rise in Plasma Ghrelin Levels Suggests a Role in Meal Initiation in Humans. *Diabetes*, 50(8), 1714–1719.

Cunningham, J. J. (1991). Body composition as a determinant of energy expenditure: A synthetic review and a proposed general prediction equation. *American Journal of Clinical Nutrition*, 54(6), 963–969.

Cypess, A. M., Lehman, S., Williams, G., Tal, I., Rodman, D., Goldfine, A. B., Kuo, F. C., Palmer, E. L., Tseng, Y. H., Doria, A., Kolodny, G. M., and Ronald Kahn, C. (2009). Identification and importance of brown adipose tissue in adult humans. *Obstetrical and Gynecological Survey*, 360(15), 1509–1517.

D'Agostino, G., Lyons, D., Cristiano, C., Lettieri, M., Olarte-Sanchez, C., Burke, L. K., Greenwald-Yarnell, M., Cansell, C., Doslikova, B., Georgescu, T., Martinez de Morentin, P. B., Myers, M. G., Rochford, J. J., and Heisler, L. K. (2018). Nucleus of the Solitary Tract Serotonin 5-HT2C Receptors Modulate Food Intake. *Cell Metabolism*, 28(4), 619–630.

Dallman, M. F. (2010). Stress-induced obesity and the emotional nervous system. *Trends in Endocrinology and Metabolism*, 21(3), 159–165.

Dallman, M. F., La Fleur, S. E., Pecoraro, N. C., Gomez, F., Houshyar, H., and Akana, S. F. (2004). Minireview: Glucocorticoids - Food intake, abdominal obesity, and wealthy nations in 2004. *Endocrinology*, 145(6), 2633–2638.

Date, Y., Murakami, N., Toshinai, K., Matsukura, S., Niijima, A., Matsuo, H., Kangawa, K., and Nakazato, M. (2002). The role of the gastric afferent vagal nerve in Ghrelin-induced feeding and growth hormone secretion in rats. *Gastroenterology*, 123(4), 1120–1128.

Daviu, N., Rabasa, C., Nadal, R., and Armario, A. (2014). Comparison of the effects of single and daily repeated immobilization stress on resting activity and heterotypic sensitization of the hypothalamic-pituitary-adrenal axis. *Stress*, 17(2), 176–185.

Dawkins, M. S., Martin, P., and Bateson, P. (1994). *Measuring Behaviour. An Introductory Guide*. *The Journal of Animal Ecology*.

Dayan, P., and Balleine, B. W. (2002). Reward, motivation, and reinforcement learning. *Neuron*, 36(2), 285–298.

Dayas, C. V., Buller, K. M., Crane, J. W., Xu, Y., and Day, T. A. (2001). Stressor categorization: Acute physical and psychological stressors elicit distinctive recruitment patterns in the amygdala and in medullary noradrenergic cell groups. *European Journal of Neuroscience*, 14(7), 1143–1152.

De Felice, L. J. (2016). A current view of serotonin transporters. *F1000Research*, 5.

de Git, K. C. G., Peterse, C., Beerens, S., Luijendijk, M. C. M., van der Plasse, G., la Fleur, S. E., and Adan, R. A. H. (2018). Is leptin resistance the cause or the consequence of diet-induced obesity? *International Journal of Obesity*, 42(8), 1445–1457.

de Kloet, E. R., Joels, M., and Holsboer, F. (2005). Stress and the brain: from adaptation to disease. *Nature Reviews Neuroscience*, 6(6), 463–475.

De Vry, J., and Schreiber, R. (2000). Effects of selected serotonin 5-HT1 and 5-HT2 receptor agonists on feeding behavior: possible mechanisms of action. *Neuroscience & Biobehavioral Reviews*, 24(3), 341–353.

Demireva, E. Y., Suri, D., Morelli, E., Mahadevia, D., Chuhma, N., Teixeira, C. M., Ziolkowski, A., Hersh, M., Fifer, J., Bagchi, S., Chemiakine, A., Moore, H., Gingrich, J. A., Balsam, P., Rayport, S., and Ansorge, M. S. (2018). 5-HT2C receptor blockade reverses SSRI-associated basal ganglia dysfunction and potentiates therapeutic efficacy. *Molecular Psychiatry*.

Demyttenaere, K. (2014). Agomelatine in treating generalized anxiety disorder. *Expert Opinion on Investigational Drugs*, 23(6), 857–864.

Denayer, T., Stöhrn, T., and Van Roy, M. (2014). Animal models in translational medicine: Validation and prediction. *New Horizons in Translational Medicine*, 2(1), 5–11.

Denmark, A., Tien, D., Wong, K., Chung, A., Cachat, J., Goodspeed, J., Grimes, C., Elegante, M., Suciu, C., Elkhayat, S., Bartels, B., Jackson, A., Rosenberg, M., Chung, K. M., Badani, H., Kadri, F., Roy, S., Tan, J., Gaikwad, S., Stewart, A., Zapolsky, I., Gilder, T., and Kalueff, A. V. (2010). The effects of chronic social defeat stress on mouse self-grooming behavior and its patterning. *Behavioural Brain Research*, 208(2), 553–559.

Dezaki, K., Hosoda, H., Kakei, M., Hashiguchi, S., Watanabe, M., Kangawa, K., and Yada, T. (2004). Endogenous Ghrelin in Pancreatic Islets Restricts Insulin Release by Attenuating Ca 2+ Signaling in β-cells. *Diabetes*, 53(12), 3142–3151.

Di Giovanni, G. (2013). Serotonin in the pathophysiology and treatment of CNS disorders. *Experimental Brain Research*, 230(4), 371–373.

Dodd, G. T., Decherf, S., Loh, K., Simonds, S. E., Wiede, F., Balland, E., Merry, T. L., Münzberg, H., Zhang, Z. Y., Kahn, B. B., Neel, B. G., Bence, K. K., Andrews, Z. B., Cowley, M. A., and Tiganis, T. (2015). Leptin and insulin act on POMC neurons to promote the browning of white fat. *Cell*, 160(1–2), 88–104.

Doherty, M. D., and Pickel, V. M. (2000). Ultrastructural localization of the serotonin 2A receptor in dopaminergic neurons in the ventral tegmental area. *Brain Research*, 864(2), 176–185.

Dourish, C. T., Clark, M. L., Fletcher, A., and Iversen, S. D. (1989). Evidence that blockade of post-synaptic 5-HT1receptors elicits feeding in satiated rats. *Psychopharmacology*, 97(1), 54–58.

Dourish, C. T., Hutson, P. H., and Curzon, G. (1985). Low doses of the putative serotonin agonist 8-hydroxy-2-(di-n-propylamino) tetralin (8-OH-DPAT) elicit feeding in the rat. *Psychopharmacology*, 86(1–2), 197–204.

Drevets, W. C., Frank, E., Price, J. C., Kupfer, D. J., Holt, D., Greer, P. J., Huang, Y., Gautier, C., and Mathis, C. (1999). PET imaging of serotonin 1A receptor binding in depression. *Biological Psychiatry*, 46(10), 1375–1387.

Dryden, S., Wang, Q., Frankish, H. M., Pickavance, L., and Williams, G. (1995). The serotonin (5-HT) antagonist methysergide increases neuropeptide Y (NPY) synthesis and secretion in the hypothalamus of the rat. *Brain Research*, 699(1), 12–18.

Duclos, M., Pereira, P. M., Barat, P., Gatta, B., and Roger, P. (2005). Increased cortisol unavailability, abdominal obesity, and the metabolic syndrome in obese women. *Obesity Research*, 13(7), 1157–1166.

Dutcher, J. M., and Creswell, J. D. (2018). The role of brain reward pathways in stress resilience and health. *Neuroscience and Biobehavioral Reviews*, 95, 559–567.

Egecioglu, E., Jerlhag, E., Salomé, N., Skibicka, K. P., Haage, D., Bohlooly-Y, M., Andersson, D., Bjursell, M., Perrissoud, D., Engel, J. A., and Dickson, S. L. (2010). Ghrelin increases intake of rewarding food in rodents. *Addiction Biology*, 15(3), 304–311.

Egido, E. M., Rodríguez-Gallardo, J., Silvestre, R. A., and Marco, J. (2002). Inhibitory effect of ghrelin on insulin and pancreatic somatostatin secretion. *European Journal of Endocrinology*, 146(2), 241–244.

Elias, C. F., Aschkenasi, C., Lee, C., Kelly, J., Ahima, R. S., Bjorbæk, C., Flier, J. S., Saper, C. B., and Elmquist, J. K. (1999). Leptin differentially regulates NPY and POMC neurons projecting to the lateral hypothalamic area. *Neuron*, 23(4), 775–786.

Elmquist, J. K., Bjørbaek, C., Ahima, R. S., Flier, J. S., and Saper, C. B. (1998). Distributions of Leptin Receptor mRNA Isoforms in the Rat Brain. *Journal of Comparative Neurology*, 395(4), 535–547.

Ely, D. L., and Henry, J. P. (1978). Neuroendocrine response patterns in dominant and subordinate mice. *Hormones and Behavior*, 10(2), 156–169.

Ferrés-Coy, A., Santana, N., Castañé, A., Cortés, R., Carmona, M. C., Toth, M., Montefeltro, A., Artigas, F., and Bortolozzi, A. (2013). Acute 5-HT1A autoreceptor knockdown increases antidepressant responses and serotonin release in stressful conditions. *Psychopharmacology*, 225(1), 61–74.

Filipenko, M. L., Beilina, A. G., Alekseyenko, O. V., Dolgov, V. V., and Kudryavtseva, N. N. (2002). Repeated experience of social defeats increases serotonin transporter and monoamine oxidase A mRNA levels in raphe nuclei of male mice. *Neuroscience Letters*, 321(1–2), 25–28.

Fine, E. J., and Feinman, R. D. (2004). Thermodynamics of weight loss diets. *Nutrition and Metabolism*, 1(1), 15.

Finger, B. C., Dinan, T. G., and Cryan, J. F. (2011). High-fat diet selectively protects against the effects of chronic social stress in the mouse. *Neuroscience*, 192, 351–360.

Finger, B. C., Dinan, T. G., and Cryan, J. F. (2012). The temporal impact of chronic intermittent psychosocial stress on high-fat diet-induced alterations in body weight. *Psychoneuroendocrinology*, 37(6), 729–741.

Fitzsimons, C. P., Herbert, J., Schouten, M., Meijer, O. C., Lucassen, P. J., and Lightman, S. (2016). Circadian and ultradian glucocorticoid rhythmicity: Implications for the effects of glucocorticoids on neural stem cells and adult hippocampal neurogenesis. *Frontiers in Neuroendocrinology*, 41, 44–58.

Flecknell, P. (2002). Reduction, refinement and replacement. *ALTEX: Alternatives to Animal Experimentation*.

Fletcher, P. J., and Davies, M. (1990). Dorsal raphe microinjection of 5-HT and indirect 5-HT agonists induces feeding in rats. *European Journal of Pharmacology*, 184(2–3), 265–271.

Flier, J. S., Harris, M., and Hollenberg, A. N. (2000). Leptin, nutrition, and the thyroid: The why, the wherefore, and the wiring. *Journal of Clinical Investigation*, 105(7), 859–861.

Froger, N. (2004). Neurochemical and Behavioral Alterations in Glucocorticoid Receptor-Impaired Transgenic Mice after Chronic Mild Stress. *Journal of Neuroscience*, 24(11), 2787–2796.

Fujita, M., Richards, E. M., Niciu, M. J., Ionescu, D. F., Zoghbi, S. S., Hong, J., Telu, S., Hines, C. S., Pike, V. W., Zarate, C. A., and Innis, R. B. (2017). CAMP signaling in brain is decreased in unmedicated depressed patients and increased by treatment with a selective serotonin reuptake inhibitor. *Molecular Psychiatry*, 22(5), 754–759.

Furtado, L. M., Somwar, R., Sweeney, G., Niu, W., and Klip, A. (2002). Activation of the glucose transporter GLUT4 by insulin. *Biochemistry and Cell Biology*, 80(5), 569–578.

Füzesi, T., Daviu, N., Wamsteeker Cusulin, J. I., Bonin, R. P., and Bains, J. S. (2016). Hypothalamic CRH neurons orchestrate complex behaviours after stress. *Nature Communications*, 7, 11937.

Galgani, J., and Ravussin, E. (2008). Energy metabolism, fuel selection and body weight regulation. *International Journal of Obesity*, 32(Suppl 7), S109-119.

García-Díaz, D. F., Campion, J., Milagro, F. I., Lomba, A., Marzo, F., and Martínez, J. A. (2007). Chronic mild stress induces variations in locomotive behavior and metabolic rates in high fat fed rats. *Journal of Physiology and Biochemistry*, 63(4), 337–346.

Gardiner, K., and Du, Y. (2006). A-to-I editing of the 5HT2C receptor and behaviour. *Briefings in Functional Genomics and Proteomics*, 5(1), 37–42.

Gargiufo, P. A., and Donoso, A. O. (1996). Distinct grooming patterns induced by intracerebroventricular injection of CRH, TRH and LHRH in male rats. *Brazilian Journal of Medical and Biological Research*, 29(3), 375–379.

Gartner, S. N., Aidney, F., Klockars, A., Prosser, C., Carpenter, E. A., Isgrove, K., Levine, A. S., and Olszewski, P. K. (2018). Intragastric preloads of L-tryptophan reduce ingestive behavior via oxytocinergic neural mechanisms in male mice. *Appetite*, 125, 278–286.

Ge, J. F., Qi, C. C., and Zhou, J. N. (2013). Imbalance of leptin pathway and hypothalamus synaptic plasticity markers are associated with stress-induced depression in rats. *Behavioural Brain Research*, 249, 38–43.

Geisler, J. G. (2011). Targeting energy expenditure via fuel switching and beyond. *Diabetologia*, 54(2), 237–244.

Gershon, M. D., and Tack, J. (2007). The Serotonin Signaling System: From Basic Understanding To Drug Development for Functional GI Disorders. *Gastroenterology*, 132(1), 397–414.

Gillies, G. E., Linton, E. A., and Lowry, P. J. (1982). Corticotropin releasing activity of the new CRF is potentiated several times by vasopressin. *Nature*, 299, 355–357.

Goel, N., Plyler, K. S., Daniels, D., and Bale, T. L. (2011). Androgenic influence on serotonergic activation of the HPA stress axis. *Endocrinology*, 152(5), 2001–2010.

Goenzalz, J. S., Peyrot, M., McCarl, L. A., Collins, E. M., Serpa, L., Mimiaga, M. J., and Safren, S. A. (2008). Depression and diabetes treatment nonadherence: a meta-analysis. *Diabetes Care*, 31(12), 2398–2403.

Golden, S. A., Covington, H. E., Berton, O., and Russo, S. J. (2011). A standardized protocol for repeated social defeat stress in mice. *Nature Protocols*, 6(8), 1183–1191.

Goto, T., Kubota, Y., Tanaka, Y., Iio, W., Moriya, N., and Toyoda, A. (2014). Subchronic and mild social defeat stress accelerates food intake and body weight gain with polydipsia-like features in mice. *Behavioural Brain Research*, 270, 339–348.

Gout, J. F., Li, W., Fritsch, C., Li, A., Haroon, S., Singh, L., … Vermulst, M. (2017). The landscape of transcription errors in eukaryotic cells. *Science Advances*, 3(10).

Gray, S. M., Meijer, R. I., and Barrett, E. J. (2014). Insulin regulates brain function, but how does it get there? *Diabetes*, 63(12), 3992–3997.

Greenbaum, D., Colangelo, C., Williams, K., and Gerstein, M. (2003). Comparing protein abundance and mRNA expression levels on a genomic scale. *Genome Biology*, 4(9), 117.

Greenberg, M. E., Xu, B., Lu, B., and Hempstead, B. L. (2009). New Insights in the Biology of BDNF Synthesis and Release: Implications in CNS Function. *Journal of Neuroscience*, 29(41), 12764–12767.

Guan, X., Yu, H., Palyha, O., McKee, K., Feighner, S., Sirinathsinghji, D., Smith, R., Van der Ploeg, L., and Howard, A. (1997). Distribution of mRNA encoding the growth hormone secretagogue receptor in brain and peripheral tissues. *Molecular Brain Research*, 48(1), 23–29.

Guiard, B. P., and Di Giovanni, G. (2015). Central serotonin-2A (5-HT2A) receptor dysfunction in depression and epilepsy: The missing link? *Frontiers in Pharmacology*, 6, 1–17.

Guo, K.-Y., Halo, P., Leibel, R. L., and Zhang, Y. (2004). Effects of obesity on the relationship of leptin mRNA expression and adipocyte size in anatomically distinct fat depots in mice. *American Journal of Physiology-Regulatory, Integrative and Comparative Physiology*, 287(1), R112-119.

Gupta, R. Das, Ramachandran, R., Venkatesan, P., Anoop, S., Joseph, M., and Thomas, N. (2017). Indirect Calorimetry: From Bench to Bedside. *Indian Journal of Endocrinology and Metabolism*, 21(4), 594–599.

Halatchev, I. G., Ellacott, K. L. J., Fan, W., and Cone, R. D. (2004). Peptide YY3-36 inhibits food intake in mice through a melanocortin-4 receptor-independent mechanism. *Endocrinology*, 145(6), 2585–2590.

Haleem, D. J. (2014). Investigations into the involvement of leptin in responses to stress. *Behavioural Pharmacology*, 25(5–6), 384–397.

Hall, K. D., Heymsfield, S. B., Kemnitz, J. W., Klein, S., Schoeller, D. A., and Speakman, J. R. (2012). Energy balance and its components: Implications for body weight regulation. *American Journal of Clinical Nutrition*, 95(4), 989–994.

Haller, J., Fuchs, E., Halász, J., and Makara, G. B. (1999). Defeat is a major stressor in males while social instability is stressful mainly in females: Towards the development of a social stress model in female rats. *Brain Research Bulletin*, 50(1), 33–39.

Hameed, S., Patterson, M., Dhillo, W. S., Rahman, S. A., Ma, Y., Holton, C., Gogakos, A., Yeo, G. S.H., Lam, B. Y.H., Polex-Wolf, J., Fenske, W., Bell, J., Anastasovska, J., Samarut, J., Bloom, S. R., Bassett, J. H. D., Williams, G. R., and Gardiner, J. V. (2017). Thyroid Hormone Receptor Beta in the Ventromedial Hypothalamus Is Essential for the Physiological Regulation of Food Intake and Body Weight. *Cell Reports*, 19(11), 2202–2209.

Hammen. (2005). Stress and depression. *Annual Review of Clinical Psychology*, 1(1), 293–391.

Han, H. S., Kang, G., Kim, J. S., Choi, B. H., and Koo, S. H. (2016). Regulation of glucose metabolism from a liver-centric perspective. *Experimental and Molecular Medicine*, 48(3).

Haque, M. S., Minokoshi, Y., Hamai, M., Iwai, M., Horiuchi, M., and Shimazu, T. (1999). Role of the sympathetic nervous system and insulin in enhancing glucose uptake in peripheral tissues after intrahypothalamic injection of leptin in rats. *Diabetes*, 48(9), 1706–1712.

Hardie, L. J., Rayner, D. V., Holmes, S., and Trayhurn, P. (1996). Circulating leptin levels are modulated by fasting, cold exposure and insulin administration in lean but not Zucker (fa/fa) rats as measured by ELISA. *Biochemical and Biophysical Research Communications*, 223(3), 660–665.

Hardwick, A. J., Linton, E. A., and Rothwell, N. J. (1989). Thermogenic effects of the antiglucocorticoid ru-486 in the rat: Involvement of corticotropin-releasing factor and sympathetic activation of brown adipose tissue. *Endocrinology*, 124(4), 1684–1688.

Harris, A. M., Jensen, M. D., and Levine, J. A. (2006). Weekly changes in basal metabolic rate with eight weeks of overfeeding. *Obesity*, 14(4), 690–695.

Harris, R. B. S., Palmondon, J., Leshin, S., Flatt, W. P., and Richard, D. (2006). Chronic disruption of body weight but not of stress peptides or receptors in rats exposed to repeated restraint stress. *Hormones and Behavior*, 49(5), 615–625.

Heiman, M. L., Ahima, R. S., Craft, L. S., Schoner, B., Stephens, T. W., and Flier, J. S. (1997). Leptin inhibition of the hypothalamic-pituitary-adrenal axis in response to stress. *Endocrinology*, 138(9), 3859–3863.

Heindel, J. J., Blumberg, B., Cave, M., Machtinger, R., Mantovani, A., Mendez, M. A., Nadal, A., Palanza, P., Panzica, G., Sargis, R., Vandenberg, L. N., and vom Saal, F. (2017). Metabolism disrupting chemicals and metabolic disorders. *Reproductive Toxicology*, 68, 3–33.

Heisler, L. K., Jobst, E. E., Sutton, G. M., Zhou, L., Borok, E., Thornton-Jones, Z., Liu, H. Y., Zigman, J. M., Balthasar, N., Kishi, T., Lee, C. E., Aschkenasi, C. J., Zhang, C. Y., Yu, J., Boss, O., Mountjoy, K. G., Clifton, P. G., Lowell, B. B., Friedman, J. M., Horvath, T., Butler, A. A., Elmquist, J. K., and Cowley, M. A. (2006). Serotonin Reciprocally Regulates Melanocortin Neurons to Modulate Food Intake. *Neuron*, 51(2), 239–249.

Hemrick-Luecke, S. K., and Evans, D. C. (2002). Comparison of the potency of MDL 100,907 and SB 242084 in blocking the serotonin (5-HT)2receptor agonist-induced increases in rat serum corticosterone concentrations: Evidence for 5-HT2Areceptor mediation of the HPA axis. *Neuropharmacology*, 42(2), 162–169.

Herman, J. P., McKlveen, J. M., Ghosal, S., Kopp, B., Wulsin, A., Makinson, R., Scheimann, J., and Myers, B. (2016). Regulation of the hypothalamic-pituitary-adrenocortical stress response. *Comprehensive Physiology*, 6(2), 603–621.

Hernandez, L., and Hoebel, B. G. (1988). Food reward and cocaine increase extracellular dopamine in the nucleus accumbens as measured by microdialysis. *Life Sciences*, 42(18), 1705–1702.

Herrera, B. M., and Lindgren, C. M. (2010). The Genetics of Obesity. *Current Diabetes Reports*, 10(6), 498–505.

Hershey, J. W. B., Sonenberg, N., and Mathews, M. B. (2012). Principles of translational control: An overview. *Cold Spring Harbor Perspectives in Biology*, 4(12).

Hesselgrave, N., and Parsey, R. V. (2013). Imaging the serotonin 1A receptor using [11C]WAY100635 in healthy controls and major depression. *Philosophical Transactions of the Royal Society B: Biological Sciences*, 368(1615).

Higgs, S., Cooper, A. J., and Barnes, N. M. (2016). The 5-HT2C receptor agonist, lorcaserin, and the 5-HT6receptor antagonist, SB-742457, promote satiety; a

microstructural analysis of feeding behaviour. *Psychopharmacology*, 233(3), 417–424.

Hill, J. (2012). PVN pathways controlling energy homeostasis. *Indian Journal of Endocrinology and Metabolism*, 16(Suppl 3), S627-636.

Hill, J. M., Lesniak, M. A., Pert, C. B., and Roth, J. (1986). Autoradiographic localization of insulin receptors in rat brain: Prominence in olfactory and limbic areas. *Neuroscience*, 17(4), 1127–1138.

Holmes, A. (2008). Genetic variation in cortico-amygdala serotonin function and risk for stress-related disease. *Neuroscience and Biobehavioral Reviews*, 32(7), 1293–1314.

Homberg, J. R., and Contet, C. (2009). Deciphering the Interaction of the Corticotropin-Releasing Factor and Serotonin Brain Systems in Anxiety-Related Disorders. *Journal of Neuroscience*, 29(44), 13743–13745.

Hommel, J. D., Trinko, R., Sears, R. M., Georgescu, D., Liu, Z. W., Gao, X. B., Thurmon, J. J., Marinelli, M., and DiLeone, R. J. (2006). Leptin Receptor Signaling in Midbrain Dopamine Neurons Regulates Feeding. *Neuron*, 51(6), 801–810.

Hornung, J. P. (2003). The human raphe nuclei and the serotonergic system. *Journal of Chemical Neuroanatomy*, 26(4), 331–343.

Hosoda, H., Kojima, M., Matsuo, H., and Kangawa, K. (2000). Ghrelin and des-acyl ghrelin: Two major forms of rat ghrelin peptide in gastrointestinal tissue. *Biochemical and Biophysical Research Communications*, 279(3), 909–913.

Hosoi, T., Kawagishi, T., Okuma, Y., Tanaka, J., and Nomura, Y. (2002). Brain stem is a direct target for leptin's action in the central nervous system. *Endocrinology*, 143(9), 3498–3504.

Howell, L. L., and Cunningham, K. a. (2015). Serotonin 5-HT2 receptor interactions with dopamine function: implications for therapeutics in cocaine use disorder. *Pharmacological Reviews*, 67(1), 176–97.

Hoyer, D., Hannon, J. P., and Martin, G. R. (2002). Molecular, pharmacological and functional diversity of 5-HT receptors. *Pharmacology Biochemistry and Behavior*, 71(4), 533–554.

Hoyer, D., and Martin, G. (1997). 5-HT receptor classification and nomenclature: Towards a harmonization with the human genome. *Neuropharmacology*, 36(4–5), 419–428.

Huang, G.-B., Zhao, T., Muna, S. S., Bagalkot, T. R., Jin, H.-M., Chae, H.-J., and Chung, Y.-C. (2013). Effects of chronic social defeat stress on behaviour, endoplasmic reticulum proteins and choline acetyltransferase in adolescent mice.

International Journal of Neuropsychopharmacology, 16(7), 1635–1647.

Huang, H. J., Zhu, X. C., Han, Q. Q., Wang, Y. L., Yue, N., Wang, J., Yu, R., Li, B., Wu, G. C., Liu, Q., and Yu, J. (2017). Ghrelin alleviates anxiety- and depression-like behaviors induced by chronic unpredictable mild stress in rodents. *Behavioural Brain Research*, 326, 33–43.

Huang, S., and Czech, M. P. (2007). The GLUT4 Glucose Transporter. *Cell Metabolism*, 5(4), 237–252.

Hube, F., Lietz, U., Igel, M., Jensen, P. B., Tornqvist, H., Joost, H. G., and Hauner, H. (1996). Difference in leptin mRNA levels between omental and subcutaneous abdominal adipose tissue from obese humans. *Hormone and Metabolic Research*, 28(12), 690–693.

Iio, W., Takagi, H., Ogawa, Y., Tsukahara, T., Chohnan, S., and Toyoda, A. (2014). Effects of chronic social defeat stress on peripheral leptin and its hypothalamic actions. *BMC Neuroscience*, 15(72), 1–7.

Iio, W., Tokutake, Y., Matsukawa, N., Tsukahara, T., Chohnan, S., and Toyoda, A. (2012). Anorexic behavior and elevation of hypothalamic malonyl-CoA in socially defeated rats. *Biochemical and Biophysical Research Communications*, 421(2), 301–304.

Ikeda, K., Maretich, P., and Kajimura, S. (2018). The Common and Distinct Features of Brown and Beige Adipocytes. *Trends in Endocrinology and Metabolism*, 29(3), 191–200.

Iñiguez, S. D., Aubry, A., Riggs, L. M., Alipio, J. B., Zanca, R. M., Flores-Ramirez, F. J., Hernandez, M. A., Nieto, S. J., Musheyev, D., and Serrano, P. A. (2016). Social defeat stress induces depression-like behavior and alters spine morphology in the hippocampus of adolescent male C57BL/6 mice. *Neurobiology of Stress*, 5, 54–64.

Iñiguez, S. D., Riggs, L. M., Nieto, S. J., Dayrit, G., Zamora, N. N., Shawhan, K. L., Cruz, B., and Warren, B. L. (2014). Social defeat stress induces a depression-like phenotype in adolescent male c57BL/6 mice. *Stress*, 17(3), 247–255.

Inui, A., Tsai, M., Amitani, H., and Asakawa, A. (2012). Stimulation of leptin secretion by insulin. *Indian Journal of Endocrinology and Metabolism*, 16(Suppl 3), S543–S548.

James, G. M., Baldinger-Melich, P., Philippe, C., Kranz, G. S., Vanicek, T., Hahn, A., Gryglewski, G., Hienert, M., Spies, M., Traub-Weidinger, T., Mitterhauser, M., Wadsak, W., Hacker, M., Kasper, S., and Lanzenberger, R. (2017). Effects of Selective Serotonin Reuptake Inhibitors on Interregional Relation of Serotonin Transporter Availability in Major Depression. *Frontiers in Human Neuroscience*, 11(48), 1–10.

Jhanwar-Uniyal, M., Beck, B., Jhanwar, Y. S., Burlet, C., and Leibowitz, S. F. (1993). Neuropeptide Y projection from arcuate nucleus to parvocellular division of paraventricular nucleus: specific relation to the ingestion of carbohydrate. *Brain Research*, 631(1), 97–106.

Jiang, D. G., Jin, S. L., Li, G. Y., Li, Q. Q., Li, Z. R., Ma, H. X., Zhuo, C. J., Jiang, R. H., and Ye, M. J. (2016). Serotonin regulates brain-derived neurotrophic factor expression in select brain regions during acute psychological stress. *Neural Regeneration Research*, 11(9), 1471–1479.

Jiang, X., Xing, G., Yang, C., Verma, A., Zhang, L., and Li, H. (2009). Stress Impairs 5-HT2A Receptor-Mediated Serotonergic Facilitation of GABA Release in Juvenile Rat Basolateral Amygdala. *Neuropsychopharmacology*, 34(2), 410–423.

Jiang, Z. C., Qi, W. J., Wang, J. Y., and Luo, F. (2014). Chronic administration of 5-HT1A receptor agonist relieves depression and depression-induced hypoalgesia. *The Scientific World Journal*, 2014, 1–7.

Johnson, P. M., and Kenny, P. J. (2010). Dopamine D2 receptors in addiction-like reward dysfunction and compulsive eating in obese rats. *Nature Neuroscience*, 13(5), 635–641.

Joseph, J. J., and Golden, S. H. (2017). Cortisol dysregulation: the bidirectional link between stress, depression, and type 2 diabetes mellitus. *Annals of the New York Academy of Sciences*, 1391(1), 20–34.

Joung, K. E., Park, K. H., Zaichenko, L., Sahin-Efe, A., Thakkar, B., Brinkoetter, M., Usher, N., Warner, D., Davis, C. R., Crowell, J. A., and Mantzoros, C. S. (2014). Early life adversity is associated with elevated levels of circulating leptin, irisin, and decreased levels of adiponectin in midlife adults. *Journal of Clinical Endocrinology and Metabolism*, 99(6), E1055-1060.

Jovanovic, H., Perski, A., Berglund, H., and Savic, I. (2011). Chronic stress is linked to 5-HT1A receptor changes and functional disintegration of the limbic networks. *NeuroImage*, 55(3), 1178–1188.

Jow, G. M., Yang, T. T., and Chen, C. L. (2006). Leptin and cholesterol levels are low in major depressive disorder, but high in schizophrenia. *Journal of Affective Disorders*, 90(1), 21–27.

Kalat, J. W. (1998) *Biological Psychology* 6th edn. Pacific Grove, CA: Brooks/Cole Pub. Co.

Kalra, S. P., Dube, M. G., Sahu, A., Phelps, C. P., and Kalra, P. S. (1991). Neuropeptide Y secretion increases in the paraventricular nucleus in association with increased appetite for food. *Proceedings of the National Academy of Sciences of the United States of America*, 88(23), 10931–10935.

Kampe, J., Tschöp, M. H., Hollis, J. H., and Oldfield, B. J. (2009). An anatomic basis for the communication of hypothalamic, cortical and mesolimbic circuitry in the regulation of energy balance. *European Journal of Neuroscience*, 30(3), 415–430.

Kanarik, M., Alttoa, A., Matrov, D., Kõiv, K., Sharp, T., Panksepp, J., and Harro, J. (2011). Brain responses to chronic social defeat stress: effects on regional oxidative metabolism as a function of a hedonic trait, and gene expression in susceptible and resilient rats. *European Neuropsychopharmacology*, 21(1), 92–107.

Kanehisa, M., Akiyoshi, J., Kitaichi, T., Matsushita, H., Tanaka, E., Kodama, K., Hanada, H., and Isogawa, K. (2006). Administration of antisense DNA for ghrelin causes an antidepressant and anxiolytic response in rats. *Progress in Neuro-Psychopharmacology and Biological Psychiatry*, 30(8), 1403–1407.

Karra, E., Chandarana, K., and Batterham, R. L. (2009). The role of peptide YY in appetite regulation and obesity. *Journal of Physiology*, 587(1), 19–25.

Kataoka, N., Hioki, H., Kaneko, T., and Nakamura, K. (2014). Psychological stress activates a dorsomedial hypothalamus-medullary raphe circuit driving brown adipose tissue thermogenesis and hyperthermia. *Cell Metabolism*, 20(2), 346–358.

Katsurada, K., Maejima, Y., Nakata, M., Kodaira, M., Suyama, S., Iwasaki, Y., Kario, K., and Yada, T. (2014). Endogenous GLP-1 acts on paraventricular nucleus to suppress feeding: Projection from nucleus tractus solitarius and activation of corticotropin-releasing hormone, nesfatin-1 and oxytocin neurons. *Biochemical and Biophysical Research Communications*, 451(2), 276–281.

Katz, R. J., Roth, K. A., and Carroll, B. J. (1981). Acute and chronic stress effects on open field activity in the rat: Implications for a model of depression. *Neuroscience & Biobehavioral Reviews*, 5(2), 247–251.

Kaufman, J., DeLorenzo, C., Choudhury, S., and Parsey, R. V. (2016). The 5-HT1A receptor in Major Depressive Disorder. *European Neuropsychopharmacology*, 26(3), 397–410.

Kim, M. S., Yoon, C. Y., Park, K. H., Shin, C. S., Park, K. S., Kim, S. Y., Cho, B. Y., and Lee, H. K. (2003). Changes in ghrelin and ghrelin receptor expression according to feeding status. *NeuroReport*, 14(10), 1317–1320.

Kineman, R. D., Gahete, M. D., and Luque, R. M. (2007). Identification of a mouse ghrelin gene transcript that contains intron 2 and is regulated in the pituitary and hypothalamus in response to metabolic stress. *Journal of Molecular Endocrinology*, 38(5), 511–521.

Kishi, T., Aschkenasi, C. J., Lee, C. E., Mountjoy, K. G., Saper, C. B., and Elmquist, J. K. (2003). Expression of melanocortin 4 receptor mRNA in the central nervous

system of the rat. *The Journal of Comparative Neurology*, 457(3), 213–235.

Kleinridders, A., Cai, W., Cappellucci, L., Ghazarian, A., Collins, W. R., Vienberg, S. G., Pothos, E. N., and Kahn, C. R. (2015). Insulin resistance in brain alters dopamine turnover and causes behavioral disorders. *Proceedings of the National Academy of Sciences*, 112(11), 3463–3468.

Klok, M. D., Jakobsdottir, S., and Drent, M. L. (2007). The role of leptin and ghrelin in the regulation of food intake and body weight in humans: A review. *Obesity Reviews*, 8(1), 21–34.

Knol, M. J., Twisk, J. W. R., Beekman, A. T. F., Heine, R. J., Snoek, F. J., and Pouwer, F. (2006). Depression as a risk factor for the onset of type 2 diabetes mellitus. A meta-analysis. *Diabetologia*, 49(5), 837–845.

Koch, C. E., Bartlang, M. S., Kiehn, J. T., Lucke, L., Naujokat, N., Helfrich-Förster, C., Reber, S. O., and Oster, H. (2016). Time-of-day-dependent adaptation of the HPA axis to predictable social defeat stress. *Journal of Endocrinology*, 231(3), 209–221.

Koch, C. E., Leinweber, B., Drengberg, B. C., Blaum, C., and Oster, H. (2017). Interaction between circadian rhythms and stress. *Neurobiology of Stress*, 6, 57–67.

Kojima, M., Hosoda, H., Matsuo, H., and Kangawa, K. (2001). Ghrelin: Discovery of the natural endogenous ligand for the growth hormone secretagogue receptor. *Trends in Endocrinology and Metabolism*, 12(3), 118–122.

Konishi, N., Otaka, M., Odashima, M., Jin, M., Wada, I., Komatsu, K., Sato, T., Kato, S., Matsuhashi, T., and Watanabe, S. (2006). Systemic stress increases serum leptin level. *Journal of Gastroenterology and Hepatology*, 21(7), 1099–1102.

Koolhaas, J. M., Bartolomucci, A., Buwalda, B., de Boer, S. F., Flugge, G., Korte, S. M., Meerlo, P., Murison, R., Olivier, B., Palanza, P., Richter-Levin, G., Sgoifo, A., Steimer, T., Stiedl, O., van Dijk, G., Wohr, M., and Fuchs, E. (2011). Stress revisited: a critical evaluation of the stress concept. *Neuroscience and Biobehavioral Reviews*, 35(5), 1291–1301.

Koolhaas, J. M., Coppens, C. M., de Boer, S. F., Buwalda, B., Meerlo, P., and Timmermans, P. J. A. (2013). The resident-intruder paradigm: a standardized test for aggression, violence and social stress. *JoVE: Journal of Visualized Experiments*, (77).

Koolhaas, J. M., de Boer, S. F., Buwalda, B., and Meerlo, P. (2017). Social stress models in rodents: Towards enhanced validity. *Neurobiology of Stress*, 6, 104–112.

Koolhaas, J. M., De Boer, S. F., De Rutter, A. J., Meerlo, P., and Sgoifo, A. (1997). Social stress in rats and mice. *Acta Physiologica Scandinavica*, 640(February),

69–72. Retrieved from QP1.A25

Kornberg, H. (2017). Metabolism. In *Encyclopædia Britannica*.

Kozera, B., and Rapacz, M. (2013). Reference genes in real-time PCR. *Journal of Applied Genetics*, 54(4), 391–406.

Kranz, G. S., Kasper, S., and Lanzenberger, R. (2010). Reward and the serotonergic system. *Neuroscience*, 166(4), 1023–1035.

Krashes, M. J., Koda, S., Ye, C. P., Rogan, S. C., Adams, A. C., Cusher, D. S., Maratos-Flier, E., Roth, B. L., and Lowell, B. B. (2011). Rapid, reversible activation of AgRP neurons drives feeding behavior in mice. *Journal of Clinical Investigation*, 121(4), 1424–1428.

Kristenssson, E., Sundqvist, M., Astin, M., Kjerling, M., Mattsson, H., Dornonville de la Cour, C., Håkanson, R., and Lindström, E. (2006). Acute psychological stress raises plasma ghrelin in the rat. *Regulatory Peptides*, 134(2–3), 114–117.

Kudryavtseva, N. N., Bakshtanovskaya, I. V, and Koryakina, L. A. (1991). Social model of depression in mice of C57BL/6J strain. *Pharmacology Biochemistry and Behavior*, 38(2), 315–320.

Kumar, J., Chuang, J. C., Na, E. S., Kuperman, A., Gillman, A. G., Mukherjee, S., Zigman, J. M., McClung, C. A., and Lutter, M. (2013). Differential effects of chronic social stress and fluoxetine on meal patterns in mice. *Appetite*, 64, 81–88.

Kursungoz, C., Ak, M., and Yanik, T. (2015). Effects of risperidone treatment on the expression of hypothalamic neuropeptide in appetite regulation in Wistar rats. *Brain Research*, 1596, 146–155.

Lam, D. D., Garfield, A. S., Marston, O. J., Shaw, J., and Heisler, L. K. (2010). Brain serotonin system in the coordination of food intake and body weight. *Pharmacology Biochemistry and Behavior*, 97(1), 84–91.

Lam, D. D., Przydzial, M. J., Ridley, S. H., Yeo, G. S. H., Rochford, J. J., O'Rahilly, S., and Heisler, L. K. (2008). Serotonin 5-HT2Creceptor agonist promotes hypophagia via downstream activation of melanocortin 4 receptors. *Endocrinology*, 149(3), 1323–1328.

Lam, Y. Y., and Ravussin, E. (2016). Analysis of energy metabolism in humans: A review of methodologies. *Molecular Metabolism*, 5(11), 1057–1071.

Larger, E. (2005). Weight gain and insulin treatment. *Diabetes and Metabolism Journal*, 31(4 Pt 2), 4S51-4S56.

Lawson, E. A., Miller, K. K., Blum, J. I., Meenaghan, E., Misra, M., Eddy, K. T., Herzog, D. B., and Klibanski, A. (2012). Leptin levels are associated with

decreased depressive symptoms in women across the weight spectrum, independent of body fat. *Clinical Endocrinology*, 76(4), 520–525.

Lazar, M. A., and Birnbaum, M. J. (2012). De-meaning of metabolism. *Science*, 336(6089), 1651–1652.

Lee, J. M., Seo, W. Y., Han, H. S., Oh, K. J., Lee, Y. S., Kim, D. K., Choi, S., Choi, B. H., Harris, R. A., Lee, C. H., Koo, S. H., and Choi, H. S. (2016). Insulin-Inducible SMILE inhibits hepatic gluconeogenesis. *Diabetes*, 65(1), 62–73.

Leigh Gibson, E. (2006). Emotional influences on food choice: Sensory, physiological and psychological pathways. *Physiology and Behavior*, 89(1), 53–61.

Leitner, B. P., Huang, S., Brychta, R. J., Duckworth, C. J., Baskin, A. S., McGehee, S., Tal, I., Dieckmann, W., Gupta, G., Kolodny, G. M., Pacak, K., Herscovitch, P., Cypess, A. M., and Chen, K. Y. (2017). Mapping of human brown adipose tissue in lean and obese young men. *Proceedings of the National Academy of Sciences*, 114(32), 8649–8654.

Leroy, P., Dessolin, S., Villageois, P., Moon, B. C., Friedman, J. M., Ailhaud, G., and Dani, C. (1996). Expression of ob gene in adipose cells: Regulation by insulin. *Journal of Biological Chemistry*, 271(5), 2365–2368.

Lesch, K. P., Bengel, D., Heils, A., Sabol, S. Z., Greenberg, B. D., Petri, S., Benjamin, J., Müller, C. R., Hamer, D. H., and Murphy, D. L. (1996). Association of anxiety-related traits with a polymorphism in the serotonin transporter gene regulatory region. *Science*, 274(5292), 1527–1531.

Lester, N., Nebel, L. E., and Baum, A. (1994). Psychophysiological and Behavioral Measurement of Stress: Applications to Mental Health. In W. R. Avison and I. H. Gotlib (Eds.), *Stress and Mental Health* (pp. 291–309). Boston, MA: Springer US.

Leventopoulos, M., Russig, H., Feldon, J., Pryce, C. R., and Opacka-Juffry, J. (2009). Early deprivation leads to long-term reductions in motivation for reward and 5-HT1A binding and both effects are reversed by fluoxetine. *Neuropharmacology*, 56(3), 692–701.

Levine, J. A. (2005). Measurement of energy expenditure. *Public Health Nutrition*, 8(7A), 1123–1132.

Lightman, S. (2016). Rhythms within rhythms: The importance of oscillations for glucocorticoid hormones. In *A Time for Metabolism and Hormones* (pp. 87–99).

Little, T. J., Horowitz, M., and Feinle-Bisset, C. (2005). Role of cholecystokinin in appetite control and body weight regulation. *Obesity Reviews*, 6(4), 297–306.

Liu, M., Weiss, M. A., Arunagiri, A., Yong, J., Rege, N., Sun, J., Haataja, L., Kaufman, R. J., and Arvan, P. (2018). Biosynthesis, structure, and folding of the insulin

precursor protein. *Diabetes, Obesity and Metabolism*, 20(S2), 28–50.

Liu, Y.-Y., Zhou, X.-Y., Yang, L.-N., Wang, H.-Y., Zhang, Y.-Q., Pu, J.-C., Liu, L.-X., Gui, S.-W., Zeng, L., Chen, J.-J., Zhou, C.-J., Xie, P. (2017). Social defeat stress causes depression-like behavior with metabolite changes in the prefrontal cortex of rats. *PloS ONE*, 12(4).

Lkhagvasuren, B., Nakamura, Y., Oka, T., Sudo, N., and Nakamura, K. (2011). Social defeat stress induces hyperthermia through activation of thermoregulatory sympathetic premotor neurons in the medullary raphe region. *European Journal of Neuroscience*, 34(9), 1442–1452.

Loh, K., Zhang, L., Brandon, A., Wang, Q., Begg, D., Qi, Y., Fu, M., Kulkarni, R., Teo, J., Baldock, P., Brüning, J. C., Cooney, G., Neely, G., and Herzog, H. (2017). Insulin controls food intake and energy balance via NPY neurons. *Molecular Metabolism*, 6(6), 574–584.

Lonçar, D., Afzelius, B. A., and Cannon, B. (1988). Epididymal white adipose tissue after cold stress in rats I. Nonmitochondrial changes. *Journal of Ultrastructure Research and Molecular Structure Research*, 101(2–3), 109–122.

Lu, X.-Y., Kim, C. S., Frazer, A., and Zhang, W. (2006). Leptin: A potential novel antidepressant. *Proceedings of the National Academy of Sciences*, 103(5), 1593–1598.

Luppino, F. S., De Wit, L. M., Bouvy, P. F., Stijnen, T., Cuijpers, P., Penninx, B. W. J. H., and Zitman, F. G. (2010). Overweight, obesity, and depression: A systematic review and meta-analysis of longitudinal studies. *Archives of General Psychiatry*, 67(3), 220–229.

Luque, C. A., and Rey, J. A. (2002). The discovery and status of sibutramine as an anti-obesity drug. *European Journal of Pharmacology*, 440(2–3), 119–128.

Lutter, M., and Elmquist, J. (2009). Depression and metabolism: linking changes in leptin and ghrelin to mood. *F1000 Biology Reports*, 1(63).

Lutter, M., Sakata, I., Osborne-Lawrence, S., Rovinsky, S. A., Anderson, J. G., Jung, S., Birnbaum, S., Yanagisawa, M., Elmquist, J. K., Nestler, E. J., Zigman, J. M. (2008). The orexigenic hormone ghrelin defends against depressive symptoms of chronic stress. *Nature Neuroscience*, 11(7), 752–753.

Madden, C. J., and Morrison, S. F. (2009). Neurons in the paraventricular nucleus of the hypothalamus inhibit sympathetic outflow to brown adipose tissue. *American Journal of Physiology-Regulatory, Integrative and Comparative Physiology*, 296(3), R831-843.

Madden, C. J., Tupone, D., Cano, G., and Morrison, S. F. (2013). Alpha 2 Adrenergic Receptor-Mediated Inhibition of Thermogenesis. *Journal of Neuroscience*, 33(5), 2017–2028.

Maffei, M., Halaas, J., Ravussin, E., Pratley, R. E., Lee, G. H., Zhang, Y., Fei, H., Kim, S., Lallone, R., Ranganathan, S., Kern, P. A., and Friedman, J. M. (1995). Leptin levels in human and rodent: Measurement of plasma leptin and ob RNA in obese and weight-reduced subjects. *Nature Medicine*, 1(11), 1155–1161.

Magalhães, C. P., de Freitas, M. F. L., Nogueira, M. I., Campina, R. C. de F., Takase, L. F., de Souza, S. L., and de Castro, R. M. (2010). Modulatory role of serotonin on feeding behavior. *Nutritional Neuroscience*, 13(6), 246–255.

Malison, R. T., Price, L. H., Berman, R., van Dyck, C. H., Pelton, G. H., Carpenter, L., Sanacora, G., Owens, M. J., Nemeroff, C. B., Rajeevan, N., Baldwin, R. M., Seibyl, J. P., Innis, R. B., and Charney, D. S. (1998). Reduced brain serotonin transporter availability in major depression as measured by [123I]-2 beta-carbomethoxy-3 beta-(4-iodophenyl)tropane and single photon emission computed tomography. *Biological Psychiatry*, 44(11), 1090–1098.

Maniam, J., and Morris, M. J. (2012). The link between stress and feeding behaviour. *Neuropharmacology*, 63(1), 97–110.

Maniscalco, J. W., Kreisler, A. D., and Rinaman, L. (2012). Satiation and stress-induced hypophagia: Examining the role of hindbrain neurons expressing prolactin-releasing peptide or glucagon-like peptide 1. *Frontiers in Neuroscience*, 6, 199.

Mann, A., Thompson, A., Robbins, N., and Blomkalns, A. L. (2014). Localization, Identification, and Excision of Murine Adipose Depots. *Journal of Visualized Experiments*, (94).

Margioris, A., and Tsatsanis, C. (2011). ACTH Action on the Adrenal. *Adrenal Physiology and Diseases*.

Martinowich, K., and Lu, B. (2008). Interaction between BDNF and serotonin: Role in mood disorders. *Neuropsychopharmacology*, 33(1), 73–83.

Matheny, M., Strehler, K. Y. E., King, M., Tümer, N., and Scarpace, P. J. (2014). Targeted leptin receptor blockade: Role of ventral tegmental area and nucleus of the solitary tract leptin receptors in body weight homeostasis. *Journal of Endocrinology*, 222(1), 27–41.

Matoušková, P., Bártíková, H., Boušová, I., Hanušová, V., Szotáková, B., and Skálová, L. (2014). Reference genes for real-time PCR quantification of messenger RNAs and microRNAs in mouse model of obesity. *PLoS ONE*, 9(1).

Mazor, R., Friedmann-Morvinski, D., Alsaigh, T., Kleifeld, O., Kistler, E. B., Rousso-Noori, L., Huang, C., Li, J. B., Verma, I. M., and Schmid-Schönbein, G. W. (2018). Cleavage of the leptin receptor by matrix metalloproteinase-2 promotes leptin resistance and obesity in mice. *Science Translational Medicine*, 10(445), 1–11.

McAllister-Williams, R. H., Ferrier, I. N., and Young, A. H. (1998). Mood and neuropsychological function in depression: The role of corticosteroids and serotonin. *Psychological Medicine*, 28(3), 573–584.

McEwen, B. S., and Reagan, L. P. (2004). Glucose transporter expression in the central nervous system: Relationship to synaptic function. *European Journal of Pharmacology*, 490(1–3), 13–24.

McGonagle, K. A., and Kessler, R. C. (1990). Chronic stress, acute stress, and depressive symptoms. *American Journal of Community Psychology*, 18(5), 681–706.

McKittrick, C. R., Caroline Blanchard, D., Blanchard, R. J., McEwen, B. S., and Sakai, R. R. (1995). Serotonin receptor binding in a colony model of chronic social stress. *Biological Psychiatry*, 37(6), 383–393.

McKittrick, C. R., Magariños, A. M., Blanchard, D. C., Blanchard, R. J., McEwen, B. S., and Sakai, R. R. (2000). Chronic social stress reduces dendritic arbors in CA3 of hippocampus and decreases binding to serotonin transporter sites. *Synapse*, 36(2), 85–94.

Meerlo, P., Overkamp, G. J. F., Daan, S., Van Den Hoofdakker, R. H., and Koolhaas, J. M. (1996). Changes in behaviour and body weight following a single or double social defeat in rats. *Stress*, 1(1), 21–32.

Mengod, G., Nguyen, H., Le, H., Waeber, C., Lübbert, H., and Palacios, J. M. (1990). The distribution and cellular localization of the serotonin 1C receptor mRNA in the rodent brain examined by in situ hybridization histochemistry. Comparison with receptor binding distribution. *Neuroscience*, 35(3), 577–591.

Mergenthaler, P., Lindauer, U., Dienel, G. A., and Meisel, A. (2013). Sugar for the brain: The role of glucose in physiological and pathological brain function. *Trends in Neurosciences*, 36(10), 587–597.

Meyer, R. M., Burgos-Robles, A., Liu, E., Correia, S. S., and Goosens, K. A. (2014). A ghrelin-growth hormone axis drives stress-induced vulnerability to enhanced fear. *Molecular Psychiatry*, 19(12), 1284–1294.

Mezuk, B., Eaton, W. W., Albrecht, S., and Golden, S. H. (2008). Depression and type 2 diabetes over the lifespan: A meta-analysis. *Diabetes Care*, 31(12), 2383–2390.

Millington, G. W. M. (2007). The role of proopiomelanocortin (POMC) neurones in feeding behaviour. *Nutrition and Metabolism*, 4, 18.

Miura, H., Ozaki, N., Sawada, M., Isobe, K., Ohta, T., and Nagatsu, T. (2008). A link between stress and depression: Shifts in the balance between the kynurenine and serotonin pathways of tryptophan metabolism and the etiology and pathophysiology of depression. *Stress*, 11(3), 198–209.

Miyagawa, K., Tsuji, M., Ishii, D., Takeda, K., and Takeda, H. (2015). Prenatal stress induces vulnerability to stress together with the disruption of central serotonin neurons in mice. *Behavioural Brain Research*, 277, 228–236.

Mo, Q., Salley, J., Roshan, T., Baer, L. A., May, F. J., Jaehnig, E. J., Lehnig, A. C., Guo, X., Tong, Q., Nuotio-Antar, A. M., Shamsi, F., Tseng, Y.-H., Stanford, K. I., and Chen, M.-H. (2017). Identification and characterization of a supraclavicular brown adipose tissue in mice. *JCI Insight*, 2(11), 1–14.

Mohammad-Zadeh, L. F., Moses, L., and Gwaltney-Brant, S. M. (2008). Serotonin: A review. *Journal of Veterinary Pharmacology and Therapeutics*, 31(3), 187–199.

Moles, A., Bartolomucci, A., Garbugino, L., Conti, R., Caprioli, A., Coccurello, R., Rizzi, R., Ciani, B., and D'Amato, F. R. (2006). Psychosocial stress affects energy balance in mice: Modulation by social status. *Psychoneuroendocrinology*, 31(5), 623–633.

Molteni, R., Calabrese, F., Cattaneo, A., Mancini, M., Gennarelli, M., Racagni, G., and Riva, M. A. (2009). Acute stress responsiveness of the neurotrophin bdnf in the rat hippocampus is modulated by chronic treatment with the antidepressant duloxetine. *Neuropsychopharmacology*, 34(6), 1523–1532.

Mongeau, R., Martin, C. B. P., Chevarin, C., Maldonado, R., Hamon, M., Robledo, P., and Lanfumey, L. (2010). 5-HT2C receptor activation prevents stress-induced enhancement of brain 5-HT turnover and extracellular levels in the mouse brain: Modulation by chronic paroxetine treatment. *Journal of Neurochemistry*, 115(2), 438–449.

Montague, C. T., Farooqi, I. S., Whitehead, J. P., Soos, M. A., Rau, H., Wareham, N. J., Sewter, C. P., Digby, J. E., Mohammed, S. N., Hurst, J. A., Cheetham, C. H., Earley, A. R., Barnett, A. H., Prins, J. B., and O'Rahilly, S. (1997). Congenital leptin deficiency is associated with severe early-onset obesity in humans. *Nature*, 387, 903–908.

Morrison, S. F., Madden, C. J., and Tupone, D. (2014). Central neural regulation of brown adipose tissue thermogenesis and energy expenditure. *Cell Metabolism*.

Morton, G. J., Meek, T. H., Matsen, M. E., and Schwartz, M. W. (2015). Evidence against hypothalamic-pituitary-adrenal axis suppression in the antidiabetic action of leptin. *Journal of Clinical Investigation*, 125(12), 4587–4591.

Morton, G. J., Meek, T. H., and Schwartz, M. W. (2014). Neurobiology of food intake in health and disease. *Nature Reviews Neuroscience*.

Morton, G. J., Niswender, K. D., Rhodes, C. J., Myers, M. G., Blevins, J. E., Baskin, D. G., and Schwartz, M. W. (2003). Arcuate nucleus-specific leptin receptor gene therapy attenuates the obesity phenotype of Koletsky (fak/fak) rats. *Endocrinology*, 144(5), 2016–2024.

Morton, G. J., and Schwartz, M. W. (2011). Leptin and the central nervous system control of glucose metabolism. *Physiological Reviews*, 91(2), 389–411.

Müller, T. D., Nogueiras, R., Andermann, M. L., Andrews, Z. B., Anker, S. D., Argente, J., Batterham, R. L., Benoit, S. C., Bowers, C. Y., Broglio, F., Casanueva, F. F., D'Alessio, D., Depoortere, I., Geliebter, A., Ghigo, E., Cole, P. A., Cowley, M., Cummings, D. E., Dagher, A., Diano, S., Dickson, S. L., Diéguez, C., Granata, R., Grill, H. J., Grove, K., Habegger, K. M., Heppner, K., Heiman, M. L., Holsen, L., Holst, B., Inui, A., Jansson, J. O., Kirchner, H., Korbonits, M., Laferrère, B., LeRoux, C. W., Lopez, M., Morin, S., Nakazato, M., Nass, R., Perez-Tilve, D., Pfluger, P. T., Schwartz, T. W., Seeley, R. J., Sleeman, M., Sun, Y., Sussel, L., Tong, J., Thorner, M. O., van der Lely, A. J., van der Ploeg, L. H.T., Zigman, J. M., Kojima, M., Kangawa, K., Smith, R. G., Horvath, T., and Tschöp, M. H. (2015). Ghrelin. *Molecular Metabolism*, 4(6), 437–460.

Musazzi, L., Tornese, P., Sala, N., and Popoli, M. (2017). Acute or Chronic? A Stressful Question. *Trends in Neurosciences*, 40(9), 525–535.

Nakazato, M., Murakami, N., Date, Y., Kojima, M., Matsuo, H., Kangawa, K., and Matsukura, S. (2001). A role for ghrelin in the central regulation of feeding. *Nature*, 409(6817), 194–198.

Naleid, A. M., Grace, M. K., Cummings, D. E., and Levine, A. S. (2005). Ghrelin induces feeding in the mesolimbic reward pathway between the ventral tegmental area and the nucleus accumbens. *Peptides*, 26(11), 2274–2279.

Nantel, J., Mathieu, M. E., and Prince, F. (2011). Physical activity and obesity: Biomechanical and physiological key concepts. *Journal of Obesity*, 2011, 1–10.

Nasrallah, C. M., and Horvath, T. L. (2014). Mitochondrial dynamics in the central regulation of metabolism. *Nature Reviews Endocrinology*, 159(10), 3596–3604.

Natarajan, R., Forrester, L., Chiaia, N. L., and Yamamoto, B. K. (2017). Chronic-Stress-Induced Behavioral Changes Associated with Subregion-Selective Serotonin Cell Death in the Dorsal Raphe. *The Journal of Neuroscience*, 37(26), 6214–6223.

NC3Rs. (2017). The 3Rs. Retrieved November 12, 2017, from https://www.nc3rs.org.uk/the-3rs

Nedergaard, J., Bengtsson, T., and Cannon, B. (2007). Unexpected evidence for active brown adipose tissue in adult humans. *American Journal of Physiology-Endocrinology and Metabolism*, 293(2), E444-452.

Nestler, E. J., and Carlezon, W. A. (2006). The Mesolimbic Dopamine Reward Circuit in Depression. *Biological Psychiatry*, 59(12), 1151–1159.

Newberg, A. B., Amsterdam, J. D., Wintering, N., Ploessl, K., Swanson, R. L., Shults,

J., and Alavi, A. (2015). 123I-ADAM Binding to Serotonin Transporters in Patients with Major Depression and Healthy Controls : A Preliminary Study. *Journal of Nuclear Medicine*, 46(6), 973–977.

Newberg, A. B., Amsterdam, J. D., Wintering, N., and Shults, J. (2012). Low brain serotonin transporter binding in major depressive disorder. *Psychiatry Research - Neuroimaging*, 202(2), 161–167.

Nguyen, D., and Xu, T. (2008). The expanding role of mouse genetics for understanding human biology and disease. *Disease Models and Mechanisms*, 1(1), 56–66.

Nguyen, N. Q., Debreceni, T. L., Bambrick, J. E., Chia, B., Wishart, J., Deane, A. M., Rayner, C. K., Horowitz, M., and Young, R. L. (2015). Accelerated intestinal glucose absorption in morbidly obese humans: Relationship to glucose transporters, incretin hormones, and glycemia. *Journal of Clinical Endocrinology and Metabolism*, 100(3), 968–976.

Nieh, E. H., Matthews, G. A., Wildes, C. P., Tye Correspondence, K. M., Allsop, S. A., Presbrey, K. N., … Tye, K. M. (2015). Decoding Neural Circuits that Control Compulsive Sucrose Seeking In Brief Decoding Neural Circuits that Control Compulsive Sucrose Seeking. *Cell*, 160(3), 528–541.

Nielsen, J. A., Chapin, D. S., Johnson, J. L., and Torgersen, L. K. (1992). Sertraline, a serotonin-uptake inhibitor, reduces food intake and body weight in lean rats and genetically obese mice. *American Journal of Clinical Nutrition*, 55(1 Suppl), 185S–189S.

Nogueiras, R., Tovar, S., Mitchell, S. E., Rayner, D. V, Archer, Z. a, Dieguez, C., and Williams, L. M. (2004). Regulation of growth hormone secretagogue receptor gene expression in the arcuate nuclei of the rat by leptin and ghrelin. *Diabetes*, 53(10), 2552–2558.

Nonogaki, K., and Kaji, T. (2018). Liraglutide, a GLP-1 Receptor Agonist, Which Decreases Hypothalamic 5-HT2A Receptor Expression, Reduces Appetite and Body Weight Independently of Serotonin Synthesis in Mice. *Journal of Diabetes Research*, 2018, 1–6.

Oakley, R. H., and Cidlowski, J. A. (2013). The biology of the glucocorticoid receptor: New signaling mechanisms in health and disease. *Journal of Allergy and Clinical Immunology*, 132(5), 1033–1044.

Obici, S., Feng, Z., Karkanias, G., Baskin, D. G., and Rossetti, L. (2002). Decreasing hypothalamic insulin receptors causes hyperphagia and insulin resistance in rats. *Nature Neuroscience*, 5(6), 566–572.

Ochi, M., Tominaga, K., Tanaka, F., Tanigawa, T., Shiba, M., Watanabe, T., Fujiwara, Y., Oshitani, N., Higuchi, K., and Arakawa, T. (2008). Effect of chronic stress on gastric emptying and plasma ghrelin levels in rats. *Life Sciences*, 82(15–16), 862–

868.

Olivares, E. L., Silva-Almeida, C., Pestana, F. M., Sonoda-Côrtes, R., Araujo, I. G., Rodrigues, N. C., Mecawi, A. S., Côrtes, W. S., Marassi, M. P., Reis, L. C., and Rocha, F. F. (2012). Social stress-induced hypothyroidism is attenuated by antidepressant treatment in rats. *Neuropharmacology*, 62(1), 446–456.

Oliver, G., and Wardle, J. (1999). Perceived effects of stress on food choice. *Physiology and Behavior*, 66(3), 511–515.

Ollmann, M. M., Wilson, B. D., Yang, Y. K., Kerns, J. A., Chen, Y., Gantz, I., and Barsh, G. S. (1997). Antagonism of central melanocortin receptors in vitro and in vivo by agouti-related protein. *Science*, 278(5335), 135–138.

Opacka-Juffry, J. (2008). The role of serotonin as a neurotransmitter in health and illness: A review. *British Journal of Neuroscience Nursing*, 4(6), 272–277.

Østergaard, L., Jørgensen, M. B., and Knudsen, G. M. (2018). Low on energy? An energy supply-demand perspective on stress and depression. *Neuroscience and Biobehavioral Reviews*, 94, 248–270.

Otabi, H., Goto, T., Okayama, T., Kohari, D., and Toyoda, A. (2017). The acute social defeat stress and nest-building test paradigm: A potential new method to screen drugs for depressive-like symptoms. *Behavioural Processes*, 135, 71–75.

Otte, C., Gold, S. M., Penninx, B. W., Pariante, C. M., Etkin, A., Fava, M., Mohr, D. C., and Schatzberg, A. F. (2016). Major depressive disorder. *Nature Reviews Disease Primers*, 2, 16065.

Ouellet, V., Labbé, S. M., Blondin, D. P., Phoenix, S., Guérin, B., Haman, F., Turcotte, E. E., Richard, D., and Carpentier, A. C. (2012). Brown adipose tissue oxidative metabolism contributes to energy expenditure during acute cold exposure in humans. *The Journal of Clinical Investigation*, 122(2), 545–552.

Oury, F., and Karsenty, G. (2011). Towards a serotonin-dependent leptin roadmap in the brain. *Trends in Endocrinology and Metabolism*, 22(9), 382–387.

Palanza, P., Brain, P. F., and Parmigiani, S. (1993). Intraspecific Aggression in Mice (Mus Domesticus): Male and Female Strategies. In M. Haug, R. E. Whalen, C. Aron, and K. L. Olsen (Eds.), *The Development of Sex Differences and Similarities in Behavior* (pp. 191–203). Dordrecht: Springer Netherlands.

Palanza, P., Gioiosa, L., and Parmigiani, S. (2001). Social stress in mice: gender differences and effects of estrous cycle and social dominance. *Physiology and Behavior*, 73(3), 411–420.

Pan, L. H., and Gilbert, F. (1993). Identification of different mechanisms of action for increases of food intake and plasma ACTH concentration following 5-HT1a receptor subtype activation in rat brain. *Psychoneuroendocrinology*, 18(2), 123–

130.

Pandey, D. K., Mahesh, R., Kumar, A. A., Rao, V. S., Arjun, M., and Rajkumar, R. (2010). A novel 5-HT2A receptor antagonist exhibits antidepressant-like effects in a battery of rodent behavioural assays: Approaching early-onset antidepressants. *Pharmacology Biochemistry and Behavior*, 94(3), 363–373.

Park, A. T., Leonard, J. A., Saxler, P. K., Cyr, A. B., Gabrieli, J. D. E., and Mackey, A. P. (2018). Amygdala-medial prefrontal cortex connectivity relates to stress and mental health in early childhood. *Social Cognitive and Affective Neuroscience*, 13(4), 430–439.

Parkinson, J. A., Olmstead, M. C., Burns, L. H., Robbins, T. W., and Everitt, B. J. (1999). Dissociation in effects of lesions of the nucleus accumbens core and shell on appetitive pavlovian approach behavior and the potentiation of conditioned reinforcement and locomotor activity by D-amphetamine. *The Journal of Neuroscience : The Official Journal of the Society for Neuroscience*, 19(6), 2401–2411.

Parsey, R. V., Hastings, R. S., Oquendo, M. A., Huang, Y. Y., Simpson, N., Arcement, J., … Mann, J. J. (2006). Lower serotonin transporter binding potential in the human brain during major depressive episodes. *American Journal of Psychiatry*, 163(1), 52–58.

Patchev, V. K., and Patchev, A. V. (2006). Experimental models of stress. *Dialogues in Clinical Neuroscience*, 8(4), 417–432.

Patterson, M., Bloom, S. R., and Gardiner, J. V. (2011). Ghrelin and appetite control in humans - Potential application in the treatment of obesity. *Peptides*, 32(11), 2290–2294.

Patterson, M., Murphy, K. G., Le Roux, C. W., Ghatei, M. A., and Bloom, S. R. (2005). Characterization of ghrelin-like immunoreactivity in human plasma. *Journal of Clinical Endocrinology and Metabolism*, 90(4), 2205–2211.

Patterson, Z. R., Ducharme, R., Anisman, H., and Abizaid, A. (2010). Altered metabolic and neurochemical responses to chronic unpredictable stressors in ghrelin receptor-deficient mice. *European Journal of Neuroscience*, 32(4), 632–639.

Patterson, Z. R., Khazall, R., MacKay, H., Anisman, H., and Abizaid, A. (2013). Central ghrelin signaling mediates the metabolic response of C57BL/6 male mice to chronic social defeat stress. *Endocrinology*, 154(3), 1080–1091.

Paxinos, G., and Franklin, K. B. J. (2004). *The mouse brain in stereotaxic coordinates*. *Academic Press* (Vol. 2nd).

Paz-Filho, G., Mastronardi, C., Wong, M.-L., and Licinio, J. (2012). Leptin therapy, insulin sensitivity, and glucose homeostasis. *Indian Journal of Endocrinology*

and Metabolism, 16(Suppl 3), S549-555.

Pellerin, L., Bouzier-Sore, A. K., Aubert, A., Serres, S., Merle, M., Costalat, R., and Magistretti, P. J. (2007). Activity-dependent regulation of energy metabolism by astrocytes: An update. *GLIA*, 55(12), 1251–1262.

Perelló, M., Chacon, F., Cardinali, D. P., Esquifino, A. I., and Spinedi, E. (2006). Effect of social isolation on 24-h pattern of stress hormones and leptin in rats. *Life Sciences*, 78(16), 1857–1862.

Perelló, M., and Zigman, J. M. (2012). The role of ghrelin in reward-based eating. *Biological Psychiatry*, 72(5), 347–353.

Peters, A. (2011). The selfish brain: Competition for energy resources. *American Journal of Human Biology*, 28(2), 143–180.

Peters, A., Kubera, B., Hubold, C., and Langemann, D. (2011). The selfish brain: Stress and eating behavior. *Frontiers in Neuroscience*, 5, 74.

Petrunich-Rutherford, M. L., Garcia, F., and Battaglia, G. (2018). 5-HT1A receptor-mediated activation of neuroendocrine responses and multiple protein kinase pathways in the peripubertal rat hypothalamus. *Neuropharmacology*, 139, 173–181.

Pickup, J. C. (2004). Inflammation and Activated Innate Immunity in the Pathogenesis of Type 2 Diabletes. *Diabetes Care*, 27(3), 813–823.

Plum, L., Belgardt, B. F., and Brüning, J. C. (2006). Central insulin action in energy and glucose homeostasis. *Journal of Clinical Investigation*, 116(7), 1761–1766.

Plum L, Schubert M, and Brüning JC. (2005). The role of insulin receptor signaling in the brain. *Trends in Endocrinology and Metabolism*, 16(2), 59–65.

Polter, A. M., and Li, X. (2010). 5-HT1A receptor-regulated signal transduction pathways in brain. *Cellular Signalling*, 22(10), 1406–1412.

Porter, C., Herndon, D. N., Chondronikola, M., Chao, T., Annamalai, P., Bhattarai, N., Saraf, M. K., Capek, K. D., Reidy, P. T., Daquinag, A. C., Kolonin, M. G., Rasmussen, B. B., Borsheim, E., Toliver-Kinsky, T., and Sidossis, L. S. (2016). Human and Mouse Brown Adipose Tissue Mitochondria Have Comparable UCP1 Function. *Cell Metabolism*, 24(2), 246–255.

Pöykkö, S. M., Kellokoski, E., Hörkkö, S., Kauma, H., Kesäniemi, Y. A., and Ukkola, O. (2003). Low plasma ghrelin is associated with insulin resistance, hypertension, and the prevalence of type 2 diabetes. *Diabetes*, 52(10), 2546–2553.

Prado-Lima, P. S., Cruz, I. B. M., Schwanke, C. H. A., Netto, C. A., and Licinio, J. (2006). Human food preferences are associated with a 5-HT2Aserotonergic receptor polymorphism. *Molecular Psychiatry*, 11(10), 889–891.

Pryce, C. R., Azzinnari, D., Sigrist, H., Seifritz, E., Fuertig, R., Ceci, A., and Hengerer, B. (2014). EPA-1343 – Chronic psychosocial stress in mice causes neuro-immune-monoamine changes in brain and depression-relevant behaviour that is reversible by anti-inflammatory treatment. *European Psychiatry*, 29(Suppl 1), 1.

Pryce, C. R., and Fuchs, E. (2017). Chronic psychosocial stressors in adulthood: Studies in mice, rats and tree shrews. *Neurobiology of Stress*, 6, 94–103.

Pryce, C. R., and Seifritz, E. (2011). A translational research framework for enhanced validity of mouse models of psychopathological states in depression. *Psychoneuroendocrinology*, 36(3), 308–329.

Qi, L., and Cho, Y. A. (2008). Gene-environment interaction and obesity. *Nutrition Reviews*, 66(12), 684–694.

Quesseveur, G., Repérant, C., David, D. J., Gardier, A. M., Sanchez, C., and Guiard, B. P. (2013). 5-HT2A receptor inactivation potentiates the acute antidepressant-like activity of escitalopram: Involvement of the noradrenergic system. *Experimental Brain Research*, 226(2), 285–295.

Rabasa, C., and Dickson, S. L. (2016). Impact of stress on metabolism and energy balance. *Current Opinion in Behavioral Sciences*, 9, 71–77.

Rabasa, C., Muñoz-Abellán, C., Daviu, N., Nadal, R., and Armario, A. (2011). Repeated exposure to immobilization or two different footshock intensities reveals differential adaptation of the hypothalamic-pituitary-adrenal axis. *Physiology and Behavior*, 103(2), 125–133.

Rainer, Q., Xia, L., Guilloux, J. P., Gabriel, C., Mocaër, E., Hen, R., Enhamre, E., Gardier, A. M., and David, D. J. (2012). Beneficial behavioural and neurogenic effects of agomelatine in a model of depression/anxiety. *International Journal of Neuropsychopharmacology*, 15(3), 321–335.

Raison, C. L., Capuron, L., and Miller, A. H. (2006). Cytokines sing the blues: Inflammation and the pathogenesis of depression. *Trends in Immunology*, 27(1), 24–31.

Ramage, L. E., Akyol, M., Fletcher, A. M., Forsythe, J., Nixon, M., Carter, R. N., van Beek, E. J.R., Morton, N. M., Walker, B. R., and Stimson, R. H. (2016). Glucocorticoids Acutely Increase Brown Adipose Tissue Activity in Humans, Revealing Species-Specific Differences in UCP-1 Regulation. *Cell Metabolism*, 24(1), 130–141.

Raspopow, K., Abizaid, A., Matheson, K., and Anisman, H. (2014). Anticipation of a psychosocial stressor differentially influences ghrelin, cortisol and food intake among emotional and non-emotional eaters. *Appetite*, 74, 35–43.

Razzoli, M., Andreoli, M., Maraia, G., Di Francesco, C., and Arban, R. (2010). Functional role of Calcium-stimulated adenylyl cyclase 8 in adaptations to

psychological stressors in the mouse: Implications for mood disorders. *Neuroscience*, 170(2), 429–440.

Razzoli, M., and Bartolomucci, A. (2016). The Dichotomous Effect of Chronic Stress on Obesity. *Trends in Endocrinology and Metabolism*, 27(7), 504–515.

Razzoli, M., Bartolomucci, A., and Carola, V. (2014). *Gene-by-Environment Mouse Models for Mood Disorders*. (T. Canli, Ed.), *The Oxford Handbook of Molecular Psychology* (Vol. 1). United Stated of America: Oxford University Press.

Razzoli, M., Carboni, L., Andreoli, M., Ballottari, A., and Arban, R. (2011b). Different susceptibility to social defeat stress of BalbC and C57BL6/J mice. *Behavioural Brain Research*, 2016(1), 100–108.

Razzoli, M., Carboni, L., Andreoli, M., Michielin, F., Ballottari, A., and Arban, R. (2011c). Strain-specific outcomes of repeated social defeat and chronic fluoxetine treatment in the mouse. *Pharmacology Biochemistry and Behavior*, 97(3), 566–576.

Razzoli, M., Carboni, L., and Arban, R. (2009). Alterations of behavioral and endocrinological reactivity induced by 3 brief social defeats in rats: Relevance to human psychopathology. *Psychoneuroendocrinology*, 34(9), 1405–1416.

Razzoli, M., Carboni, L., Guidi, A., Gerrard, P., and Arban, R. (2007). Social defeat-induced contextual conditioning differentially imprints behavioral and adrenal reactivity: A time-course study in the rat. *Physiology and Behavior*, 92(4), 734–740.

Razzoli, M., Domenici, E., Carboni, L., Rantamaki, T., Lindholm, J., Castrén, E., and Arban, R. (2011a). A role for BDNF/TrkB signaling in behavioral and physiological consequences of social defeat stress. *Genes, Brain and Behavior*, 10(4), 424–433.

Razzoli, M., Frontini, A., Gurney, A., Mondini, E., Cubuk, C., Katz, L. S., Cero, C., Bolan, P. J., Dopazo, J., Vidal-Puig, A., Cinti, S., and Bartolomucci, A. (2016). Stress-induced activation of brown adipose tissue prevents obesity in conditions of low adaptive thermogenesis. *Molecular Metabolism*, 5(1), 19–33.

Reber, S. O., Birkeneder, L., Veenema, A. H., Obermeier, F., Falk, W., Straub, R. H., and Neumann, I. D. (2007). Adrenal insufficiency and colonic inflammation after a novel chronic psycho-social stress paradigm in mice: Implications and mechanisms. *Endocrinology*, 148(2), 670–682.

Reimer, M. K., Pacini, G., and Ahrén, B. (2003). Dose-dependent inhibition by ghrelin of insulin secretion in the mouse. *Endocrinology*, 144(3), 916–921.

Riad, M., Garcia, S., Watkins, K. C., Jodoin, N., Doucet, É., Langlois, X., El Mestikawy, S., Hamon, M., and Descarries, L. (2000). Somatodendritic localization of 5-HT1A and preterminal axonal localization of 5-HT1B serotonin

receptors in adult rat brain. *Journal of Comparative Neurology*, 417(2), 181–194.

Ricca, V., Nacmias, B., Cellini, E., Di Bernardo, M., Rotella, C. M., and Sorbi, S. (2002). 5-HT2A receptor gene polymorphism and eating disorders. *Neuroscience Letters*, 323(2), 105–108.

Richardson-Jones, J. W., Craige, C. P., Guiard, B. P., Stephen, A., Metzger, K. L., Kung, H. F., Gardier, A. M., Dranovsky, A., David, D. J., Beck, S. G., Hen, R., and Leonardo, E. D. (2010). 5-HT1A Autoreceptor Levels Determine Vulnerability to Stress and Response to Antidepressants. *Neuron*, 65(1), 40–52.

Richter, E. A., and Hargreaves, M. (2013). Exercise, GLUT4, and Skeletal Muscle Glucose Uptake. *Physiological Reviews*.

Riediger, T., Traebert, M., Schmid, H. A., Scheel, C., Lutz, T. A., and Scharrer, E. (2003). Site-specific effects of ghrelin on the neuronal activity in the hypothalamic arcuate nucleus. *Neuroscience Letters*, 341(2), 151–155.

Riga, D., Theijs, J. T., De Vries, T. J., Smit, A. B., and Spijker, S. (2015). Social defeat-induced anhedonia: effects on operant sucrose-seeking behavior. *Frontiers in Behavioural Neuroscience*, 9, 195.

Risch, N., Herrell, R., Lehner, T., Liang, K. Y., Eaves, L., Hoh, J., … Merikangas, K. R. (2009). Interaction between the serotonin transporter gene (5-HTTLPR), stressful life events, and risk of depression: A meta-analysis. *JAMA - Journal of the American Medical Association*, 301(23), 2462–2471.

Rodríguez, E. M., Blázquez, J. L., and Guerra, M. (2010). The design of barriers in the hypothalamus allows the median eminence and the arcuate nucleus to enjoy private milieus: The former opens to the portal blood and the latter to the cerebrospinal fluid. *Peptides*, 31(4), 757–776.

Rogers, P., McKibbin, P. E., and Williams, G. (1991). Acute fenfluramine administration reduces neuropeptide Y concentrations in specific hypothalamic regions of the rat: Possible implications for the anorectic effect of fenfluramine. *Peptides*, 12(2), 251–255.

Rogers, R. C., and Hermann, G. E. (1985). Gastric-vagal solitary neurons excited by paraventricular nucleus microstimulation. *Journal of the Autonomic Nervous System*, 14(4), 351–362.

Romieu, I., Dossus, L., Barquera, S., Blottière, H. M., Franks, P. W., Gunter, M., Hwalla, N., Hursting, S. D., Leitzmann, M., Margetts, B., Nishida, C., Potischman, N., Seidell, J., Stepien, M., Wang, Y., Westerterp, K., Winichagoon, P., Wiseman, M., and Willett, W. C. (2017). Energy balance and obesity: what are the main drivers? *Cancer Causes and Control*, 28(3), 247–258.

Rosenblatt, S., Chanley, J. D., Sobotka, H., and Kaufman, M. R. (1960). Interrelationships between electroshock, the blood-brain barrier, and

catecholamines. *Journal of Neurochemistry*, 5, 172–176.

Rossi, M. A., and Stuber, G. D. (2017). Overlapping Brain Circuits for Homeostatic and Hedonic Feeding. *Cell Metabolism*, 27(1), 42–56.

Roth, A., Kyzar, E. J., Cachat, J., Stewart, A. M., Green, J., Gaikwad, S., O'Leary, T. P., Tabakoff, B., Brown, R. E., and Kalueff, A. V. (2013). Potential translational targets revealed by linking mouse grooming behavioral phenotypes to gene expression using public databases. *Progress in Neuro-Psychopharmacology and Biological Psychiatry*, 40, 312–325.

Rouach, V., Bloch, M., Rosenberg, N., Gilad, S., Limor, R., Stern, N., and Greenman, Y. (2007). The acute ghrelin response to a psychological stress challenge does not predict the post-stress urge to eat. *Psychoneuroendocrinology*, 32(6), 693–702.

Rubin, R. R., Ma, Y., Peyrot, M., Marrero, D. G., Price, D. W., Barrett-Connor, E., and Knowler, W. C. (2010). Antidepressant medicine use and risk of developing diabetes during the diabetes prevention program and diabetes prevention program outcomes study. *Diabetes Care*, 33(12), 2549–2551.

Rygula, R., Abumaria, N., Domenici, E., Hiemke, C., and Fuchs, E. (2006). Effects of fluoxetine on behavioral deficits evoked by chronic social stress in rats. *Behavioural Brain Research*, 174(1), 188–192.

Rygula, R., Abumaria, N., Flügge, G., Hiemke, C., Fuchs, E., Rüther, E., and Havemann-Reinecke, U. (2006). Citalopram counteracts depressive-like symptoms evoked by chronic social stress in rats. *Behavioural Pharmacology*, 17(1), 19–29.

Saad, M. F., Bernaba, B., Hwu, C. M., Jinagouda, S., Fahmi, S., Kogosov, E., and Boyadjian, R. (2002). Insulin regulates plasma ghrelin concentration. *Journal of Clinical Endocrinology and Metabolism*, 87(8), 3997–4000.

Saadat, N., IglayReger, H. B., Myers, M. G., Bodary, P., and Gupta, S. V. (2012). Differences in metabolomic profiles of male db/db and s/s, leptin receptor mutant mice. *Physiological Genomics*, 44(6), 374–381.

Sachs, B. D., Ni, J. R., and Caron, M. G. (2015). Brain 5-HT deficiency increases stress vulnerability and impairs antidepressant responses following psychosocial stress. *Proceedings of the National Academy of Sciences*, 112(8), 2557–2562.

Sacks, H., and Symonds, M. E. (2013). Anatomical Locations of Human Brown Adipose Tissue. *Diabetes*, 62(6), 1783–1790.

Saito, M. (2013). Brown adipose tissue as a regulator of energy expenditure and body fat in humans. *Diabetes and Metabolism Journal*.

Salamone, J. D., and Correa, M. (2012). The Mysterious Motivational Functions of

Mesolimbic Dopamine. *Neuron*, 76(3), 470–485.

Salamone, J. D., Steinpreis, R., McCullough, L., Smith, P., Grebel, D., and Mahan, K. (1991). Haloperidol and nucleus accumbens dopamine depletion suppresses lever pressing for food but increase free food consumption in a novel food-choice procedure. *Psychopharmacology*, 104(4), 515–521.

Sanders, A. C., Hussain, A. J., Hen, R., and Zhuang, X. (2007). Chronic blockade or constitutive deletion of the serotonin transporter reduces operant responding for food reward. *Neuropsychopharmacology*, 32(11), 2321–2329.

Sanghez, V., Razzoli, M., Carobbio, S., Campbell, M., McCallum, J., Cero, C., Ceresini, G., Cabassi, A., Govoni, P., Franceschini, P., de Santis, V., Gurney, A., Ninkovic, I., Parmigiani, S., Palanza, P., Vidal-Puig, A., and Bartolomucci, A. (2013). Psychosocial stress induces hyperphagia and exacerbates diet-induced insulin resistance and the manifestations of the Metabolic Syndrome. *Psychoneuroendocrinology*, 38(12), 2933–2942.

Sapolsky, R. M. (2015). Stress and the brain: Individual variability and the inverted-U. *Nature Neuroscience*, 18(10), 1344–1346.

Sapolsky, R. M., Romero, L. M., and Munck, A. U. (2000). How do glucocorticoids influence stress responses? Integrating permissive, suppressive, stimulatory, and preparative actions. *Endocrine Reviews*, 21(1), 55–89.

Sargent, P. A., Husted Kjaer, K., Bench, C. J., Rabiner, E. A., Messa, C., Meyer, J., Gunn, R. N., Grasby, P. M., and Cowen, P. J. (2000). Brain serotonin(1A) receptor binding measured by positron emission tomography with [11C]WAY-100635: Effects of depression and antidepressant treatment. *Archives of General Psychiatry*, 52(2), 174–80.

Savignac, H. M., Finger, B. C., Pizzo, R. C., O'Leary, O. F., Dinan, T. G., and Cryan, J. F. (2011). Increased sensitivity to the effects of chronic social defeat stress in an innately anxious mouse strain. *Neuroscience*, 192, 524–536.

Sawchenko, P. E., Li, H.-Y., and Ericsson, A. (2000). Circuits and mechanisms governing hypothalamic responses to stress: a tale of two paradigms. *Progress in Brain Research*, 122(2000), 61–78.

Schaeffer, M., Langlet, F., Lafont, C., Molino, F., Hodson, D. J., Roux, T., Lamarque, L., Verdié, P., Bourrier, E., Dehouck, B., Banères, J.-L., Martinez, J., Méry, P-F., Marie, J., Trinquet, E., Fehrentz, J.-A., Prévot, V., and Mollard, P. (2013). Rapid sensing of circulating ghrelin by hypothalamic appetite-modifying neurons. *Proceedings of the National Academy of Sciences of the United States of America*, 110(4), 1512–1517.

Scherer, T., OHare, J., Diggs-Andrews, K., Schweiger, M., Cheng, B., Lindtner, C., Zielinski, E., Vempati, P., Su, K., Dighe, S., Milsom, T., Puchowicz, M., Scheja, L., Zechner, R., Fisher, S. J., Previs, S. F., and Buettner, C. (2011). Brain insulin

controls adipose tissue lipolysis and lipogenesis. *Cell Metabolism*, 13(2), 183–194.

Schildkraut, J. J. (1965). The catecholamine hypothesis of affective disorders: a review of supporting evidence. *The American Journal of Psychiatry*, 122(5), 509–522.

Schipper, L., Harvey, L., van der Beek, E. M., and van Dijk, G. (2018). Home alone: a systematic review and meta-analysis on the effects of individual housing on body weight, food intake and visceral fat mass in rodents. *Obesity Reviews*, 19(5), 614–637.

Schmid, C. L., Raehal, K. M., and Bohn, L. M. (2008). Agonist-directed signaling of the serotonin 2A receptor depends on beta-arrestin-2 interactions in vivo. *Proceedings of the National Academy of Sciences of the United States of America*, 105(3), 1079–1084.

Schneiderman, N., Ironson, G., and Siegel, S. D. (2008). STRESS AND HEALTH: Psychological, Behavioral, and Biological Determinants. *Annual Review of Clinical Psychology*, 1, 607–628.

Schoffelen, P. F. M., and Plasqui, G. (2018). Classical experiments in whole-body metabolism: open-circuit respirometry—diluted flow chamber, hood, or facemask systems. *European Journal of Applied Physiology*, 118(1), 33–49.

Schwartz, M. W., Seeley, R. J., Campfield, L. A., Burn, P., and Baskin, D. G. (1996). Identification of targets of leptin action in rat hypothalamus. *Journal of Clinical Investigation*, 98(5), 1101–1106.

Scotney, H., Symonds, M. E., Law, J., Budge, H., Sharkey, D., and Manolopoulos, K. N. (2017). Glucocorticoids modulate human brown adipose tissue thermogenesis in vivo. *Metabolism: Clinical and Experimental*, 70, 125–132.

Scott, K. (2012). Effects of Chronic Social Stress on Obesity. *Current Obesity Reports*, 1(1), 16–25.

Scott, M. M., Lachey, J. L., Sternson, S. M., Lee, C. E., Elias, C. F., Friedman, J. M., and Elmquist, J. K. (2009). Leptin targets in the mouse brain. *Journal of Comparative Neurology*, 514(5), 518–532.

Segerstrom, S. C., and Miller, G. E. (2004). Psychological stress and the human immune system: A meta-analytic study of 30 years of inquiry. *Psychological Bulletin*, 130(4), 601–630.

Selye, H. (1936). A syndrome produced by diverse nocuous agents. *Nature*, 138, 32.

Selye, H. (1976). *Stress without Distress*. *Psychopathology of Human Adaptation*.

Serrats, J., Mengod, G., and Cortés, R. (2005). Expression of serotonin 5-HT2C receptors in GABAergic cells of the anterior raphe nuclei. *Journal of Chemical*

Neuroanatomy, 29(2), 83–91.

Shah, M., and Vella, A. (2014). Effects of GLP-1 on appetite and weight. *Reviews in Endocrine and Metabolic Disorders*, 15(3), 181–187.

Shimizu, H., Arima, H., Ozawa, Y., Watanabe, M., Banno, R., Sugimura, Y., Ozaki, N., Nagasaki, H., and Oiso, Y. (2010). Glucocorticoids increase NPY gene expression in the arcuate nucleus by inhibiting mTOR signaling in rat hypothalamic organotypic cultures. *Peptides*, 31(1), 145–149.

Shimizu, H., Arima, H., Watanabe, M., Goto, M., Banno, R., Sato, I., Ozaki, N., Nagasaki, H., and Oiso, Y. (2008). Glucocorticoids increase neuropeptide Y and agouti-related peptide gene expression via adenosine monophosphate-activated protein kinase signaling in the arcuate nucleus of rats. *Endocrinology*, 149(9), 4544–4553.

Skibicka, K. P., and Grill, H. J. (2009). Hypothalamic and hindbrain melanocortin receptors contribute to the feeding, thermogenic, and cardiovascular action of melanocortins. *Endocrinology*, 150(12), 5351–5361.

Small, D. M., Jones-Gotman, M., and Dagher, A. (2003). Feeding-induced dopamine release in dorsal striatum correlates with meal pleasantness ratings in healthy human volunteers. *NeuroImage*, 19(4), 1709–1715.

Smith, K. A., Fairburn, C. G., and Cowen, P. J. (1997). Relapse of depression after vapid depletion of tryptophan. *Lancet*, 349(9056), 915–919.

Sneddon, L. U., Halsey, L. G., and Bury, N. R. (2017). Considering aspects of the 3Rs principles within experimental animal biology. *Journal of Experimental Biology*, 220(17), 3007–3016.

Snyder, J. S., Soumier, A., Brewer, M., Pickel, J., and Cameron, H. A. (2011). Adult hippocampal neurogenesis buffers stress responses and depressive behaviour. *Nature*, 476(7361), 458–461.

Solati, J., Salari, A. A., and Bakhtiari, A. (2011). 5HT(1A) and 5HT(1B) receptors of medial prefrontal cortex modulate anxiogenic-like behaviors in rats. *Neuroscience Letters*, 504(3), 325–329.

Sotty, F., Folgering, J. H. A., Brennum, L. T., Hogg, S., Mørk, A., Hertel, P., and Cremers, T. I. F. H. (2009). Relevance of dorsal raphe nucleus firing in serotonin 5-HT2C receptor blockade-induced augmentation of SSRIs effects. *Neuropharmacology*, 57(1), 18–24.

Speakman, J. R. (2013). Measuring energy metabolism in the mouse - theoretical, practical, and analytical considerations. *Frontiers in Physiology*, 4, 34.

Spencer, S. J., Xu, L., Clarke, M. A., Lemus, M., Reichenbach, A., Geenen, B., Kozicz, T., and Andrews, Z. B. (2012). Ghrelin regulates the hypothalamic-pituitary-

adrenal axis and restricts anxiety after acute stress. *Biological Psychiatry*, 72(6), 457–465.

Spoida, K., Masseck, O. A., Deneris, E. S., and Herlitze, S. (2014). Gq/5-HT2c receptor signals activate a local GABAergic inhibitory feedback circuit to modulate serotonergic firing and anxiety in mice. *Proceedings of the National Academy of Sciences*, 111(17), 6479–6484.

Stechman, M. J., Ahmad, B. N., Loh, N. Y., Reed, A. A. C., Stewart, M., Wells, S., Hough, T., Bentley, L., Cox, R. D., Brown, S. D.M., and Thakker, R. V. (2010). Establishing normal plasma and 24-hour urinary biochemistry ranges in C3H, BALB/c and C57BL/6J mice following acclimatization in metabolic cages. *Laboratory Animals*, 44(3), 218–225.

Sternson, S. M., Shepherd, G. M. G., and Friedman, J. M. (2005). Topographic mapping of VMH → arcuate nucleus microcircuits and their reorganization by fasting. *Nature Neuroscience*, 8(10), 1356–1363.

Stockmeier, C. A., Shapiro, L. A., Dilley, G. E., Kolli, T. N., Friedman, L., and Rajkowska, G. (1998). Increase in serotonin-1A autoreceptors in the midbrain of suicide victims with major depression-postmortem evidence for decreased serotonin activity. *The Journal of Neuroscience*, 18(18), 7394–7401.

Strack, A. M., Bradbury, M. J., and Dallman, M. F. (1995). Corticosterone decreases nonshivering thermogenesis and increases lipid storage in brown adipose tissue. *American Journal of Physiology-Regulatory, Integrative and Comparative Physiology*, 268(1), R183-191.

Sun, Y., Wang, P., Zheng, H., and Smith, R. G. (2004). Ghrelin stimulation of growth hormone release and appetite is mediated through the growth hormone secretagogue receptor. *Proceedings of the National Academy of Sciences of the United States of America*, 101(13), 4679–4684.

Sutton, R. E., Koob, G. F., Le Moal, M., Rivier, J., and Vale, W. (1982). Corticotropin releasing factor produces behavioural activation in rats. *Nature*, 297, 331–333.

Swiss Confederation. MEXT Chapter 1 General Provisions, Ministry of Education, Culture, Sports, Science and Technology, Japan § (2011).

Szyszkowicz, J. K., Wong, A., Anisman, H., Merali, Z., and Audet, M. C. (2017). Implications of the gut microbiota in vulnerability to the social avoidance effects of chronic social defeat in male mice. *Brain, Behavior, and Immunity*, 66, 45–55.

Tamashiro, K. L. K., Nguyen, M. M. N., and Sakai, R. R. (2005). Social stress: From rodents to primates. *Frontiers in Neuroendocrinology*, 26(1), 27–40.

Tatsumi, Y., Morimoto, A., Miyamatsu, N., Noda, M., Ohno, Y., and Deura, K. (2015). Effect of body mass index on insulin secretion or sensitivity and diabetes. *American Journal of Preventive Medicine*, 48(2), 128–135.

Tecott, L. H., Sun, L. M., Akana, S. F., Strack, A. M., Lowenstein, D. H., Dallman, M. F., and Julius, D. (1995). Eating disorder and epilepsy in mice lacking 5-HT2C serotonin receptors. *Nature*, 374, 542–546.

The Jackson Laboratory. (n.d.). Mouse Genetics - The mouse as a model for human disease. Retrieved November 10, 2017, from https://www.jax.org/personalized-medicine/why-mous

Tiryakioglu, O., Ugurlu, S., Yalin, S., Yirmibescik, S., Caglar, E., Yetkin, D. O., and Kadioglu, P. (2010). Screening for Cushing's syndrome in obese patients. *Clinics (São Paulo, Brazil)*, 65(1), 9–13.

Torres, S. J., and Nowson, C. A. (2007). Relationship between stress, eating behavior, and obesity. *Nutrition*, 23(11–12), 887–894.

Toyoda, A., Iio, W., Matsukawa, N., and Tsukahara, T. (2015). Influence of chronic social defeat stress on digestive system functioning in rats. *Journal of Nutritional Science and Vitaminology*, 61(3), 280–284.

Trayhurn, P., Thomas, M. E., Duncan, J. S., and Rayner, D. V. (1995). Effects of fasting and refeeding on ob gene expression in white adipose tissue of lean and obese (oblob) mice. *FEBS Letters*, 368(3), 488–490.

Tsankova, N. M., Berton, O., Renthal, W., Kumar, A., Neve, R. L., and Nestler, E. J. (2006). Sustained hippocampal chromatin regulation in a mouse model of depression and antidepressant action. *Nature Neuroscience*, 9(4), 519–525.

Tschöp, M. H., Speakman, J. R., Arch, J. R. S., Auwerx, J., Brüning, J. C., Chan, L., Eckel, R. H., Farese, R. V., Galgani, J. E., Hambly, C., Herman, M. A., Horvath, T. L., Kahn, B.B., Kozma, S. C., Maratos-Flier, E., Müller, T. D., Münzberg, H., Pfluger, P. T., Plum, L., Reitman, M. L., Rahmouni, K., Shulman, G. I., Thomas, G., Kahn, C. R., and Ravussin, E. (2011). A guide to analysis of mouse energy metabolism. *Nature Methods*, 9(1), 57–63.

Tschop, M., Smiley, D. L., and Heiman, M. L. (2000). Ghrelin induces adiposity in rodents. *Nature*, 407(6806), 908–913.

Tsubone, T., Masaki, T., Katsuragi, I., Tanaka, K., Kakuma, T., and Yoshimatsu, H. (2005). Ghrelin regulates adiposity in white adipose tissue and UCP1 mRNA expression in brown adipose tissue in mice. *Regulatory Peptides*, 130(1–2), 97–103.

Tsuneki, H., Tokai, E., Sugawara, C., Wada, T., Sakurai, T., and Sasaoka, T. (2013). Hypothalamic orexin prevents hepatic insulin resistance induced by social defeat stress in mice. *Neuropeptides*, 47(3), 213–219.

Uemura, E., and Greenlee, H. W. (2006). Insulin regulates neuronal glucose uptake by promoting translocation of glucose transporter GLUT3. *Experimental Neurology*, 198(1), 48–53.

Ueta, C. B., Fernandes, G. W., Capelo, L. P., Fonseca, T. L., Maculan, F. D. A., Gouveia, C. H. A., Brum, P. C., Christoffolete, M. A., Aoki, M. S., Lancellotti, C. L., Kim, B., Bianco, A. C., Ribeiro, M. O. (2012). β1 Adrenergic receptor is key to cold-and diet-induced thermogenesis in mice. *Journal of Endocrinology*, 214(3), 359–365.

UK Home Office. (2017). *Annual Statistics of Scientific Procedures on Living Animals Great Britain 2016*.

Ulrich-Lai, Y. M., Figueiredo, H. F., Ostrander, M. M., Choi, D. C., Engeland, W. C., and Herman, J. P. (2006). Chronic stress induces adrenal hyperplasia and hypertrophy in a subregion-specific manner. *AJP: Endocrinology and Metabolism*, 291(5), E965-973.

Unger, T. J., Calderon, G. A., Bradley, L. C., Sena-Esteves, M., and Rios, M. (2007). Selective Deletion of Bdnf in the Ventromedial and Dorsomedial Hypothalamus of Adult Mice Results in Hyperphagic Behavior and Obesity. *Journal of Neuroscience*, 27(52), 14265–14274.

Ussar, S., Haering, M. F., Fujisaka, S., Lutter, D., Lee, K. Y., Li, N., Gerber, G. K., Bry, L., and Ronald Kahn, C. (2017). Regulation of glucose uptake and enteroendocrine function by the intestinal epithelial insulin receptor. *Diabetes*, 66(4), 886–896.

Valentino, R. J., Lucki, I., and Van Bockstaele, E. (2010). Corticotropin-releasing factor in the dorsal raphe nucleus: Linking stress coping and addiction. *Brain Research*, 1314, 29–37.

Van de Kar, L. D., Javed, A., Zhang, Y., Serres, F., Raap, D. K., and Gray, T. S. (2001). 5-HT2A receptors stimulate ACTH, corticosterone, oxytocin, renin, and prolactin release and activate hypothalamic CRF and oxytocin-expressing cells. *The Journal of Neuroscience : The Official Journal of the Society for Neuroscience*, 21(10), 2572–3579.

Van Den Beukel, J. C., Grefhorst, A., Quarta, C., Steenbergen, J., Mastroberardino, P. G., Lombés, M., Delhanty, P. J., Mazza, R., Pagotto, U., Van Der Lely, A. J., and Themmen, A. P. N. (2014). Direct activating effects of adrenocorticotropic hormone (ACTH) on brown adipose tissue are attenuated by corticosterone. *FASEB Journal*, 28(11), 4857–4867.

Van Den Top, M., Lee, K., Whyment, A. D., Blanks, A. M., and Spanswick, D. (2004). Orexigen-sensitive NPY/AgRP pacemaker neurons in the hypothalamic arcuate nucleus. *Nature Neuroscience*, 7(5), 493–494.

Vandamme, T. F. (2014). Use of rodents as models of human diseases. *Journal of Pharmacy and Bioallied Sciences*, 6(1), 2–9.

Virtue, S., and Vidal-Puig, A. (2013). Assessment of brown adipose tissue function. *Frontiers in Physiology*, 4, 1–18.

Voigt, J. P., and Fink, H. (2015). Serotonin controlling feeding and satiety. *Behavioural Brain Research*, 277, 14–31.

Voigt, J. P., Schade, R., Fink, H., and Hörtnagl, H. (2002). Role of 5-HT1A receptors in the control of food intake in obese Zucker rats of different ages. *Pharmacology Biochemistry and Behavior*, 72(1–2), 403–409.

Volkow, N. D., Wang, G. J., and Baler, R. D. (2011). Reward, dopamine and the control of food intake: Implications for obesity. *Trends in Cognitive Sciences*, 15(1), 37–46.

Volkow, N. D., Wang, G. J., Fowler, J. S., Logan, J., Jayne, M., Franceschi, D., Wong, C., Gatley, S. J., Gifford, A. N., Ding, Y. S., and Pappas, N. (2002). "Nonhedonic" food motivation in humans involves dopamine in the dorsal striatum and methylphenidate amplifies this effect. *Synapse*, 44(3), 175–180.

Vollmayr, B., Keck, S., Henn, F. A., and Schloss, P. (2000). Acute stress decreases serotonin transporter mRNA in the raphe pontis but not in other raphe nuclei of the rat. *Neuroscience Letters*, 290(2), 109–112.

Vom Saal, S., Franks, P., Boechler, M., Palanza, P., and Parmigiani, S. (1995). Nest defense and survival of offspring in highly aggressive wild Canadian female house mice. *Physiology & Behavior*, 58(4), 669–678.

Ward, S. J., Lefever, T. W., Jackson, C., Tallarida, R. J., and Walker, E. A. (2008). Effects of a Cannabinoid1 Receptor Antagonist and Serotonin2C Receptor Agonist Alone and in Combination on Motivation for Palatable Food: A Dose-Addition Analysis Study in Mice. *Journal of Pharmacology and Experimental Therapeutics*, 325(2), 567–576.

Waterson, M. J., and Horvath, T. L. (2015). Neuronal Regulation of Energy Homeostasis: Beyond the Hypothalamus and Feeding. *Cell Metabolism*, 22(6), 962–970.

Wauson, S. E. R., Sarkodie, K., Schuette, L. M., and Currie, P. J. (2015). Midbrain raphe 5-HT1A receptor activation alters the effects of ghrelin on appetite and performance in the elevated plus maze. *Journal of Psychopharmacology*, 29(7), 836–844.

Wehrwein, E. A., Orer, H. S., and Barman, S. M. (2016). Overview of the Anatomy, Physiology, and Pharmacology of the Autonomic Nervous System. *Comprehensive Physiology*, 6(3), 1239–1278.

Wei, S., Ji, X., Wu, C., Li, Z., Sun, P., Wang, J., Zhao, Q., Gao, J., Guo, Y., Sun, S., and Qiao, M. (2014). Resident intruder paradigm-induced aggression relieves depressive-like behaviors in male rats subjected to chronic mild stress. *Medical Science Monitor*, 20, 945–952.

Westerterp, K. R. (2017). Control of energy expenditure in humans. *European Journal*

of Clinical Nutrition.

Westerterp, K. R. (2017). Doubly labelled water assessment of energy expenditure: principle, practice, and promise. *European Journal of Applied Physiology*, 117(7), 1277–1285.

Wharton, S. (2016). Current Perspectives on Long-term Obesity Pharmacotherapy. *Canadian Journal of Diabetes*, 40(2), 184–191.

WHO. (2016). *ICD-10 Version:2016*. *Who*.

Willeit, M., Praschak-Rieder, N., Neumeister, A., Pirker, W., Asenbaum, S., Vitouch, O., Tauscher, J., Hilger, E., Stastny, J., Brucke, T., and Kasper, S. (2000). [123I]-beta-CIT SPECT imaging shows reduced brain serotonin transporter availability in drug-free depressed patients with seasonal affective disorder. *Biological Psychiatry*, 47(6), 482–489.

Williams, A. R., and Dourish, C. T. (1992). Effects of the putative 5-HT1Areceptor antagonist NAN-190 on free feeding and on feeding induced by the 5-HT1Areceptor agonist 8-OH-DPAT in the rat. *European Journal of Pharmacology*, 219(1), 105–112.

Willner, P. (1984). The validity of animal models of depression. *Psychopharmacology*, 83(1), 1–16.

Willner, P. (2017). The chronic mild stress (CMS) model of depression: History, evaluation and usage. *Neurobiology of Stress*, 6, 78–93.

Wong, D. T., Perry, K. W., and Bymaster, F. P. (2005). Case history: The discovery of fluoxetine hydrochloride (Prozac). *Nature Reviews Drug Discovery*, 4(9), 764–774.

Wood, M. W., and Hart, L. A. (2007). Selecting appropriate animal models and strains: Making the best use of research, information and outreach. *Aatex*, 14(Special Issue), 303–306.

Wood, S. K., and Bhatnagar, S. (2014). Resilience to the effects of social stress: Evidence from clinical and preclinical studies on the role of coping strategies. *Neurobiology of Stress*, 1, 164–173.

Woods, S. (2003). Gastrointestinal Satiety Signals I. An overview of gastrointestinal signals that influence food intake. *AJP: Gastrointestinal and Liver Physiology*, 286(1), G7-13.

Woods, S. C., and Seeley, R. J. (2000). Adiposity signals and the control of energy homeostasis. *Nutrition*, 16(10), 894–902.

World Health Organization. (2017). *Depression and other common mental disorders: global health estimates*. *World Health Organization*. https://doi.org/CC BY-NC-

SA 3.0 IGO

Xu, B., Goulding, E. H., Zang, K., Cepoi, D., Cone, R. D., Jones, K. R., Tecott, L. H., and Reichardt, L. F. (2003). Brain-derived neurotrophic factor regulates energy balance downstream of melanocortin-4 receptor. *Nature Neuroscience*, 6, 736–742.

Xu, X., Wei, Y., Guo, Q., Zhao, S., Liu, Z., Xiao, T., Liu, Y., Qiu, Y., Hou, Y., Zhang, G., and Wang, K. (2018). Pharmacological Characterization of H05, a Novel Serotonin and Noradrenaline Reuptake Inhibitor with Moderate 5-HT2A Antagonist Activity for the Treatment of Depression. *Journal of Pharmacology and Experimental Therapeutics*, 365(3), 624–635.

Yager, L. M., Garcia, A. F., Wunsch, A. M., and Ferguson, S. M. (2015). The ins and outs of the striatum: Role in drug addiction. *Neuroscience*, 301, 529–541.

Yamada, C., Saegusa, Y., Nahata, M., Sadakane, C., Hattori, T., and Takeda, H. (2015). Influence of aging and gender differences on feeding behavior and ghrelin-related factors during social isolation in mice. *PLoS ONE*, 10(10).

Yamaoka, K., and Tango, T. (2012). Effects of lifestyle modification on metabolic syndrome: A systematic review and meta-analysis. *BMC Medicine*, 10(138).

Yamashita, P. S. D. M., De Bortoli, V. C., and Zangrossi, H. (2011). 5-HT2C receptor regulation of defensive responses in the rat dorsal periaqueductal gray. *Neuropharmacology*, 60(2–3), 216–222.

Yang, C., Fujita, Y., Ren, Q., Ma, M., Dong, C., and Hashimoto, K. (2017). Bifidobacterium in the gut microbiota confer resilience to chronic social defeat stress in mice. *Scientific Reports*.

Yarandi, S. S., Peterson, D. A., Treisman, G. J., Moran, T. H., and Pasricha, P. J. (2016). Modulatory effects of gut microbiota on the central nervous system: How gut could play a role in neuropsychiatric health and diseases. *Journal of Neurogastroenterology and Motility*, 22(2), 201–212.

Yasuda, T., Masaki, T., Kakuma, T., and Yoshimatsu, H. (2003). Centrally administered ghrelin suppresses sympathetic nerve activity in brown adipose tissue of rats. *Neuroscience Letters*, 349(2), 75–78.

Ye, J. (2013). Mechanisms of insulin resistance in obesity. *Frontiers of Medicine*, 7(1), 14–24.

Yeo, G. S. H., and Heisler, L. K. (2012). Unraveling the brain regulation of appetite: Lessons from genetics. *Nature Neuroscience*, 15(10), 1343–1349.

Yohn, C. N., Gergues, M. M., and Samuels, B. A. (2017). The role of 5-HT receptors in depression Tim Bliss. *Molecular Brain*, 10(1).

Young, P., Arch, J. R. S., and Ashwell, M. (1984). Brown adipose tissue in the parametrial fat pad of the mouse. *FEBS Letters*, 167(1), 10–14.

Yousufzai, M. I. U. A., Harmatz, E. S., Shah, M., Malik, M. O., and Goosens, K. A. (2018). Ghrelin is a persistent biomarker for chronic stress exposure in adolescent rats and humans. *Translational Psychiatry*, 8.

Yu, Y. H., Vasselli, J. R., Zhang, Y., Mechanick, J. I., Korner, J., and Peterli, R. (2015). Metabolic vs. hedonic obesity: A conceptual distinction and its clinical implications. *Obesity Reviews*, 16(3), 234–247.

Zellner, D., Loaiza, S., Gonzalez, Z., Pita, J., Morales, J., Pecora, D., and Wolf, A. (2006). Food selection changes under stress. *Physiology & Behavior*, 87(4), 789–793.

Zhang, H., Yin, J., Li, D., Zhou, X., and Li, X. (2007). Tryptophan enhances ghrelin expression and secretion associated with increased food intake and weight gain in weanling pigs. *Domestic Animal Endocrinology*, 33(1), 47–61.

Zhang, J., Fan, Y., Li, Y., Zhu, H., Wang, L., and Zhu, M. Y. (2012). Chronic social defeat up-regulates expression of the serotonin transporter in rat dorsal raphe nucleus and projection regions in a glucocorticoid-dependent manner. *Journal of Neurochemistry*, 123(6), 1054–1068.

Zhao, Y., Zhang, Q., Shao, X., Ouyang, L., Wang, X., Zhu, K., and Chen, L. (2017). Decreased Glycogen Content Might Contribute to Chronic Stress-Induced Atrophy of Hippocampal Astrocyte volume and Depression-like Behavior in Rats. *Scientific Reports*, 7, 1–14.

Zheng, H., Patterson, L. M., Rhodes, C. J., Louis, G. W., Skibicka, K. P., Grill, H. J., Myers, M. G., and Berthoud, H.-R. (2010). A potential role for hypothalamomedullary POMC projections in leptin-induced suppression of food intake. *American Journal of Physiology-Regulatory, Integrative and Comparative Physiology*, 298(3), 720–728.

Zhou, Y., and Rui, L. (2013). Leptin signaling and leptin resistance. *Frontiers in Medicine*, 7(2), 207–222.

Zigman, J. M., Jones, J. E., Lee, C. E., Saper, C. B., and Elmquist, J. K. (2006). Expression of ghrelin receptor mRNA in the rat and the mouse brain. *The Journal of Comparative Neurology*, 494(3), 528–548.

APPENDIX 1

Animal ID and schedule of experiments

- **Animal overview - Experiment A**

Group	Cage	Ear marking	ID	Phenotype	Parents	Date of Birth
CON	S1	R	1	BL/6	BW 66	25/04/2016
CON	S1	L	2	BL/6	BW 66	25/04/2016
CON	S2	R	3	BL/6	BW 72	29/04/2016
CON	S2	L	4	BL/6	BW 72	29/04/2016
CON	S5	R	9	BL/6	BW 75	29/04/2016
CON	S5	RL	11	BL/6	BW 75	29/04/2016
CON	S7	R	14	BL/6	BW 71	02/05/2016
CON	S7	L	15	BL/6	BW 71	02/05/2016
CON	S8	R	17	BL/6	BW 71	02/05/2016
CON	S8	L	18	BL/6	BW 71	02/05/2016
CON	S10	R	21	BL/6	BW 74	02/05/2016
CON	S10	L	22	BL/6	BW 74	02/05/2016
CSS	S5	R	5	BL/6	BW 73	29/04/2016
CSS	S6	L	6	BL/6	BW 73	29/04/2016
CSS	S7	R	7	BL/6	BW 73	29/04/2016
CSS	S8	L	8	BL/6	BW 73	29/04/2016
CSS	S10	L	10	BL/6	BW 75	29/04/2016
CSS	S12	R	12	BL/6	BW 75	29/04/2016
CSS	S13	L	13	BL/6	BW 75	29/04/2016
CSS	S16	RL	16	BL/6	BW 71	02/05/2016
CSS	S19	R	19	BL/6	BW 74	02/05/2016
CSS	S20	L	20	BL/6	BW 74	02/05/2016
CSS	S23	R	23	BL/6	BW 76	02/05/2016
CSS	S24	L	24	BL/6	BW 76	02/05/2016

- **Schedule - Experiment A**

Date		Procedure	Group 1	Procedure	Group 2
11/07/2016	Weigh	Handling		Handling	
12/07/2016	Weigh	Handling		Handling	
13/07/2016	Weigh	Handling		Handling	
14/07/2016	Weigh	Handling		Handling	
15/07/2016	Weigh	Activity Test		Activity Test	
16/07/2016					
17/07/2016					
18/07/2016	Weigh	CSS1			
19/07/2016	Weigh	CSS2		CSS1	
20/07/2016	Weigh	CSS3		CSS2	
21/07/2016	Weigh	CSS4		CSS3	
22/07/2016	Weigh	CSS5		CSS4	

23/07/2016	Weigh	CSS6		CSS5	
24/07/2016	Weigh	CSS7		CSS6	
25/07/2016	Weigh	CSS8	Faeces	CSS7	
26/07/2016	Weigh	CSS9		CSS8	Faeces
27/07/2016	Weigh	CSS10		CSS9	
28/07/2016	Weigh	CSS11	Glucose Test	CSS10	
29/07/2016	Weigh	CSS12		CSS11	Glucose Test
30/07/2016	Weigh	CSS13		CSS12	
31/07/2016	Weigh	CSS14		CSS13	
01/08/2016	Weigh	CSS15		CSS14	
02/08/2016	Weigh		Faeces	CSS15	
03/08/2016			Euthanize CSS		Faeces
04/08/2016			Euthanize CON		Euthanize CSS
05/08/2016					Euthanize CON

- **Animal overview - Experiment B**

Group	**Cage**	**Ear marking**	**ID**	**Phenotype**	**Parents**	**Date of Birth**
CON	S3	R	27	BL/6	BW 73	23/05/2016
CON	S3	L	28	BL/6	BW 73	23/05/2016
CON	S5	R	31	BL/6	BW 70	23/05/2016
CON	S5	L	32	BL/6	BW 70	23/05/2016
CON	S7	R	36	BL/6	BW 75	23/05/2016
CON	S7	L	37	BL/6	BW 75	23/05/2016
CON	S8	R	38	BL/6	BW 72	28/05/2016
CON	S8	L	39	BL/6	BW 72	28/05/2016
CSS	S25	R	25	BL/6	BW 67	25/05/2016
CSS	S26	L	26	BL/6	BW 67	25/05/2016
CSS	S29	R	29	BL/6	BW 73	23/05/2016
CSS	S30	L	30	BL/6	BW 73	23/05/2016
CSS	S33	R	33	BL/6	BW 75	23/05/2016
CSS	S34	L	34	BL/6	BW 75	23/05/2016
CSS	S35	RL	35	BL/6	BW 75	23/05/2016
CSS	S40	RL	40	BL/6	BW 72	28/05/2016
CSS	S41	R	41	BL/6	BW 69	22/05/2016
CSS	S42	L	42	BL/6	BW 69	22/05/2016

- **Schedule - Experiment B**

Date		Procedure
08/08/2016	Weigh	Handling
09/08/2016	Weigh	Handling
10/08/2016	Weigh	Handling
11/08/2016	Weigh	Activity test
12/08/2016		Transfer to T'Spital
13/08/2016		Adaptation
14/08/2016		Adaptation
15/08/2016	Weigh	-
16/08/2016	Weigh	-
17/08/2016	Weigh	-
18/08/2016	Weigh	Baseline 1
19/08/2016	Weigh	Baseline 2
20/08/2016	Weigh	Baseline 3
21/08/2016	Weigh	Baseline 4
22/08/2016	Weigh	Baseline 5
23/08/2016	Weigh	CSS1
24/08/2016	Weigh	CSS2
25/08/2016	Weigh	CSS3
26/08/2016	Weigh	CSS4
27/08/2016	Weigh	CSS5
28/08/2016	Weigh	CSS6
29/08/2016	Weigh	CSS7
30/08/2016	Weigh	CSS8
31/08/2016	Weigh	CSS9
01/09/2016	Weigh	CSS10
02/09/2016	Weigh	CSS11
03/09/2016	Weigh	CSS12
04/09/2016	Weigh	CSS13
05/09/2016	Weigh	CSS14
06/09/2016	Weigh	CSS15 + Stress 1
07/09/2016	Weigh	Stress 2
08/09/2016	Weigh	Stress 3
09/09/2016	Weigh	Stress 4
10/09/2016	Weigh	Stress 5
11/09/2016	Weigh	Stress 6
12/09/2016	Weigh	Stress 7 + Euthanize
13/09/2016		Transfer cages back

- **Animal overview - Experiment C**

Group	Cage	Ear marking	ID	Phenotype	Parents	Date of Birth
CON	S1	R	1	BL/6	BW 9	04/03/2017
CON	S1	L	2	BL/6	BW 9	04/03/2017
CON	S2	R	3	BL/6	BW 89	12/03/2017
CON	S2	L	4	BL/6	BW 89	12/03/2017
CON	S6	R	11	BL/6	BW 1	15/04/2017
CON	S6	L	12	BL/6	BW 1	15/04/2017
CON	S7	R	13	BL/6	BW 7	15/04/2017
CON	S7	L	14	BL/6	BW 7	15/04/2017
CON	S8	L	15	BL/6	BW 7	15/04/2017
CON	S8	R	16	BL/6	BW 7	15/04/2017
CON	S10	R	20	BL/6	BW 13	27/04/2017
CON	S10	L	21	BL/6	BW 13	27/04/2017
CSS	S3	R	5	BL/6	BW 89	12/03/2017
CSS	S3	L	6	BL/6	BW 89	12/03/2017
CSS	S4	R	7	BL/6	BW 89	12/03/2017
CSS	S4	L	8	BL/6	BW 89	12/03/2017
CSS	S5	R	9	BL/6	BW 8	28/03/2017
CSS	S5	L	10	BL/6	BW 8	28/03/2017
CSS	S9	R	17	BL/6	BW 12	27/04/2017
CSS	S9	L	18	BL/6	BW 12	27/04/2017
CSS	S9	RL	19	BL/6	BW 12	27/04/2017
CSS	S11	R	22	BL/6	BW 6	01/05/2017
CSS	S11	L	23	BL/6	BW 6	01/05/2017
CSS	S11	RL	24	BL/6	BW 6	01/05/2017

- **Schedule - Experiment C**

Date		**Procedure Group 1**	**Procedure Group 2**
19/06/2017		Handling	Handling
20/06/2017		Handling	Handling
21/06/2017		Handling	Handling
22/06/2017		Handling	Handling
23/06/2017	Weigh	Handling	Handling
24/06/2017	Weigh		
25/06/2017	Weigh		
26/06/2017	Weigh	Activity Test	Activity Test
27/06/2017	Weigh	T'Spital	T'Spital
28/06/2017	Weigh		
29/06/2017	Weigh	Baseline 1	
30/06/2017	Weigh	Baseline 2	
01/07/2017	Weigh	Baseline 3	
02/07/2017	Weigh	Baseline 4	
03/07/2017	Weigh	Baseline 5	
04/07/2017	Weigh	Baseline 6/CSS 1	Baseline 1
05/07/2017	Weigh	CSS 2	Baseline 2
06/07/2017	Weigh	CSS 3	Baseline 3
07/07/2017	Weigh	CSS 4 + Behav	Baseline 4
08/07/2017	Weigh	CSS 5	Baseline 5
09/07/2017	Weigh	CSS 6	Baseline 6/CSS 1
10/07/2017	Weigh	CSS 7	CSS 2
11/07/2017	Weigh	CSS 8 + Behav	CSS 3
12/07/2017	Weigh	CSS 9	CSS 4 + Behav
13/07/2017	Weigh	CSS 10	CSS 5
14/07/2017	Weigh	CSS 11	CSS 6
15/07/2017	Weigh	CSS 12 + Behav	CSS 7
16/07/2017	Weigh	CSS 13	CSS 8 + Behav
17/07/2017	Weigh	CSS 14	CSS 9
18/07/2017	Weigh	CSS 15 / Stress 1	CSS 10
19/07/2017	Weigh	Stress 2	CSS 11
20/07/2017	Weigh	Stress 3	CSS 12 + Behav
21/07/2017	Weigh	Stress 4	CSS 13
22/07/2017	Weigh	Stress 5	CSS 14
23/07/2017	Weigh	Stress 6 (12:00 h)	CSS 15 / Stress 1
24/07/2017	Weigh	Euthanize	Stress 2
25/07/2017	Weigh		Stress 3
26/07/2017	Weigh		Stress 4
27/07/2017	Weigh		Stress 5
28/07/2017	Weigh		Stress 6 (12:00 h)
29/07/2017			Euthanize

- **Animal overview – Immunohistochemistry experiment**

Group	Cage	Ear marking	ID	Phenotype	Parents	Date of Birth
CON	S1	R	1	WT	Z84	16/07/2012
CON	S1	L	2	WT	Z84	16/07/2012
CON	S5	L	12	WT	Z88	25/07/2012
CON	S5	RL	13	WT	Z88	25/07/2012
CON	S6	L	15	WT	Z89	25/07/2012
CON	S6	RL	16	WT	Z89	25/07/2012
CON	S7	R	17	WT	Z98	25/07/2012
CON	S7	L	18	WT	Z98	25/07/2012
CON	S10	L	25	WT	Z99	29/07/2012
CON	S10	RL	26	WT	Z99	29/07/2012
CSS	S1	RL	3	WT	Z84	16/07/2012
CSS	S2	R	4	WT	Z87	18/07/2012
CSS	S2	L	5	WT	Z87	18/07/2012
CSS	S4	R	9	WT	Z83	25/07/2012
CSS	S4	L	10	WT	Z83	25/07/2012
CSS	S5	R	11	WT	Z88	25/07/2012
CSS	S8	R	20	WT	Z100	28/07/2012
CSS	S8	L	21	WT	Z100	28/07/2012
CSS	S9	L	23	WT	Z102	28/07/2012
CSS	S10	R	24	WT	Z99	29/07/2012

- **Brains for autoradiography**

5-HT2A	5-HT2C	5-HT1A	Bregma (mm)
mPFC & NAcc	mPFC & NAcc	mPFC & NAcc	2.00 (Fig. 14)
Amy	Amy	Amy	-1.00 (Fig. 40)
Hipp & VTA	Hipp & VTA	Hipp & VTA	-2.80 (Fig. 54)
-	-	DRN	-4.16 (Fig. 65)
LC	-	-	-5.34 (Fig. 75)

Brain	Done	Comments
CON 24	17.11.2015	Hipp and VTA missing. One slide more on 5-HT1A+ slide
CON 23	17.11.2015	x
CSS 18	18.11.2015	x
CSS 21	18.11.2015	x
CON 14	18.11.2015	Damaged on the left side (dorsal)
CSS 2	19.11.2015	x
CON 6	19.11.2015	x
CSS 1	19.11.2015	x
CSS 25	23.11.2015	x
CON 5	23.11.2015	Damaged on the left side (ventral)
CSS 16	23.11.2015	x
CON 19	25.11.2015	x
CSS 3	25.11.2015	Cracked on the dorsal side
CON 15	26.11.2015	Less well perfused
CON 10	26.11.2015	x
CSS 4	26.11.2015	Cracked on the dorsal side

APPENDIX 2

Reagents and solutions

- **Chapter 3/4/5 – Reverse transcription**

Master Mix
4.2µL RNase-free water + 2µl Buffer + 2µl Random primers + 0.8µl dNTPs + 1µl enzyme

- **Chapter 3/4/5 - qPCR**

SYBR Mix
6µL RNase-free water + 1µl 20x FW + 1µl 20x RV + 10µl 2x SYBR + 2µl cDNA

NTC
8µL RNase-free water + 1µl 20x FW + 1µl 20x RV + 10µl 2x SYBR

- **Chapter 4 – Immunohistochemistry**

Materials:
- Phosphate Buffered Saline (PBS) tablets, Cat. P4417, Sigma, UK
- Hydrogen peroxide H_2O_2 (30%) , Cat. 216763, Sigma, UK
- Triton™ X-100, Cat. X100, Sigma, UK
- VECTASTAIN Elite ABC KIT, Cat. PK-6100, Vector Laboratories
- 3'3 Diaminobenzidine, Cat. D8001, Sigma, UK
- 1st Antibody (Rabbit Anti-GHS-R1a), Cat. H-031-31, Phoenix Pharmaceuticals
- Ammonium nickel (ii) sulfate hexahydrate, Cat. A1827, Sigma, UK
- Histomount medium, Cat. HS-103, National Diagnostics, UK

Phosphate Buffer Solution PBS (10mM)
1 tablet + 200mL of $_dH_2O$

1% H_2O_2 in PBS
100µL (30%) H_2O_2 + 2900µL of (10mM) PBS

10% PBST stock
1mL Triton X-100 + 9mL PBS

0.01% PBST
200µL 10% PBST + 200mL PBS

Blocking solution (10% Normal Goat Solution)
2700µL (0.01% PBST) + 300µL NGS

1stAb (Rabbit Anti-GHS-R1a) 1:250
890µL (10mM) PBS + 30µL NGS + 80µL Ab

Blank
970µL (10mM) PBS + 30µL NGS

2nd Ab (Goat anti-rabbit IgG ABC kit)
10mL (10mM) PBS+ 150µL NGS + 50µL biotinylated anti-rabbit Ab

ABC complex
100µL reagent A (Avidin DH) + 100µL reagent B (Biotinylated Horseradish Peroxidase H) + 10mL (10mM) PBS

DAB ammonium-nickel-sulphate working solution
0.05% DAB + 0.05% Nickel-ammonium-sulphate + 0.3% H_2O_2, pH 7.2
- Reagents mixed in the following sequence:
(1) 5ml PBS
(2) 500µl 0.5% DAB
(3) 250µl 1% Nickel-ammonium-sulphate
(4) 250µl 0.3% H_2O_2

- **Chapter 4 – Glucose tolerance test**

Glucose solution
The dose of glucose is 2 g/kg body weight
Animal ~ 30g.

1g BW - 2mg glucose
30g – x (60mg)

Administered as 20% D-glucose in PBS
2g – 10mL PBS
60mg – x (300µL)

- **Chapter 5 – Autoradiography**

Materials:
- [O-methyl-^{3}H]WAY 100635, Cat. ART 1554, specific activity: 83.0 Ci/mmol, radioactive concentration: 1 mCi/ml, American Radiolabel Chemicals, UK
- [^{125}I]DOI, Cat. ARI 0147, American Radiolabel Chemicals, UK
- [^{3}H]Ketanserin, NET791, Perkin Elmer, UK
- Pargyline hydrochloride, Cat. P8013, Sigma-Aldrich
- Serotonin, Cat. 14927, Sigma, UK
- Prazosin hydrochloride, Cat, P7791, Sigma, UK
- Tetrabenazine, Cat, T2952, Sigma, UK
- Methysergide maleate, Cat, 1064, Tocris Biosciences, UK
- MDL 100907, Cat. 4173, Tocris Bioscience, UK
- RS 102221, Cat. 1050, Tocris Bioscience, UK
- Metol, Cat. 69705, Sigma, UK
- Soldium Sulfite, Cat. S0505, Sigma, UK
- Hydroquinone, Cat. H17902, Sigma, UK
- Sodium carbonate monohydrate, Cat. S4132, Sigma, UK
- Potassium bromide, Cat. P0838, Sigma, UK

Solutions for pH meter adjustment and calibration
pH 4 – BDH®, Prod. No. 33189, Buffer powder diluted in 100mL of $_{d}H_2O$
pH 7.00 ± 0.02 @ 25°C – BDH®, Prod. No. 3327420, Lot. CP079M1, Buffer capsules diluted in 100mL of $_{d}H_2O$
pH 10.00 ± 0.02 @ 25°C – Russel, Buffer powder diluted in 100mL of $_{d}H_2O$
pH Meter is a laboratorial instrument that measures the concentration of H^+ on a solution and indicates its acidity or alkalinity based on its previous calibration, with the solutions above.

Tris-HCl Buffer stock (0.5M)
1L – 0.5mol
250mL – x (0.125mol)
M.W. = 121.14 g/mol
1mol – 121.14 g
0.125mol – x (15.125g)
- 15.125g of Tris diluted in 250mL of $_dH_2O$

Tris-HCl working solution (50mM)
$C_iV_i = C_fV_f$
0.5mol x 250mL = 0.05mol x V_f?
V_f = 2500mL
- 2250mL of $_dH_2O$ to be added to the stock solution

5-HT1a – [^{3}H]WAY 100635

2nM of [^{3}H] WAY 100635
1mCi/mL = 1000µCi/mL
50µCi/vial
80Ci/mmol = 80µCi/nmol

1000µCi – 1mL
80µCi – x (0.08mL)
0.08mL – 1nmol
1000mL – x (12,500nmol)
12.5µM
$C_iV_i = C_fV_f$
12.5µM x V_i = 2nM x 34mL (32 slides)
- V_f = 5.5µL of stock solution

Pargyline stock (5mM)1L - $5x10^{-3}$ mol
5mL – x ($25x10^{-6}$mol)
M.W.:195.69 g/mol
1 mol – 195.69g
$25x10^{-6}$mol – x (4.89mg)
- 4.89mg of pargyline in 5mL of Tris-HCl

Pargyline for incubation (10µM)
$C_iV_i = C_fV_f$
5mM x V_i = 10µM x 34mL (32 slides)
- V_f = 68µL of stock solution

5-HT stock (5mM)
1L - $5x10^{-3}$ mol
5mL – x ($25x10^{-6}$mol)
M.W.:212.68g/mol
1mol – 212.68g
$25x10^{-6}$mol – x (5.31mg)
- 5.31mg of 5-HT in 5mL of Tris-HCl

5-HT for block incubation (10µM)
$C_iV_i = C_fV_f$
5mM x V_i = 10µM x 2mL (1 slide)
- V_f = 4µL of stock solution

Working Buffer Solution for total binding
[O-methyl-^{3}H] WAY 100635 + Pargyline + Tris-HCl Buffer

5.5µL of (2nM) [O-methyl-^{3}H] WAY
68µL of (5mM) pargyline
34ml of (50mM) Tris-HCl buffer

Block Solution
$(HOCH_2)_3CNH_2$ (Tris) + Pargyline + [O-methyl-^{3}H] WAY 100635 + 5-HT

4µL of (5mM) unlabelled 5-HT
2mL (50mM) Working Buffer Solution

5-HT2a – [^{3}H]Ketanserin

1nM of [^{3}H]Ketanserin
1mCi/mL = 1000µCi/mL
50µCi/vial
43Ci/mmol = 43µCi/nmol

1000µCi – 1mL
43µCi – x (0.043mL)

0.043mL – 1nmol
1000mL – x (23,255nmol)
23.3µM

$C_iV_i = C_fV_f$
23.3µM x V_i = 1nM x 34mL (32 slides)
- V_f = 1.5µL of stock solution

Prazosin stock (1mM)
1L - $1x10^{-3}$ mol
10mL – x (10^{-5}mol)
M.W.:383.401g/mol
1mol – 383.401g
10^{-5}mol – x (3.8mg)
- 3.8mg of Prazosin in 10mL of $_dH_2O$

Tetrabenazine stock (1mM)
1L - $1x10^{-3}$ mol
10mL – x (10^{-5}mol)
M.W.:317.427g/mol
1mol – 317.427g
10^{-5}mol – x (3.2mg)
- 3.2mg of Tetrabenazine in 10mL of ethanol

Methysergide stock (1mM)
1L - $1x10^{-3}$ mol
5mL – x ($5x10^{-6}$mol)
M.W.:487.56g/mol
1mol – 487.56g
$5x10^{-6}$mol – x (2.4mg)
- 2.4mg of Methysergide in 5mL of Tris-HCl

Methysergide for block incubation (400µM)
$C_iV_i = C_fV_f$
1mM x V_i = 200µM x 5mL
- V_i = 1mL of stock solution
TrisPT Buffer Solution (pre-incubation and ligand binding)
$(HOCH_2)_3CNH_2$ (Tris) + $C_{19}H_{21}N_5O_4$ (Prazosin) + $C_{19}H_{27}NO_3$ (Tetrabenazine)

100µL of (1mM) stock Prazosin
10µL of (1mM) stock Tetrabenazine
100mL of (50mM) Tris-HCl buffer

Working Buffer Solution
[^{3}H]ketanserin + TrisPT Buffer

4.7µL of (1nM) [^{3}H]ketanserin
45ml of (50mM) TrisPT buffer
} 1nM double strength [^{3}H]ketanserin

Block Solution
$(HOCH_2)_3CNH_2$ (Tris) + $C_{21}H_{27}N_3O_2$ (methysergide) + ^3H $C_{22}H_{22}FN_3O_3$ (ketanserin)

2.5ml of (400µM) methysergide
2.5ml of (2nM) ketanserin.
} 5ml of 200µM methysergide

5-HT2c – [^{125}I]DOI

0.2nM of [^{125}I]DOI
171.6µCi/mL
2200Ci/mmol = 2200uCI/nmol

171.6µCi – 1mL
2200µCi – x (12.8mL)

12.8mL – 1nmol
1000mL – x (78nmol)
78nM

$C_iV_i = C_fV_f$
78nM x V_i = 0.2nM x 50mL (48 slides)
- V_f = 128µL of stock solution

Assay Buffer (2.5L)
50mM Tris-HCl pH 7.4 – 15.1425g
0.5mM EDTA – 0.365g
10mM $MgSO_4.7H_2O$ – 6.155g
0.1% Ascorbic Acid – 2.5g
0.1% BSA – 2.5g
10uM Pargyline – 3.975

MDL 100907 stock (1mM)
1L – 10^{-3}mol
5mL – x ($5x10^{-6}$mol)
M.W = 373.49g/mol
1mol – 373.49g

$5x10^{-3}$mol – x (1.86mg)
- 1.86mg of MDL 100907 in 5mL of DMSO

MDL 100907 for incubation (100nM)
$C_iV_i = C_fV_f$
1mM x V_i = 100nM x 50mL (48 slides)
- V_f = 5.5µL of 1mM stock solution

RS 102221 stock (1mM)
1L – 10^{-3}mol
5mL – x ($5x10^{-6}$mol)
M.W = 649.08g/mol
1mol – 649.08g
$5x10^{-3}$mol – x (3.25mg)
- 3.25mg of RS 102221 in 5mL of DMSO

RS 102221 for block incubation (10µM)
$C_iV_i = C_fV_f$
1mM x V_i = 10µM x 3mL (2 slides)
- V_f = 30µL of stock solution

Working Buffer Solution for total binding
[^{125}I]DOI + MDL 100907 + Assay buffer

102µL of (0.2nM) [^{125}I]DOI
4µL of (1mM) MDL 100907
40mL of Assay Buffer

Block Solution
RS 102221 + Working buffer solution

30µL of (1mM) RS 102221
3mL of Working Buffer Solution

Developing Solution
2500mL dH_2O
8g Metol
360g Soldium Sulfite
32g Hydroquinone
210g Sodium Carbonate
20g Potassium Bromide
Cold dH_2O until 4L solution

- In order to prepare developing solution, 2.5L of distilled water was warmed up until it reached 50 degrees Celsius. It was added a pinch of sodium sulphite to inhibit the initial oxidation of the metal for then add metol. Once dissolved, remaining sodium sulfate was added to the solution as well as the other chemicals, in order of appearance. Once reagents were dissolved, solution was covered in foil film for light protection and used on the following day.

Stop Solution
H_20 + 2 drops of $C_2H_4O_2$ (acetic acid)

Fixer Solution (2.5L total volume)
250 ml of the Fixer stock + 2250 ml of distilled water

- Stir the solution thoroughly for a few minutes

APPENDIX 3

Standard curves

- **Chapter 4 – ELISA**

Ghrelin

Absorbance (A_{490}/A_{620}) was measured within 5 minutes and ghrelin concentration was determined via interpolation using the standard curve generated by plotting absorbance *versus* the corresponding concentration of ghrelin standard, as shown below.

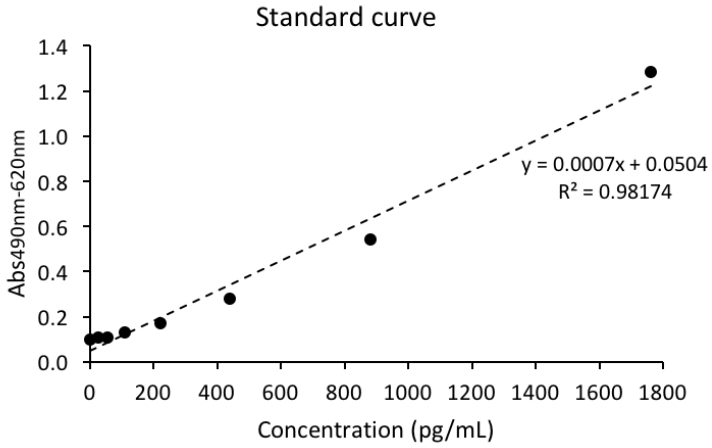

Figure 4. Standard curve of known active ghrelin concentration and the respective coefficient of correlation.

Leptin

Absorbance (A_{490}/A_{620}) was measured within 30 minutes and leptin concentration was determined via interpolation using the standard curve generated by plotting absorbance *versus* the corresponding concentration of leptin standard, as shown below.

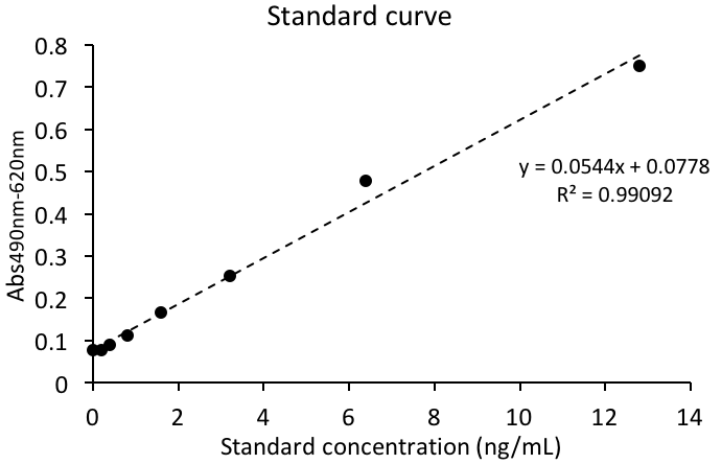

Figure 5. Standard curve of known leptin concentration and the respective coefficient of correlation.

Insulin

Absorbance (A_{490}/A_{620}) was measured within 30 minutes and insulin concentration was determined via interpolation using the standard curve generated by plotting absorbance *versus* the corresponding concentration of mouse insulin standard, as shown below.

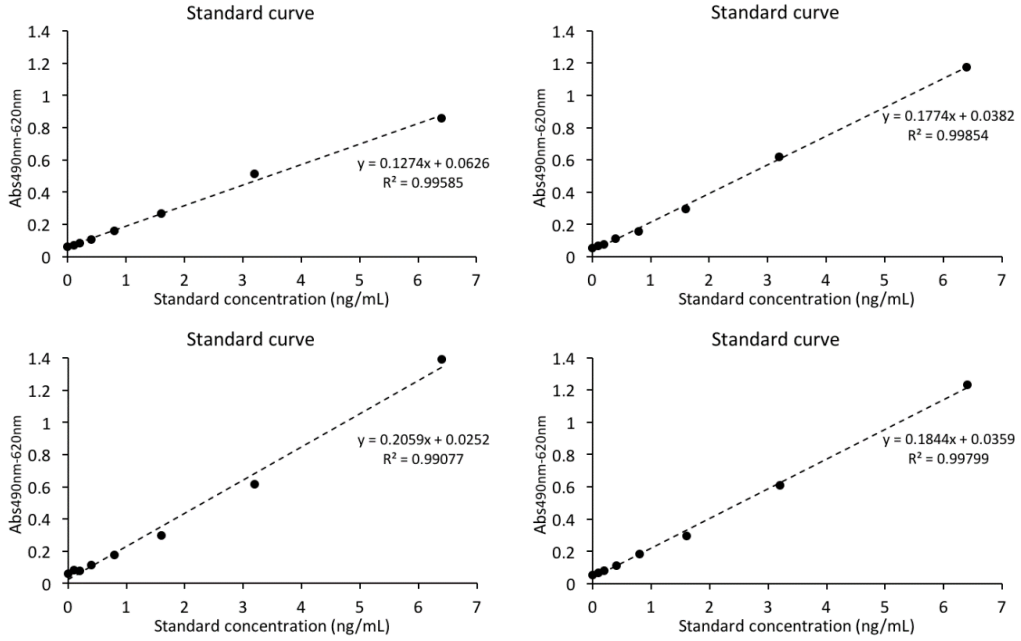

Figure 3. Standard curves of known insulin concentration and the respective coefficient of correlation; total of 4 ELISA kits used.

- **Chapter 4 – Autoradiography**

5-HT1A – [^{3}H] WAY 100635

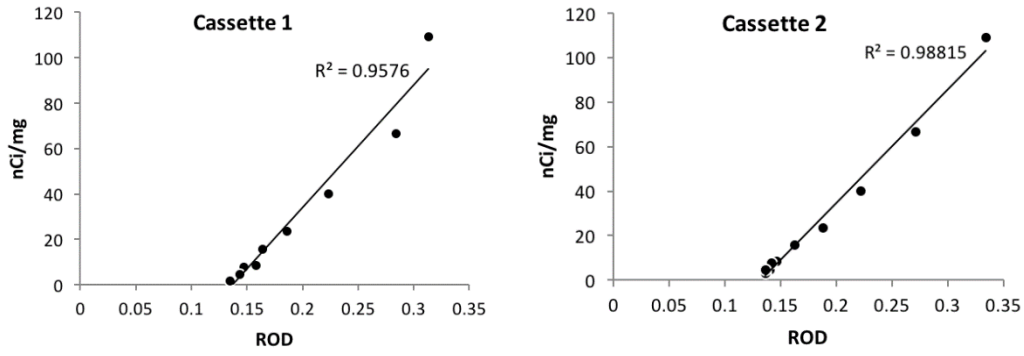

Figure 5.5. [O-methyl-^{3}H]WAY 100635 films' standard curves developed for analysis of specific binding of 5-HT1A receptors according to the respective Relative Optical Density.

5-HT2A – [^{3}H] WAY 100635

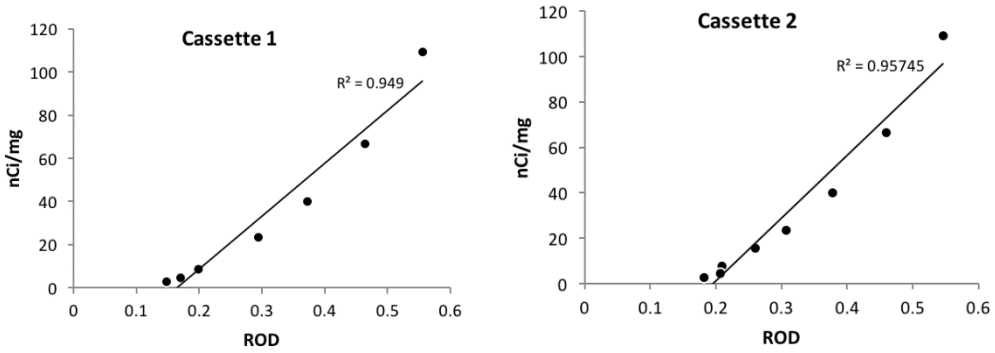

Figure 13. [^{3}H]Ketanserin films' standard curves developed for analysis of specific binding of 5-HT2A receptors according to the respective Relative Optical Density.

APPENDIX 4

Abstracts for conferences

[1]*Department of Life Sciences, University of Roehampton, London, United Kingdom*
[2]*Preclinical Laboratory for Translational Research into Affective Disorders, Department of Psychiatry, Psychotherapy & Psychosomatics, Psychiatric Hospital, University of Zurich, Switzerland*
[3]*Department of Food Science, Faculty of Science, Food Microbiology, University of Copenhagen, Denmark*

FENS 2016

The Effects of Chronic Psychosocial Stress on Ghrelin Receptor Immunoreactivity in the Hypothalamus and Ventral Tegmental Area

Simone Nascimento[1], Giorgio Bergamini[2], Carina M Brugger[1], Atieh Fallah Rokni[1], Luma Alem Martins[1], Christopher R Pryce[2], Jolanta Opacka-Juffry[1] and Michael Patterson[1]

Introduction: Stress is known to affect feeding behavior in humans and animals. The direction of this effect is dependent on the stressor and individual, but there is good evidence linking chronic social stress with overeating. In the mouse chronic social stress (CSS) stress model, increased feeding is observed. Elevated circulating levels of ghrelin are thought to contribute to this effect.
Aim: The aim of this study was to investigate the effect of CSS on ghrelin receptor (GSHR-1a) immunoreactivity in areas of the hypothalamus (arcuate nucleus – ARC and ventromedial hypothalamus – VMH) and the ventrotegmental area (VTA).
Methods: Adult male C57BL/6 mice were exposed to psychosocial stress with loss of social control for 15 days, 1-10 minutes daily (CSS). Control mice were handled daily in parallel. All in vivo procedures were conducted under a permit for animal experimentation (Switzerland). Indirect immunohistochemistry (IHC) with stereology was used to identify GHRS-1a positive cells in the brain regions of interest.
Results: The effects of CSS on central GHSR-1a immunopositive cell density appeared to be region-dependent. While no effects were observed within the VTA and VMH, the GHRS-1a immunopositive cell density was elevated in the ARC in CSS compared with control mice.
Conclusion: Chronic social defeat stress in mice can lead to upregulation of the ghrelin receptor in the hypothalamic arcuate nucleus which may contribute to the stress-related overeating observed in this experimental stress model.

BNA 2017

Effects of chronic social stress on 5-HT1A, 2A, and 2C receptor binding in mouse brain regions associated with reward processing

Simone Nascimento[1], Michaela Buerge[2], Simon Beyan[1], Cherrelle Lewis[1], Vivekan Varathanathan[1], Christopher R Pryce[2], Michael Patterson[1], Jolanta Opacka Juffry[1]

Introduction and aim: Serotonin (5-HT), via its various receptors, each of which is expressed in discrete brain regions, modulates aversion and reward processing and is implicated in various psychopathologies including eating disorders and depression. In mice, chronic social stress in adulthood leads to increased food intake in the absence of weight gain but reduces effortful motivation to obtain gustatory reward. The aim of this study was to investigate for stress effects on three 5-HT receptors, namely 1A, 2A and 2C, by quantifying their specific binding in some brain regions underlying reward processing: medial prefrontal cortex (mPFC), hippocampus (HIPP), amygdala (Amy), nucleus accumbens (NAcc), ventral tegmental area (VTA), dorsal raphe nucleus (DRN) and locus coeruleus (LC).

Methods: Adult male C57BL/6 mice were exposed to chronic social stress (CSS) or control handling (CON) for 15 days. Brains were collected on day 16. In coronal sections, receptor autoradiography was applied to quantify specific binding of 5-HT1A, 5-HT2A and 5-HT2C, using [3H]WAY100635, [3H]ketanserin and [125I]DOI, respectively.

Results: 5-HT1A binding was significantly increased (236%) in DRN of CSS compared with CON mice. 5-HT2A was significantly decreased in VTA (32%) and Amy (10%) of CSS compared with CON mice. 5-HT2C binding was significantly decreased (42%) in DRN of CSS compared with CON mice. There were no significant CSS effects in the other regions.

Conclusion: These region- and receptor type-specific stress-induced changes in 5-HT receptor binding might contribute to the deficit in gustatory motivation. On-going studies will investigate for stress-induced changes in homeostatic regulation.

FENS 2018

The Effects of Chronic Social Stress on Energy Balance and The Potential Role of Neuroendocrine Regulators of Feeding

Simone Nascimento[1], Christopher R Pryce[2], Jolanta Opacka-Juffry[1] and Michael Patterson[1]

Introduction and Aim: Stress is known to affect energy metabolism in humans and animals and regulation of feeding and energy expenditure (EE) are thought to contribute to this effect. This study aimed to investigate the effects of chronic social stress (CSS) on food intake (FI), body weight (BW), white adipose tissue (WAT), EE, respiratory exchange ratio (RER), and peripheral and central neuroendocrine regulators of feeding.

Methods: Adult male C57BL/6 mice were exposed to 15 days of social stress, 1-10 minutes daily (CSS), or control handling. FI and BW were measured daily. Indirect calorimetry was performed prior to and following CSS. At termination, blood was collected for ghrelin and leptin determination, WAT was weighed, and brains were collected for quantification of expression of central mRNA leptin and ghrelin and their respective receptors.

Results: Relative to controls, CSS mice had similar FI, attenuated increase in BW, no change in EE, increased RER, increased plasma ghrelin, decreased plasma leptin, decreased WAT mass, and decreased mRNA leptin expression. Increased RER indicates greater carbohydrate utilization in CSS versus CON mice. The similar EE with a relatively low BW indicates greater requirement of EE for other metabolic processes, possibly brain function.

Conclusion: Chronic social stress in mice led to peripheral metabolic changes consistent with increased energetic requirements and with important implications for brain function: Firstly, changes in central regulators of energy metabolism and feeding would be expected and are under investigation. Secondly, stress-induced changes in the brain may further increase its energy demands with functional consequences.

FENS 2018

The Effects of Chronic Social Stress on Gut Microbiome

Simone Nascimento[1], Maria Wiese[3], Christopher R Pryce[2], Michael Patterson[1], Jolanta Opacka-Juffry[1] and Adele Costabile[1]

Introduction and Aim: The brain's response to stress has a direct effect on the gut, and stress is known to increase the permeability of the gut lining, which gives gut bacteria easier access to both the immune and the central nervous system. This study aimed to investigate the effects of chronic social stress (CSS) on the gut microbiota composition in the mouse model, in which immune, neural and behavioural changes have been demonstrated.
Methods: Adult male C57BL/6 mice were exposed to 15 days of social stress, 1-10 minutes daily (CSS), or control handling. On days 7 and 15 freshly-voided faeces were collected from each mouse and stored at -80°C until the analysis, in which total bacterial DNA was extracted from the faeces and the gut microbiota composition was characterized by next-generation sequencing of the V3 to V4 region of the 16S rRNA gene. The 16S rDNA sequences within the assembled metagenomes were taxonomically selected using the Qiime pipeline and the Greengenes database. Biostatistic analyses of metagenomic data were performed with R and nonparametric ANOSIM significance tests.
Results: ANOSIM data have shown significantly increased populations of *Bacteroides* spp. (Bacteroidaceae) and *F. prausnitzii* (Ruminococcaceae) in CSS versus control between days 7 and 15.
Conclusion: Our data demonstrate an impact of long-term social stress on the gut microbiota composition. This pilot study with its rigorous 16S rRNA sequencing of gut microbiome contributes novel observations on the effects of chronic social stress that can be of relevance to its immune and neural outcomes.

PHARMACOLOGY 2018

Animal-Model Evidence for Involvement of Leptin in the Regulation of Stress-induced Changes in Energy Balance

Simone Nascimento[1], Christopher R Pryce[2], William Powell[1], Michaela Uebel[1], Jolanta Opacka-Juffry[1] and Michael Patterson[1]

Introduction: Stress is known to affect energy balance in humans and animals, due to its effects on both feeding and energy expenditure. The adipokine leptin contributes to the regulation of energy balance and could be a mediator of stress effects thereon. This study in mice investigated the effects of chronic social stress (CSS) on food intake, body weight (BW), energy expenditure (EE), respiratory exchange ratio (RER), white adipose tissue (WAT) mass, and peripheral levels of leptin and central expression of its receptor.

Methods: Adult male C57BL/6 mice were exposed to 15 days of social stress, 1-10 minutes daily (CSS), or control handling. Food intake and BW were measured daily. Indirect calorimetry was performed prior to and following CSS. At termination, blood was collected for plasma leptin immunoassay, WAT for quantification of expression of mRNA leptin (*Lep*) and leptin receptor (*Lepr*), and brains for frozen tissue microdissection and brain region-specific mRNA *Lepr* quantification using RT-PCR (arcuate nucleus of hypothalamus, paraventricular nucleus, ventromedial hypothalamus, ventral tegmental area, nucleus accumbens, medial prefrontal cortex).

Results: Relative to controls, CSS mice had similar food intake, lower BW gain (-69%, $p<0.005$), a trend to significantly increased EE ($p<0.07$), increased RER ($p<0.005$), lower plasma leptin level (-90%, $p<0.0001$), lower WAT mass (-42%, $p<0.001$), lower WAT *Lep* mRNA expression (0.54 fold change, $p<0.01$), similar WAT and brain-region specific *Lepr* mRNA expression. Therefore, CSS led to reduced conversion of food intake to increased BW, coupled with a trend to increased EE associated with a relative increase in carbohydrate metabolism. The lower plasma leptin levels are consistent with the increase in energy demand.

Conclusion: Chronic social stress in mice led to peripheral metabolic changes consistent with an increase in energy needs that were not met by a corresponding increase in energy intake. These changes included decreases in WAT mass, plasma leptin and WAT *Lep* mRNA expression. These findings suggest that altered leptin signalling might be a major determinant of attempted maintenance of energy balance in the face of stress and a potential target for treatment of stress-related changes in energy balance.